REPUBLIC OF TURKEY

YILDIZ TECHNICAL UNIVERSITY

GRADUATE SCHOOL OF NATURAL AND APPLIED SCIENCES

DETERMINATION OF AGEING PROPERTIES OF TURKISH STONES AND INVESTIGATION THE EFFECTIVENESS OF DIAMMONIUM PHOSPHATE CONSOLIDANT

Selen Ezgi ÇELİK

DOCTOR OF PHILOSOPHY THESIS

Department of Chemical Engineering

Chemical Engineering Program

Advisor

Prof. Dr. Fatma Jale GÜLEN

June, 2021

REPUBLIC OF TURKEY

YILDIZ TECHNICAL UNIVERSITY

GRADUATE SCHOOL OF NATURAL AND APPLIED SCIENCES

DETERMINATION OF AGEING PROPERTIES OF TURKISH STONES AND INVESTIGATION THE EFFECTIVENESS OF DIAMMONIUM PHOSPHATE CONSOLIDANT

A thesis submitted by Selen Ezgi ÇELİK in partial fulfillment of the requirements for the degree of DOCTOR OF PHILOSOPHY is approved by the committee on 30.06.2021 in Department of Chemical Engineering, Chemical Engineering Program.

Prof. Dr. Fatma Jale GÜLEN

Yıldız Technical University

Advisor

Approved By the Examining Committee

Prof. Dr. Fatma Jale GÜLEN, Advisor
Yıldız Technical University ______________________

Assoc. Prof. Dr. Nurcan TUĞRUL, Member
Yıldız Technical University ______________________

Prof. Dr. İsmail AYDIN, Member
Istanbul University Cerrahpasa ______________________

Prof. Dr. İsmail İNCİ, Member
Istanbul University Cerrahpasa ______________________

Assoc. Prof. Dr. Nil ACARALI, Member
Yıldız Technical University ______________________

I hereby declare that I have obtained the required legal permissions during data collection and exploitation procedures, that I have made the in-text citations and cited the references properly, that I haven't falsified and/or fabricated research data and results of the study and that I have abided by the principles of the scientific research and ethics during my Thesis Study under the title of Determination of Ageing Properties of Turkish Stones and Investigation the Effectiveness of Diammonium Phosphate Consolidant supervised by my supervisor, Prof. Dr. Fatma Jale GÜLEN. In the case of a discovery of false statement, I am to acknowledge any legal consequence.

Selen Ezgi ÇELİK

Signature

This study was supported by the Scientific and Technological Research Council of Turkey (TUBITAK) 2214-A Programme Grant No: 1059B141700359

Dedicated to my dearest daughter

and my soon-to-be-born son

ACKNOWLEDGEMENTS

First of all, I would like to thank my supervisor Prof. Dr. Fatma Jale GÜLEN, for her dedicated support and guidance. I would also like to thank Assoc. Prof. Dr. Nurcan TUĞRUL for her encouraging and helpful instructions among the project. I would like to thank Prof. Dr. Ismail AYDIN for his support, time, mentorship and sincerity since my bachelor days.

From the bottom of my heart I would like to express my gratitude to Prof. Heather VILES from Oxford University. Her world-renowned expertise has given me a knowledge and vision that I could not even imagine. In addition, I would like to express my endless gratitude to Dr. Mona EDWARDS and Mrs. Hong Zhang, who provided all kinds of help to me within OxRBL, Dr. Martin COOMBES who contributed greatly to the soft capping studies, Dr. Katrin WILHELM who provided me important information during my data analysis, and Prof. Dr. Tim DE KOCK and Dr. Scott ORR for DRMS analysis.

I would like to thank my colleagues Dr. H İrem ÖZGÜNDÜZ and A. Bilal ÖZTÜRK, who did not spare their support during my laboratory studies.

I would like to thank Mercan Doğaltaş for Ankara stones, Saray Taş for Nevşehir stones and Ahlat Taş for Bitlis stones and to Dr. Şükrü KAYA for providing Mardin stone samples from both the field and the quarry.

I would like to express my gratitude to my parents and my dear brother, who have supported and encouraged me in every path I have taken.

Finally, I would like to express my endless love to my beloved husband Hüseyin ÇELİK, who has been my source of peace and my biggest supporter in the world since the day he entered my life, to my dear daughter, my source of happiness, Şehrazat, whose love in my heart cannot be compared to anyone else, and to my soon-to-be-born son, who cheered up my thesis writing process with his little kicks. Thank you all for being in my life.

Selen Ezgi ÇELİK

TABLE OF CONTENTS

LIST OF SYMBOLS

°C	Celsius Degree
ΔE	Distance of Colors
GPa	Gigapascal
HLD	Hardness Unit of Equotip Impact Device D
MPa	Megapascal
μm	Micrometer
γ	Unit Weight
a_w	Water Activity

LIST OF ABBREVIATIONS

ANOVA	Analysis of variance
ASTM	American Society for Testing and Materials
BC	Before Christ
CIE	International Commission on Illumination
DAP	Diammonium Phosphate
DRMS	Drilling Resistance Measurement System
ESEM	Environmental Scanning Electron Microscope
HAP	Hydroxyapatite
ICOMOS	International Council on Monuments and Sites
IR	Infrared
ISCS	International Scientific Committee for Stone
MIP	Mercury Intrusion Porosimetry
PRESS	Predicted Residual Sum of Squares
RH	Relative Humidity
RILEM	International Union of Laboratories and Experts in Construction Materials, Systems and Structures
TEOS	Tetraethyl Orthosilicate
UNESCO	United Nations Educational, Scientific and Cultural Organization
UPV	Ultrasonic Pulse Velocity
USB	Universal Serial Bus
UV	Ultraviolet
XRD	X-ray Powder Diffraction

LIST OF FIGURES

LIST OF TABLES

ABSTRACT

Determination of Ageing Properties of Turkish Stones and Investigation the Effectiveness of Diammonium Phosphate Consolidant

Selen Ezgi ÇELİK

Department of Chemical Engineering

Doctor of Philosophy Thesis

Advisor: Prof. Dr. Fatma Jale GÜLEN

Conservation of built heritage is an important subject for both culturally and scientifically. Stone, as the dominant component of the structures, has the major importance among the materials. There has been a great interest and research on stone conservation for decades. However, for being a natural resource, there are hundreds of different stone types used in cultural heritage sites and each site should have been treated individually because of that uniqueness.

In this study, different types of Turkish stones (Ankara, Bitlis, Mardin and Nevsehir) have been investigated. They have been chosen for being not only important for geoheritage of Anatolia, but also a construction material for valuable architectural heritage.

In the first part of the study, manual weathering cycles (frost-thaw and thermal degradation) have been applied. Thermal degradation experiment plan has been created by using Design Expert 7.0 software. The results have been compared with automated ageing cycles that took place in the weathering cabinet.

In the second part of the study, DAP (Diammonium Phosphate) treatment has been applied on raw samples and effectiveness of the consolidant have been evaluated by analyzing surface hardness, surface roughness, ultrasonic pulse velocity, drilling resistance, color and hydric properties.

As the last part of the study, a soft capping (plant covering) simulation has been performed on Mardin and Nevsehir stones. The data of temperature difference has been collected and results have been analyzed by comparing the samples.

Keywords: Cultural heritage, stone, consolidant treatment, ageing, experimental design.

ÖZET

Türkiye'ye Özgü Taşlarda Yaşlanma Özelliklerinin Belirlenmesi ve Diamonyum Fosfat Koruyucusunun Etkinliğinin İncelenmesi

Selen Ezgi ÇELİK

Kimya Mühendisliği Anabilim Dalı

Doktora Tezi

Danışman: Prof. Dr. Fatma Jale GÜLEN

Yapısal kültürel mirasın korunması hem kültürel hem de bilimsel açıdan önemli bir konudur. Bu yapıların esas malzemesi olan taş ise, diğerlerinin yanında ayrı bir öneme sahiptir. Bu konuya olan ilgi uzun yıllardır sürmekte ve araştırmalar yapılmaktadır. Ancak, doğal bir malzeme olması dolayısıyla, her bir kültürel miras alanında birbirinden farklı özellikte taşlar bulunmakta ve bu nedenle her bir malzeme için yeniden inceleme yapılması gerekmektedir.

Bu çalışmada Türkiye'ye ait dört farklı taş türü (Ankara, Bitlis, Mardin ve Nevşehir) incelenmiştir. Taşlar, sadece Anadolu'nun jeolojik mirası açısından önemli olmakta kalmayıp aynı zamanda, mimari miras için de önemli yapı unsurları oluşlarından dolayı tercih edilmişlerdir.

Çalışmanın ilk kısmında, laboratuvar koşullarında manuel olarak yaşlandırma çevrimleri (donma-çözünme, sıcaklık bozunması) gerçekleştirilmiştir. Sıcaklık bozunması denemeleri gerçekleştirilirken Design Expert 7.0 yazılımı kullanılarak deneysel tasarımdan faydalanılmıştır. Sonuçlar, iklimlendirme kabini kullanılarak otomatik olarak yapılan çevrimler ile kıyaslanarak sunulmuştur.

Çalışmanın ikinci kısmında, işlem görmemiş taş örnekleri üzerinde DAP (Diamonyum fosfat) uygulaması yapılmıştır. Etkinliğinin incelenmesi için, yüzey sertliği, yüzey pürüzlülüğü, ultrasonik dalga hızı, delinme mukavemeti, renk ve hidrik özellikler analiz edilmiştir.

Çalışmanın son kısmında ise, Mardin ve Nevşehir taşları üzerinde yumuşak kaplama (bitkiyle örtme) tekniğinin simülasyonu gerçekleştirilmiştir. Simülasyon sonucunda, sıcaklık farkı verileri toplanmış ve sonuçlar karşılaştırılarak analiz edilmiştir.

Anahtar Kelimeler: Kültürel miras, koruyucu uygulaması, yaşlandırma, deneysel tasarım.

1
INTRODUCTION

1.1 Literature Review

The Republic of Turkey is one of the richest countries in the world in terms of cultural heritage thanks to nearly 4 million registered movable and immovable artefacts (Republic Of Turkey Ministry Of Culture and Tourism, 2021). As of 2021, there are a total of 85 assets, 4 mixed (cultural / natural), 3 natural and 78 cultural, registered on the UNESCO World Heritage List (Republic Of Turkey Ministry Of Culture and Tourism, 2021). The main material of most of these works is stone and among them there are archaeological and ethnographic works of world importance. Conserving these works with the right methods is of vital importance for the cultural richness of our country.

Stone artefacts in the external environment degrade over time due to many different effects such as atmospheric conditions (seasonal or daily temperature differences, wind, freeze-thaw cycles, acid rain, salt effect, air pollution), human factors (physical damage, graffiti, improper practices) and biological factors (micoorganisms and plants) (Siegesmund et al., 2002). Therefore, it is important to take care of these artefacts with scientific methods and conservation science covers these problems.

One of the most important subject among the area of conservation science is damage determination. For this purpose, in addition to observations and investigations in the field (Wedekind et al., 2018), (Inkpen et al., 2012) aging studies are also carried out under laboratory conditions (Andriani & Germinario, 2014; Smith et al., 2011). At the end of these aging studies, mathematical expressions based on different properties are developed for each stone examined. However, these studies are carried out by making many trials due to different reasons such as the high number of parameters affecting, the difference in geographical conditions or different chemical structures of the stones. Besides, the trials are aimed at detecting the damages that have occurred over a long period of time. Therefore, in such studies, there is a need to use laboratory techniques such as accelerated aging methods or to reduce the number of experiments with mathematical arrangements such as experimental design methods.

Another important class of conservation science in stone works is the application and development of consolidants. Consolidants are used to improve mechanical strength of stones. Basically consolidants are divided into three classes: organic, inorganic and lime-based. Although being commonly used in the market and research widely, they all have certain disadvantages (Borsoi et al., 2016; Matteini et al., 2011; Naidu et al., 2015; Sassoni et al., 2011, 2013, 2015).

Bio-inspired solutions have become increasingly popular in recent years. HAP has many advantages over these alternatives, including improved mechanical structure in 48 hours, formulation in aqueous solution without harmful chemicals, acid corrosion resistance, providing deep penetration depth through its low viscosity, not affecting hydric properties on the surface, not causing recognisable color change, giving opportunity to further treatments by not plugging the pores and leaving the surface hydrophilic (Graziani et al., 2016; Liu & Zhang, 2007; Sassoni et al., 2011, 2015). Consolidation effect of the phosphate compound is largely due to a reaction between DAP (Diammonium phosphate) and $CaCO_3$ in the substrate, which produces HAP as a product. Although resulting in an improvement on several performance parameters for both calcite rich and silicate rich stones, studies usually concluded that compatibility between substrate and consolidant is necessary for effective application (Molina et al., 2018; Sassoni et al., 2013). As a result, investigating the efficacy of DAP on stones with low $CaCO_3$ content is still an important research topic that needs to be investigated.

1.2 Objective of the Thesis

The purpose of this study is (i) to determine the aging properties based on freeze-thaw and thermal decomposition by using Design Expert 7.0 software, using experimental design methods on four different stone samples unique to Turkey, and express them mathematically; (ii) stopping or slowing down the degradation process by the application of diammonium phosphat (DAP), which is observed to occur naturally on the stones and provide effective protection, and (iii) to simulate soft capping technique, which is one of the green protection methods compatible with nature and observe the effectiveness. For this purpose, various physical and mechanical analyses were performed and the results were analysed statistically.

1.3 Hypothesis

The sensitivity towards cultural heritage items throughout the world is increasing day by day. The number of scientific studies conducted in this context is also increasing rapidly. With this thesis work, it is aimed to bring the different aging properties of Ankara, Bitlis, Mardin and Nevsehir stones that unique to Turkey and the effectiveness of DAP and soft capping application in these stones to the literature.

By evaluating the data obtained from the freeze-thaw cycles to be made in the first part of this study, it is expected to present information regarding the strength of the stone samples in cold conditions that they can be exposed to in different regions of Anatolia. Similarly, the effects of daily and seasonal temperature differences will be revealed with thermal degradation experiments. It is expected that the data obtained from these studies will be useful for the age determination of the structures through reverse engineering by evaluating them together with the data that can be obtained from the field later.

Following the DAP application to be carried out in the second part of the study, it is expected that this new generation material, which has many advantages compared to traditional preservatives, will be presented as a product that can be evaluated in our country. By adding external Ca^{2+} source, it is predicted to increase efficiency on Ankara, Bitlis and Nevsehir stones which have low carbonate content and therefore expected to show low efficiency of DAP.

With the soft capping mimmicking to be carried out in the last part of the study, a simulation of the vegetal cover protection technique, which has never been applied in Turkey before, will be simulated and an alternative that can be applied to reduce temperature differences and protect the structure from further wear, especially in areas that are very difficult to protect in the form of ruins will be presented as a useful method.

2
DETERIORATION MECHANISMS OF STONE

The deterioration of stone works and the binding elements of structures follows mechanisms similar to the deterioration of stones in nature. For example, the degradation textures in historical quarries are almost the same as the degradation textures that occur in historical buildings. In this section, the different types of degradation on stone works will be explained, based on the weathering effects in nature.

Knowing and identifying the different types of degradation is vital in determining the method of protection to be applied on the structure later on. To be given an analogy with medical science, this situation can be compared to the investigation of the environmental conditions of the person before the development of any disease, and to start the treatment process by examining the environmental conditions in case of a disease and then, if possible, regulating it.

• Elements of Degradation

The deterioration of stone works is mostly due to environmental factors (such as rain, wind, frost, temperature difference, soluble salts) and rarely to human factors (such as bad restoration practices, atmospheric pollutants, graffiti).

The general acceptance in the literature is that degradation is studied in four classes (Schnabel, 2014).

i. Mechanical Decay: The type of decay caused by damage triggered by the forces acting on the stone.
ii. Physical Decay: The type of degradation in which the stresses occurring in the internal structure of the stone cause the stone to crack and deeper physical damage.

iii. Chemical Degradation: The type of degradation that causes the minerological composition of the stone to change due to factors such as crystallization or dissolution.

iv. Biological Degradation: The type of degradation that mostly occurs by microbiological organisms and can function through a wide variety of mechanisms.

Although the types of decay can be classified independently of each other, it should be kept in mind that one degradation can trigger another and often more than one type is observed over the same structure.

Another important factor in the occurrence of damage, as well as the environmental conditions, is the characteristics that depend on the location and structure of the building. For example, whether it is exposed to rain or daylight, whether it is at a height that can cause capillary water rise, its general architecture (protective features of the roof, surface treatments, structure of windows, etc.), whether it has structural problems (such as leaking roof) and finally, properties such as internal structure, mechanical properties, porosity of the stone. Detailed information about these features are presented in Sections 2.2 and 2.3.

2.1 Elements of Degradation

2.1.1 Mechanical Degradation

Porous building materials, by their nature, consist of atoms with strong covalent bonds and some ionic character. These bonds prevent crystals from deforming plastically. As a result, these materials are tough and brittle.

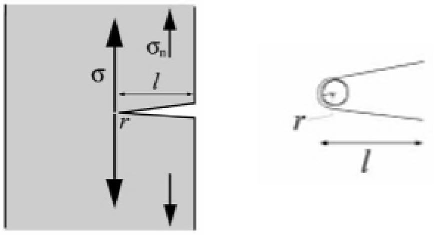

r = Radius of curvature at the apex of the crack
l = depth of crack

σ = stress at the crack apex
σ_n = average stress
k = stress intensity factor

$$\sigma = \left(1 + 2\sqrt{\frac{1}{r}}\right) \sigma_n$$

$$k = \left(1 + 2\sqrt{\frac{1}{r}}\right)$$

Figure 2.1 Stress concentration under tensile stress (Doehne & Price, 2010)

The tensile strength of brittle materials is much lower than the compressive strength and is generally not considered a reliable parameter. However, the main reason for the growth of cracks is usually the tensile stresses the structure is exposed to.

As can be seen in the formula, the larger the crack is, the larger the stress density factor (k), in other words after the crack formation starts, it does not stop unless a special intervention takes place.

While performing architectural protection treatments, these theoretical foundations should be paid attention to and the surfaces of building materials should be protected in a way that they do not create new stress points.

Whether a structural member will be subjected to tensile stress depends mainly on its position in the structure. All horizontal structures have the potential to be exposed to this problem. One of the good examples that can be given to this situation is lintels (Figure 2.2). The lower parts of the lintels are subjected to tensile stress, while the upper parts are subjected to compression stress. In this case, even the smallest crack that may occur in the opposite direction causes dangerous situations. In order to prevent this, arches that have been used in keystone since the Roman period have been made (Figure 2.2). In these structures, it is aimed to prevent crack formation and stress concentration by creating compression stress on the lower surfaces of stones (Schnabel, 2014).

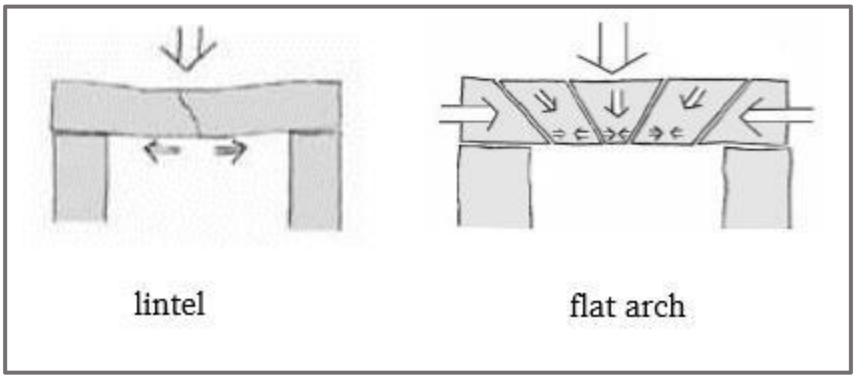

Figure 2.2 Stresses on linten and flat arch (Doehne & Price, 2010)

Physical damages occurring under compression stress are not caused by cracks or gaps, but from protrusions on the surface (Figure 2.3).

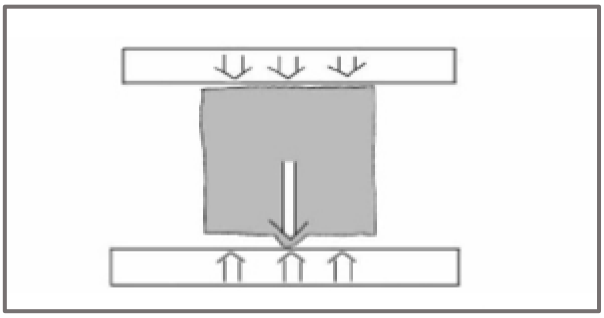

Figure 2.3 Stress concentration under compression (Doehne & Price, 2010)

Stress concentration caused by compression can be very dangerous, especially for heavy building blocks. Ancient masters, who knew this very well, either put mortar between the stones to take precautions (as in the Egyptian pyramids) or they did not require the use of mortar by smoothing the load-bearing surfaces very carefully (such as Gothic cathedrals in Europe or Inca walls in Peru).

2.1.2 Deterioration Due to Temperature Difference

2.1.2.1 Warm Up - Cool Down Cycles

All matter on the earth's surface expands by absorbing energy with solar radiation, which consists of UV, IR and visible light during the day, and cools and contracts by emitting IR during the night. Structures open to the atmosphere are also exposed to the effects of expansion and compression caused by daily or seasonal temperature cycles.

In materials with low heat conduction coefficients (eg stone), a shear stress occurs between the surface and the center during both the heating and cooling stages of thermal cycles (Figure 2.4). If two materials with very different expansion coefficients are used side by side, outward bending and even rupture of the material with high expansion coefficient may occur over time.

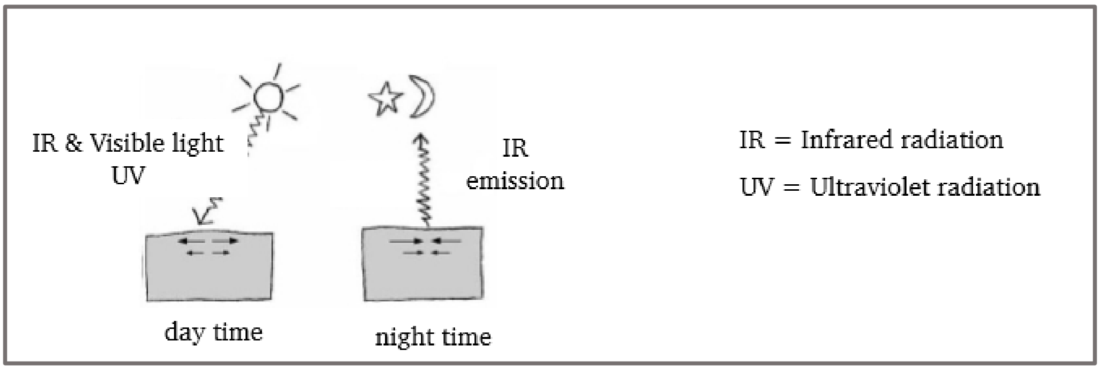

Figure 2.4 UV and IR emissions during day time and night time (Doehne & Price, 2010)

The thermal expansion coefficients of the materials frequently used together in buildings are shown in Table 2.1. Architectural protection is more difficult in buildings where different materials are used adjacent to each other, and it is recommended that the interfaces are supported with an intermediate element.

Table 2.1 Thermal expansion coefficients of different construction materials (Schnabel, 2014)

(Linear expansion per unit length per degree centigrade)			
Brick	7×10^{-6}	Carbon fibers	1.5×10^{-6}
Cement Concrete	$8\text{-}10 \times 10^{-6}$	Titanium	8×10^{-6}
Wood, along fibers *	5×10^{-6}	Iron	11×10^{-6}
Wood, across fibers *	50×10^{-6}	Copper, bronze	16×10^{-6}
Polyester / glass reinforced	$20\text{-}30 \times 10^{-6}$	Stainless steel	16×10^{-6}
Lead	28×10^{-6}	Aluminum	24×10^{-6}
* *The thermal expansion coefficients of different stones and wood species are different, an average figure is presented here.*			

Table 2.2 Thermal expansion coefficients for magmatic, metamorphic and sedimentary rocks (Siegesmund & Snethlage, 2011)

(Linear expansion per unit length per degree centigrade)				
Rock Class	Rock Type	Average	Min	Max
Magmatic	8 Rock Types	7.4×10^{-6}	5×10^{-6}	10×10^{-6}
Metamorphic	5 Marbles	11×10^{-6}	8×10^{-6}	15×10^{-6}
	1 gneiss, 1 schist	7.9×10^{-6}	6×10^{-6}	9×10^{-6}
	2 quarzitic rocks	12.5×10^{-6}	11×10^{-6}	14×10^{-6}
Sedimentary	2 calcareous sandstones	7.5×10^{-6}	7×10^{-6}	8×10^{-6}
	2 limestones	4×10^{-6}	2×10^{-6}	6×10^{-6}
	1 travertine	5×10^{-6}	4×10^{-6}	6×10^{-6}
	5 sandstones	10.8×10^{-6}	9.5×10^{-6}	12×10^{-6}

As well as the fact that the stones have different expansion numbers, another important issue is the different and anisotropic expansion coefficients of the minerals in them. In Figure 2.5, temperature-dependent variations of the linear expansion coefficients of different minerals are shown. As can be seen in the figure, when examining the degradation due to temperature, not only the matrix structure but also the different elements in the mineralogical composition should be taken into consideration. Due to the anisotropic structure, some crystals may separate from the structure over time and increase porosity and decrease cohesion.

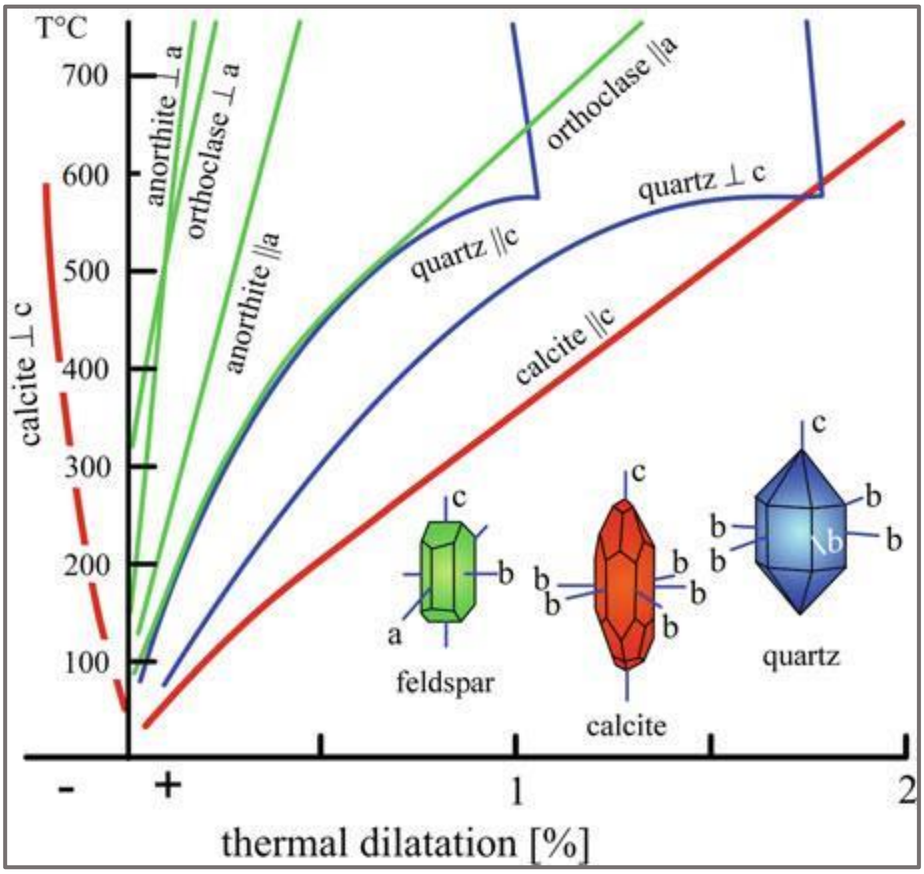

Figure 2.5 Thermal dilatation – temperature relation for different minerals (Winkler, 1997)

In general, temperature cycles set up between 20 ° C and 90 ° C cause mechanical damage to the stone. However, when the same amount of temperature difference is applied at -40 ° C, it does not result the as much as damage if the sample is not wet. This is because the expansion is temperature dependent.

2.1.2.2 Freeze - Thaw Damage

When the outdoor temperature reaches low degrees, the water inside the porous structure turns into ice crystals. During this crystallization, an average volume increase of 9% occurs. If there is too much water inside the pores, the stone will be damaged by internal stresses during ice crystal formation.

The pores must be large for damage to occur, because due to the high surface tension of the water, freezing cannot occur in the small pores. However, due to the negative pressure created by the frozen water, the liquid water is transported to the freezing zone by capillary (*cryosuction*). This causes the water in the small pores to feed the frozen water in the large pores.

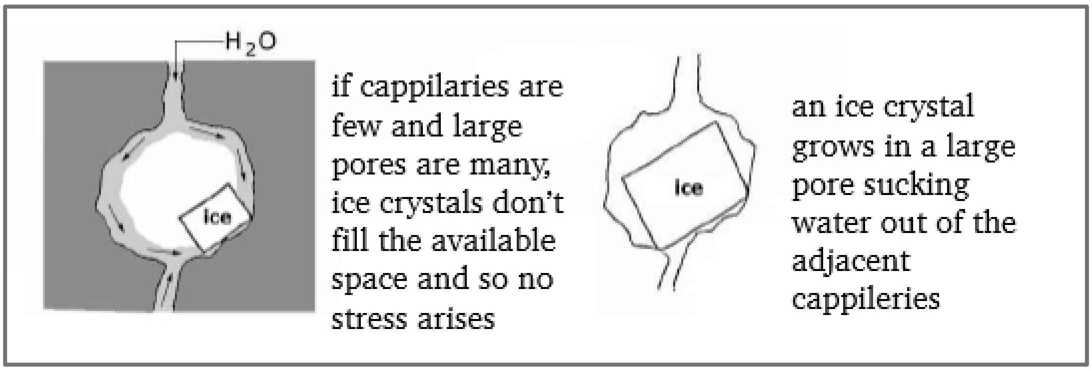

Figure 2.6 Growth of ice crystals in a porous material (Doehne & Price, 2010)

Freezing damage may cause particulate decomposition or scaling. Unlike salt degradation, it is observed more with low evaporation rates, that is, in stones saturated with water with high absorption rate.

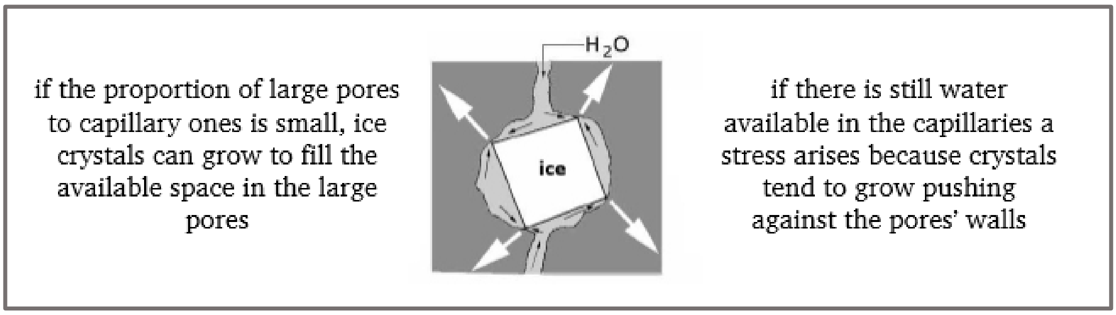

Figure 2.7 Frost damage (Doehne & Price, 2010)

2.1.3 Salt Damage

It is a type of degradation in which salt damage, chemical degradation and mechanical degradation occur at the same time. In theory, it is based on the principle that soluble salts crystallize in porous structures and cause stress in the internal structure of the pore. This tension causes cracking in the inner structure of the stone and causes mechanical weakening.

The presence of water or moisture is essential for salt to damage the stone. For this reason, knowing how water moves in the structure is of great importance in dealing with salt damage (Charola, 2000).

The source of the salt in the stone can be internal or external, usually observed as a combination of the two. Internal salts are salts that emerged from the material itself or from salt-rich dolomitic and cement based mortars by dissolution or chemical transformation (Arnold & Zehnder, 1989). For example, Portland cement often contains basic sulphates, or bricks which are not properly fired may contain sodium sulphate. Extrinsic salts can be marine effect, animal excrement, agriculture, dissolution of frozen salts, microorganisms, conservation practices (eg glass wool insulation), or salts carried by capillary uplift from groundwater (Siegesmund & Snethlage, 2011).

There are very few cases where salt damage is due to a single salt type. Usually two or more salts are present at the same time. This coexistence affects the behavior and solubility of the salts. As a general rule, if salts do not have a common ion, the solubility of both salts (such as sodium chloride and calcium sulphate dihydrate) increases due to the increase in ionic strength. This amount of increase is much higher for salt with lower solubility. If salts have common ions (such as sodium sulphate and sodium chloride), the solubility of both salts is reduced due to the common ion effect. However, it should be kept in mind that not all salts follow these rules.

At a given temperature, the vapor pressure of salt solution is smaller than that of pure water. The higher the concentration of the salt solution, the lower the vapor pressure, and the minimum when the solution reaches its saturation point. The sum of vapor pressure is determined by the salt solution's composition and temperature. This vapor pressure is known as "equilibrium relative humidity" since water vapor pressure can be expressed as % RH. Salts do not have "equilibrium RH" when mixed and they oscillate in a range (Price & Brimblecombe, 1994). When combined with the hygroscopic and capillary properties of the structure, it causes salt damage to be more harmful. These properties can be found in various geochemistry reference books such as (Krauskopf, 1979) or (Goudie & Viles, 1997).

2.1.3.1 Types of Salt Damage

There are four fundamental types of degradation caused by salt damage, efflorescence, contour scaling, honeycomb weathering and granular disintegration. The process by which the damage occurs is determined by the stone's materials, salt, and environmental factors. The stones that are most susceptible to salt damage are those with high pores that show rapid water absorption and evaporation kinetics.

- **Efflorescence**

Efflorescence is the least damaging to stone among other types of salt damage. It is based on the crystallization of salts by nucleation only on the surface of the stone. The most common salt types which cause efflorescence are chlorides (NaCl, KCl), sulphates (Na_2SO_4, $MgSO_4$, $CaSO_4$), carbonates ($CaCO_3$, $MgCO_3$) and nitrates (KNO_3, $NaNO_3$).

This type of damage occurs directly related to the capillary rise of water. Therefore, it is not generally observed in stones with low capillarity or stones covered with an anti-capillary barrier such as clay. Efflorescence is observed as white-gray spots on the undersides of the structures, usually just above the capillary fringe line. For this type of damage to occur, the capillary rise must be higher than the evaporation rate. It is a type of damage that can occur not only on the outer walls but also on the inner surfaces of buildings.

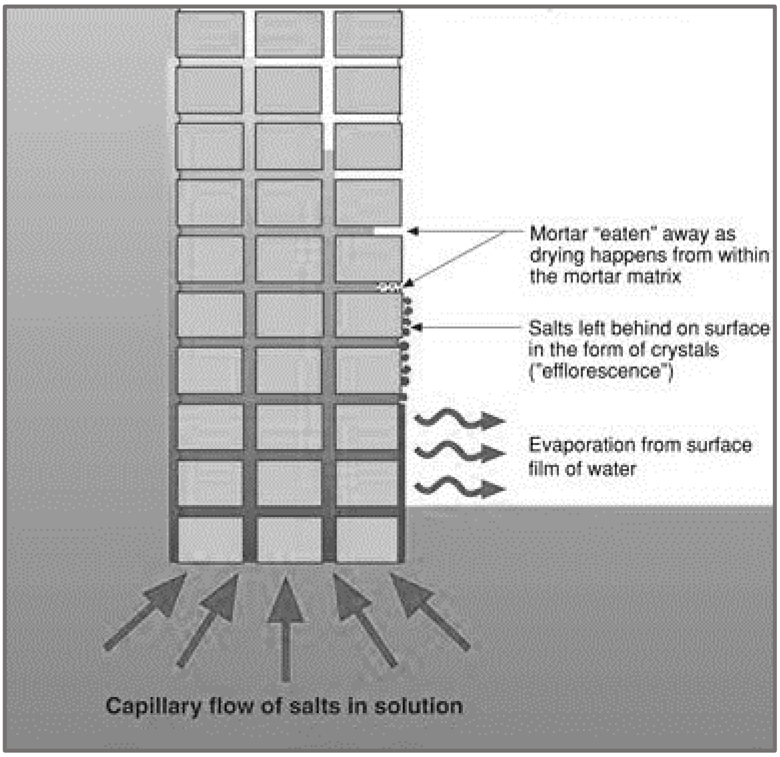

Figure 2.8 Efflorescence mechanism by capillary action

- **Contour Scaling**

If the evaporation is faster than the capillary rise, the salt solution may not reach the surface before evaporating. In this case, evaporation and therefore salt crystallization take place inside the porous structure and create a stress inside the stone that can cause damage. This deep crystallization causes cracks under the surface and causes a layer up to a few centimeters to separate from the surface. This is called contour scaling.

Figure 2.9 Contour scaling on Villiers-Adam church, Val d'Oise, France (limestone) (Angeli, 2007)

- **Granular disintegration**

This type of damage occurs in environments with high humidity, when the stone surface cannot be washed by rain or any other source of water. It follows a similar mechanism to flaking, but separation from the surface occurs with smaller pieces.

Figure 2.10 Granular disintegration on St Etienne church, Fécamp, Seine-Maritime, France (limestone). This church is located 300m of the sea (Angeli, 2007).

- **Pitting (or honeycomb-like degradation)**

It is a special type of granular disintegration. This distinct and generally regular pit texture can be in depths from a few centimeters to decimeters. The part separated from the wall with its hollow structure leaves a honeycomb-like image on the surface.

Figure 2.11 Honeycomb weathering on St Etienne church, Fecamp, Seine-Maritime, France (limestone). This church is located 300m of the sea (Angeli, 2007).

2.1.4 Mechanical Damage from Water and Wind

Mechanical erosion occurs on surfaces exposed to constantly flowing water. This causes more damage to stones with weaker grain boundaries. This type of decay becomes more dangerous by causing dissolution in carbonate stones. In addition, the dissolution effect increases with acid rain caused by atmospheric pollutants and increases the damage.

This type of damage is seen especially in the fortresses established on the hills and the walls of the old settlements. If strong winds accompany the rain, the amount of damage increases. Usually the softest element (eg mortar) begins to dissolve and erode. Subsequently, strong elements such as stones and bricks may also be subject to erosion.

Another factor that causes this type of erosion is the fine materials carried by the wind. If the building is made of silicate type stones, the damage will be stronger (Rob, 2004). Figure 2.12 shows a castle wall eroded by wind and rain.

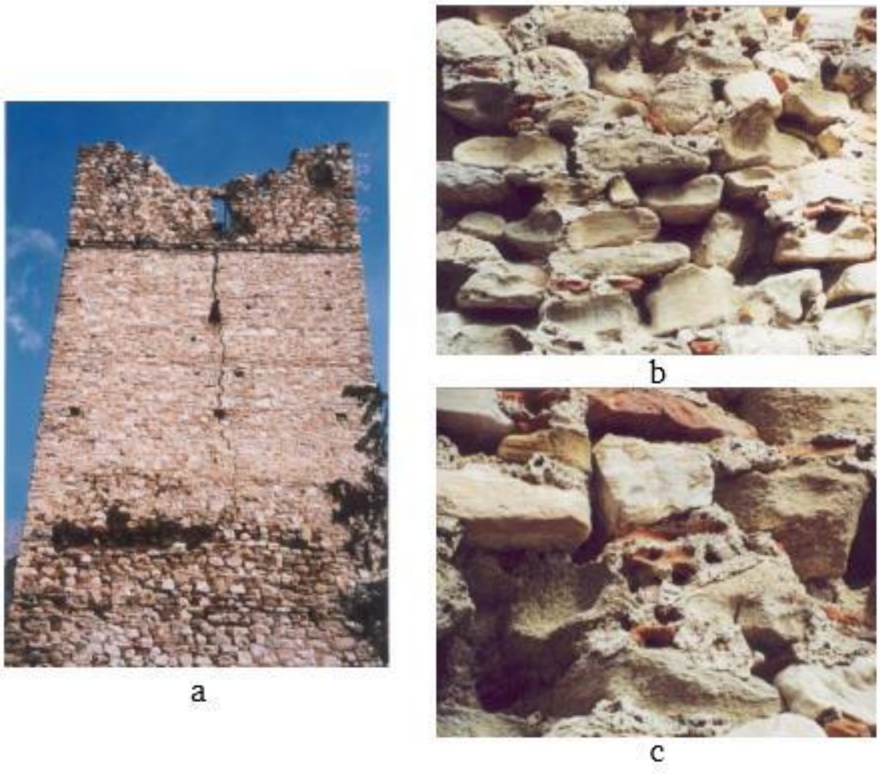

Figure 2.12 a. Tower of the castle of Serbia (North Greece – 11th Century) suffering from erosion. **b.** and **c.** details of the eroded lime mortar (Rob, 2004)

2.1.5 Iron and Steel Corrosion

Ferrous materials may have been placed in stone structures as a mechanical support element. Corrosion on the iron surface causes an increase in volume. If these metal supports are placed in brittle materials such as stone or cement without taking precautions, the tensile stress caused by corrosion over time may be strong enough to break the stone. One of the oldest ways to prevent this is to use lead in the joints (Figure 2.13).

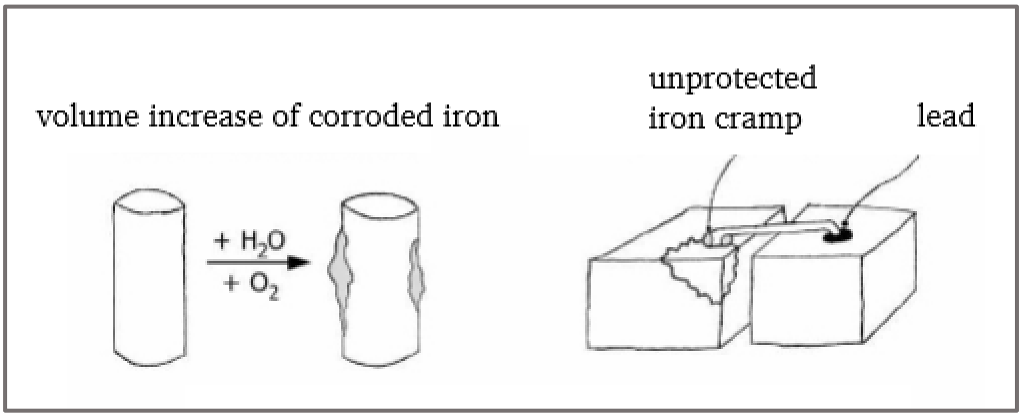

Figure 2.13 Stress caused by corrosion of iron inside stone

2.1.6 Atmospheric Pollution

- **Soiling**

Atmospheric pollution is responsible for many damages on natural stones. The least harmful of these is spotting. Soiling is the event that pollutants such as fly ash and flue gas adhere to the surface and cause blackening on the stone surface. It is frequently observed in buildings close to the road and in buildings in the city. Apart from the aesthetical deformations, it may cause the hydraulic properties of the stone to change and bring about different problems; adhering particles, low surface tension makes the stone more hydrophobic. This may lead to different problems such as reduced interaction with water and the inability of water inside the building to come out.

Figure 2.14 Example of soiling

- **Gypsum Formation**

Although the gypsum formation looks quite similar to soiling, it should be distinguished very carefully as it follows a different chemical structure. It usually occurs in parts of structures that are not exposed to water flow (such as under bridges or under statues). It is based on the principle that the SO_2 gas in the atmosphere reacts with calcite ($CaCO_3$) in the stone or the atmosphere and forms gypsum ($CaSO_4.2H_2O$) by releasing CO_2.

The thickness of this gypsum crust can reach 3 cm. Although gypsum is normally a transparent white color, pollutants in the atmosphere accumulate on this layer as in staining and cause a black crust to form. The interface between the stone and the shell formed is very fragile and over time, the surface of the stone begins to rupture. During the ruptures, fragments are separated from the surface of the stone and mechanical damage occurs.

- **Acid rains**

It is the phenomenon of dissolution on stone surfaces due to sulfuric and nitric acid caused by industrial pollution. This effect causes serious damage not only to structures but also to nature. In regions with high pollution, the pH of acid rain reaches values as low as 4.5. However, in recent years, especially with the trend towards renewable energy, the damage caused by acid rain has been decreasing (Angeli, 2007).

Acid rain damage, also known as acid corrosion, is most often observed in calcareous ($CaCO_3$ constituent) materials. Limestone stones, such as white marble, travertine, limestone, calcareous tuff, or lime-based binders, are examples of these stones (Schnabel, 2014).

The damage caused by acid rain is mainly based on the chemical reactions given below. However, in practice, these reactions proceed with much more complex mechanisms, with effects such as the adhesion of gases in the atmosphere to the surface or existence of different substances on the surface acting as catalysts.

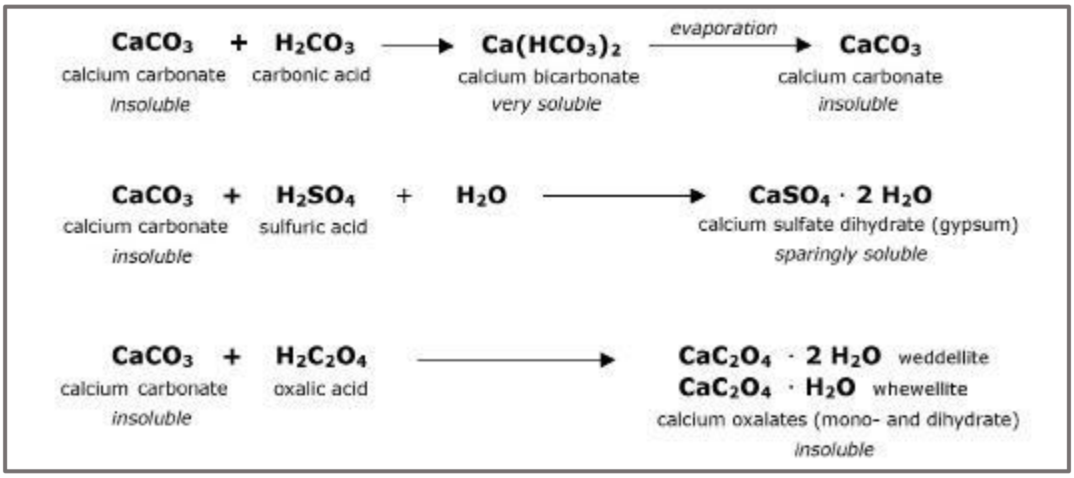

Figure 2.15 Acid attack of calcareous materials (Schnabel, 2014)

If the resulting product is soluble in water (such as calcium bicarbonate or calcium sulphate), the dissolved products may move to a different location from where the reaction takes place and cause re-accumulation there, or if the amount of water is low, it may settle in the same place. If the product formed is calcium bicarbonate, it turns back to calcium carbonate when the water in the environment evaporates.

- **Water and Acid Damage on Volcanic Rocks**

Granite, basalt and other volcanic rocks containing crystalline silica (quartz) are resistant to acid, but various silica-alumina minerals can be affected by rain or moisture according to the following reactions.

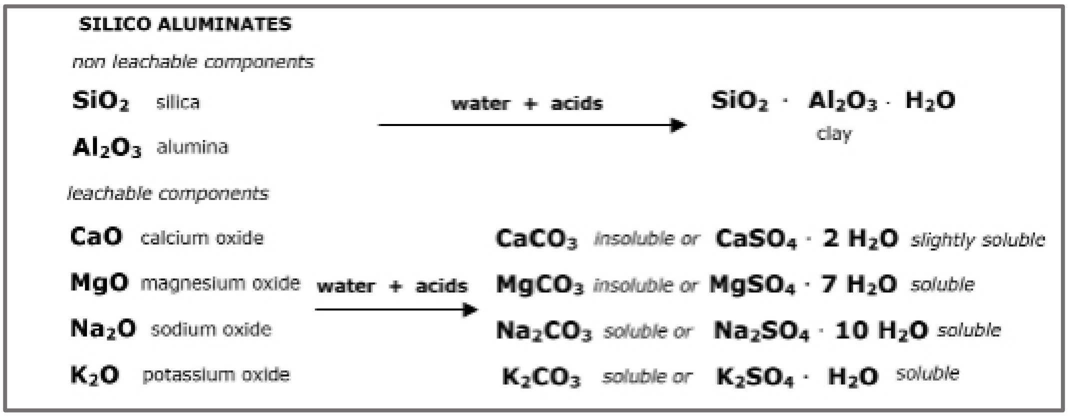

Figure 2.16 Leaching of volcanic rocks by acid water (Schnabel, 2014)

Silica-aluminates (such as feldspar, mica, chlorides) undergo a slow transformation with the humidity in the atmosphere. During this process, metal oxides selectively undergo acid reactions and become soluble in water by converting to carbonate or sulphates. This causes damage due to their removal from the surface and material loss.

2.1.7 Biological Damage

From a biological point of view, stones are very difficult environments to live on. They are poor in nutrients, vary widely in terms of moisture content, and are vulnerable to atmospheric influences such as wind, rain, and sun. However, there is no sterile stone that doesn't host microorganisms in any part of the world. These microorganisms living in the stone environment can be classified into two categories; i. those living in the stone surfaces are called *epilithic*, and ii. those living in the spaces within the stone are called *endolithic*. (Siegesmund & Snethlage, 2011)

The microorganism layer that forms a visible layer on the surface on the material and appears harmless to the surface is called *biopatina*. These layers can be removed with various antimicrobial agents, but these treatments are likely to leave a discoloration.

The most important factor determining whether there is a microbial growth on the stone surface is the presence of water. Therefore, porous stones with high water absorption capacity generally host bacterial and fungal colonization in a wide range of species. On the other hand, stones with low pores or easily drying are not microbiologically preferred hosts.

The types of microorganisms can be examined according to their water activity; while bacteria need higher water activity ($a_w > 0.98$), lichens and fungi appear to survive in places with lower ($a_w > 0.65$) water activity and tolerate longer periods under complete drying. However, bacteria are more resistant to high salt concentrations in water (Rivadeneyra et al., 2004). For this reason, bacteria are generally seen in high humidity and salty environments, where fungi are not common. However, it should be kept in mind that there are fungal species that are exceptional, and it should be remembered when investigating microbiological damage, that biodiversity always makes exceptions to general rules. Excellent reviews of the topic are provided by (Warscheid & Braams, 2000), (Caneva vd., 2008); (Scheerer vd., 2009). Other useful overviews are given by (Wakefield & Jones, 1998); (Ciferri vd., 2000) and (Crispim & Gaylarde, 2005).

Figure 2.17 Examples of the growth of algae on masonry monuments

Microbiological organisms have positive effects as well as negative effects on stone surfaces. In the literature studies, it is seen that there are still studies on "bioprotection vs biodeteroation" (Bartoli vd., 2014; Concha-Lozano vd., 2012; de la Rosa vd., 2013; Di Bonaventura vd., 1999; Favero-Longo & Viles, 2020; Gulotta vd., 2018; Pinna, 2014; Viles, 2005). Different studies have been reported from the bioprotection framework. For example, it has been suggested that different erosion levels are seen on stones with and without lithobionts (organisms live on/ir stone) and therefore, it has been suggested to create an umbrella-like protection (Mottershead & Lucas, 2000; Özvan vd., 2015). Comparing the lichen coated and uncoated stones in open air for 1 year, it has been observed that lichens play the role of a protective physical layer against weathering factors (McIlroy de la Rosa vd., 2014). Or it has been observed that *Hedera Helix L* type ivy protects the stone structure from atmospheric pollution of the city (Sternberg vd., 2010) or freeze-thaw damage (Coombes vd., 2018). In drier climates, microorganisms living on the surface can form a protective layer on the surface through chemical reactions and protect the stone in the long term (Dorn, 2013; Taylor-George vd., 1983). In addition, a varnish effect may occur on the surface with metals such as Mn and Fe accumulated in bacterial sheats (Dorn, 2013; Gorbushina, 2003; Parchert vd., 2012). Finally, it is also known that an effective protection layer is obtained on stones by the formation of oxalate layers with the effect called biomineralization (Rampazzi vd., 2004; Souza-Egipsy vd., 2004)(Souza-Egipsy et al. 2004), (Rampazzi 2019). Table 2.3 summarizes the biodeteriative and bioprotective roles of organism.

Table 2.3 Biodeteriorative and bioprotective roles often reported (●) or hypothesized/debated (?) for various types of lithobiontic organisms. It is worth noting that each potential role has to be considered species-specific and cannot be generalized for all the members of each group. (Favero-Longo & Viles, 2020)

				Higher Plants	Bryophytes *	Lichens	Microbial Biofilms		
							Algea	Cyanobacteria	Micro-colonial fungi
Biodeteriorative roles	During life	Biogeophysical	“Rooting”	■	■	■			■
			Wetting/drying			■	■	■	
			Enhanced thermal stresses		?	■	■	■	■
		Biogeochemical	Biomineralization		■	■		■	■
			Acid/complex dissolution	■	■	■	■	■	?
		Aesthetic loss	Surface coverage/ soiling	■	■	■	■	■	■
	After death	Remnant biocrusts	Disfiguring patina	?	■	■	■	■	■
Bioprotective roles	During life	Shielding	Umbrella effect	■	■	■	?	?	
			Reduced thermal stress	■	■	■	■	?	
			From pollutants	■	?	?	?	?	
		Biogeochemical	Rock varnish & case hardening			■		■	■
			Biomineralization		■	■		■	
		Aesthetic/ biodiversity enhancement	Greening’ walls	■	■	■	■	■	
	After death	Remnant biocrusts	Protective patina	?	■	■	■	■	■

2.2 The Effect of Stone Properties on Decay

In terms of conservation science, besides the environmental conditions of the buildings, the properties of the materials from which they are made should be examined carefully. In this section, some basic properties of stones will be mentioned. More detailed information can be found in geology reference books, which include features of rocks.

2.2.1 Mineralogical Composition

Knowing the mineralogical structure of the stone is very critical in understanding its interaction with its environment and accurately determining the damage that may occur. Not all minerals are subject to the same degradation. For example, calcite dissolves very easily in water, while quartz is almost inert. Degradation can also occur due to the different properties of different minerals within the same structure.

Sedimentary, igneous, and metamorphic rocks are the three geological groups of rocks. Igneous rocks, such as lava, may be extrusive or intrusive, such as granite. Variations in the pressures and depths at which igneous rocks form, the presence of magma, and the time taken to solidify determine the composition and size of minerals present. Generally speaking, bigger minerals are the product of deeper pressures and longer solidifying periods.

Main minerals in igneous rocks have differing resistance to weathering processes. The crystalline structure of various minerals, as well as their arrangement, can influence how susceptible igneous rocks are to degradation. The fundamental shapes of the atoms are as chains, as double chains, as loops, as sheets, and as three-dimensional networks. The fewer oxygen atoms are shared, the more resistant the mineral would normally be. The numerous mechanisms are vulnerable to weathering in different areas of their networks. Pyroxenes are long-chain minerals, for example, which undergo chemical weathering along the mineral's cleavage planes.

Goldrich proposed a straightforward ordering of minerals based on their relative weathering susceptibility, known as a mineral stability sequence. (Figure 2.18).

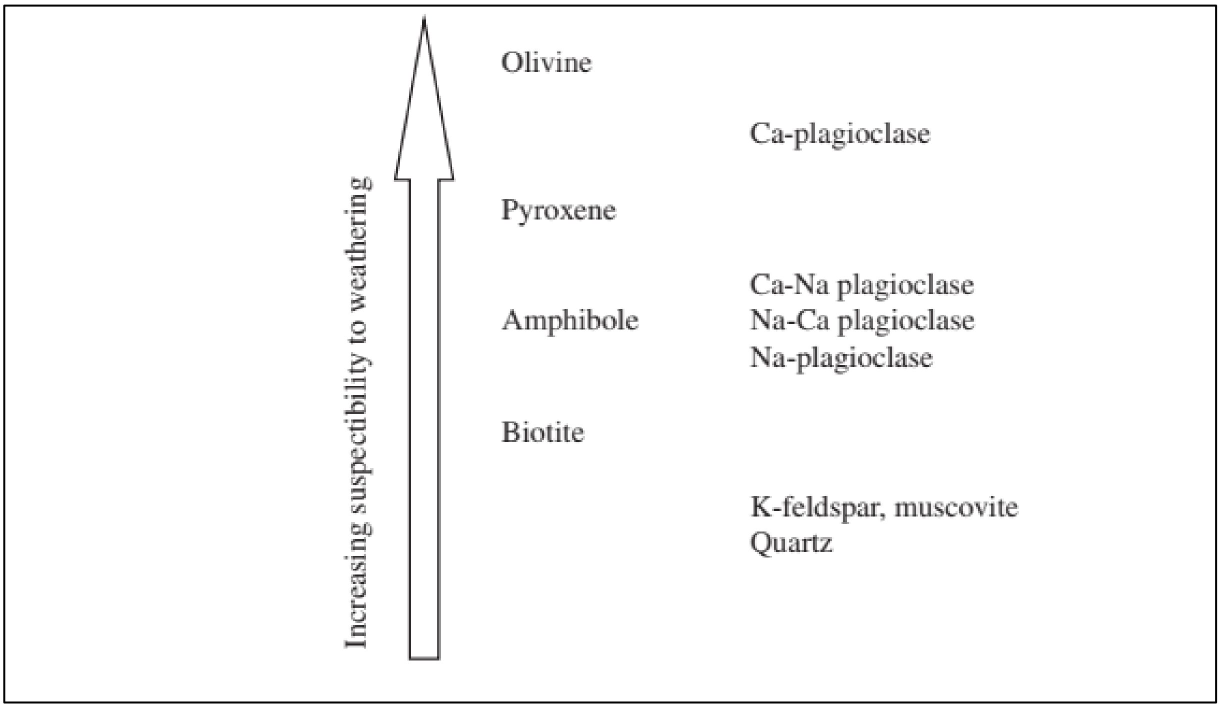

Figure 2.18 Goldrich's sequence of mineral stability (May & Jones, 2006)

Weathering materials from other rocks form sedimentary rocks. These compounds build up in lakes and seas, forming sand deposits. Sedimentary rocks can vary in texture from very finely bedded limestones to rough-bedded, unsorted sandstones. The discontinuities caused by changes in the environment in which the sediment is collected, such as from the lagoon to the deeper sea, may be relatively inconspicuous relative to the discontinuities induced by changes in the atmosphere in which the sediment is deposited. This means that whilst certain sedimentary rocks may have large discontinuities, they may be broadly scattered and therefore of little consequence while the stone is in the formation. In high-bedded rocks, such as certain types of sandstones, planes of structural collapse may be inherent. These bedding planes represent more distinct phases of deposition and may be essential for the stone's degradation once it's in place. When the rock is strained, the bedding planes can also act as liquid entry points and weakness areas.

Metamorphic rocks are either igneous or sedimentary rocks which have been modified by pressure or heat action. Marble is an example of a metamorphic rock, a calcareous rock whose crystalline composition has been changed by heat or pressure. Metamorphic rocks generally more resistant than the initial sedimentary rocks to degradation agents. The almost absolute lack of pore space and structure decreases the potential to penetrate the substance through weathering agents.

The deterioration of any stone, no matter what form, depends on the capacity of the weathering agents to act on the minerals that make up the rock. On structures such as mineral grain margins, alteration appears to be localized. This operation could either be supported or inhibited by rock properties. Similarly, if altered, the products of weathering must be extracted in order to prevent further contact of rock minerals and weathering agents. The main properties of any stone for its weathering behaviour are its mechanical strength, its solubility, its porosity (a reference for the ability of erosion agents to penetrate it) and the history of the rock (its memory).

2.2.2 Hydric Properties

The hydric properties of the stone are one of the most critical properties in terms of its long-term durability, because water is the carrier medium of many damage factors such as salt, pollutants, chemicals. These water-borne substances diffuse between the pores of the stone and crystallize by a mechanism determined by their drying kinetics. As a rule of thumb, it can be said that stones with low capillarity are more resistant to weathering. The reason for this is that less water is transported into porous structures. Stones with rapid capillary rise suffer more from both salt and frost effects.

In addition, the mineralogical properties of the structure also affect its behaviour towards water. Metamorphic stones containing some clays, especially smectite, are more susceptible to swelling with water than other types. When the clay swells with water in the stone, it causes tension inside the structure and can cause damage up to spilling in layers.

2.2.3 Having Different Strength Zones

This feature is not a direct cause of damage, but the heterogeneous structure of the stone may cause different amounts of stress and therefore cracks. The most common reason for this situation is that the stone has a bedding structure. For example, this is thought to be one of the reasons for honeycomb-like degradation.

This difference in properties is usually observed in sandstones with different metamorphosis layers.

2.2.4 Stone-Stone and Stone-Binder Compatibility

The chemical, physical and mineralogical compatibility of the materials used in the structure, is one of the most critical decisions in the long-term stability. The importance of this situation can be observed in the rapid deterioration after restoration works where wrong materials were used.

Looking at the examples in the field, it is seen that the most important feature of the damage is caused by the differences in the hydric properties of the stones. When one stone has a higher capillary than the other, the capillary continuity of the structure is disrupted and water begins to accumulate in the more capillary stone (usually the softer stone). This accumulation causes degradation over time. A similar situation arises when the hydric properties of the binder are different then the main stone.

2.3 Features of the Building

In addition to the properties of the stones, the properties of the structure are also important in terms of decay dynamics. These features are generally related to phenomena such as location, exposure to sun, and strength, which are the result of architectural decisions.

2.3.1 Location of Stones

As mentioned earlier in this chapter, the same stones kept in the same building under the same climatic conditions may show different decay characteristics from each other. Properties such as their altitude, exposure to atmospheric conditions such as sun and wind directly affect the degradation.

However, it is not uncommon to use more than one type of stone on the same structure. For example, stones with high strength and low capillarity are generally used in basements or columns, while the softest stones are generally used in decorations due to their easy processing.

2.3.2 Locating in the Shade / Sun

In buildings where pollution is observed heterogeneously, the effect of location can be clearly seen. Generally, areas in the sun are subject to degradation such as color change, while areas in the shade may be exposed to biological attacks and gypsum formation due to their higher humidity.

2.3.3 Mechanical Load

All structures are under mechanical load due to their own loads. This is particularly critical in building elements where the load is concentrated over a small area (upper parts of the arches or alcoves). In addition, if the structure is built on sloping terrain or in a landslide area, mechanical load may cause damage.

2.4 Human Factors

The increasing interest in cultural heritage day by day, while increasing the sensibility to the protection of buildings, on the other hand, increases the potential for harm from people. Unfortunately, this damage can be conscious or unconscious. For example, stone floors are worn under heavy visitors unconsciously or damage can be created on the stone by direct intervention (such as scraping and graffiti) consciously.

However, there are also damages indirectly caused by human influence. The most important example of this is atmospheric pollution.

Wrong choices made during restoration are also counted among human errors. These errors are usually due to the use of incompatible materials selected for financial concerns.

Finally, even if all stages are carried out in accordance with the standards and carefully, it is inevitable that various damages will occur during the operations until the stone is removed from the quarry and used in the building. Table 2.4 summarizes these operations and their outputs. Accordingly, when approaching a damaged structure, it should be kept in mind that th

ere may be degradation during production, transportation or construction even before the building is erected.

Table 2.4 Secondary and tertiary factors affecting natural stone during extraction, processing, and after the placement.(Přikryl, 2013)

Process	**Response**
Extraction and processing	
The rock microfabric's physical reaction and modification during extraction from the rock mass	Stress release (dilation) of a rough block (microcrack formation)
Various rock fabric alteration phenomenon, such as surface retreat (owing to abrasion, granular disintegration, subsurface microcrack formation, etc.)	Cutting and dressing of raw blocks of finished materials changes the stone surface
Drilling, chopping, and dressing with water	Increased moisture content, potential breakdown of water-soluble phases, and the formation of new phases in natural stone's pore system (e.g. water-soluble salts, chemicals)
Post-emplacement	
Interactions with the environment on a physical and chemical level	The order in which weathering or decay processes occur varies significantly depending on the stone's composition, environment, and other factors
Interactions with the environment's components, both physical and chemical	Stone characteristics change as a result of differences in physical behavior (e.g. thermal dilation, wetting–drying, or freezing–thawing) between stone and surrounding materials (mortars, other forms of stone, metallic components) or chemical variations in these materials (e.g. rusting of stone)
Maintenance	Removal of foreign materials (crusts, salts, polychromy deposits, etc.) from natural stone, absorption of new substances by cleaning chemicals, and modification of rock microfabric by mechanical cleaning methods cause physical and chemical changes to natural stone during cleaning. Natural stone undergoes physical and chemical changes through conservation, resulting in changes in the rock microfabric and physical properties due to the use of consolidants (e.g. porosity or surface permeability reduction).

3

ACCELERATED AGING STUDIES

3.1 Aging and Stability

All ordered structures tend to become disordered by the second law of thermodynamics. This disorder is measured by entropy, and all isolated systems want to reach their maximum entropy. Cultural heritage materials are also no exception, but from a material science perspective, unlike other engineering fields, the area studied is not new materials, but very large samples that have often been exposed to the influence of time. Therefore, determining the effects that occur over time is of particular importance for this field.

Changes in the material may occur due to different mechanisms, as explained in Section 2. Although mechanical and human damages are generally rapid and preventable, chemical damages (such as biochemical, light or heat effects) cannot be prevented and are slow-progressing effects. Therefore, mechanical and human effects can be reduced through laws and restrictions, but slowing down chemical damage is difficult and requires technical equipment and knowledge.

Weathering and therefore the determination of durability in stones has been an ongoing problem since ancient builders. The oldest known written source on this subject belongs to Vitruvius in 15 BC. Accordingly, before starting a building, older structures made with similar stones should be examined and careful action should be taken while quarrying and afterwards. In the relevant text, this suggestion is as follows: “two years before the commencement of building, the stones should be extracted from the quarries in the summer seasons, by no means in winter, and they should then be exposed to the vicissitudes and action of the weather. Those which after two years 'exposure are injured, may be used in the foundations, but those which continue sound after this ordeal, will endure in the parts above ground” (Morgan 1960). After the ancient era, researchers continued to make studies and suggestions about the durability of the stone.

The initiation of research in the laboratory to examine the durability dates back to the 18th century (West, 2000). The first documented test to take place under laboratory conditions was conducted by Thury in 1828. In this method, also known as the Mr. Brard's test, the changes on the natural stone were investigated using a combination of freeze-thaw and salt effect (Prikrly, 2013). In the continuation of these studies, in 1908, Hirshwald went one step further, and the idea of classifying stones according to their weathering and decay textures and introducing a scoring system was proposed.

Throughout the 20th century, studies have been carried out to examine the durability of natural stones, with changes made on four factors: i. Philosophy of durability determination; ii. Selection of the process used to examine ageing conditions, iii. Conditions and duration of durability test, iv. The properties that change before and after the process. Accordingly, the summary presented by Prikryl is shown in Table 3.1 to summarize the principles of approach.

Table 3.1 Overview of principal approaches to the durability assessment of natural stone (Přikryl, 2013)

Type of Approach	Principle	Methods of Evaluation	Duration	Advantages	Drawbacks and limitations
Accelerated laboratory durability tests	Modeling of the effects of various deterioration factors (specifically freeze–thaw, salt crystallization, and/or wetting–drying cycles) on free-standing normal specimens.	Changes in weight, porosity, dynamic elastic properties, and uniaxial compressive strength are all factors to consider.	Days–weeks	Simple equipment Cheap and quick evalutions at given conditions Use of standradized tests for determination of physical properties before and after the test	Regular conditions of the test (duration of cycles, temperature variations, etc.) are generally far from the reality Use of single damage process Fixed number of cycles Due to the measurement of transition in physical properties just before and after the experiment, obervation of the dynamics of changes is usually unlikely.

Table 3.1 Overview of principal approaches to the durability assessment of natural stone (Přikryl, 2013) (ctd)

Complex environemntal or stress testing	On free-standing standard specimens stored in an environmental box or cabinet, a combination of many deterioration mechanisms (e.g. freeze–thaw + moisture variance + presence of deleterious gases) is used.	Change of weight, dynamic elastic properties, porosity, uniaxial compressive strength	Weeks - months	In comparison to the previous method, the test conditions (cycle length, temperature variation, etc.) are similar to real conditions. Usage of standardized testing to determine physical properties before and after the evaluation is a possibility.	Expensive equipment Fixed number of cycles Observation of dynamics of the changes generally impossible owing to evaluation of changes of physical properties only before and after the experiment

Table 3.1 Overview of principal approaches to the durability assessment of natural stone (Přikryl, 2013) (ctd)

Exposure site testing	Material (regular specimens) is placed on exposure racks in real-world environments (generally outdoors)	Visual characteristics (colour change), weight change, ± dynamic elastic properties, ± destructive tests (strength)	Months to years	Higher level of confidence of test results owing to real environment Possible testing (non-destructive) of physical properties during the experiment	Range of environments needed if material to be used globally Stone specimens are not in contact with other construction materials (in contrast to within the real structure) Impractical duration of the test if rapid results are required Larger amounts of specimens in the case of application of destructive tests

Table 3.1 Overview of principal approaches to the durability assessment of natural stone (Přikryl, 2013) (ctd)

Practical experience	The materials used in the structure interact with the surrounding materials and are subject to realistic environmental conditions over time.	In situ observation of weathering or decay patterns ± sampling followed by testing of physical properties ± comparative digital photography, photogrammetry, laser scanning, ground penetrating radar, IR thermography	Depending on the age of the building, it may be hundreds or thousands of years	The highest level of confidence Materials exposed to real conditions Weathering or decay forms that haven't been reproduced in any of the previous simulations	Weathering or decay patterns seen in one ecosystem cannot be extrapolated to another (important in the case of climate change). Limited test specimen availability (regular and adequate sampling is normally not permitted on many monuments) In situ properties may be altered by test specimen preparation (e.g., washing out of weathered materials). Physical properties generally missing for fresh materials

The first three of these approaches can be considered as an artificial simulation of ageing, but practical experience should be taken into account in a different class. These practical tests provide more realistic results in real conditions, but it is difficult to reach scientific conclusions because of uncontrolled conditions, and performing large-scale tests in the real field may not comply with the "conservation" purpose of conservation sciences. Accelerated aging tests in the laboratory are the most used methods for the remaining methods. Detailed information about these tests will be presented in Section 3.2.

3.2 Accelerated Aging

Accelerated aging is a research technique based on observing the effects that materials will be exposed to in their natural environment for a long time, by applying more severe changes (higher temperature, higher concentration, etc.) in a controlled laboratory environment.

Feller (1994) divided the purpose of accelerated aging tests into three groups: (i) to classify materials according to their physical and chemical stability in a short time; (ii) estimating the long-term service life of materials at expected service conditions; (iii) to determine the degradation mechanisms that occur in the structure through controlled experiments under laboratory conditions. In this way, detailed information about the deterioration process can be obtained by removing a degradation texture (Feller, 1994).

When the stone materials within the scope of cultural heritage are examined, it is seen that accelerated aging applications in literature studies are carried out for different purposes;

• In order to determine damage mechanisms

• In order to predict the long-term effects of an applied consolidant,

• In cases where it is not possible to examine naturally aged specimens, to get damaged stones and to determine the restorative effect of the applied consolidant or treatment on damaged stones

When accelerated aging studies in the literature are examined since 2017, it is seen that more than 50% of the examined stone types are sedimentary carbonate rocks (Alves, 2020). This type is followed by magmatic rocks and sedimentary detrial rocks. When examined in terms of types of aging tests, it is seen that the highest ratio is in salt tests, then freeze-thaw and chemical reactants as can be seen in Figure 3.1. Here, "S" refers to any salt test in which salt damage is examined, regardless of type, procedure or environmental conditions. The "F" (freeze-thaw), "T" (thermal cycles) and "H" (heating) groups are all related to the temperature, but in freeze-thaw the damage caused by the increase in the volume of water in the pores is examined, while T deals with temperature fluctuations similar to seasonal cycles, and H is about high temperature effects (also known as thermal shock). The "CR" (chemical reactants) group has been used for all kinds of tests where chemical reactions are dominant. Here, the source of the reaction can be atmospheric contaminants, effects such as dissolution with solution or leaching (Alves, 2020).

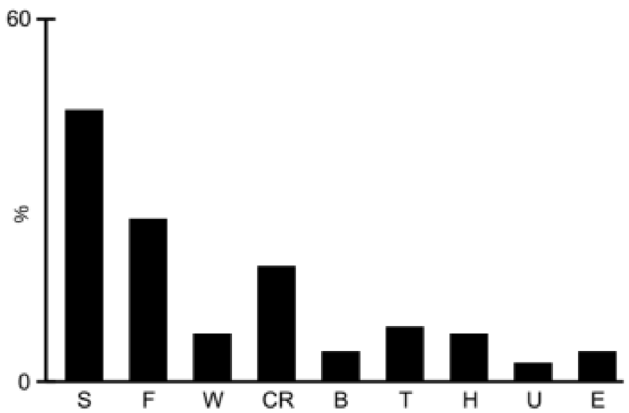

Figure 3.1 Data was gathered from literature for ageing studies. S: Salt weathering, F: Freeze-thaw, W: Wetting-drying, CR: Chemical reactants, B: Biological colonization, T: Thermal cycles, H: Heating, U: UV radiation, E: Exposure to weathering agents in the outdoors (Alves,2020).

3.2.1 Thermal Ageing Tests

Thermal ageing, as presented in detail in Chapter 2, is the total degradation due to seasonal or daily temperature differences that occurs in the stone or the elements applied on it. The most fundamental method to accelerate thermal ageing is to expose the sample to the temperature effect in accordance with a predetermined schedule in weathering cabinets where temperature and humidity can be controlled. Samples are subjected to various mechanical, chemical or physical tests before and after (sometimes after certain test numbers at intermediate stages) to examine their durability.

Thermal degradation in stone materials within cultural heritage is often studied together with thermal shock. Thermal shock (or thermal damage) generally used for exposing materials to very high temperatures, often to simulate fire damage (Andriani & Germinario, 2014; Hajpal & Török, 2004; Ozguven & Ozcelik, 2013, 2014; Sengun, 2014; H. Yavuz vd., 2010). This type of damage is not included in this thesis as it tests the damages that the material can never be exposed to under normal climatic conditions and is not covered by material aging techniques.

In recent years, there is ongoing trend to measure the durability of the treatments developed rather than the aging parameters of the stones themselves (Garcia-Talegon vd., 1998; Inigo vd., 2004; Iucolano vd., 2019; Sena da Fonseca vd., 2017; Tesser vd., 2018). The most important reason for this situation is that a significant part of the treatments developed are polymeric and they show much more dramatic changes in both micro and macro properties compared to stone with the effect of temperature.

When the literature studies are analysed, the most studied types in terms of stone types are marble (Eren Sarıcı, 2016; Ferrero & Marini, 2001; Andrew S Goudie & Viles, 2000; Mahmutoglu, 1998; Ozguven & Ozcelik, 2014; Rodríguez-Gordillo & Sáez-Pérez, 2006) and limestone (Al-Omari vd., 2014; Andriani & Germinario, 2014; Germinario vd., 2015; Ozguven & Ozcelik, 2014), followed by granite (Lam dos Santos vd., 2011) and sandstone (Mahmutoglu, 1998; Wang vd., 2016; Zhang, 2015). In addition, there are specific examples that examine more local stones (Al-Omari vd., 2014; Demirdag, 2013), as in this thesis. While some of these papers are based on a single species, some covers comparison studies. Although the sizes of the samples used varied, the shape of the samples do not differ much; mostly cubic or prismatic, sometimes cylindrical samples were preferred. On the other hand, the cycles applied varies greatly in studies. The preferred analysis frequency may be after every 4-5 cycles (Eren Sarıcı, 2016; Andrew S Goudie & Viles, 2000; Mahmutoglu, 1998), every 10-20 cycles (Demirdag, 2013; Germinario vd., 2015; Wang vd., 2016) or before and after the whole experiment (Andriani & Germinario, 2014; Ferrero & Marini, 2001; Lam dos Santos vd., 2011; Ozguven & Ozcelik, 2014; Poli vd., 2006; BS-EN 14066,2013)

The feature to be analysed at the end of the thermal tests is shaped according to the focus of the study. In studies that want to observe changes in microstructure, properties such as SEM, open porosity, UPV, apparent density, while observing changes in mechanical properties, compressive strength, elastic module, flexural strength, Knoop micro-hardness, surface hardness, microcracks count, linear expansion, residual strength and Young's modulus are also performed. However, the examination of color change as an important physical property often comes across. This analysis is frequently used in samples where thermal tests are performed, especially after applying polymeric treatments.

When the literature studies are examined, it can be said that thermal ageing simulations, which are frequently encountered as "weathering" or "accelerated weathering", have certain rules in the basic sense, but there is no consensus determined by the researchers with certain rules. While some of the scientists prefer to examine in more "gentle" or realistic conditions with the cycles they prepared based on the meteorological data of the region under investigation (Germinario vd., 2015), some may prefer to make examinations in more "aggressive" conditions in order to observe the temperature effects more clearly and quickly (Andrew S Goudie & Viles, 2000; Lam dos Santos vd., 2011). However, as can be found in some of the studies, it may be possible to examine both natural temperature cycles and thermal shock effects that can be observed in cases of fire etc. within the same study (Andriani & Germinario, 2014). In this case, it is possible to evaluate the degradation in the samples as a function of temperature, but it should be kept in mind that very high temperatures cause damage that would never occur under normal conditions. The most well-known example given by researchers who claim that high temperature experiments are not realistic is *boiled eggs*. No matter how long it stays at room temperature, an egg can never be "cooked", but it undergoes an irreversible transformation in boiling water at 100°C in as little as five minutes (Artioli, 2010). If it is necessary to learn from this situation, it should be evaluated by which mechanism the method we apply damages the stone and whether the temperature is above a threshold value such as the activation energy, and therefore whether it enables reactions that cannot occur under normal conditions.

Although it is common to observe the effect of a single factor at the laboratory scale, the samples are never under a single effect under real conditions. In normal conditions, decomposition factors such as moisture, water, salt are also added to the temperature effect. Therefore, although rare, extensive studies including these effects are encountered in literature studies as can be found in Section 3.2.5.

On the other hand, the behaviour of adjacent materials used against temperature can also accelerate the degradation with temperature (Steiger vd., 2011). For this reason, one of the factors to be evaluated in the selection of the material used during the restoration should be thermal properties (especially the expansion coefficient).

There are standards prepared for accelerated temperature tests, both in the industrial field and in the cultural heritage such as BS 14066:2013 *Natural stone test methods - Determination of resistance to ageing by thermal shock* or BS EN

16140:2011 *Determination of sensitivity to changes in appearance produced by thermal cycles.* The establishment of these standards is of great importance for conservation scientists to understand the properties of the structures they are interested in.

In summary, accelerated temperature cycles (TS) are one of the basic techniques frequently applied in the literature. The most frequently changed parameters are temperature, application time, cycle amounts and whether there is a water bath. Depending on the purpose of the study, different mechanical or physical analysis methods are applied. Since the chemical structure does not change generally, chemical analysis is not used. In recent years, especially with the widespread use of polymeric treatments, there are also examples where these products are put into thermal tests.

Although there are standards for tests based on thermal cycles, there is no method agreed upon by the researchers, and there are very few studies deals with application of tests. For this reason, within the scope of this thesis, different parameters of thermal cycles were examined simultaneously at different levels and suggestions were made for the development of tests.

3.2.2 Salt Tests

The damage caused by salt to porous structures, together with its mechanisms, is described in Chapter 2. In this section, aging studies using salt tests will be included.

Accelerated salt crystallization tests are tests performed in the laboratory in extreme conditions, usually by immerse all or part of the stones in salt solutions with higher than normal concentrations in order to simulate and accelerate salt damage that occurs under normal conditions. These tests are used to determine the stability of stones used in buildings and the damage caused by the presence of salt. The tests are generally low-cost, technically simple, and reliable because they give results similar to natural salt damage mechanisms (Zooli, 2020). As seen in Figure 3.1, salt tests constitute the largest proportion of accelerated aging tests on stones (Alves, 2020).

In Figure 3.2, a summary of the characteristics of the salt crystallization process, the influencing factors and the resulting damage types is given (Doehne, 2002). As can be seen in the figure, there are many parameters that affect the tests. Of these, substrate properties are not usually a selection factor, but before starting the tests, determining the physical properties of the substrate is of great importance for the correct interpretation of the damage mechanism. Solution properties; except for the case that it belongs to a structure for which damage assessment is attempted, it is generally at the initiative of the researchers in scientific studies. The most important properties regarding solution and salt are the type and concentration of the salt (or salts) used. The most important parameter regarding environmental conditions is the humidity and ventilation of the environment where the test is performed.

At the end of the tests, different damage mechanisms can be observed depending on the process. Damage may occur with mechanisms such as efflorescence, subflorescence and etc, which are explained in detail in Chapter 2 and shown in Figure 3.2.

Salt tests performed under laboratory conditions is much more easily observable and much more damaging than thermal tests. In Figure 3.3, the visuals of the tests where the parameters were changed at different levels are presented (Doehne, 2002). The tests were carried out by partial immersion method using limestone substrate and sodium sulphate solutions.

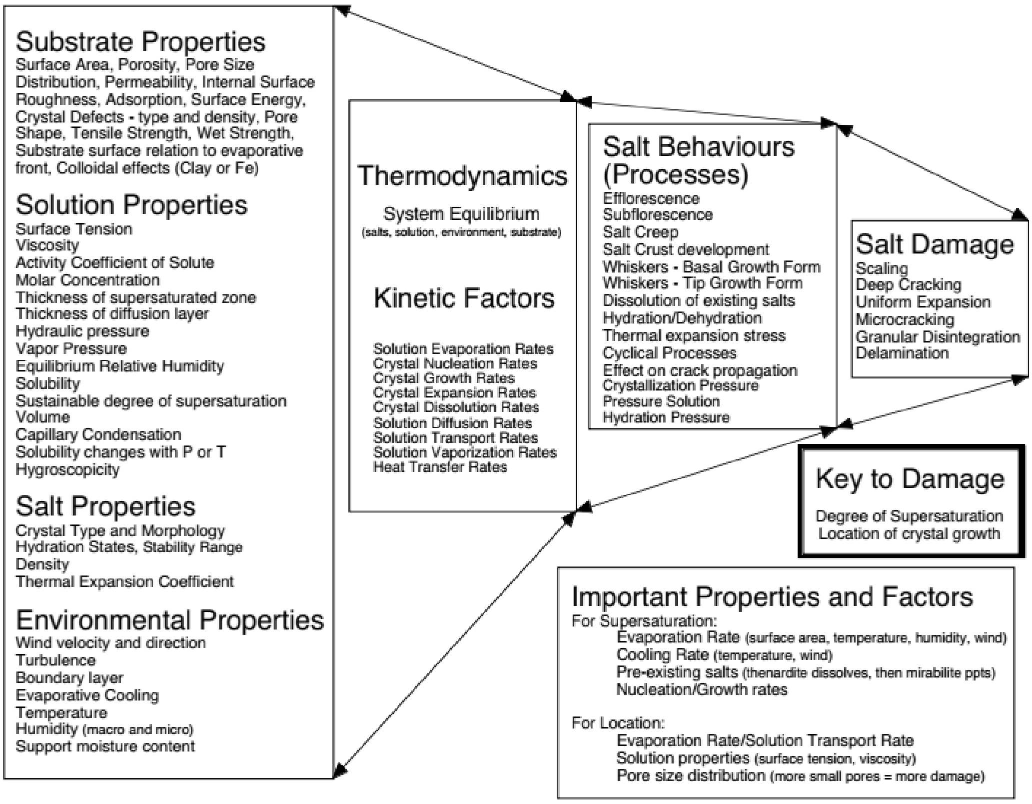

Figure 3.2 Diagram of properties, factors and behaviours in the salt crystallization process (Doehne, 2002)

Choice of the salt solution is highly dependant on the nature of the stone. However, Na_2SO_4 solution is one of the most popular ones, because it creates a volume increase of 300% during transformation of Na_2SO_4 to $Na_2SO_4.10H_2O$ (Price & Brimblecombe, 1994). This value is about 173% for $MgSO_4.H_2O$-$MgSO_4.7H_2O$ couple (Rothert vd., 2007) and NaCl does not have a hydrated form because of its molecular structure. Therefore, easiest way to simulate and accelerate salt damage is to use salts like Na_2SO_4 which have higher hydration expansion ratios. It is also possible to see the results of SOx effect on the stone, which is quite important due to atmospheric pollution, by use of sulphate-included solution.

On the other hand, actual salt damage in the field is not always based on sodium sulphate. Therefore, the damage caused by other salts (and salt mixtures) should also be examined. When the literature studies are investigated, it can be seen that most of the researches were carried out with solutions containing sodium sulphate (Benavente, 2001; Benavente vd., 2007; Diaz Gonçalves & Brito, 2014; Flatt, 2002; A. S. Goudie, 1999; López-Arce vd., 2010; Lopez-Arce & Doehne, t.y.; Molina vd., 2018; Ordóñez vd., 1997; A.B. Yavuz & Topal, 2007; Ali Bahadır Yavuz & Topal, 2016) and there is a literature gap for other salts. The most used salt solution after sodium sulphate is NaCl baths designed to examine the effect of sea salt (Aly vd., 2015; Van vd., 2007) Some of the studies are based on comparing different salts separately or using them as a mixture (Diaz Gonçalves & Brito, 2014; El-Gohary, t.y.; La Iglesia vd., 1997; McCabe vd., 2007; Rodriguez-Navarro & Doehne, 1999; Williams & Robinson, 1981).

As in thermal tests, sample sizes and geometric shapes may differ in salt tests. The frequency of analysis also varies. The main features analysed at the end of salt tests are density, color change, porosity, ESEM, microscopic imaging, surface roughness, UPV, weight, water absorption, MIP and XRD. XRD is used to observe the change of the chemical structure, weight and UPV to understand how much salt enters the structure, surface roughness, ESEM, color change to observe the change of the surface, and MIP to examine the state of pores. In addition, measurements such as modulus of elasticity or compressive strength are made to determine the mechanical weakening caused by salt in the structure.

There are standards developed for salt tests as well as thermal tests such as; EN 12370:2020 - *Natural stone test methods - Determination of resistance to salt crystallisation*, BS EN 14147 *Natural stone test methods -Determination of resistance to ageing by salt mist,* RILEM 25-PEM (1980) and ASTM D5240/5240M 20- *Standard Test Method for Evaluation of the Durability of Rock for Erosion Control Using Sodium Sulfate or Magnesium Sulfate.* In addition, the "271-ASC: Accelerated laboratory test for the assessment of the durability of materials with respect to salt crystallization" was established in 2016 within RILEM (International Union of Laboratories and Experts in Construction Materials, Systems and Structures) and there are studies to prepare a comprehensive standard by this committee.

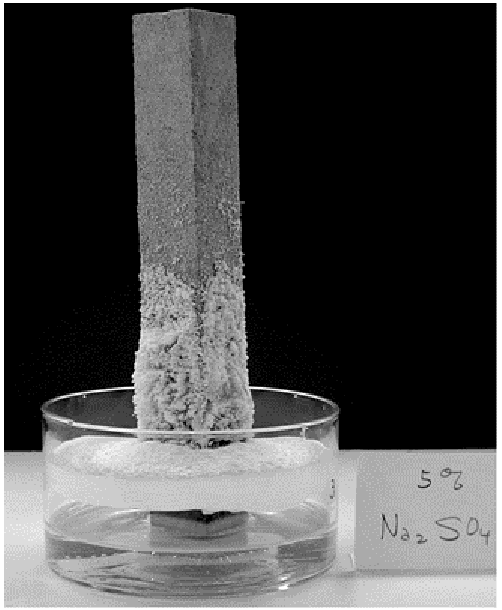	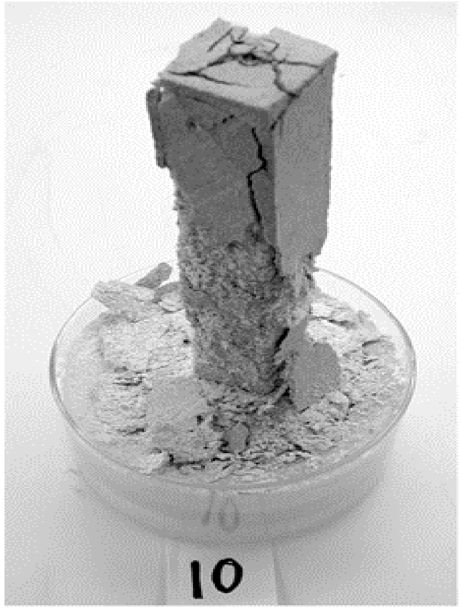	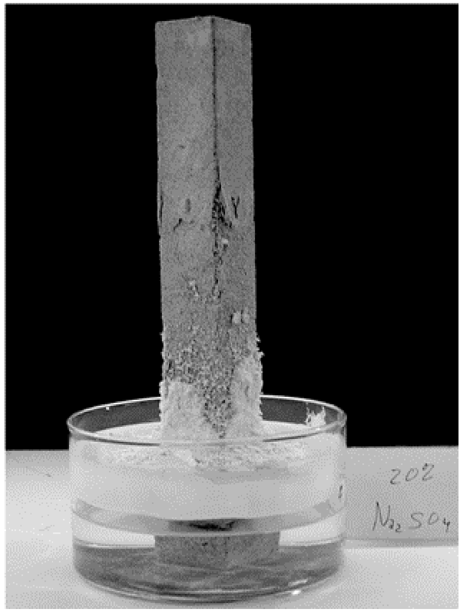	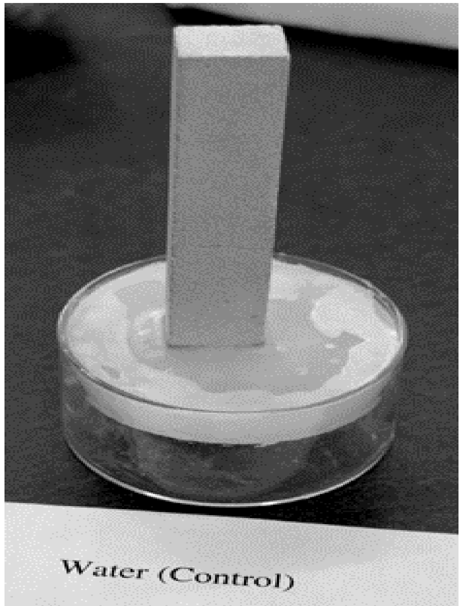
Bath limestone block after exposure to 5% solution of sodium sulphate in high air exchange environment (10x/hr) for two weeks. Note substantial efflorescence.	Bath limestone block after exposure to 15% solution of sodium sulphate in high air exchange environment (10x/hr) for four weeks. Note extensive contour scaling	Bath limestone block after exposure to 20% solution of sodium sulphate in high air exchange environment (10x/hr) for two weeks. Note less efflorescence and greater damage due to subsurface crystallization.	Bath limestone block exposed to water (control). Note no loss of stone surface

Figure 3.3 Visual examples of salt crystallization experiments (Doehne, 2002)

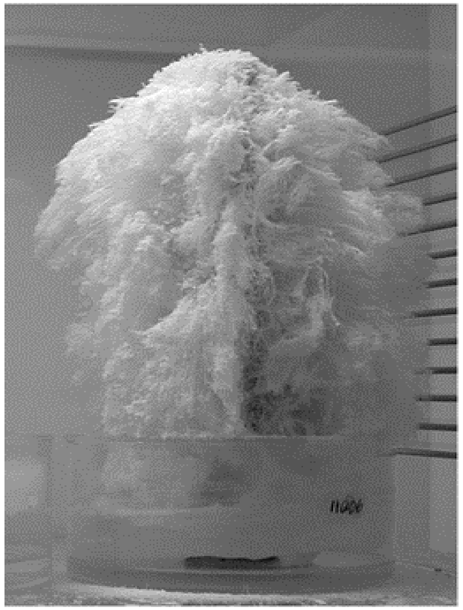			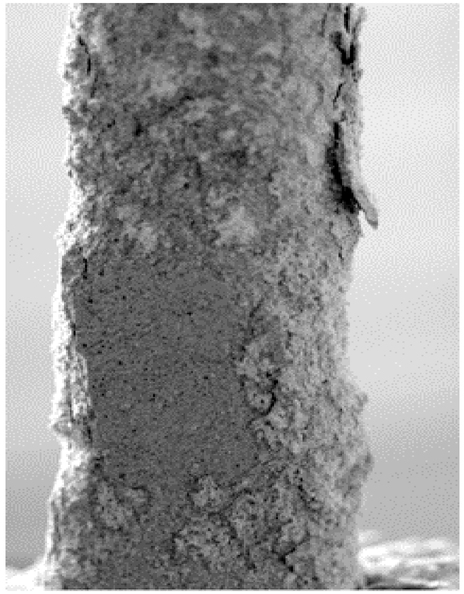
Bath limestone block after exposure to 20% solution of sodium sulphate in low air exchange environment, 3 months. Note extensive efflorescence of mirabilite	Opposite side of Bath limestone block after exposure to 20% solution of sodium sulphate in high air exchange environment (10x/hr). Note pile of scales at base of sample	Bath limestone after exposure to 20% solution of sodium sulphate in high air exchange environment (10x/hr), 3 months. Note contour scaling. Note scales at base.	Surface detail of Bath limestone block after exposure to 20% solution of sodium sulphate. Note partially attached contour scales (spall fragments).

Figure 3.3 Visual examples of salt crystallization experiments (Doehne, 2002) (ctd)

3.2.3 Freeze – Thaw Tests

Freeze-thaw tests are one of the oldest methods used when examining the weathering of stones. It is attributed to De Thury in 1928, the first recorded known to have been carried out in the laboratory (Martínez-Martínez vd., 2013). As seen in Figure 3.1, it is still the most applied accelerated aging test in the literature after salt crystallization tests.

The changes occurring in the structure by freezing-thawing are explained in detail in Section 2.

The basic approach in accelerated freeze-thaw tests is based on the principle of cooling the stone to a certain temperature (usually between -5°C and -30°C and mostly at -20°C) in a controlled environment and then thawing by submerging it in a room temperature (usually 20°C) water bath (Akkurt vd., 2008; Altindag vd., 2004; Ghobadi vd., 2016; Ghobadi & Torabi-Kaveh, 2014; Karaca vd., 2010). These cycles are used to simulate the changes in stones in cold regions where daily or seasonal temperature difference is high. Unlike thermal and salt tests, the temperatures tested are not kept at levels that stones would not normally be exposed to. However, the "acceleration" factor is based on the principle of repeated cycles in short periods of time and accelerating the thawing by putting it in water.

Sample shapes in freeze-thaw tests can be cubic (Amirkiyaei vd., 2020; Karaca vd., 2010), cylindrical (Hu vd., 2019) or rectangular prism. Sample sizes also vary. Although different types of stones have been investigated in the literature, studies are generally made for highly porous stones (Bakis, 2019; Ghobadi vd., 2016; Ghobadi & Torabi-Kaveh, 2014; Karaca vd., 2010).

During the cycles, the water freezes between the micro pores of the stone, causing an increase in volume of approximately 9%. This expansion causes the formation of tensile stress points and damage to the micropores. In soluble rocks, this situation is even more damaging, because during thawing, the water filled into the micro cracks formed in the previous step thaws some of the rock and causes the pores to grow. In this case, the mechanism of damage occurs both mechanically and by material loss (Ghobadi & Torabi-Kaveh, 2014).

When the literature studies were examined, it has seen that freeze-thaw tests caused changes in strength, compressibility, porosity, pore size distribution, permeability and the mineral content (Ghobadi vd., 2016). For the determination of physical properties, density (Karaca vd., 2010; Mutlutürk vd., 2004), color (Garcia-Talegon vd., 1998; Ozcelik vd., 2012, 2012; Uğur & Toklu, 2020), porosity (Altindag vd., 2006; Ghobadi vd., 2016; Ghobadi & Torabi-Kaveh, 2014; Karaca vd., 2010; H. Yavuz vd., 2006; Huseyin Yavuz, 2011), weight loss (Altindag vd., 2006; Ghobadi & Torabi-Kaveh, 2014; Karaca vd., 2010; Huseyin Yavuz, 2011) volume loss (Martínez-Martínez vd., 2013; H. Yavuz vd., 2006) analyses are used. For the determination of mechanical properties, point load index (Altindag vd., 2004; Ghobadi & Torabi-Kaveh, 2014; Topal & Sözmen, 2003; Uğur & Toklu, 2020), Brazilian tensile strength (Altindag vd., 2004, 2006; Ghobadi & Torabi-Kaveh, 2014), UPV (Akkurt vd., 2008; Altindag vd., 2004, 2006; Amirkiyaei vd., 2020; Ghobadi vd., 2016; Martínez-Martínez vd., 2013; Mutlutürk vd., 2004; Uğur & Toklu, 2020; H. Yavuz vd., 2006, s. 200), uniaxial compressive strength (Ghobadi vd., 2016; Karaca vd., 2010), bending strength (Altindag vd., 2006) are used. Finally, mineralogical analysis (Ghobadi vd., 2016; Topal & Sözmen, 2003, s. 200) is used to observe changes in chemical properties.

Freeze-thaw tests are mostly applied for the stones from the regions with high day-night or seasonal temperature differences. For this reason, most of the studied samples are carried out in areas where continental climatic conditions are dominant or in the northern regions. In addition, salt damage comes to the fore in places near the coast and where more temperate climatic conditions prevail.

There are also existing standards for freeze-thaw tests as in salt and thermal tests such as EN 12371 - *Natural Stone tests methods: determination of frost resistance.*

Figure 3.4 shows the samples broken at the end of 150 F-T cycles (Tan vd., 2011). The fracture of the samples in different axes may be a result of the bedding or the previous damage in their structures.

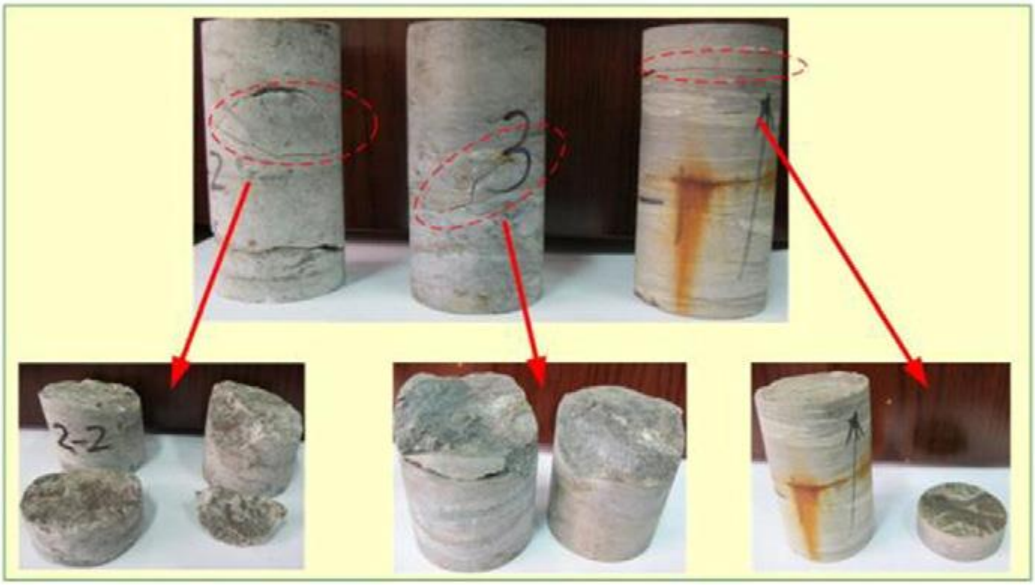

Figure 3.4 The macroscopic damage process of biotite granite under 150 F-T cycle between +40°C and - 40°C (Tan vd., 2011)

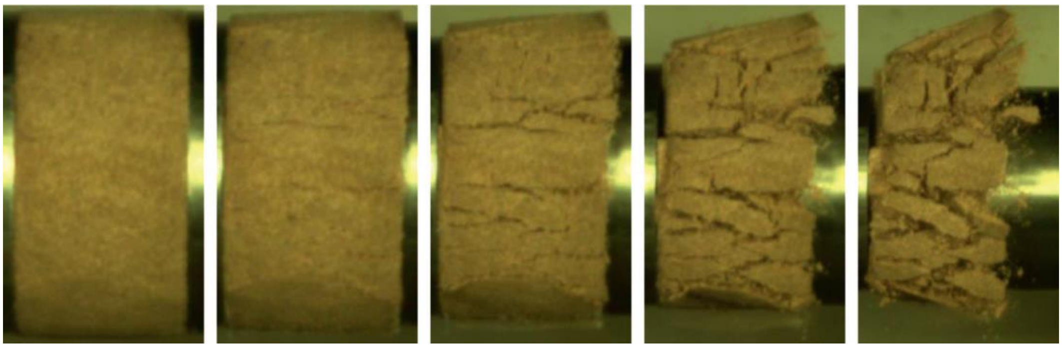

Figure 3.5 The macroscopic damage process of yellow sandstone under F-T cycle at - 30°C. (Hu,2019)

Figure 3.5 shows a visual of a study in which one cycle was completed by keeping it for 6 hours at -30°C and 2 hours in water at 25°C and a total of 8 cycles were made. It appears to be subjected to mechanical degradation.

3.2.4 Other Ageing Tests

Other than freeze-thaw, salt crystallization and thermal effect, there are some other tests used to determine accelerated ageing properties of stones, by using chemical agents, UV effect or biological colonization. Although these tests are not common as the first mentioned they still supply important data and needs to be investigated more.

- **Pollution**

  Pollution tests are usually carried to undercover the mechanism of black crust or the effect of acid rains on stones (Bernal & Bello, 2003; Camuffo vd., 1983; Jaynes & Cooke, 1987). Concentrated H_2SO_3 acid solution is used to accelerate SO_2 effect (Olaru vd., 2010).
- **UV**

  UV tests can be used to determine the durability of consolidants (especially polymeric treatments) (Bracci & Melo, 2003; Zornoza-Indart vd., 2017), understand the effect of solar radiation on heritage stones (Sáez-Pérez & Rodríguez-Gordillo, 2008), as a pre-ageing step for further analysis (Wasserman, 2004) or just simply to understand the effect of UV on stone surfaces (Careddu & Marras, 2013).
- **Biological Colonization**

  Rather than being used as an accelerating method, biological colonization studies usually used for observing the organism growth the stones in real environments (Briones & Viles, 2018; ElBaghdady vd., 2019), determining the effectiveness of biocides (Zarzuela vd., 2018) or inspecting the possible negative effect of other types of treatments (rather than biocides) on colonization (Barriuso vd., 2017).

3.2.5 Comparative Studies

In some literature studies, comparisons can be made by applying different accelerated aging tests simultaneously on the same sample or treatment. In this case, differences in observed properties may occur depending on the nature of the test. This result shows that the “old” material is the result of a more dynamic process that can walk through different mechanisms, rather than a single-choice deformation process depending on time.

Figure 3.6 shows the results of freeze-thaw and thermal shock tests performed on the same sample. When these results are examined, for example, while a decrease is observed in thermal shock tests for apparent porosity, an increase in freeze-thaw results is observed. This is because at the end of freeze-thaw intervals, the number and aperture of microfractures increases. During the thermal shock processes, heating produced expansion of minerals that were not able to recover quickly when cooled, resulting in an increase in the amount and aperture of microfractures. However, in the Schmidt test results, it was seen that the results were decreased in both tests (Huseyin Yavuz, 2011, s. 20).

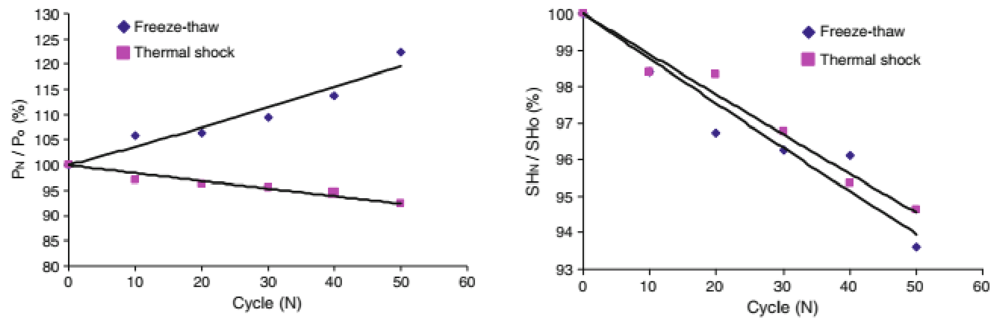

Figure 3.6 (Left) Porosity change by cycle. (Right) Schmidt hardness change by cycle.

3.3 Mathematical Modelling and Durability Indices

One goal of accelerated aging studies is to investigate whether a mathematical expression of aging can be found. For this purpose, studies are conducted that reveal the relationship of certain properties to cycle numbers and whether this correlates with the natural aging process. For example, Table 3.2 shows durability indicators compiled by (Viles, 2013) for salt crystallization tests.

Table 3.2 Durability indicators for salt crystallization tests (Viles, 2013)

Portland Stone durability predictor	Durability predictor = (100 × SC) = (0.5 × M) SC, saturation coefficient M, microporosity as per cent of total porosity
Durability index	DI = wet strength/dry strength (based on modulus of rupture, uniaxial compressive strength of tensile strength)
Static rock durability index	RDI = Is – 0.1(SST + 5WA)]SGsd Is, average dry and saturated point load index SST, MgSO4 soundness test value SWA, water absorption SGssd, saturated and surface dried relative density
Index of rock durability	IRD = (R/Rt) (N + 2a) R, final compressive strength Rt = 1MPa N, porosity a, mantissa of swelling strain
Durability factor	D = Cs2P Cs, saturation coefficient P, total porosity
Weathering susceptibility index	WSI = Pc/St Pc, pore size distribution and pore radius St, tensile strength
Limestone durability estimator	LDI = (P Sc)0.5 P, porosity Sc, saturation coefficient

Table 3.2 Durability indicators for salt crystallization tests (Viles, 2013) (ctd)

Durability dimensional estimator	DDE = $\Sigma[Dv(ri)/ri]$ Dv, pore-size distribution ri, pore size Pconc, connected porosity
Petrophysical durability estimator	PDE = X/σ X, pore structure characteristics σ, material strength
Alteration index estimator	AI = $\ln[100C/(E s)]$ C, capillary coefficient E, evaporation coefficient σ, tensile strength
Alteration velocity estimator	AV = Vp Vp, ultrasonic pulse velocity
Salt susceptibility index	SSI = $(Ipc + Ipm0.1)(Pm5/Pc)$ Ipc, index of total connected porosity Ipm0.1, index of micropores $<0.1\mu m$ Pm5, microporosity of pores $<5\mu m$ Pc, total connected porosity

However, as stated in the same publication, such equivalents, while appealing for their simplicity, are lacking in showing the simultaneous damage of different effects.

In addition to aging balances established for different (especially mechanical) properties, there are also reaction balances on which the chemical deterioration of some rocks is based. Various information on chemical aging can be obtained as a result of analyzes such as XRD and AAS performed on samples taken from rocks of known species. Table 3.3 shows the chemical aging indices compilation made by (Topal & Sözmen, 2003). According to this table, it can be said that information about aging can be obtained especially by examining the degradation processes of oxides.

Table 3.3 A summary of chemical weathering indices (Topal & Sözmen, 2003)

Weathering potential index	$[K_2O + Na_2O + CaO\ \ H_2O+]\ 100/$
(WPI) (mole ratio)	$[SiO_2 + Al_2O_3 + Fe_2O_3 + TiO_2 + CaO + MgO + Na_2O + K_2O]$
Product index (PI) (mole ratio)	$(SiO_2)\ 100/(SiO_2 + TiO_2 + Fe_2O_3 + Al_2O_3)$
Ruxton's ratio (R) (mole ratio)	SiO_2/Al_2O_3
Parker index (P) (mole ratio)	$[(2Na_2O/0.35)+(MgO/0.9) + 2K_2O/0.25)+(CaO/0.7)]\ 100$
Vogt ratio (V) (mole ratio)	$(Al_2O_3 + K_2O)/(MgO + CaO + Na_2O)$
Modified weathering potential index (MWPI) (mole ratio)	$[Na_2O + K_2O + CaO + MgO]\ \ 100/$ $[Na_2O + K_2O + CaO + MgO +$ $SiO_2 + Al_2O_3 + Fe_2O_3]$
Chemical index of alteration (CIA) (mole ratio)	$[Al_2O_3/(Al_2O_3 + CaO + Na_2O + K_2O)]\ \ 100$
Lixiviation index (b) (mole ratio)	$[(K_2O + Na_2O)/Al_2O_3]$ weathered / $\{[(K_2O + Na_2O)/Al_2O_3]$ fresh + $(CaO/MgO)\}$
Alumina to calcium– sodium oxide ratio (ACN) (mole ratio)	$[Al_2O_3/(Al_2O_3 + CaO + Na_2O)]\ \ 100$
Alumina to potassium– sodium oxide ratio (ALK) (mole ratio)	$[K_2O/(Na_2O + K_2O)]\ \ 100$
Loss on ignition (LoI)	H_2O+ content (in weight) of specimen heated to 900– 1000 jC
Mobiles index (Imob) (mole ratio)	$[(K_2O + Na_2O + CaO)$fresh $\ \ (K_2O + Na_2O + CaO)$weathered]/ $[(K_2O + Na_2O + CaO)$fresh]
Mobility index (MI)	(Rp Rwi)/(Rw Rpi) Rw = the percentage by weight of the stable constituent in the weathered product; Rp = the percentage by weight of the stable constituent in the parent rock; Rip= the percentage by weight of nonstable constituent i in the parent rock; Riw= the percentage by weight of the nonstable constituent i that remains in the weathered product

However, it is seen that different mechanisms are proposed by different authors for such indices, even for rocks of the same type. This shows that a certain consensus could not be reached in the literature. However, establishing such equivalences is important in terms of examining the chemical dimensions of damage mechanisms.

As shown in Section 3.2.5, not every accelerated test affect the properties in the same way, which emphasizes once again the necessity of determining the nature of the damage mechanisms during damage assessment and examination of the aging degree of the material. Therefore, durability indices are scientifically useful parameters that should always be carefully considered.

4
TECHNIQUES AND MATERIALS USED IN STONE CONSERVATION

Restoration and conservation of cultural heritage deals with preserving the historical sites, artefacts or objects. They may be overlapping in some fields but there are certain differences. While restoration often aims to return a building or object to its original condition, conservation focuses on preserving in its current state. Other fundamental difference between two is that, restoration may involve structural strengthening works, while conservation generally deals with items or buildings structurally sound.

There are various of different requirements to preserve a masonry building both in restoration and conservation. For example, restoration works, such as, architectural strengthening of the building, changing of structural elements, or adding support elements are under architects and civil engineers responsibility. On the other hand, strengthening the mechanical properties of the stone, application of repellents to eliminate the water absorption problem, cleaning and protecting against a salt problem are within the work area of conservation experts. In this thesis, restoration studies will be briefly mentioned and conservation methods (especially techniques based on chemical product development) will be examined in detail.

Approaching a structure in terms of conservation science can be compared to a physician approaching a patient medically. This analogy has been tried to be shown in the analogy established in Figure 4.1. According to the figure, firstly, the damage should be determined in the structure (examination), then a cleaning process should be applied (surgery) if necessary, other actions should be taken to remove the damage (treatment), the results of the applications should be examined (tests) and then measures should be taken to prevent damage (preventive medicine).

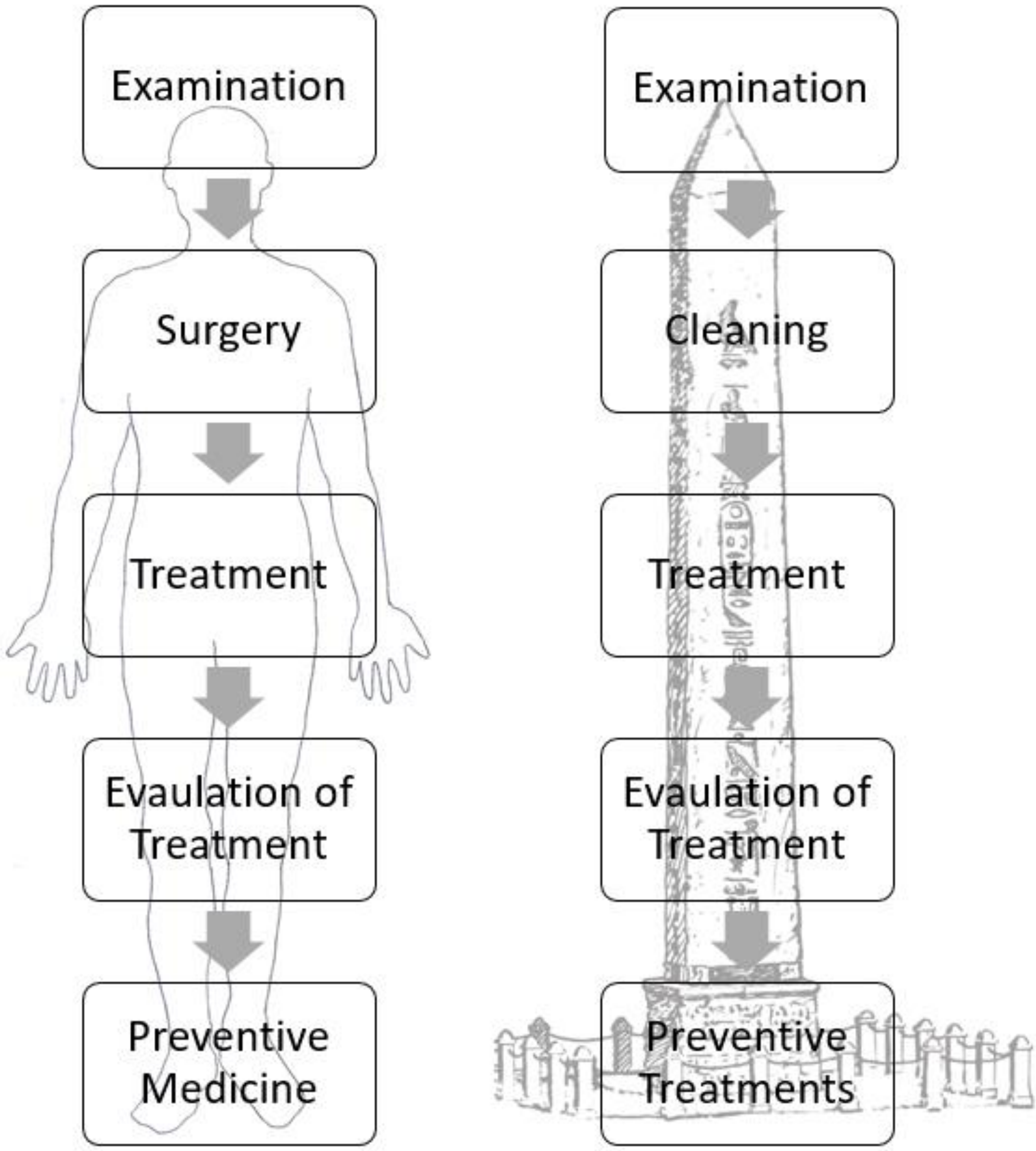

Figure 4.19 Analogy between medicine and conservation science

4.1 Damage Assessment

4.1.1 Evaluation the Soundness of Stone

There are certain applications for detecting damages in masonry structures. Structural problems are determined by restoration experts. In the conservation perspective, the features to be checked are as follows (Winkler, 1997).

- Geological information about the stone from which the building was created:

If possible determining the source-related properties such as, the type of stone, its quarry, mineral content, bedding condition etc.

- Investigation of Physical Damage

a. Cracks

b. Scaling and flaking by hygric action, frost or salts

c. Surface crumbling, detection of traces of efflorescent salts

d. Porosity

e. Ultrasound testing

f. Moisture testing

- Investigation of Chemical Damage

a. Change in color

b. Efflorescence

c. Quick chemical semiquantitative analyses

There are reports of various international organizations for the standardization of damage assessment. One of the most important of these organizations is ICOMOS (International Council on Monuments and Sites). According to the ICOMOS directive published in 2008, the weathering in stones can be classified as shown in Table 4.1. (Siegesmund & Snethlage, 2011)

Table 4.1 Stone degradation classification (ICOMOS-ISCS 2008) (Siegesmund & Snethlage, 2011)

ALTERATION – DAMAGE – DECAY – DEGRADATION – DETERIORATION – WEATHERING				
CRACK AND DEFORMATION	DETACHMENT	FEATURES INDUCED BY MATERIAL LOSS	DISCOLORATIO N AND DEPOSIT	BIOLOGICAL COLONISATIO N
CRACK	BLISTERING	ALVEOLIZATION	CRUST	LICHEN
(Fracture; Star Crack; Hair	BURSTING	(Coving)	(Black Crust; Salt Crust)	MOSS
Crack; Craquelé; Splitting)	DELAMINATION	EROSION	DEPOSIT	MOULD
DEFORMATION	DISINTEGRATIO N	(Differential Erosion; Loss of	DISCOLORATIO N	PLANTS
	(Crumbling; Granular	Components or of Matrix;	(Coloration, Bleaching, Moist	
	Disintegration like Powdering,	Rounding; Roughening)	Area; Staining)	
	Chalking, Sanding, Sugaring)	MECHANICAL DAMAGE	EFFLORESCENC E	
	FRAGMENTATI ON	(Impact Damage; Cut; Scratch;	ENCRUSTATION	
	(Splintering; Chipping)	Abrasion; Keying)	FILM	
	PEELING	MICROKARST	GLOSSY ASPECT	
	SCALING	MISSING PART	GRAFFITI	
	(Flaking; Contour Scaling)	(Gap)	PATINA	
		PERFORATION	SOILING	
		PITTING	SUBFLORESCEN CE	
See Figure 4.2	See Figure 4.3, 4.4	See Figure 4.5, 4.6	See Figure 4.7, 4.8	See Figure 4.9

Images of these types of degradation are presented in Figure 4.2 – 4.9. These damages can be briefly summarized as follows:

Deformation and Crack: "Deformation" refers to a change of shape without lack of consistency that causes a stone to bend, buckle, or twist. (Figure 4.2 a,b)

Specific fissures that are apparent to the naked eye that arise from the separating of one component from another are known as "cracks" (Figure 4.2 c,d). They have the potential to trigger detachment patterns such as bursting or fragmentation.

Detachment: The weathering forms that display disintegration of stone systems on a macroscopic and microscopic scale are classified as detachment. It may be seen in different forms.

Material Loss: It encompasses all descriptions of stone material losses. (Figure 4.5 and 4.6).

Discoloration and Deposit: It covers all forms characterizing a modification of stone color and deposit on the stone surface or near the stone surface (Figure 4.7 and 4.8).

Biological Damage: It relates to the occupation of the stone by bacteria, cyanobacteria, algae, fungi, and lichen, among other species (Figure 4.9). Other species, such as animals nesting on and in stone, may also cause biological harm.

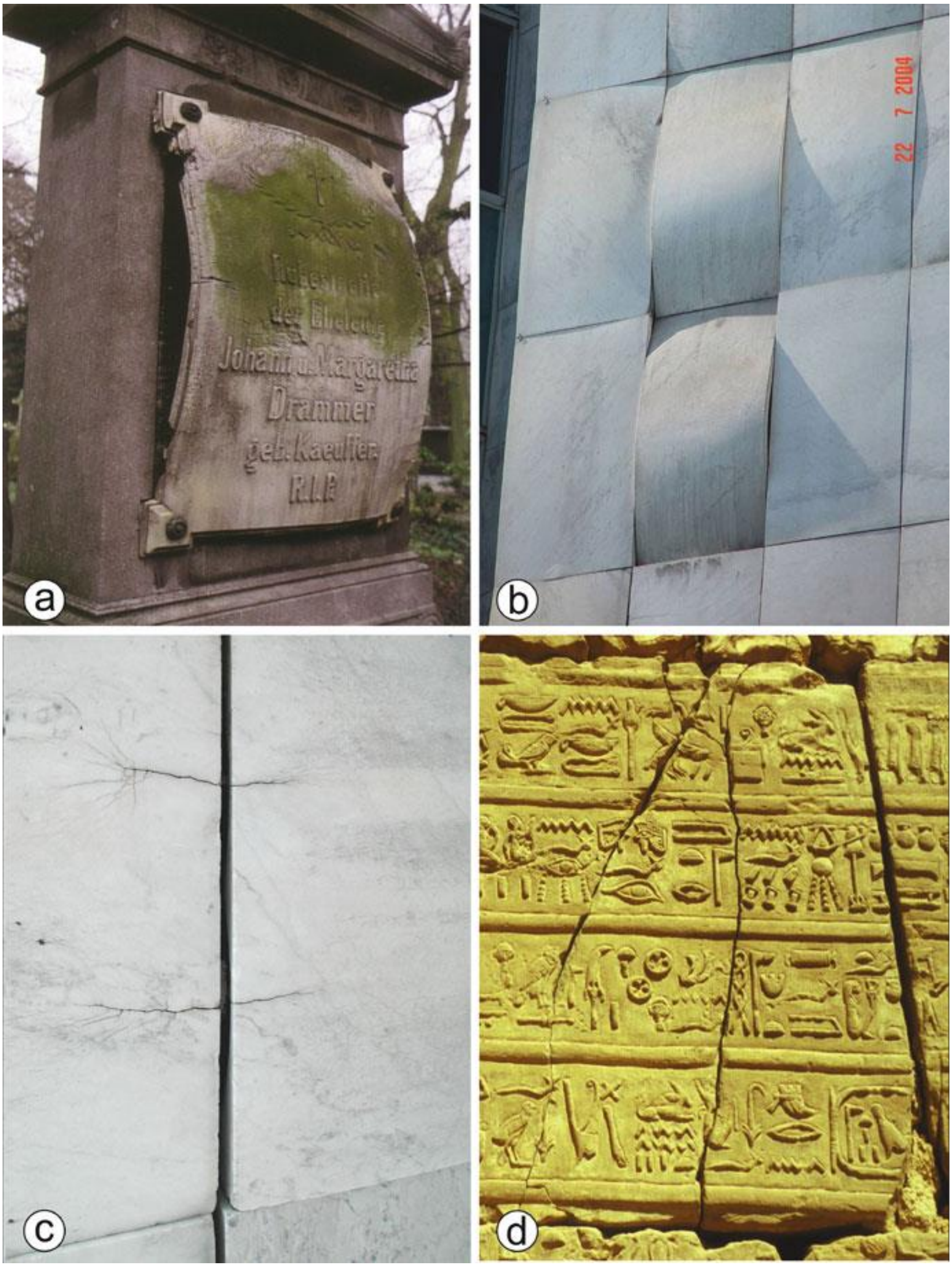

Figure 4.2 Deformation and crack: (**a**) marble bowing (Germany), (**b**) marble bowing (Croatia (**c**) iron corrosion related crack (Germany), and (**d**) crack (Egypt) (Siegesmund & Snethlage, 2011)

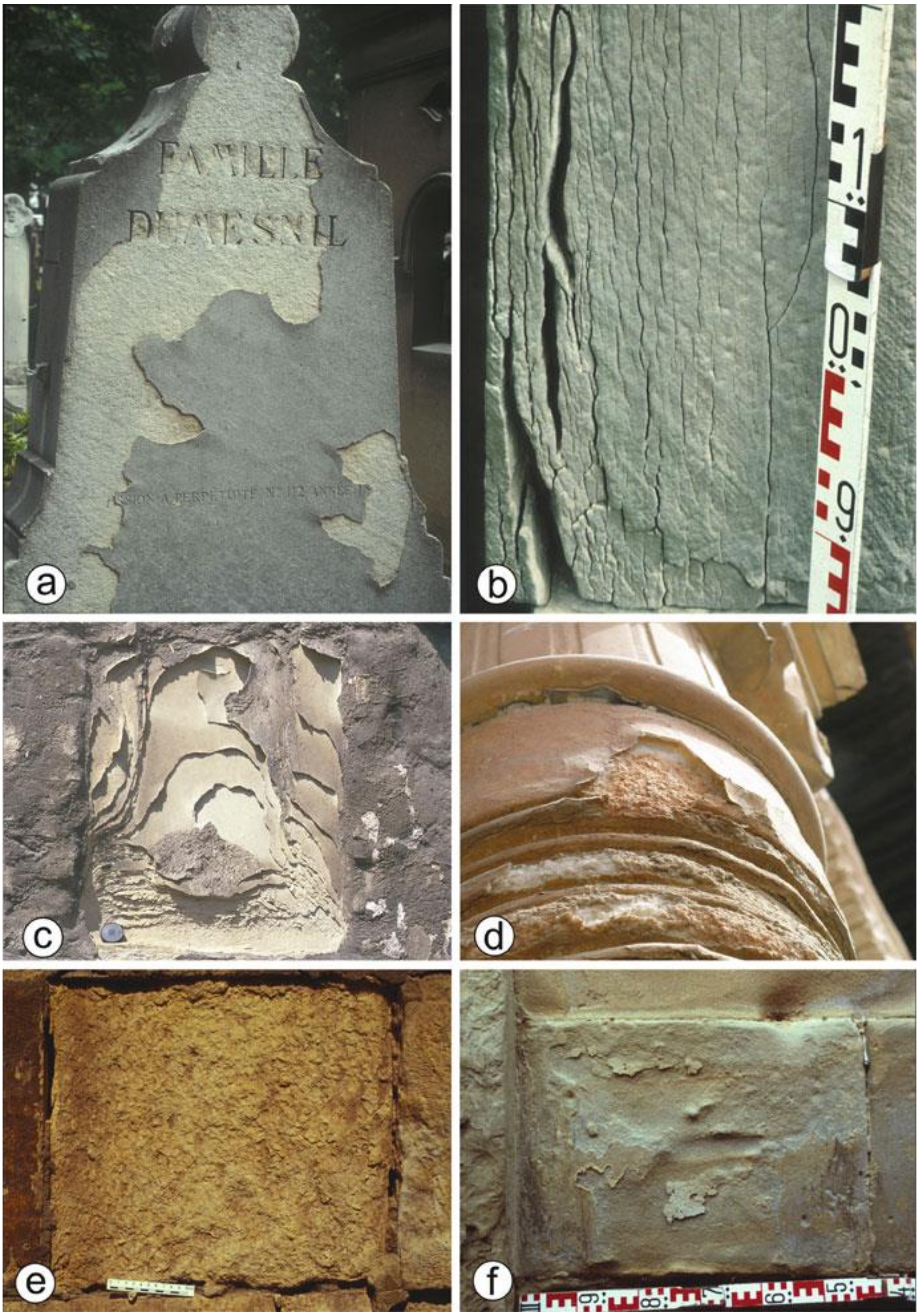

Figure 4.3 Detachment 1: (**a**) peeling on limestone (France), (**b**) delamination on sandstone (Germany), (**c**) exfoliation on sandstone (Germany) (**d**) granular disintegration in Alhambra (Spain), (**e**) multiple flaking on limestone, (Egypt), and (**f**) single flaking on sandstone, (Germany) (Siegesmund & Snethlage, 2011)

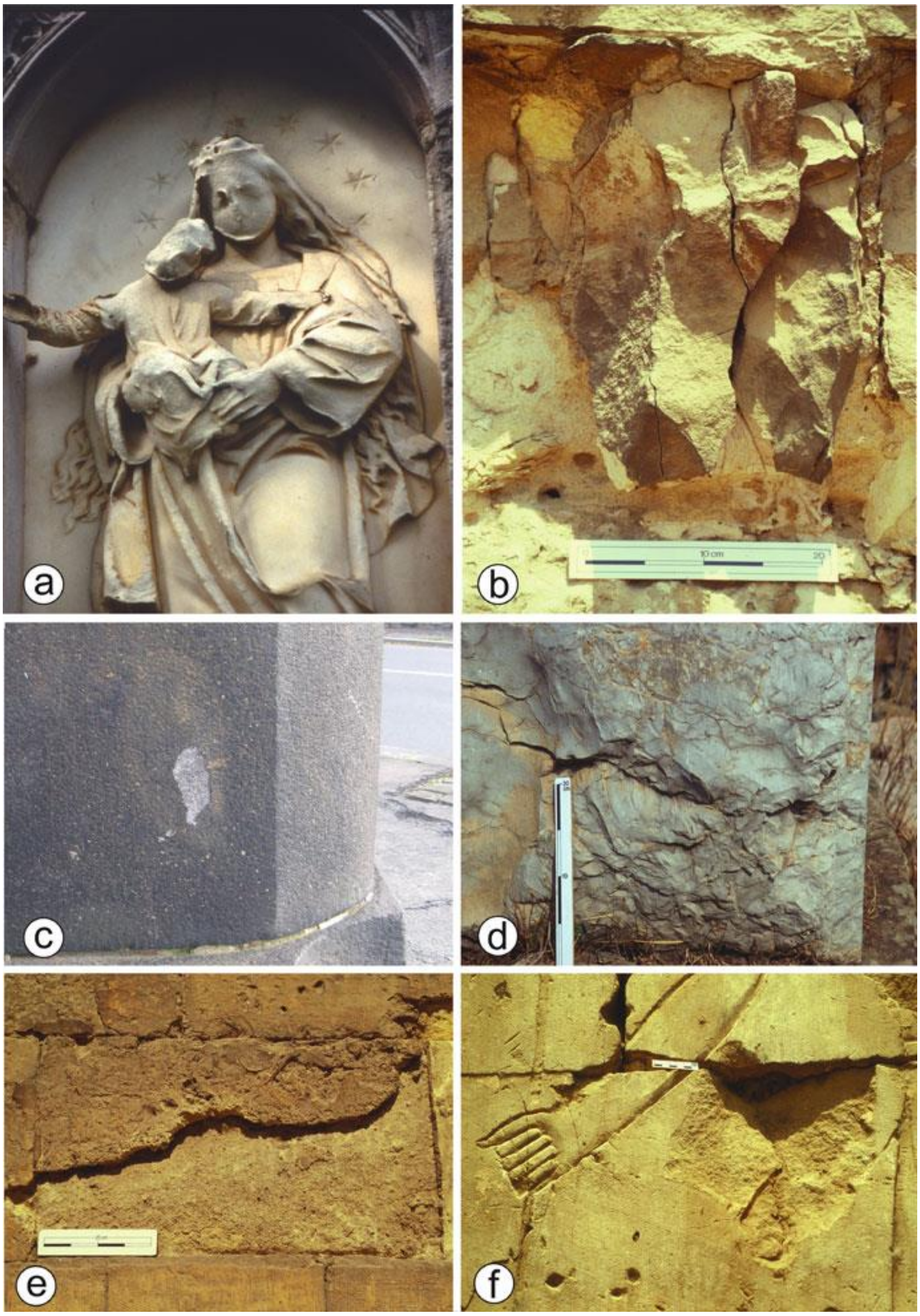

Figure 4.4 Detachment 2: (**a**) disintegration – marble sugaring (Germany), (**b**) disintegration – crumbling on limestone (Egypt), (**c**) blistering on granite, (Germany) (**d**) fragmentation - splintering on limestone(Greece), (**e**) contour scaling on limestone (Egypt), and (**f**) bursting on sandstone (Egypt) (Siegesmund & Snethlage, 2011)

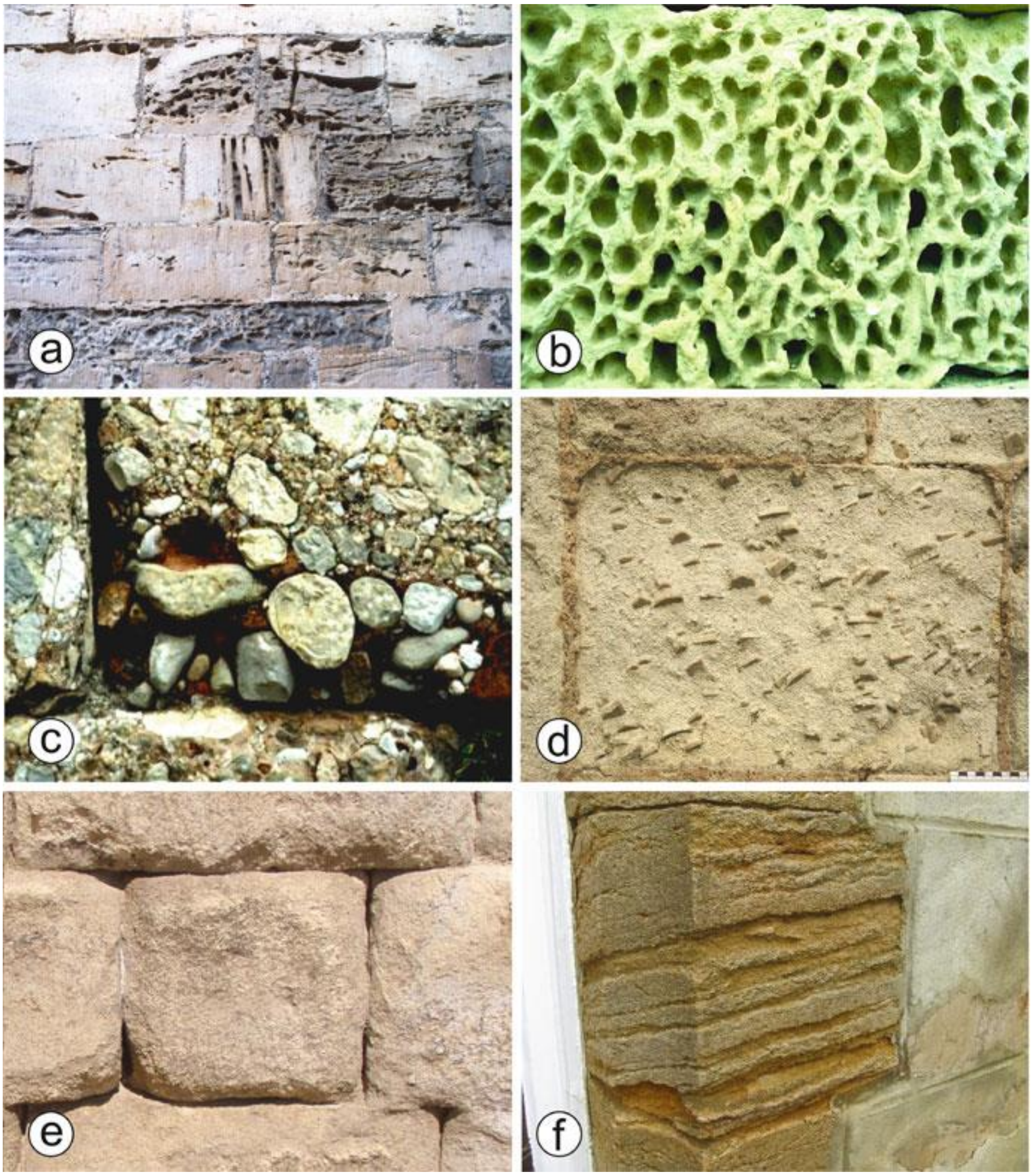

Figure 4.5 Material loss 1: (**a**) alveolization on sandstone (Denmark), (**b**) alveolization on limestone (Malta), (**c**) erosion (Spain), (**d**) erosion (Germany), (**e**) erosion (Germany), and (**f**) differential erosion on limestone (U.K.) (Siegesmund & Snethlage, 2011)

Figure 4.6 Material loss 2: (**a**) microkarst (Germany) (**b**) microkarst on limestone (Turkey), (**c**) pitting (Italy), (**d**) cut (Germany), (**e**) missing part (Budapest), and (**f**) mechanical damage on sandstone (Cambodia) (Siegesmund & Snethlage, 2011)

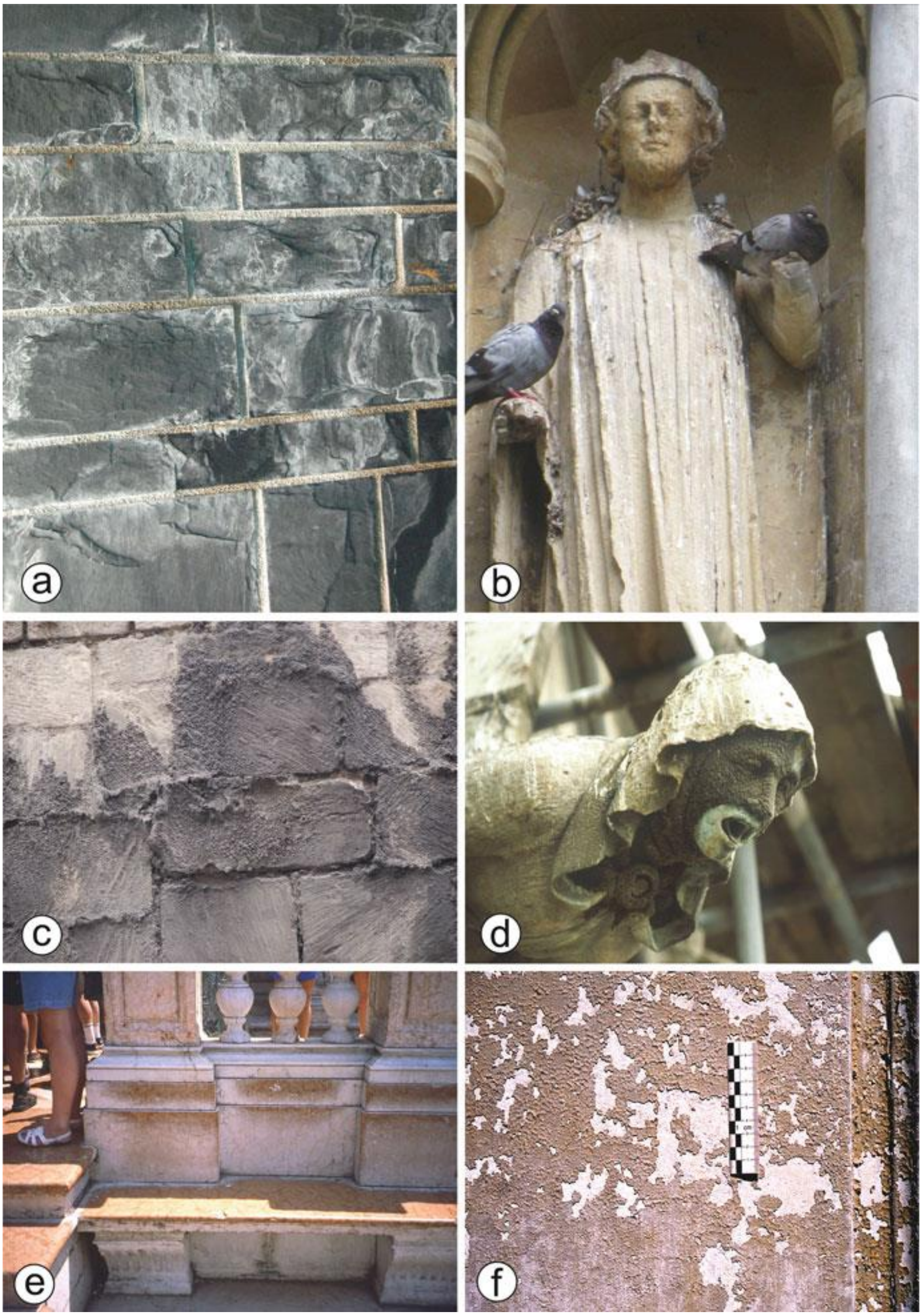

Figure 4.7 Discoloration and deposit 1: (**a**) encrustation on slate (Germany), (**b**) deposit of pigeon droppings (U.K.), (**c**) gypsum crust (Germany), (**d**) gypsum crust (Germany) (**e**) bleaching and glossy aspect (Italy), and (**f**) film: old oil paint on sandstone (Germany) (Siegesmund & Snethlage, 2011)

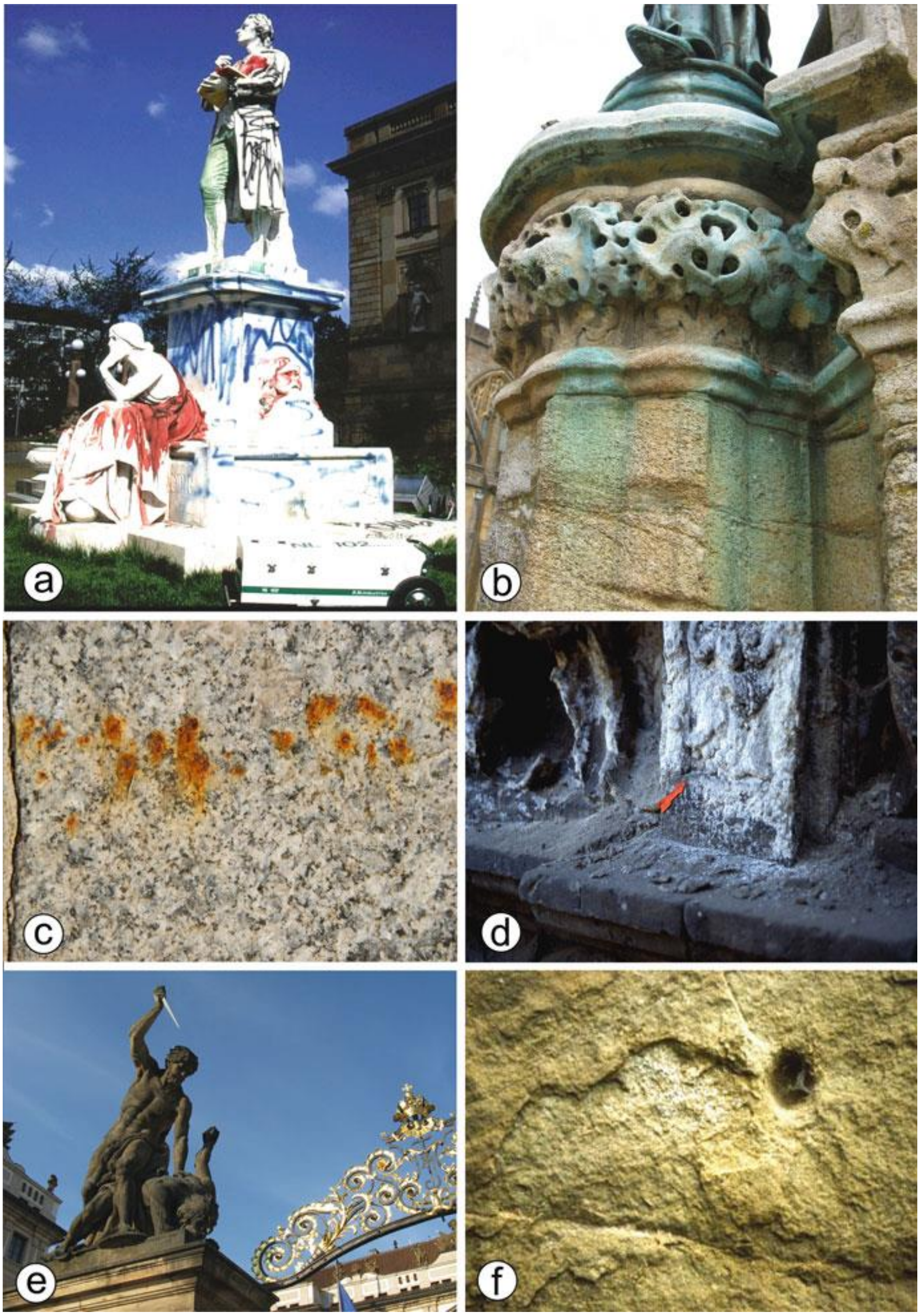

Figure 4.8 Discoloration and deposit 2: (**a**) graffiti on marble (Germany) (**b**) discoloration: staining on limestone (U.K.), (**c**) discoloration: staining (Germany) (**d**) salt efflorescence (Germany), (**e**) patina on sandstone (Czech Republic), and (**f**) subflorescence (Germany) (Siegesmund & Snethlage, 2011)

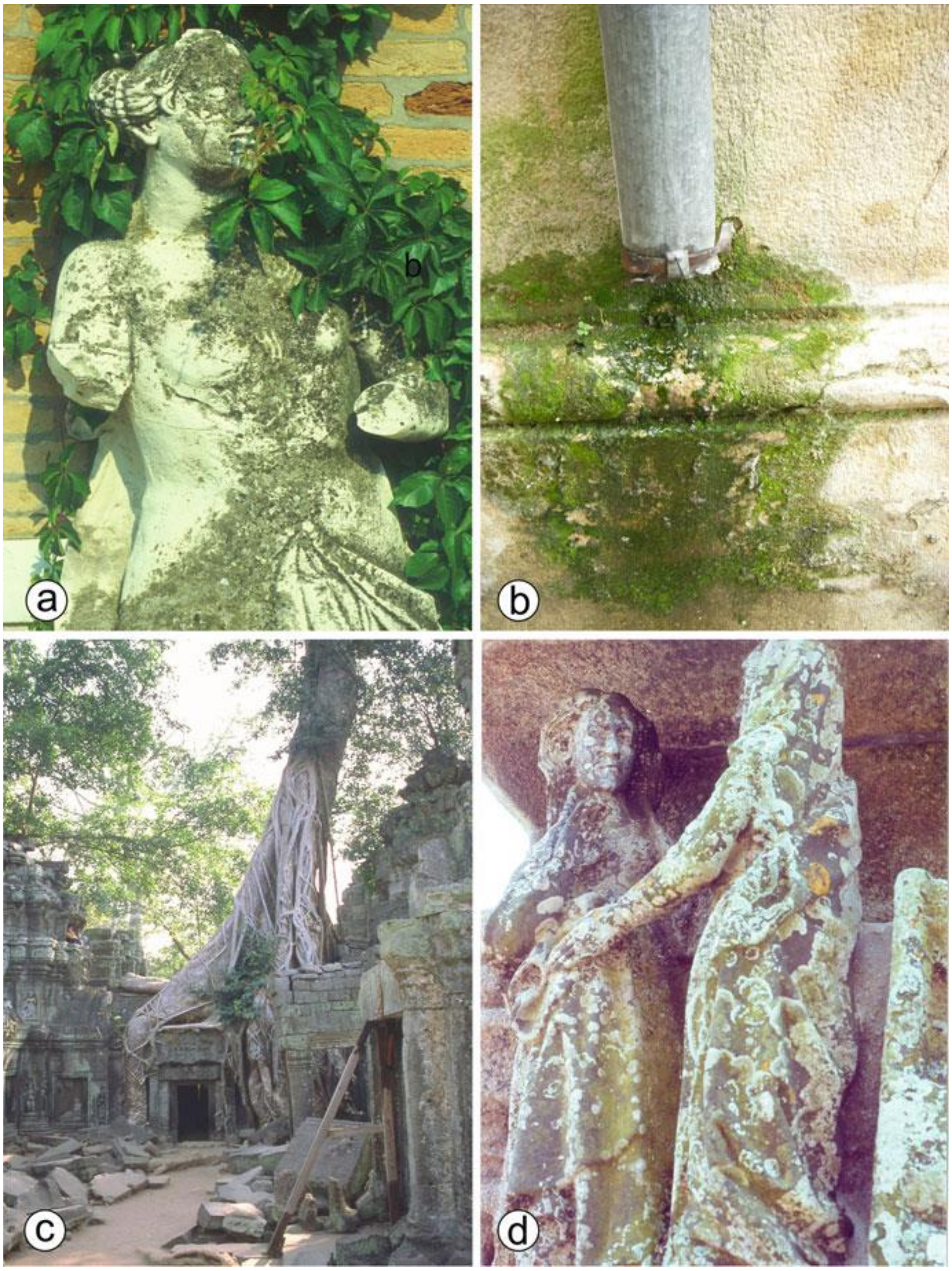

Figure 4.9 Biological damage: (**a**) Colonization of a statue with lichen, moss and higher plants , (**b**) development of biofilms, (**c**) secondary diameter growth of the roots of a fig tree (**d**) Lichen on granite (Siegesmund & Snethlage, 2011)

4.1.2 Mapping

In structures made of natural stones or works of art such as sculptures, the types of damage mentioned in the previous section can be found simultaneously. Or, different types of damage may have occurred in different parts of the same building. It is therefore recommended, if possible, to make a damage map of the structure after the damage status has been determined.

The mapping process can have several goals (Siegesmund & Snethlage, 2011):

• Recording the current state of the damage: It is important for scientific purposes or can be used as a reference for the starting point of conservation practice.

• Identifying more heavily damaged areas in the building and collecting the necessary information: With this information, more intensive applications can be made in different parts of the building. For example, theoretically, damage from salt and capillary rising water is known to occur at lower levels. With the information obtained through mapping, the level of the conservation practices can be determined.

• Determination of the size and depth of the damage: It is an important information set especially in terms of cost calculation.

Mapping work requires an intensive workforce and experienced staff. After photographing the building in detail, maps are created using various visual processing software. However, one of the most important issues here is to analyze the damages occurred correctly. Most of the time, various technical analyzes are used in addition to visual inspection.

When mapping, the types of stone used in the building, changed parts (if any), and the type and level of damage can be shown. Since this area is a relatively new field in conservation studies, standards for notation have not been developed. Figure 4.10 and Figure 4.11 shows damage maps of two different structures.

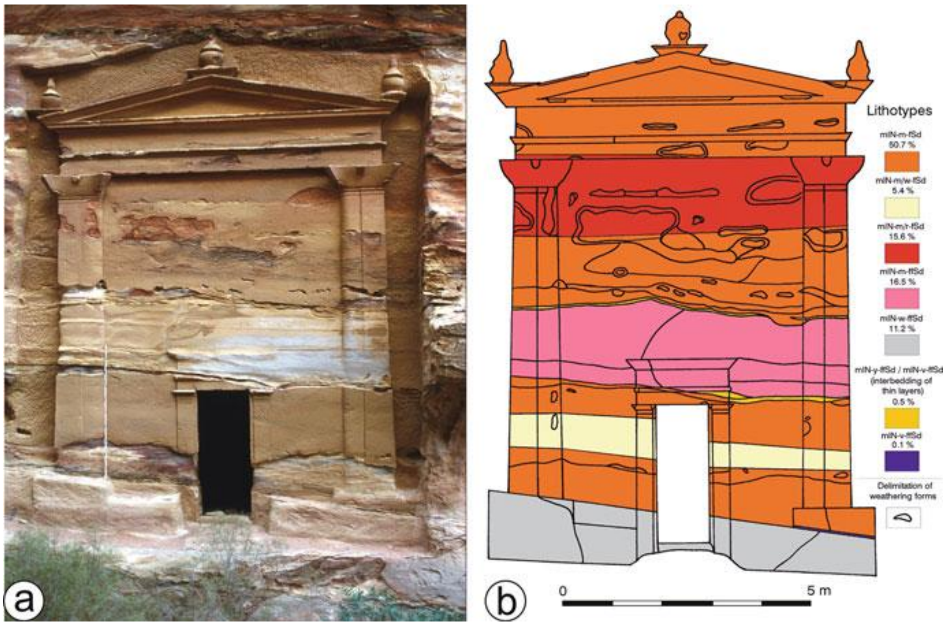

Figure 4.10 Lithological map of a tomb in Petra (Siegesmund & Snethlage, 2011)

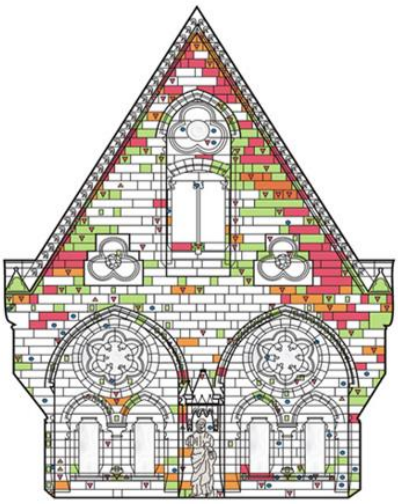

Object: Church St. Lucas Zwickau - Planitz	**Date:** Oct. 1995
Component: Westgable	**Scale:** 1:40

features	comment	color (feature dominant)	symbol (feature secondary)
without damage			
relief	advise to essential method: stabilisation		
flaking and scaling, weakly	advise to essential method: stabilisation after removing loose pieces		
flaking and scaling, strongly	advise to essential method: replacement or addition of stones		
mechanical break out and loss of stone, older additons	advise to essential method: after removing loose pieces addition of stones		

Figure 4.11 Lithological and damage map of St. Lukas Church, Germany

4.2 Cleaning

The cleaning process is the first conservation step after damage assessment. It can be done for several goals. The technical purpose of the cleaning process is to remove atmospheric or rain-based pollutants such as soot, grease and dust, or gypsum or other salts formed as a result of the chemical reaction between the original material and acidic pollutants. The aesthetic purpose of the process is removal of disfigurements, exposing the nature, colour, or specifics of structures or sculptures, and bringing a building's or sculpture's appearance together after it has been altered or restored (Siegesmund & Snethlage, 2011). For this reason, in the field, the cleaning process is made for both comprehensive protection applications, and also in periodic maintenance.

Although the cleaning process is included in the conservation process in almost all cases, the degree and method of cleaning varies widely. Although this situation has been tried to be standardized by objective procedures (Andrew vd., 1994; Werner, 1991; Young, 1993) there are still issues that are not agreed upon. For example, when determining the degree (or success) of cleaning, the color change that occurs after the process is taken into account. In some restoration implementations, as required by the legislation of the countries or the decisions of the boards, the stones that are clean enough to look as new as newly extracted from the quarry are targeted, while in some places, the effects of the aging of the building are not completely eliminated.

However, there are also standards such as "*BS 8221-1: 2012 Code of practice for cleaning and surface repair of buildings - Part 1: Cleaning of natural stone, brick, terracotta and concrete*." that can be used as a guide, especially when determining the measures to be taken and implementation methods.

As in the different conservation steps, there are various risks of damage in the cleaning process. The most important risks are the loss of original material (attention should be paid especially on surfaces with fine workmanship), crack formation (can occur when aggressive cleaning is applied to brittle stones), and accumulation of soluble salts (can occur after chemical cleaning methods) (Schnabel, 2014).

When the literature studies are examined, it is seen that there are also publications that argue that the patina formed over time protects the stone, so cleaning procedures should be eliminated or reduced. However, most of the studies conducted in recent years have shown that removing the patina makes the stone more stable in the long term (Siegesmund & Snethlage, 2011).

Cleaning processes can be examined under four main headings according to the technique applied: Cleaning with water, mechanical cleaning, poultice, laser cleaning. The most common methods, target pollutants and risks are shown in Table 4.2 (Siegesmund & Snethlage, 2011).

Table 4.2 Selection of main cleaning methods (Siegesmund & Snethlage, 2011)

Method	Parameter	Application	Risks
Cold Water	Spraying without pressure optional detergents	Gypsum crusts, Dense stone	Moistening of masonry
Pressurized water	Cold/warm/hot 10–20°C/60–90°C	Gypsum crusts, Dense stones	Water penetration through open joints
	Up to 150 bars (15 MPa)		Material loss from friable surfaces
Water steam	140–180°C	Gypsum crusts, Dense and porous stones	Material loss from sanding and flaking surfaces
	20–40 bars (2–4 Mpa)		
Cleaning poultices	Active agents: EDTA, $(NH_4)_2CO_3$ poultice	Gypsum crusts, especially on limestone and marble	Full adherence of the poultice to the surface
	Ionic exchanger poultice with CO_3^{2-} and OH^-	Transformation of gypsum to calcite	Formation and migration of salts: $(NH_4)_2SO_4$
	Poultice materials: Clay mixtures of Attapulgite, Sepiolite, Bentonite, methyl cellulose, cellulose, highly dispersed silica, etc.	Testing and observing correct application time	Dissolution of calcite by EDTA
			Difficult removal of thin grey clay remains

Table 4.2 (ctd) Selection of main cleaning methods (Siegesmund & Snethlage, 2011)

Particle jet	Particle materials: glass slag, natural sand, quartz sand, hollow glass spheres	All kind of soiling	Dust development
		Dense and hard materials	Loss of flakes and loose material
		Dry or wet	Risk for loose paint layers
Micro particle jet	Particle materials: calcite, corundum, quartz powder, hollow glass spheres, fine sand	All kind of soiling and stones	Dust development
			Risk for loose paint layers possible
	Particle size 0.05–0.1 mm	Dry or wet	
Laser	Nd YAG laser	All kind of soiling	Discoloration of pigments
	Adjustment of pulse frequency, puls duration and beam focus	Especially on light stones like marble and limestone	Color change of stone through removal of coloring clay layers

4.2.1 Water Cleaning

Water-based cleaning processes are still widely used in the field, despite other advanced techniques. It plays an important role in removing water-soluble pollutants such as gypsum. There are different application techniques available: (Schnabel, 2014; Siegesmund & Snethlage, 2011).

i. Mild water spray: Here, it is aimed to wash the dirty layer on the stone by flowing the water through thin hoses for days and sometimes weeks. It is an effective method if the pollutants are gypsum or similar water-soluble layers, but often not sufficient. The biggest risk of the method is the possibility that the stone will hold too much water. This situation becomes more risky, especially when there are joints. In addition, as in rain, depending on the atmospheric conditions, fast drying occurs in some areas due to the effect of sun and wind, while it dries late in some places, which may cause the building not to be cleaned homogeneously.

   In this method, using warm or hot water increases the cleaning efficiency slightly, but considering the application difficulty, it does not appear as an effective method.

Figure 4.12 Wet mist cleaning of Gustav Adolf monument in Gothenburgh (Lindborg 1995)

ii. Pressurized water: In this method, cleaning is done by using pressurized water. Since it requires less water, the risk of water absorption is reduced. However, it is a more aggressive method for stone since the mechanical effect also occurs here. There may be material loss from the surface.

iii. Steam jet: In this method, steam is obtained by heating the water up to 140-180 °C in a closed container and coming to a pressure of 20-40 bar. Then, the operator opens the nozzle and allows water vapor to come from a small head. There is also a mechanical effect here, so it must be applied carefully. It also requires careful health and safety regulations because of high temperature and pressure.

Figure 4.13 A large steam cleaner being used to clean ashlar with a 45° fan nozzle

4.2.2 Cleaning Poultices

In cases where the water is not sufficient, chemical reactions can be used for cleaning. In these applications, mild agents (instead of aggressive chemicals) are used to not damage the stone or other existing coatings. Therefore, they must remain in contact with the surface for a relatively long time. This is usually achieved by impregnating a kind of paste (poultice) made of cellulosic materials or a compressed structure (sheets of paper) with a solution containing a chemical agent and adhering this mixture to the surface (Figure 4.13). During the application, the paste is applied to the stone, usually covered with a plastic or aluminum layer. Then the protective layer is removed and the poultice is kept on the surface until it dries, and it is cleaned from the surface afterwards.

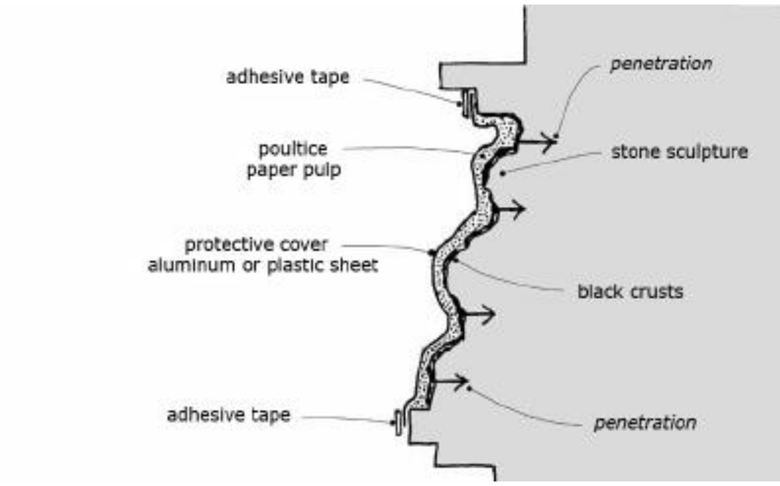

Figure 4.14 Cleaning by poultice (Schnabel, 2014)

If the stone contains oil-based nonpolar contaminants (such as fuel oil, tar or grease), clay poultices provide very effective cleaning. However, in this case, an apolar liquid (e.g. white spirit) should be used as a solvent medium instead of water.

The most commonly used poultice agents in the field are EDTA and ammonium carbonate. (Schnabel, 2014; Siegesmund & Snethlage, 2011). On the other hand, in recent years, studies with natural latex have started to become widespread again. (Siegesmund & Snethlage, 2011).

As with other methods, using poultice has its own risks. For example, if there is paint or a similar application on the surface, poultice can dissolve the organic material in the application. Another danger is that the clay minerals in the medium in the poultice leave a white or yellow stain after the poultice leaves the surface. For this reason, the contact surface is tried to be protected by placing Japanese paper between the stone and the poultice during the application.

Figure 4.15 Removal of poultice

4.2.3 Mechanical and Abrasive Cleaning

In cases where wet cleaning methods are not sufficient, it may be necessary to use mechanical methods. Although more aggressive methods have been tried for mechanical cleaning such as spinning discs, lately, particle jet or micro-particle jet techniques are used. Particle sizes used in the particle jet vary between 0.1 mm - 0.5 mm and between 0.05 and 0.1 mm in micro particle jet (Siegesmund & Snethlage, 2011). The material of the particle can be blast furnace glass slag, natural sand with mica or with calcite, quartz sand with rounded or broken grains, hollow glass spheres (Schnabel, 2014). When applying the method, a more aggressive or softer application can be obtained depending on the pressure and particle used. The effects of different particle sizes are shown in Figure 4.16. Accordingly, it is seen that large diameter particles cause larger pits and therefore are suitable for thicker contaminant layers and small diameter particles should be used in cases where more careful study is required.

Abrasive cleaning can be made dry or wet. The factors to be considered in case of dry preparation are the hardness, speed, concentration, application distance of the particles, the configuration of nozzle and the application angle. In aqueous methods, the application is made by adding water from a separate line. In this method, the pressure of water and air and the amount of water fed, among other parameters, should be carefully controlled. [BS 8221-1: 2012]

The stones that this method is used most frequently are the hard microcrystalline calcareous stone, on which a thick and hard layer is continuously deposited. Mechanical cleaning is especially useful during the restoration of historical fountains over which hard water flows. However, the most important constraint is that it is too aggressive to be used in renderings, stuccoes, soft sandstone or limestone. It is also not recommended for hard stones containing large crystals such as white marble and granite, as it may cause the crystals to separate.

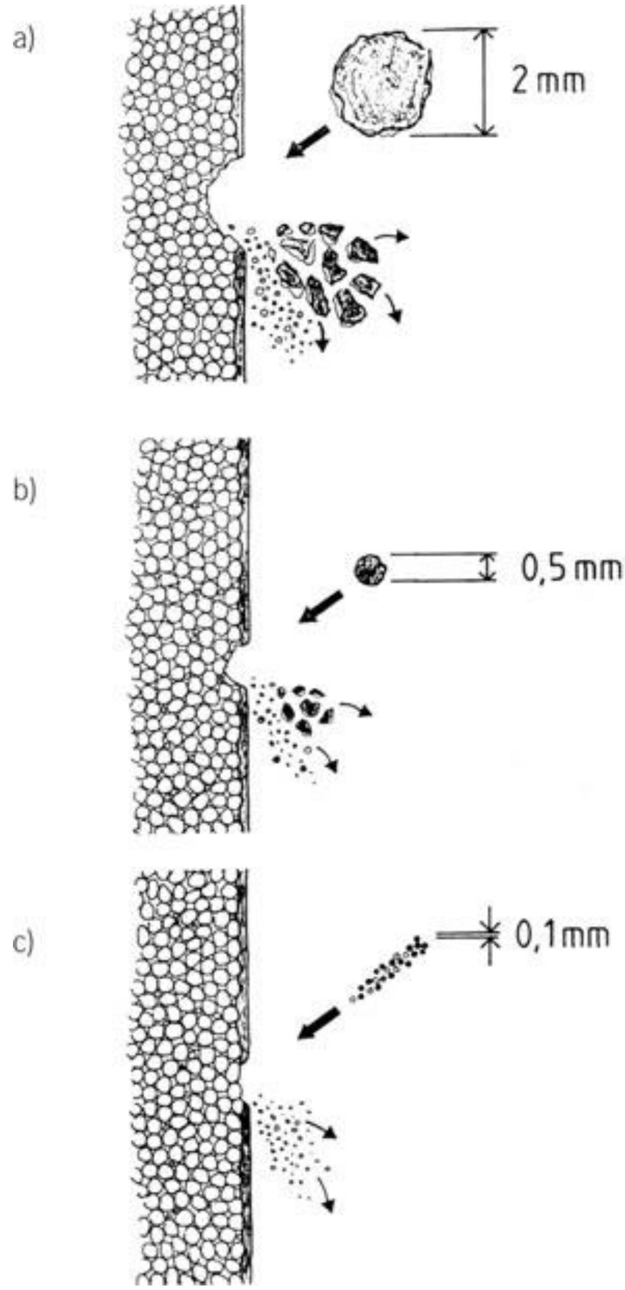

Figure 4.16 Potential hazard of different mechanical cleaning types (a) sandblasting, (b) particle jet, (c) micro particle jet (Siegesmund & Snethlage, 2011)

Figure 4.17 Application of mechanical cleaning

4.2.4 Laser Cleaning

Laser technology was first used in the field of cultural heritage as an archiving method for hologramming Venice sculptures (Asmus vd., 1973). Meanwhile, when the laser was seen to clear the black incrustation on the surface, it was found that it could also be used for cleaning purposes. However, laser technology was used only on materials such as museum artefacts made from stone, wood, ceramic and ivory until the 1990s due to the weight of the devices (Siegesmund & Snethlage, 2011). After the 1990s, with the transportation of equipment, the use of materials in stone works exposed to open air has become widespread.

The basic principle of laser cleaning is as follows; a laser beam impacts the surface, and the energy of the infrared beam is dissipated by the sudden heating and expansion of light-absorbing material on the surface, such as particles rich in carbon, and the nearly instantaneous vaporization of moisture in the surface layer, which acts to remove surface dirt (Doehne & Price, 2010). However, in some studies, it has been observed that the efficiency increases if water is used just before the application (Siedel & Hubrich, 2000).

The biggest advantage of the laser is that it is absorbed by dark colors and reflected by light colors. This ensures that the black layers formed on light colored stones such as marble and limestone are removed and the cleaning is completed without any material abrasion from the stone. This situation is theoretically related to the difference in energy holdings; for example vaporization of black crust requires 6.8 J/cm^2, black fungi 0.3-0.5 J / cm^2, mold 0.1-0.2 J / cm^2 and marble 17 J / cm^2. Accordingly, it is theoretically not possible to damage the marble surface with the amount of energy adjusted to remove black crust (Siegesmund & Snethlage, 2011).

The most commonly used laser in practice is of the Nd: YAG laser in its Q- switched option. The core of this kind of laser is an Yttrium Aluminum Garnet doped with Neodymium (Siegesmund & Snethlage, 2011).

The energy threshold level, pulse length, pulse frequency, and the focus and/or distance of the laser beam to the surface can all be adjusted to match the laser's performance to the mission. (Siegesmund & Snethlage, 2011). After determining these parameters, focusing can be made up to an area of 1 mm to several cm^2.

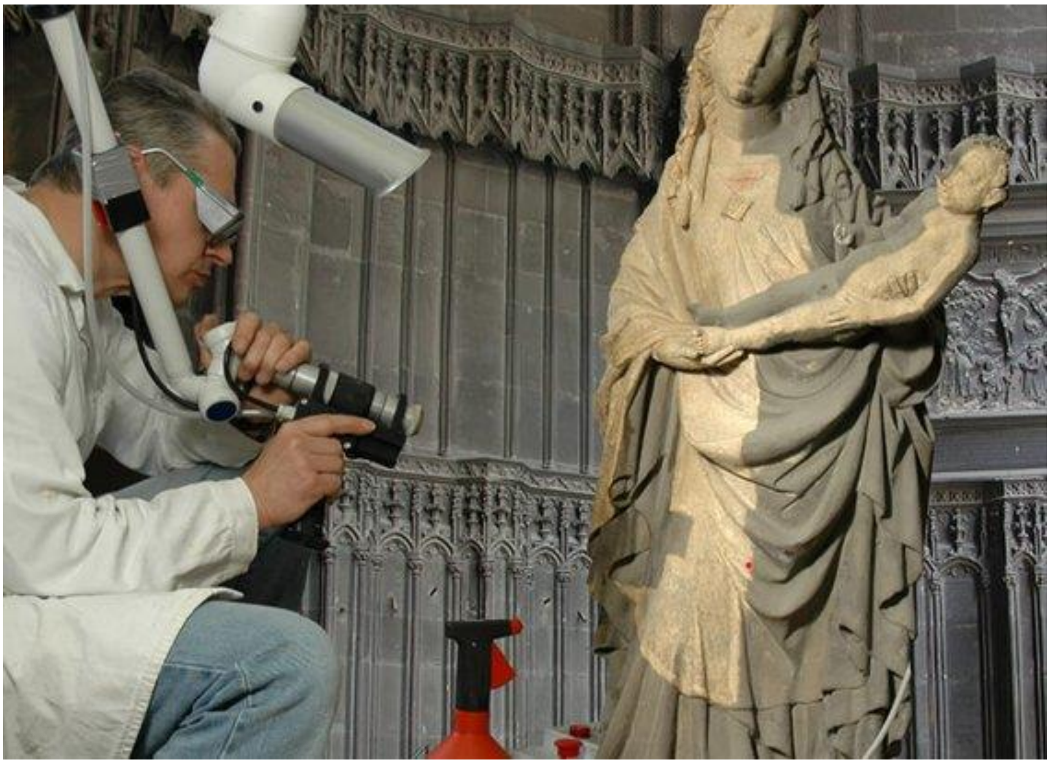

Figure 4.18 Stephan's Cathedral was laser cleaned with 30,000 hours of work in 7 years. Despite the long workforce, it has been calculated that it is less costly than cleaning applications that can be done with traditional methods due to reasons such as the large number of details in the building and its spread over a wide area.

Various advantages and disadvantages have been revealed in studies comparing laser cleaning with other methods. The most important advantages are selectivity, being dust-free, having no need for water, and can be applied on fragile and fine decoration. However, the tools are very costly, require high energy costs during application, and high-level occupational safety measures. For this reason, field workers often recommend using a combination of more than one technique to meet economic and technical requirements (Kwiatkowski vd., 2004; Łukaszewicz & Niemcewicz, 2008).

Another controversial issue regarding laser is the yellowing of the stones. This has been evaluated by various researchers and put forward as one of the disadvantages of laser. However, recent studies show that yellowing is not caused by laser, but a phenomenon acquired by the stone itself during its natural degradation and can be taken as the boundary layer between the black layer and the stone core (Pouli vd., 2008) . However, if pigments are present such as lead white, azurite, malachite, ocher and other natural pigments that contain hydroxyl groups, laser is known to cause damage. This situation can be even more troublesome if the binder medium of the paint is organic. However, stable elements such as smaltite, cobalt blue, hematite and green earth are not affected by laser. For this reason, pigment and binder analysis should be done before laser cleaning which will be performed on painted surfaces (European Commission. Raphael Programme & Domstiftung Regensburg, 2001)

4.3 Treatments

The most important and comprehensive part of the conservation work includes the basic practices for damage elimination after damage assessment and cleaning. These applications may be more restorative, architectural or constructive in cases where structural integrity is impaired or mechanical strength is reduced. For lighter damage due to material degradation, conservation experts take place.

The first of these works is to repair higher damage based on physical or mechanical healing such adhesion of detached parts. In this process, it is aimed to reassemble the parts by selecting suitable materials (such as epoxy resins, stainless steel, glass-reinforced polyester). There is a simple demonstration of joining a broken statue arm in Figure 4.19.

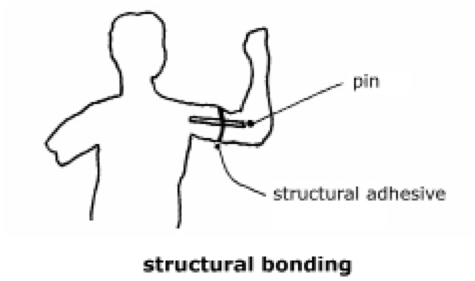

Figure 4.19 Structural bonding of a sculpture (Schnabel, 2014)

Another application is grounting. Grouting is the name given to a rock consolidation technology based on the injection of fluid materials (grouts, normally cement-based mixtures or synthetic resins) that can harden inside the cracks (Schnabel, 2014). Although these applications are not strong enough to be structural intervention, they can be considered as the most important strengthening works on a layer that can be counted on the surface.

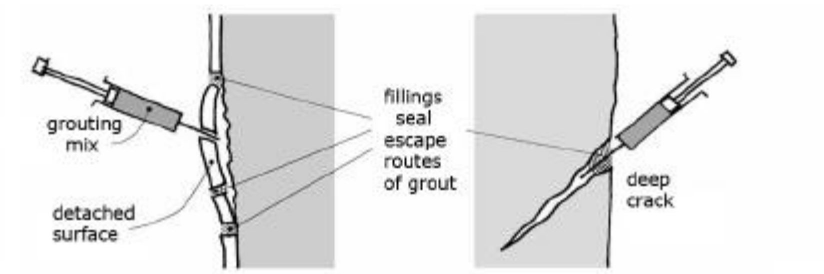

Figure 4.20 Surface grouting application (Schnabel, 2014)

Filling all cracks and voids in the surface of deteriorated materials is a fundamental point in the present practice of conservation of architectural surfaces as in grouting. The main purpose of this application is to repair the stress areas that will occur here in case of a discontinuity without causing any greater damage. The materials used in the application are more flexible and closer to the structure of stone than grouting. Generally, lime-mortar is used, but in case of deep cavities, mixed applications with aggregates and hydraulic cement can be made. If necessary, colored stone powders can be added to match the color.

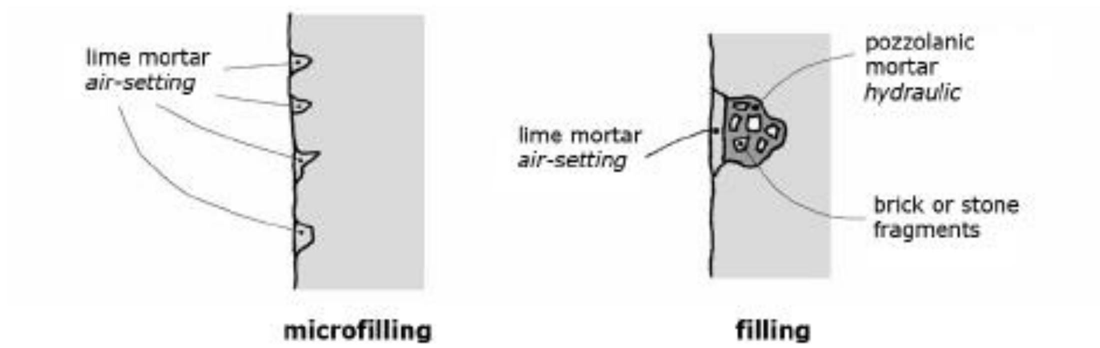

Figure 4.21 Microfilling (left) and filling (right) treatments (Schnabel, 2014)

4.3.1 Consolidants

Stones used within the scope of cultural heritage degrade over time by being exposed to environmental effects. One of these degradation mechanisms is the loss of mechanical strength due to the loss of minerals in the pore structures of the stones and the enlargement of the intergranular spaces. When the grain structure of a newly mined stone is examined, it is seen that the cohesion mainly derives from the cohesion provided by "mineral bridges" and mechanical indentation (mechanical interlocking effect). Therefore, the loss of cohesion means the breakdown or weakening of these agglomerating mechanisms that typically occur in zones located near the surface, at a major or minor depth (Sena da Fonseca vd., 2018).

With the use of consolidants, it is aimed to provide mechanical improvement by re-establishing the cohesion between the particles of the stones. Consolidant can operate by two types of mechanisms; locking the grains by filling the interstices between the loosened grains (Figure 4.22 a,b) and “gluing” grains together by forming adhesive bridges between adjacent grains. An illustration of the applications using alkoxysilanes is shown in Figure 4.22.

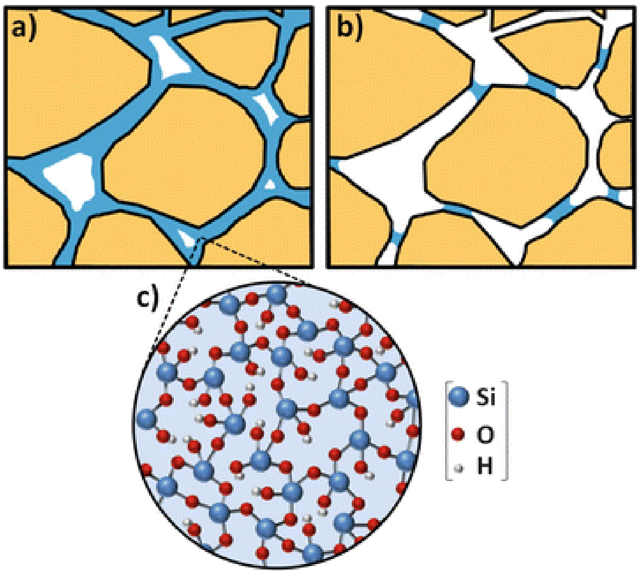

Figure 4.22 Consolidant effect of alkoxysilane at molecular level (Sena da Fonseca vd., 2018)

Consolidant use should be decided on the damage type of the stone. For example, it is not correct to apply consolidant for stones that undergo powdering, sugaring or sanding style degradation. It is usually carried out as a pillar of large-scale conservation plans and then supported by surface protectors.

There are several features that consolidants should have for good implementation;

• It should have low viscosity and low contact angle for high penetration rate into the stone surface.

• After applying in liquid form and obtaining a certain penetration, it needs to stiffen or set once it is in place in order to strengthen the stone. This can be done by three different mechanisms; I. It can be applied in a molten state at high temperature and harden when cooled (eg wax). However, in this application, applying wax at high temperatures is risky in terms of work safety and during application the wax becomes sticky and it has the potential to hold various dirt. In addition, it is not a useful application in the long term, as re-melting may occur in areas exposed to high sunlight. ii. To apply consolidants by carrying them in a volatile solvent medium. Here, it is controversial to what depth the volatile solvent penetrates before evaporating. It can also carry some of the consolidant to the surface during evaporation. iii. Use of low viscosity solution that produces a solid product through chemical reaction. This is the mechanism on which the most frequently used products in recent years are based (Doehne & Price, 2010).

Figure 4.23 shows two consolidant applications that have reached and not reached sufficient penetration. Accordingly, it is seen that sufficient and correct application should cover the whole damaged area and some sound core (Schnabel, 2014).

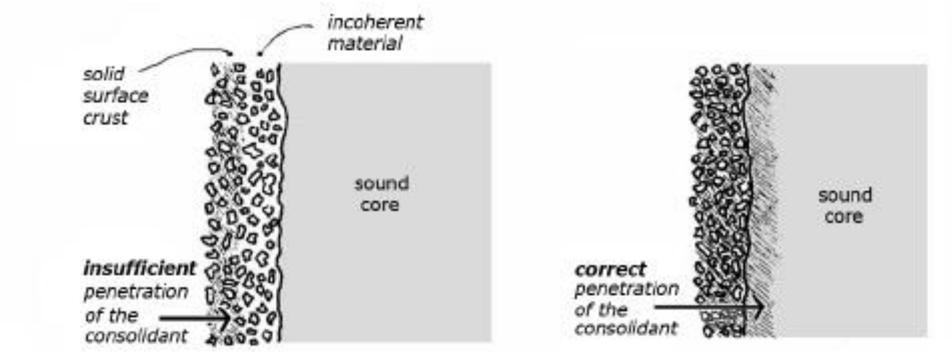

Figure 4.23 Depth of penetration of a consolidant

• **Application**

Consolidants are usually applied to the surface of the stone by brush, spray, pipette, or by immersion and are drawn into the stone by capillary action. In Figure 4.24, HAP application from (Franzoni vd., 2015) is shown. Accordingly, the samples were exposed to HAP application with brushing, poultice and immersion and different properties were tested. At the end of the study, when the comparison of the absorbed material based on weight measurements was examined, it was observed that the efficiency of the application method changed depending on the geometric shape of the sample.

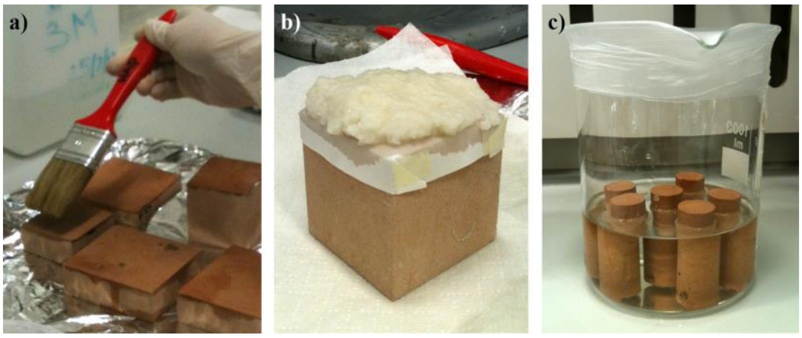

Figure 4.24 Application methods of consolidants; a. brushing b. poultice c. immersion (Franzoni vd., 2015)

• **Types**

Organic and inorganic (including lime-based) consolidants are the primary alternatives on the field. They all have both benefits and drawbacks, and they also need improvement. A large number of organic products have polymeric formulations (e.g. epoxy resins, polyacrylates, polymethacrylates, polyesters and polyvinyls). They can provide mechanical strength by accumalating solid particles inside pores, either by inserting macromolecules into pores and evaporating solvents (thermoplastic polymers) or by creating cross-linking reactions with an external curing agent (thermoset polymers) (Sassoni vd., 2011). While they tend to increase mechanical strength, they have non-negligible drawbacks, such as reduced penetration depth, biodeterioration sensitivity, UV-ray instability, hydrophobic surface structure and changing water transport properties, and when they display poor compatibility with inorganic substrate, they can cause significant degradation of microstructural or physical properties and make the stone prone to atmospheric effects (Matteini vd., 2011).

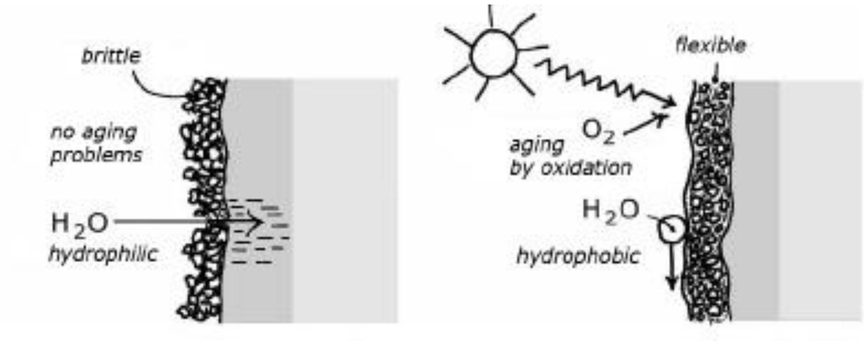

Figure 4.25 Consolidation by impregnation. (Left) inorganic consolidant, (right) organic consolidant (Schnabel, 2014)

Inorganic consolidants are generally based on the addition of a chemical intermediate into the pores. Insoluble crystal structures and mechanical strength are provided by chemical reactions such as hydrolysis (as in TEOS), carbonation (as in lime-water) or direct reaction with stone (as in phosphate treatments). Silicate-based consolidants, such as TEOS, are more effective on silicate-based stones. On sandstone grains, they react with silanole groups and produce a consolidation effect by forming covalent bonds. However they are not as successful for carbonate stones if they are used without external reagents due to lack of-OH groups to react, thus bonding happens only physically (Naidu vd., 2015; Sassoni vd., 2011, 2013, 2015). On the other hand, lime-based consolidants are based on the concept of lime ($Ca(OH)_2$) being inserted into stone. $CaOH_2$ interacts with atmospheric CO_2 and generates $CaCO_3$. The freshly developed $CaCO_3$ is compatible with calcite, forming bonds between grains and reinforcing the stone. It also has drawbacks, however, besides the chemical compatibility, such as slow reaction rate and creating a color difference by aggregation due to low water lime solubility.

Nano-lime-based research is still underway in the area in order to prevent these issues. When achieving high penetration values (up to 40 mm) (Borsoi vd., 2016), lime-based consolidants may be transported back to the surface during drying, which may contribute to near-surface particle aggregation and a lack of substrate consolidation (Rodriguez-Navarro & Ruiz-Agudo, 2018)

- **Bioinspired Solutions**

There has been an on-going demand for bio-inspired technologies in recent years. Pioneer research began by studying preserved masonry sites without human interference. (Huang Kezhong, 2003; X Wang, 2004). These studies showed that minerals such as calcium oxalate (CaC_2O_4), fluorapatite ($Ca_5(PO_4)_3F$) and hydroxyapatite (HAP) ($Ca_5(PO_4)_3(OH)$) functioned as protective biomimetic films (de Buergo & González, 2003; Del Monte vd., 1987; Garcia-Vallès vd., 1998; Liu vd., 2006, 2010; Liu & Zhang, 2007; Monte, 2017; Rampazzi vd., 2004; Yang vd., 2012).

HAP has some benefits among these alternatives, such as enhancing mechanical structure within 48 hours, creation in aqueous solution without harmful chemicals, being protective against acid corrosion, having deep penetration depth by its low viscosity, not influencing hydric properties on the surface, not causing identifiable color change, giving opportunities for more treatments by not affecting hydric properties on the surface (Graziani vd., 2015, 2016; Sassoni, 2018; Sassoni vd., 2011). Therefore, phosphate based treatments are mainly focused on HAP formation in recent years.
Most of the consolidation effect of the phosphate compound is based on the reaction between the substrate DAP (Diammonium hydrogen phosphate) and $CaCO_3$, resulting in the product HAP. From the reaction in equation 4.1, it can be seen that Ca^{2+} ions are required for HAP to form. For this cause, most of the experiments were focused on samples of calcareous and marble and there is still inadequate knowledge in the literature on the impact of HAP on a broader spectrum of stone forms, such as low-carbonate stone material. (Molina vd., 2018; Sassoni vd., 2013) .

$$CaCO_3 + (NH_4)_2HPO_4 \rightarrow Ca_{10}(PO_4)_6(OH)_2 + (NH_4)_2CO_3 + CO_2 + H_2O \qquad (4.1)$$

Consolidant studies have an important place in the literature. According to Web of Science data, there are 102 publications published in this field between 2015-2020. When the contents of these articles are analysed, it is seen that the most intensive study (36/102) was done in the field of research of nanomaterial additives. After that research on DAP (24/102) seems to have interest from researchers. It can be said that DAP is the current leading consolidant in research by considering the variety of nano materials. On the other hand, although having certain disadvantageous (such as causing yellowing or changing hydric properties) TEOS is still being researched by significant amount of scientists (19/102). This can be related coherence between siliceous stones and TEOS and more work need to done to material development for this type of rocks. Moreover, search for new materials as consolidant is also another rising research topic (11/102). On the other hand, the popularity of polymeric consolidants seems to be decreased over the years (5/102), probably because of observation of negative side effects.

Although most of these studies have been carried on material investigation (95/102), there are also significant amount of researches on developing analytical techniques (16/102) and understanding the behaviour in outdoor conditions (15/102). Furthermore, it should be noted that some of these studies overlapping and hard to distinguish in between.

By means of the stone type, there is still a major interest in limestone and carbonate-based stones, and there are less studies on sandstone and others. So it can be said that, there is a research lack for other kind of stones.

Table 4.3 Literature summary on SCI-EXP indexed published articles with keywords “consolidant” and “stone” between 2015-2020

	FIELD STUDY	ANALYSIS TECHNIQUE	TYPE OF THE CONSOLIDANT					STONE TYPE		FIELD STUDY	ANALYSIS TECHNIQUE	TYPE OF THE CONSOLIDANT					STONE TYPE
			POLYMERIC MATERIALS	DAP	NEW MATERIALS	TEOS	NANO MATERIALS					POLYMERIC MATERIALS	DAP	NEW MATERIALS	TEOS	NANO MATERIALS	
1							*	Carbonate	52				*				Limestone
2									53	*						*	
3	*						*	Limestone	54							*	
4		*							55	*			*			*	
5				*				Carbonate	56	*			*				Limestone
6						*	*	Granite	57							*	
7				*					58						*	*	Andesite
8									59				*	*			Limestone
9						*			60		*						Limestone
10						*	*		61				*	*			Marble
11							*	Limestone	62				*				
12	*								63				*				Limestone
13	*							Sandstone	64				*				Limestone
14							*	Carbonate	65				*				Carbonate
15					*			Sandstone	66					*			Basalt
16							*		67								
17							*	Limestone	68							*	Limestone
18	*						*		69	*							
19	*			*			*		70							*	
20				*					71			*		*	*		
21						*		Limestone	72		*						Limestone
22		*						Marble	73				*				Carbonate
23									74						*		Sandstone
24		*							75								Limestone
25							*	Tuff	76				*				Marble

Table 4.3 (ctd) Literature summary on SCI-EXP indexed published articles with keywords “consolidant” and “stone” between 2015-2020

26					*				77						*	*	Limestone
27							*		78						*	*	
28					*			Limestone	79							*	Tuff
29			*						80				*				
30						*			81				*				
31									82			*					
32				*					83							*	
33						*	*		84	*			*				Marble
34	*						*		85				*	*			
35		*						Limestone	86						*		
36						*	*		87							*	
37						*			88							*	
38		*							89	*	*						
39		*							90							*	
40		*			*				91		*						
41						*			92		*						Tuff
42							*		93						*	*	Sandstone
43	*								94		*						
44									95		*				*		
45									96			*					
46			*	*		*			97	*							
47	*					*	*	Limestone	98		*		*				Limestone
48							*		99					*			Granite
49							*		100							*	
50				*			*		101				*				
51					*				102		*						

94

However, consolidants have also an important commercial potential. For this reason, projects developed on the subject receive satisfying funding.

In one of these projects (under EU-Horizon 2020 programme), contribution of nanoparticles have been investigated by comparing commercial and research products (2014) (Figure 4.26). According to this graph, as of 2015, the most commonly used consolidant type is alkoxy-silane and oligomers, both in research and commercial terms. However, in scientific research, it can be seen that low molecular weight inorganics and biomineralization based consolidants are on the rise. When these data are evaluated together with the table 4.3 covering the period between 2015-2020, it is seen that this increase has continued in recent years and has been ahead of polymeric materials. Similarly, when comparing in terms of solvent, it is observed that there is a balanced distribution between organic, aqueous and solventless for the consolidants in the market, while the most intensive work in the research area is for organic solvent. However, it can be said that this distribution has passed to aqueous with the increase in the use of inorganic substances in recent years (Table 4.3).

When evaluated in terms of the types of stones, it is seen that limestone, sandstone and marble are mostly studied in the research area, followed by low amount of granite and then much lower amounts of other stones. This situation continues similarly in the studies conducted between 2015-2020.

Finally, in terms of the application methods, it is known that the researched methods are mostly applied with brush, immersion and spraying, while it is known that the immersion method is not applicable in practice and the brush and spray method are mostly applied.

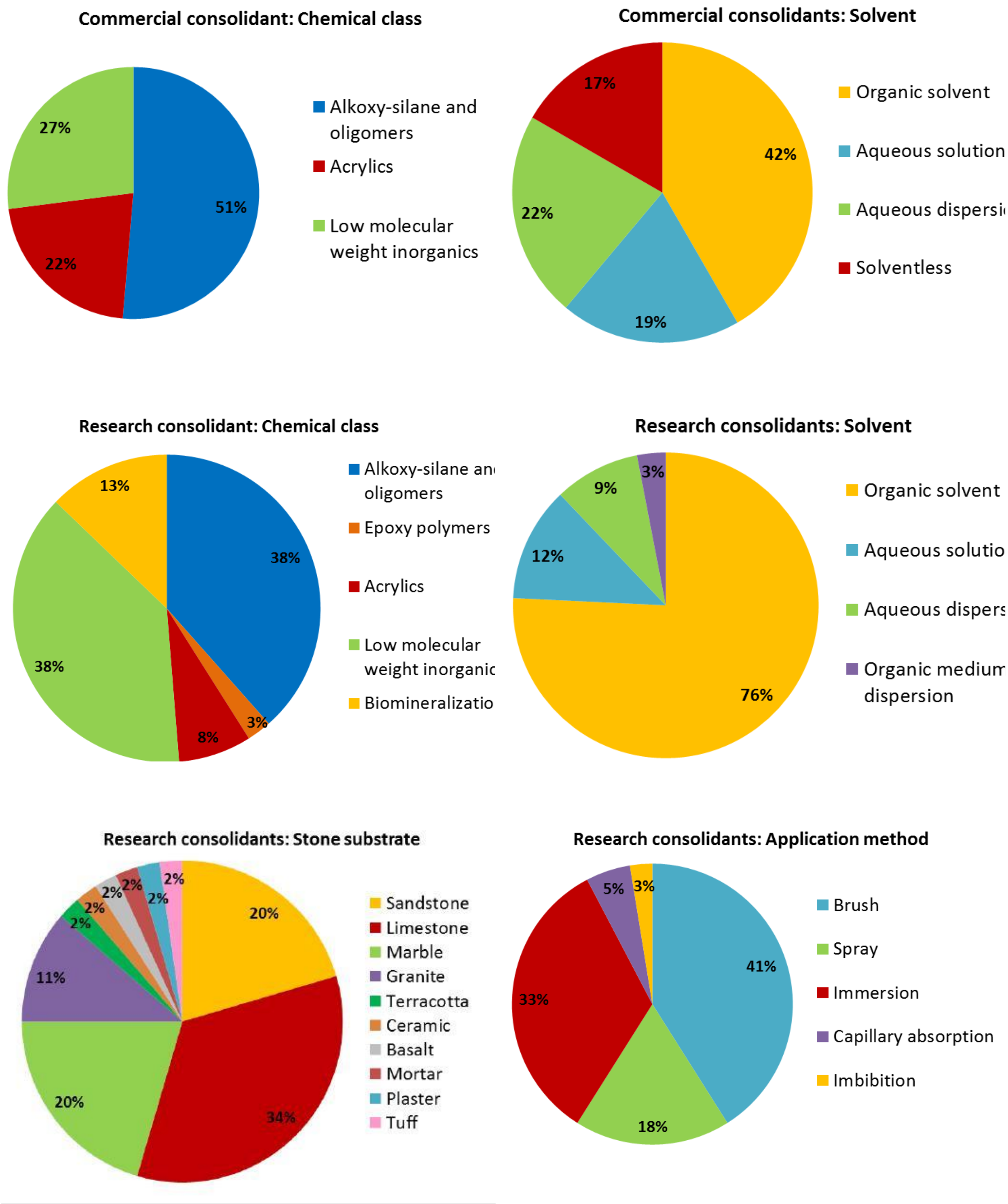

Figure 4.26 Research and market data of masonry consolidants (Gherardi & Toniolo, 2015)

4.3.2 Surface Treatments

Surface protection treatments used in stones have a wide category that includes products with many different functions; such as protective water repellents, emulsions, antigraffiti coatings, salt inhibitors, protective oxalate layers, sacrificial lime coatings, colloidal silica, biocides, and bioremediation treatments.

Since the 1970s, product development studies have been carried out in order to improve the mechanical properties (consolidation) and protect the surface of the stone (surface treatments) with the same product. However, it was observed that although both water repellency and mechanical improvement properties were observed in consolidants such as TEOS, this approach did not yield very effective results. Explaining it with medical analogy, it is very difficult to expect the same drug to both fight flu infections and heal a broken foot. For this reason, today this purpose has been abandoned and shifted to applying two (or more) different products on top of each other, if necessary (Doehne & Price, 2010).

There are different chemical surface protectors in commercial and literature studies. The distributions of these products are shown in Figure 4.27. Accordingly, it can be seen that, as of 2015, approximately 80% of the surface treatment in the market and in the research area is polymeric in origin and although they show distribution within themselves, the most used class is silanes. The most important reason for this situation is that these products are used as water repellents. However, different classes such as oxalates and aliphatic polyesters are seen in the research areas, unlike the products on the market. The reason for such a wide chemical distribution is that surface treatments serve many different functions, and various products have been developed to meet different requirements.

When evaluated in terms of solvent type, it is seen that there is a great similarity in market and research areas, only some products in the market are solvent free.

It is seen that nanoparticles, which are widely used in recent consolidant studies (Table 4.3), are also used in surface treatments. Since the use of nanoparticles is a relatively new field, it is expected that different materials are being tested in the research area than the ones on the market.

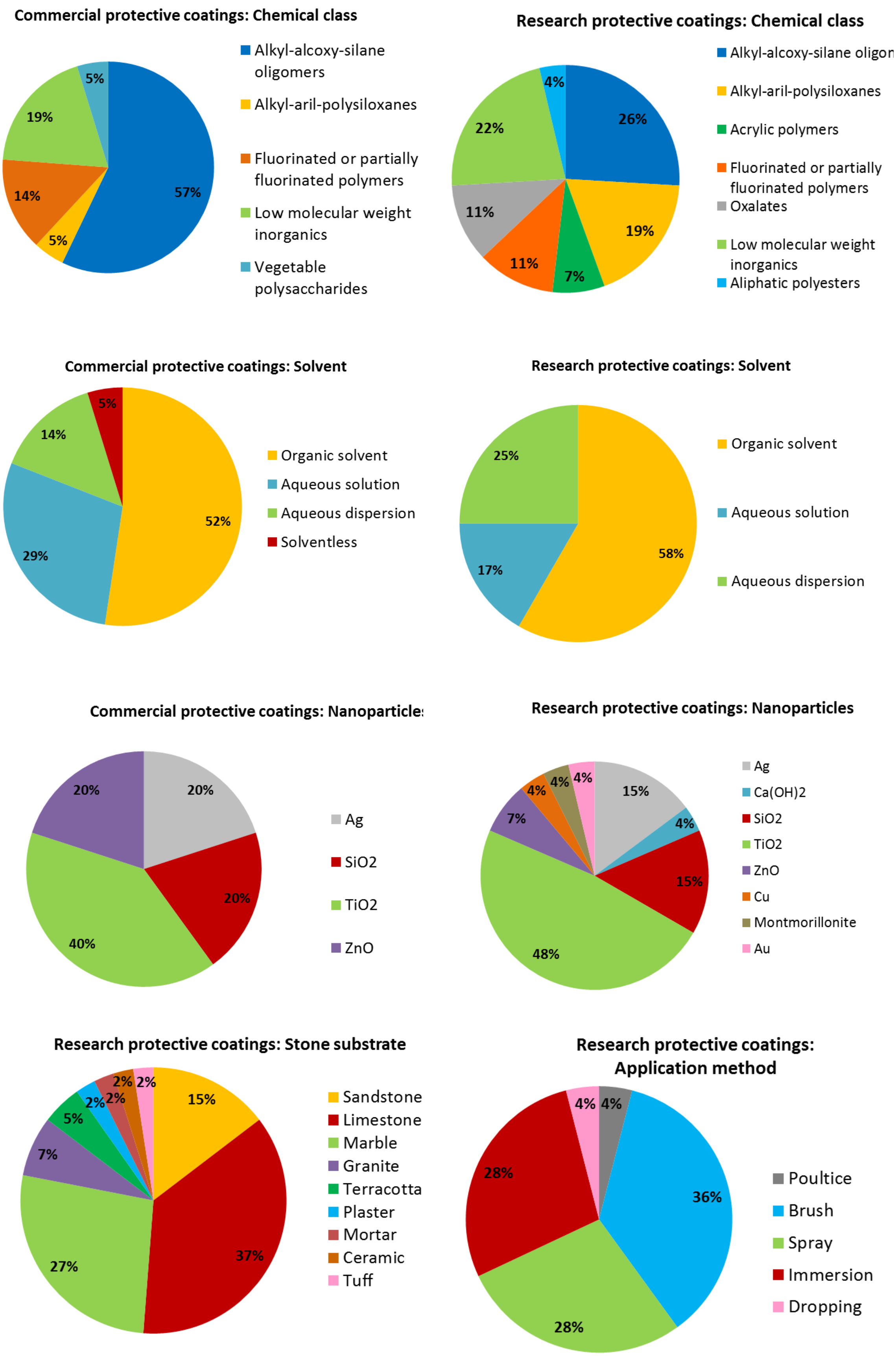

Figure 4.27 Research and market data of protective coatings (Gherardi & Toniolo, 2015)

In terms of stone types, it is seen that the most intense research area in parallel with consolidant is in sandstone, limestone and marble, followed by other stones (and building materials).

Finally, when the comparison is made in terms of application methods, it should be stated that the most used methods in the research field are brush, spray and immersion, as in consolidant; but it should be noted that it is difficult to apply the immersion technique in the field and it is usually applied with brush and poultice or spray.

Popular Products used in Conservation Industry

In this section, more detailed information about the most used products, water repellents and biocides, will be presented.

- **Water Repellents**

Although the use of water repellents is controversial, they have been used and developed as a surface protector for many years. Since water is the main source of many damage mechanisms, a lot of damage is prevented by removing water. The most commonly used water repellents are alkoxysilanes, silicon and fluoropolymers (Doehne & Price, 2010).

Hydrophobic applications make the surface water repellent but do not affect vapor permeability. Therefore, it increases the risk of damage in the environment where hydroscopic salts are present. The salts carried to the inner surface of the stone in the water vapor accumulate in the boundary area of the hydrophobic layer with the stone. Meanwhile, the water vapor passing into the liquid phase cannot leave the stone due to the hydrophobic layer and a dense accumulation occurs in this area. This causes more damage to the stone than if there is no hydrophobic application. For this reason, the use of water repellents should be avoided in areas with degradation due to salt damage.

Another disadvantage of this application is the need to cover the entire surface during application. In cases where such a holistic application cannot be done (or not done intentionally), water accumulation occurs in certain areas and more damage occurs (Siegesmund & Snethlage, 2011). On the other hand, it has been observed that water repellent applications made in earlier dates have lost their effect in the long term and require more repetitions than expected (Siegesmund & Snethlage, 2011).

Because of all this, the use of water repellents is the most controversial of all surface treatments. Application may be considered in places with heavy rainfall and therefore exposed to heavy damage, but it is not recommended to be applied in buildings located adjacent to other buildings with open one facade or which are under dry climate conditions.

Figure 4.28 Effect of silicone base water repellent (from product sheet of Flora Metallic Flooring© TR-813)

- **Biocides**

Although the use of biocide is controversial, it is still applied to prevent damage caused by fungi, bacteria, algea and lichen. However, there are more considerations that should be considered before use than the other conservation applications, because microorganisms have complex structures. The microorganisms are difficult to control in outdoor where the environmental conditions (especially temperature and humidity) are dynamic. In addition, more than one microorganism is usually present at the same time. In this case, it should be analyzed well which microorganism to fight against. Because the application for lichen and the application for bacteria are not the same for example.

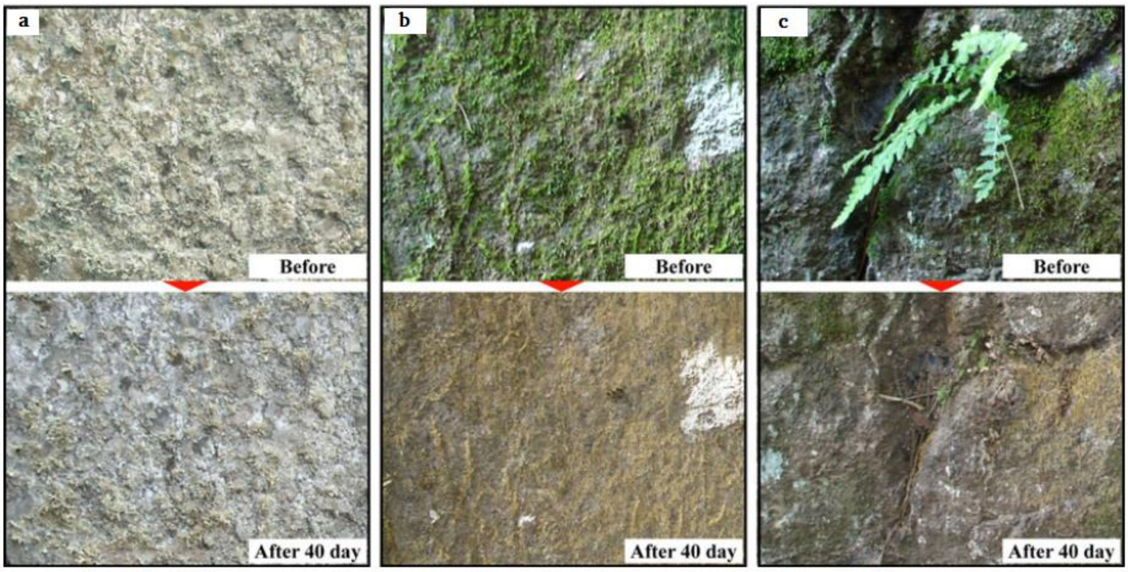

Figure 4.29 a. Difference between before and 40 days after biocide treatment of lichens. **b.** Difference between before and 40 days after biocide treatment of bryophytes. **c.** Difference between before and 40 days after biocide treatment of high plants. (Lee vd., 2011).

If there is damage to the stone caused by biological attack and the application of biocide is decided, the first thing to do is cleaning. For this, the chemical composition and the hardness of the stone must be analyzed. The microorganism type is also important for the cleaning phase. For example, if algal and cyanobacterial layers are completely dry before cleaning, they can be removed from the surface by a mechanical method such as brushing or microparticle jet. In general, it is not recommended to clean the stone with pressurized or superheated steam because these applications cause microorganisms to penetrate deeper with water.

As with all other surface protectors, there are features that are expected to meet in biocides. The most important of these is that it must kill harmful microorganisms and prevent them from growing again. However, it should have no effect on the appearance of the stone and make the stone turn yellow over time, etc. It should not undergo a change under environmental conditions, leave the surface with rain or deteriorate under UV effect (Doehne & Price, 2010). In addition, it is desired to have low viscosity for good penetration during application (Siegesmund & Snethlage, 2011). One way to increase the application efficiency is to moisten the surface to activate the biofilm. For this purpose, it is recommended to wet the surface a few hours before applying the biocide without using pressure.

The effect of Biocide on the environment and human health is also carefully examined. Products used in Europe are regulated by the European Biocide Directive (http://ec.europa.eu/environment/biocides/index.htm) and the use of certain toxic materials such as organo-tin or mercury and other heavy-metal components is prohibited (Siegesmund & Snethlage, 2011).

It is a method widely used in the field to be used with hydrophobic applications to increase the anti-microbial effect. In this way, it is aimed to prevent new damage occurrences.

4.4 Evaluation of Effectiveness of Treatments

Although many laboratory tests are performed beforehand, the effectiveness of protective or reparative practices should be determined after applications. Some of the studies conducted for this purpose aimed to look from a larger perspective and suggest strategic approaches (Price, 1982). Others have suggested more “tailor-made” tests for each application by considering stone, environment and treatment, arguing that a single procedure cannot be applied to all situations (Fassina vd., 1994). However, this approach made it difficult to compare the studies of the researchers with each other. For this reason, developing standards has been seen as one of the best options.

The reviews to be carried out after the implementation should be evaluated in two stages: effectiveness to be measured shortly after implementation and performance evaluation in the long term. While conducting these examinations, it should always be considered that which criteria can give sufficient information about whether the application is recommended or not.

While characterizing the stones with surface treatments, testing some features that seem independent of the purpose of the application provides a general knowledge. These are porosity, pore distribution, appearance and penetration depth of the application. However, tests for the purpose of the application (eg consolidant) are also very important; such as water uptake, Scotch tape test, surface hardness, DRMS, UPV. It can be said that some tests have been standardized in the field; For example, if a water-repellent application has been applied, it is common practice to then measure the contact angle and water absorption.

It is also an important issue to carry out long-term examinations of the applications. For this reason, it is a wise approach to return to the field again at specified time intervals after the application is made.

Different international standards were tried to be established on the subject. 25-PEM and 59-TPM groups working under the roof of RILEM are one of the groups that made the most efforts in this regard. In addition, there are studies performed by EN and CEN Technical Commitee 346. Detailed information about these can be found on the websites of the standards.

5

MATERIALS AND METHOD

5.1 Stone

In this study, the stones of Ankara, Bitlis, Mardin and Nevsehir were used as substrate as shown in Figure 5.1. All the samples are unique for Anatolia and valuable for the geological and architectural heritage of the region. They are used for construction of cultural elements such as Seljuk Tombs (Bitlis stone), Midyat city (Mardin stone), Second Building of the Turkish Parliament (Ankara Stone) and Cappadocia city (Nevsehir stone). They have different physical characteristics such as porosity, hydric behaviour and density) which enables comparison of the effect of treatments on a range of stone types. Geographically, they come from different areas of Turkey and they have different geological properties representing the geodiversity of Anatolia (Figure 5.2) (Kazancı & Gürbüz, 2014).

Figure 5.20 Appearance of raw samples. From left to right; Mardin, Ankara, Nevsehir and Bitlis stones

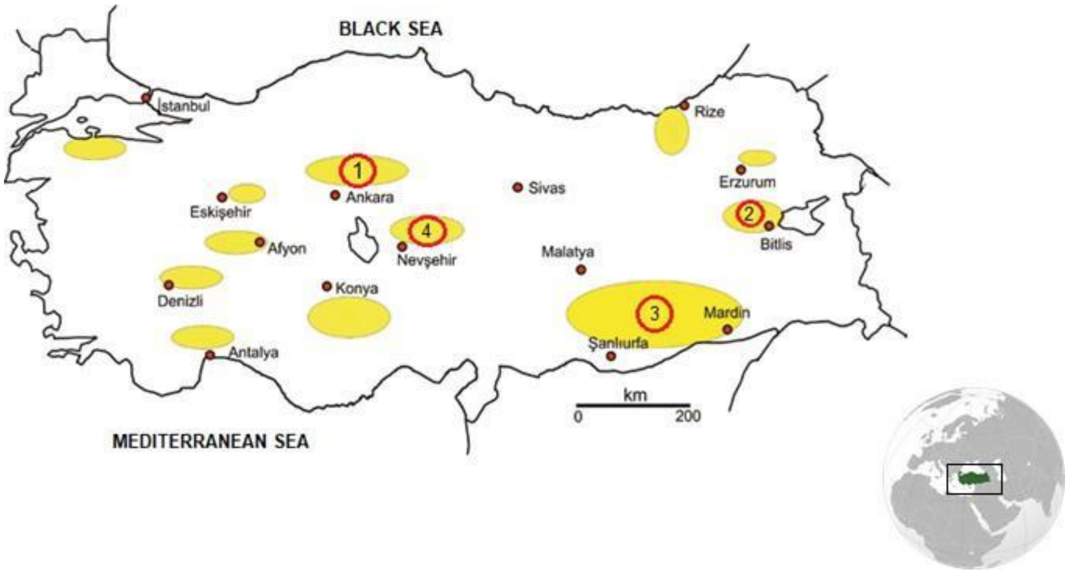

Figure 5.21 Geoheritage stones of Turkey. Numbered areas show the locations of samples (Kazancı & Gürbüz, 2014)

5.1.1 Ankara Stone

Ankara region is a geologically rich area which is located in ENE-WSW basin and has different kind of rocks such as andesite, tuff and agglomerate which is formed from mesoscopic to recent (Arıkan et al., 2007; Orhan et al., 2006; Sari et al., 2010; Yavuz, 2011). Among these types, andesite is the most common one because of its durability, hardness, attractive appearance and is used widely for monuments, walls, pavements and kerbs (Arıkan et al., 2007; Binal, 2009; Orhan et al., 2006; Sari et al., 2010; Yavuz, 2011). The andesite has a porphyritic texture with plagioclase and quartz phenocrysts embedded within a microlite matrix (Orhan et al., 2006). Although having similar chemical composition, Ankara andesite have been classified into different categories by several researchers and institutes (Arıkan et al., 2007; Sari et al., 2010). The classifications are as follow; according to Geological Society of America (1963) Dark Gray (N4), Light Gray (N6), Pink (5RP4/2) and Light Pink (5P6/2); according to Kasapoglu (1980) bluish gray, pink and blackish violet; according to Ayday (1989), pink andesite (A type), dark pink – gray andesite (B type) and black andesite (C type). A type is the most weathered one and C type is the freshest one in this sort.

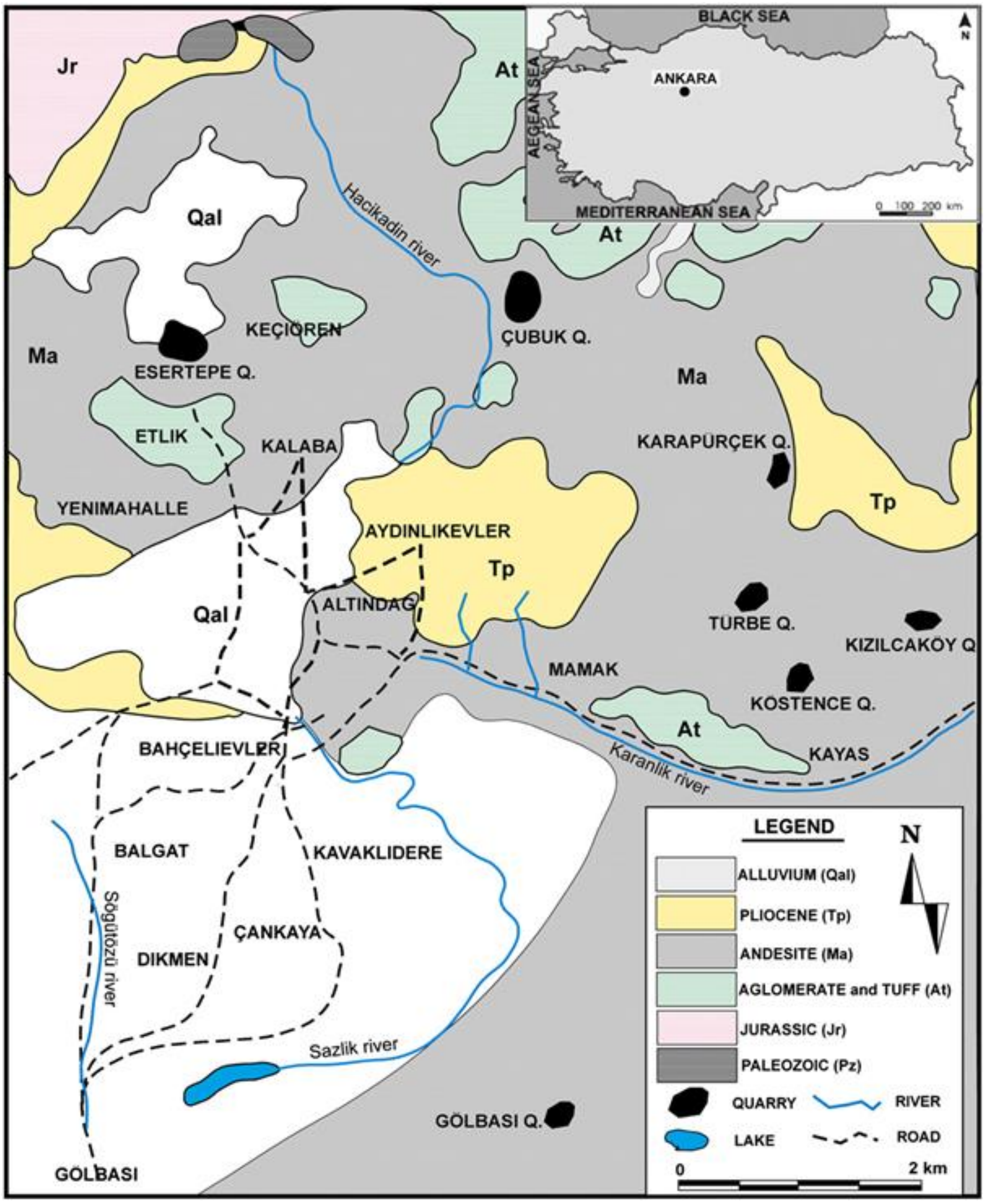

Figure 5.3 Location and geologic map of Ankara andesite area (Sari et al., 2010)

Chemical composition and physical - mechanical properties of Ankara andesite can be found in Table 5.1 and Table 5.2, respectively.

Table 5.1 Chemical composition of Ankara andesite

Oxides	%
SiO_2	55-62
Al_2O_3	15-20
Fe_2O_3	4-5
CaO	2-5
MgO	2-5
SO_3	0-1
Na_2O	0-2
K_2O	0-3
TiO_2	0-1

Table 5.2 Physical and mechanical properties of Ankara andesite

Parameter	Range	Reference
Uniaxial compressive strength (UCS)	22-115 53-128 83.72-87.50 72.15-119.89	(Arıkan et al., 2007) (Sari et al., 2010) (Binal, 2009) (Sonmez et al., 2006)
Unit weight (γ) (kN/m^3)	22-25 20.75-21.120 23.84-24.70	(Arıkan et al., 2007) (Binal, 2009) (Sonmez et al., 2006)
P wave velocity (m/s)	2198-4114 3828.66 (+-92.86)	(Arıkan et al., 2007) (Yavuz, 2011)
Tensile strength (MPa)	2.4-8.4	(Arıkan et al., 2007)
Block punch strength index (MPa)	6.2-26.7	(Arıkan et al., 2007)
Porosity (%)	7.9-19.5 8.76 (+- 0.90) 8.13-9.42	(Arıkan et al., 2007) (Yavuz, 2011) (Binal, 2009)
Water absorption (%)	3.80-4.42 3.81 (+-) 0.42	(Binal, 2009) (Yavuz, 2011)

By means of cultural value, Ankara andesite have been used since Roman times until today (Sari et al., 2010). However, the most important era for andesite is the early years of republican period.

(a)

(b)

(c)

Figure 5.4 Culturally important buildings made of Ankara andesite. a. The War of Independence Museum (housed in the First Turkish Grand National Assembly Building) b. Ankara railway station c. Rebuplic Museum (housed in the Second Turkish Grand National Assembly Building)

In this thesis, we have used black andesite (C type) supplied from local quarries (Kozak Granit). Physical characteristics of the raw stone can be found Table 5.3.

Table 5.3. Physical characteristics of the raw Ankara stone

Open Porosity (%)	10.527 (±0.003)
Unit Weight (γ) (kN/m^3)	22.532 (±0.806)
Ultrasonic Pulse Velocity (km/s)	3.798 (±0.124)
Surface Roughness (μm)	25.022 (±8.766)
Surface Hardness (HLD)	664.796 (±111.136)
Water Absorption (%) • BS EN 13755 Standard	4.533 (±0.101)

** In additional to this data, other properties such as XRD analysis or color values can be found in other sections.*

5.1.2 Bitlis (Ahlat) Stone

Ahlat, a district of Bitlis, is located in Eastern Anatolian Region of Turkey and surrounded by Nemrut and Suphan mountains. Because of these volcanic mountains the area is abundant with ignimbrite quarries. Ahlat stone, as a Nemrut ignimbrite, is widely used in the region since Seljuk time.

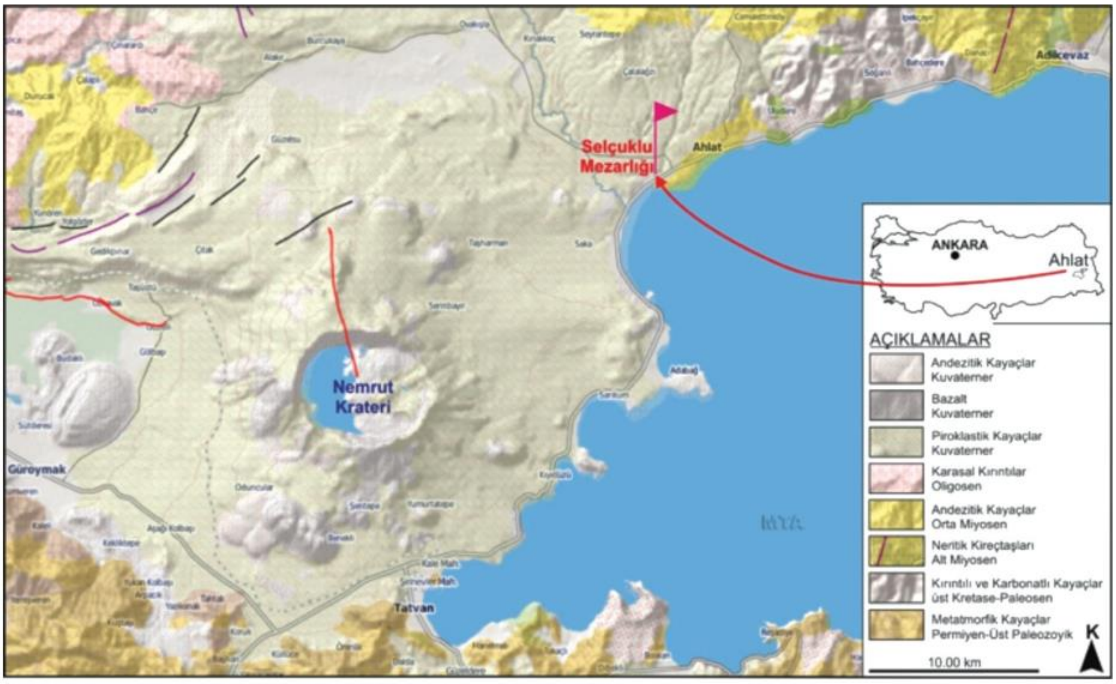

Figure 5.5 Geological map of Ahlat region (Akın et al., 2016)

From geological aspect, ignimbrites are volcanic pyroclastic rocks, which formed during volcanic eruptions with high temperature and gas pressure. They contain pumice, volcanic glass, lithic materials (Akın et al., 2017; Baykara & Işık, 2016; Özvan et al., 2015). Nemrut ignimbrites, are formed during pre-caldera stage of Nemrut mountain and they contain sanidine, plagioclase, linopyroxene and hornblende phenocryst in porphyritic matrix (Akın et al., 2017; Özvan et al., 2015). The difference in amount of these materials and welding degrees result different type of ignimbrites. The most important criterion on the differentiation is the color of the rocks caused by welding degrees. From bottom to top, the color changes from black / brown to red / grey (Akın et al., 2017).

Table 5.4 and Table 5.5 shows the chemical composition and physicomechanical properties of Ahlat stone. The data presented here belongs to dark brown type which is used in our study. Lightweight of the stone can be seen by dry unit weight, this is an important parameter to be used as construction material.

The variations in the table shows the differences between ignimbrites as mentioned above. It is also another point that there is a need of standardized classification among the stone to prevent confusion within researchers.

Table 5.4 Chemical composition of Bitlis stone

SiO_2 (%)	64.05	66.80
Al_2O_3 (%)	15.33	15.53
Na_2O (%)	5.46	5.85
Fe_2O_3 (%)	4.90	4.49
K_2O (%)	4.81	5.11
CaO (%)	2.00	1.46
MgO (%)	0.53	0.20
TiO_2 (%)	0.42	0.38
MnO (%)	-	0.14
P_2O_5 (%)	-	0.07
Reference	(Erdal, 2004)	(Özvan et al., 2015)

Table 5.5 Physical properties of Bitlis stone

Property	Range	Reference
Dry unit weight (kN/m^3)	11.0 – 12.4 14.95 – 16.54 18.63 – 18.83	(Akın et al., 2017) (Özvan et al., 2015) (Erdal, 2004)
Saturated unit weight (kN/m^3)	15.0 – 17.1 17.85 – 19.12	(Akın et al., 2017) (Özvan et al., 2015)
Apparent porosity (%)	28.1 – 38.5 25.11 – 30.47 26.62 – 28.09	(Akın et al., 2017) (Özvan et al., 2015) (Erdal, 2004)
Water absorption by weight (%)	31.3 – 46.5 15.27 – 18.71 18.3 – 20.2	(Akın et al., 2017) (Özvan et al., 2015) (Erdal, 2004)
Uniaxial compressive strength (MPa)	1.5 - 3.8 10.05 – 15.01 9.5 – 13.4	(Akın et al., 2017) (Özvan et al., 2015) (Erdal, 2004)
P-wave velocity (m/s)	1711 – 2600	(Özvan et al., 2015)
Bending strength (MPa)	1.59 – 1.66	(Erdal, 2004)
Water absorption in boiling water by mass (%)	30.2 – 36.9	(Erdal, 2004)
Abrasion (cm^3/50 cm^2)	26.5 – 27.0	(Erdal, 2004)

Table 5.6 shows the data on the raw Bitlis stones used in this thesis.

Table 5.6 Physical properties of raw Bitlis stone

Open Porosity (%)	32.479 (±0.509)
Unit Weight (γ) (kN/m^3)	14.355 (±0.148)
Ultrasonic Pulse Velocity (km/s)	2.512 (±0.051)
Surface Roughness (μm)	25.962 (±3.823)
Surface Hardness (HLD)	391.296 (±44.890)
Water Absorption (%) • BS EN 13755 Standard	20.181 (±0.092)

* *In additional to this data, other properties such as XRD analysis or color values can be found in other sections.*

Cultural importance of Ahlat stone is majorly known by Seljuk artefacts, such as *kumbet*s (Figure 5.6) and baths but especially the cemetery (Figure 5.7) (Özvan et al., 2015). There are approximately 1500 tombstones within 210.000 m^2 area, which means a magnificent area and number of artefacts in terms of conservation (Avsar & Güleç, 2019) The tombstones have highly important historical value in terms of the information on the carvings and the artistic features. The cemetery has been on the UNESCO World Heritage Tentative List since 2000, and the process is monitored by the ministry. Therefore, it is curial to handle the area interdisciplinary and take serious actions in terms of conservation.

Figure 5.6 Seljuk Kumbet (Özvan et al., 2015)

Figure 5.7 Ahlat cemetery (Avsar & Güleç, 2019)

5.1.3 Mardin Stone

Midyat stone, which is also known as Midyat formation, is a unique stone for Anatolia. From geological aspect, the stone has high carbonate contents, and is sourced from the Mardin region in the southeast of Turkey. The dominant geological unit of the region is limestone formed during the eocene and myocene periods. Horsts and grabens formed as a result of tectonic activities constitute the basic shape of the region. Graben regions caused accumulation for myocene and quaternary clays. These savings resulted in the creation of fertile agricultural lands for Mardin, Nusaybin, Cizre, Kızıltepe and Silopi regions (Figure 5.8). Mardin is approximately 1082 m above sea level and is founded on clay deposits continuing in the horizontal axis. The Eocene Hoya formation, known as Midyat stone, covers Diyarbakır, Siirt and Adıyaman regions outside the provincial borders of Mardin. The Hoya formation has a thickness of 50 to 600 m and the Midyat stone is collected from the quarries that are still open in the region (Kaya, 2008; Önenç et al., 2006; Şahin et al., 2013). Midyat stone has a partially dolomitic structure, with fine grains and high porosity. It is usually well-jointed and this high karstification creates small and medium scale caves. Currently, there are four quarries and fifteen workshops that collect and shape Midyat stone (Kazancı & Gürbüz, 2014; Şahin et al., 2013)

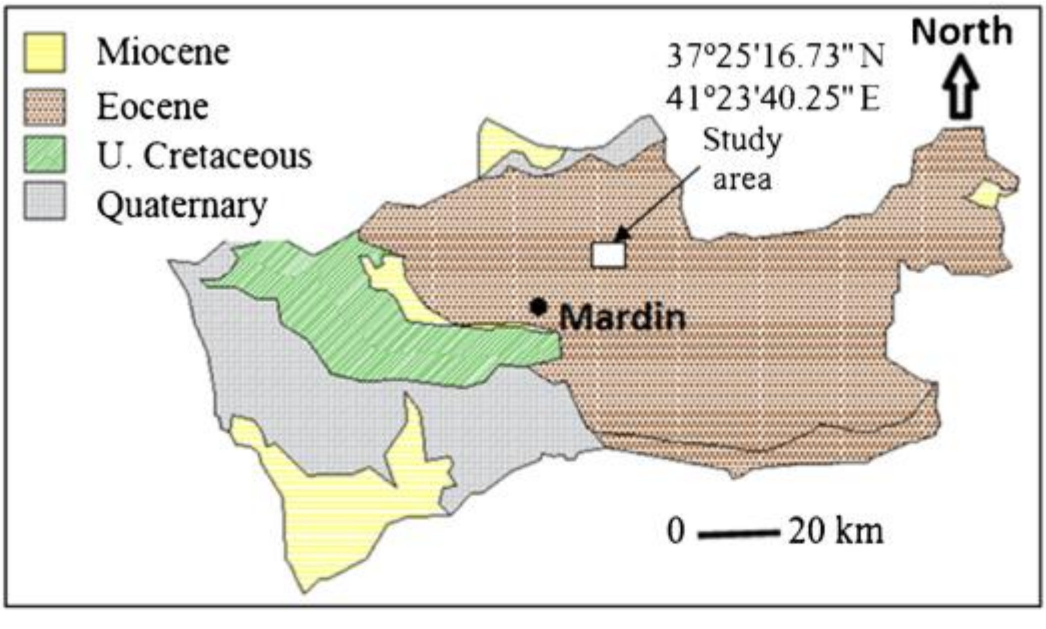

Figure 5.8 Geology map of Mardin (Agan & Cicek, 2020)

It has been used as a construction material for a long time because of its availability, low heat transfer coefficient (which aids the creation of a comfortable indoor environment), ease of carving so it can be used as a decorative element on the façades or extensions such as windows, doors etc, low maintenance requirement and stable characteristics over time. Therefore, it is still used by the local people as the main construction material.

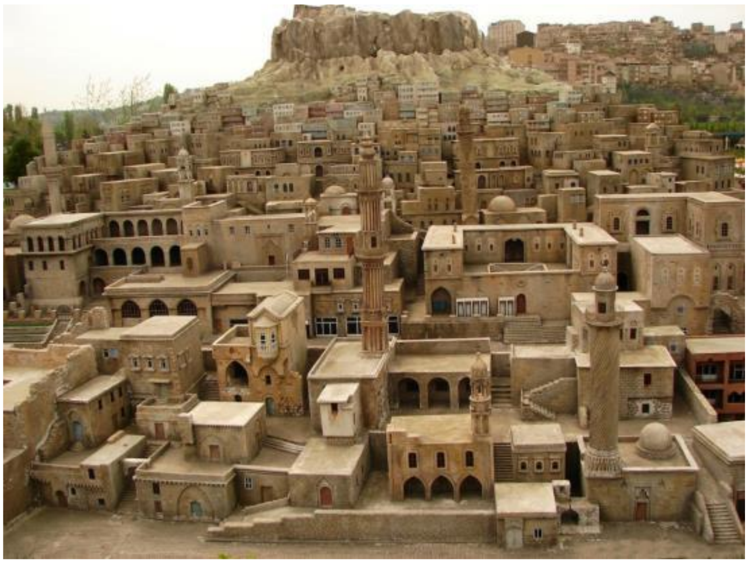

Figure 5.9 Midyat city constructed with Midyat stone

Midyat stone has a partially dolomitic structure, with fine grains and high porosity. When looking at the regional stratigraphy, it can be seen that it is found in Middle Upper Eocene age (Kaya, 2008; Önenç et al., 2006; Ozkaya, 1974). It is usually well-jointed and this high karstification creates small and medium scale caves. Currently, there are four quarries and fifteen workshops that collect and shape Midyat stone (Kazancı & Gürbüz, 2014; Şahin et al., 2013)

The stone is also important for the cultural heritage of the area. There are currently 1145 registered cultural assets in Mardin city and 965 of them are made from Midyat or Mardin stone (Günal, 2011). Some of them are quite old and important such as Zeynel Abidin Mosque Complex and Mor Yakup (Saint Jacob) Church (Figure 5.10) which was built in 320 AD and under UNESCO protection or Mor Hananyo Monastery which was built in 493 AD (Figure 5.11).

Chemical, physico-mechanical and thermal properties of Mardin stone are shown in Table 5.7, Table 5.8 and Table 5.9 respectively.

Figure 5.10 Zeynel Abidin Mosque and Mor Yakup Church

Figure 5.11 Hor Mananyo Monastery

Table 5.7 Chemical composition of Midyat stone

Mineral	%
CaO	45.36 ± 0.15
MgO	29.47 ± 0.10
SiO_2	1.42 ± 0.01
Fe_2O_3	1.24 ± 0.01
Al_2O_3	0.34 ± 0.01
SO_3	0.12 ± 0.01
Cr_2O_3	0.10 ± 0.01
BaO	0.10 ± 0.01
CuO	0.10 ± 0.01
V_2O_5	0.05 ± 0.01
As_2O_3	0.04 ± 0.01
SrO	0.03 ± 0.01
PbO	0.03 ± 0.01
Undefined	1.32 ± 0.13
Loss on ignition	20.24 ± 0.60
Reference	(Agan & Cicek, 2020)

Table 5.8 Physico-mechanical propertie of Mardin (Midyat) stone

Property	Range	Reference
Dry unit weight (kN/m^3)	16.57 16.9 ± 0.2	(Kaya, 2008) (Agan & Cicek, 2020)
Specific gravity	2,102 2,74	(Kaya, 2008) (Agan & Cicek, 2020)
Density (kg/m^3)	1680 1490 1960	(Agan & Cicek, 2020) (Özışık, 1985) (Semerci, 2008)
Apparent porosity (%)	27,63 16,2 28	(Kaya, 2008) (Agan & Cicek, 2020) (Semerci, 2008)
Water absorption by weight (%)	11,81 20,3 7,96	(Kaya, 2008) (Agan & Cicek, 2020) (Semerci, 2008)
Void ratio (%)	15,	(Agan & Cicek, 2020)
Uniaxial compressive strength (MPa)	22,67 23,39	(Agan & Cicek, 2020) (Semerci, 2008)
P-wave velocity (km/s)	2,81	(Semerci, 2008)
Bending strength (MPa)	3,4	(Agan & Cicek, 2020)
Modulus of elasticity (GPa)	21,3 21,4	(Agan & Cicek, 2020) (Semerci, 2008)
Poisson's ratio	0.20 ± 0.04	(Agan & Cicek, 2020)

Table 5.9 Thermal properties of Mardin (Midyat) stone

Property	Range	Reference
Specific heat ($J.kg^{-1}.°C^{-1}$)	881 1032	(Agan & Cicek, 2020) (Özışık, 1985)
Thermal diffusivity ($m^2.s\text{-}1.10^{-7}$)	4,18 4,68	(Agan & Cicek, 2020) (Özışık, 1985)
Thermal conductivity ($W.m^{-1}.K^{-1}$)	0,91 0,72	(Agan & Cicek, 2020) (Özışık, 1985)

Table 5.10 shows the physical information on the raw Mardin stone, collected within this thesis.

Table 5.10 Physical properties of Mardin stone

Open Porosity (%)	0.179 (±0.031)
Unit Weight (γ) (kN/m^3)	12.459 (±0.956)
Ultrasonic Pulse Velocity (km/s)	3.561 (±1.004)
Surface Roughness (μm)	27.760 (±8.664)
Surface Hardness (HLD)	290.778 (±74.636)
Water Absorption (%) • BS EN 13755 Standard	12.721 (±4.287)

5.1.4 Nevsehir Stone

The Cappadocia area, which covers approximately 40.000 km^2, lays on rich deposit of volcano-sedimentary sequences (Figure 5.12) (Erguler, 2009) (Topal & Doyuran, 1998). Covered by volcanos such as Erciyes, Melendiz and Hasandag the area is rich with volcanic rocks such as tuff, andesite and basalt (Erguler, 2009). Rock units found in this region covers Pre-Miocene basement rocks, alternations of Lower Miocene sedimentary rocks (red mudstone, sandstone, and conglomerates), Miocene volcano–sedimentary unit (Urgup Formation), and Quaternary deposits. Among these formations, the Urgup Formation, having around 400 m thickness, is the main lithological unit which formed famous fairy chimneys. (Erguler, 2009).

Ürgüp Formation comprises two levels of lava flows and nine Upper Miocene to Pliocene welded to non-welded rhyolitic ignimbrites interbedded with pumice-fall deposits, pyroclastic surge, and continental deposits including fluvial sediments (and calcareous-marly beds of lacustrine environment (Mauro Francesco, La Russa et al., 2014). Although having different sub-formations (Le Pennec et al., 1994) (such as Zelve, Cemilköy, Gördeles etc.) Kavak and Tahar formation are important, since they form most of the fairy chimneys and historical sites (Mauro Francesco, La Russa vd. 2014; Erguler 2009; Topal ve Doyuran 1998; 1997)(Dinçer & Bostancı, 2019).

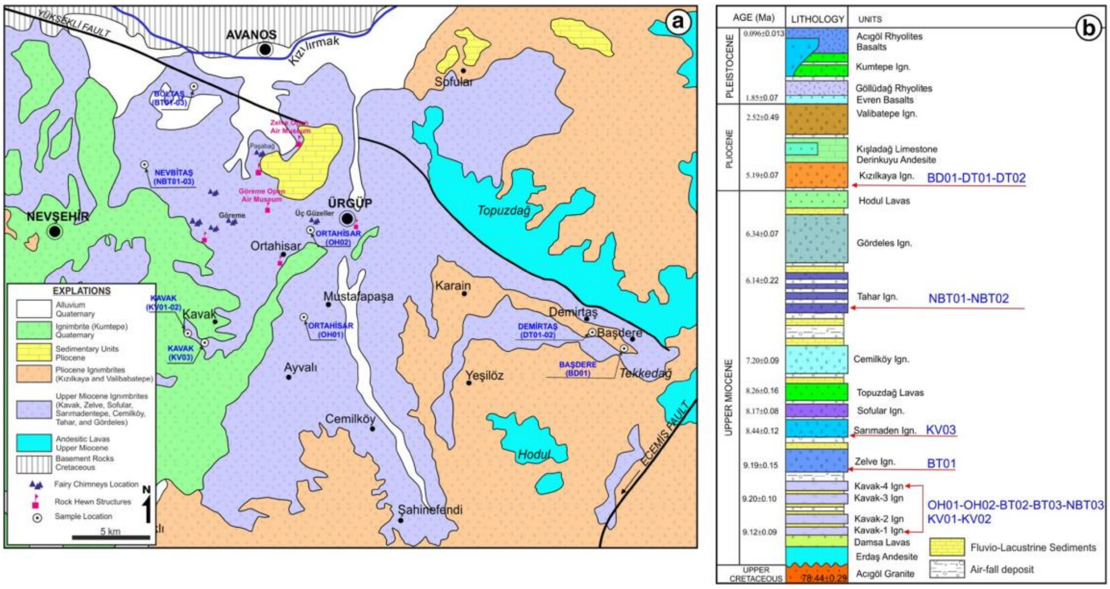

Figure 5.12 Geological map of Nevsehir region (Dinçer & Bostancı, 2019)

The literature data for composition and material properties of Cappadocian tuff is shown in Table 5.11, Table 5.12 respectively. The listed values belong to Kavak formation which is used in this study.

Table 5.11 Chemical composition of Nevsehir stone

Mineral	**%**	**%**	**%**
Plagioclase ($CaAl_2Si_2O_8$ (anorthite), $NaAlSi_3O_8$ (albite))	89.0	85.0	70.2
Quartz (SiO_2)	9.2	-	14.8
Feldspar ($KAlSi_3O_8$ – $NaAlSi_3O_8$ – $CaAl_2Si_2O_8$)	1.8	10.0	12.8
Biotite $K(Mg,Fe)_3(AlSi_3O_{10})(F,OH)_2$	-	5.0	2.2

Table 5.12 Physico-mechanical propertie of Nevsehir stone

Property	Range	Reference
Dry unit weight (kN/m^3)	13.60 (±0.11) 13.6 12.4 – 14.4 13.3 - 14.3 15.98 – 11.43	(Topal & Doyuran, 1997)* (Erguler, 2009) (Ulusay, 2006) [Tuncay (2009)] (Dinçer & Bostancı, 2019)
Apparent porosity (%)	38.29 (±0.38) 28.7 21-27 18.28 – 35.14	(Topal & Doyuran, 1997) (Erguler, 2009) [Tuncay (2009)] (Dinçer & Bostancı, 2019)
Water absorption by weight (%)	21.60 (±0.27) 17.0 11.52 – 28.03	(Topal & Doyuran, 1997) (Erguler, 2009) (Dinçer & Bostancı, 2019)
Uniaxial compressive strength (MPa)	6.63 (±0.67) 8.12 2.3 – 9.1 3.6 – 5.0 5.91 – 32.56	(Topal & Doyuran, 1997) (Erguler, 2009) [Ulusay, 2006] [Tuncay (2009)] (Dinçer & Bostancı, 2019)
P-wave velocity (km/s)	2.09 (±0.84) 1.23 – 2.30 1.23 – 2.79	(Topal & Doyuran, 1997) [Ulusay, 2006] (Dinçer & Bostancı, 2019)
Modulus of elasticity (GPa)	3.08 (±0.49) 1.14	(Topal & Doyuran, 1997) (Erguler, 2009)
Poisson's ratio	0.20 (+0.02)	(Topal & Doyuran, 1997)
Point load strength (MPa)	0.48 (±0.10)	(Topal & Doyuran, 1997)
Schmidt rebound hardness	27 (±3.3)	(Topal & Doyuran, 1997)
Tensile strength (MPa)	0.91	(Erguler, 2009)

**The corresponding values are belong to dry-vertical measurements.*

Table 5.13 shows the physical information on the raw Nevsehir stone, collected within this thesis.

Table 5.13 Physical properties of Nevsehir stone

Open Porosity (%)	27.891 (±5.022)
Unit Weight (γ) (kN/m^3)	12.940 (±0.350)
Ultrasonic Pulse Velocity (km/s)	36.142 (±8.860)
Surface Roughness (μm)	2.107 (±0.072)
Surface Hardness (HLD)	244.222 (30.855)
Water Absorption (%) • BS EN 13755 Standard	24.480 (±1.492)

By means of cultural importance, Cappadocia region stands in Central Anatolia and covers Nevşehir, Kayseri, Niğde and Aksaray provinces. The area is one of the most attractive touristic sites in Turkey (which attracted almost 4 milion torusits in 2019 thanks to its unique natural, historical and cultural value, which is also part of the world Heritage List since 1985. The famous landscape is mostly defined by the rock pillars formed by differential weathering, which known as *fairy chimneys* (Özşen et al., 2017). However, the rich culture of the region is not only about natural wonders but also covers cultural elements such rock-hewn churches, enormous man-made underground cities and monuments (Erguler, 2009) which all made of local stones.

Figure 5.13 *Fairy chimneys* in Capadoccia (Nevsehir) region

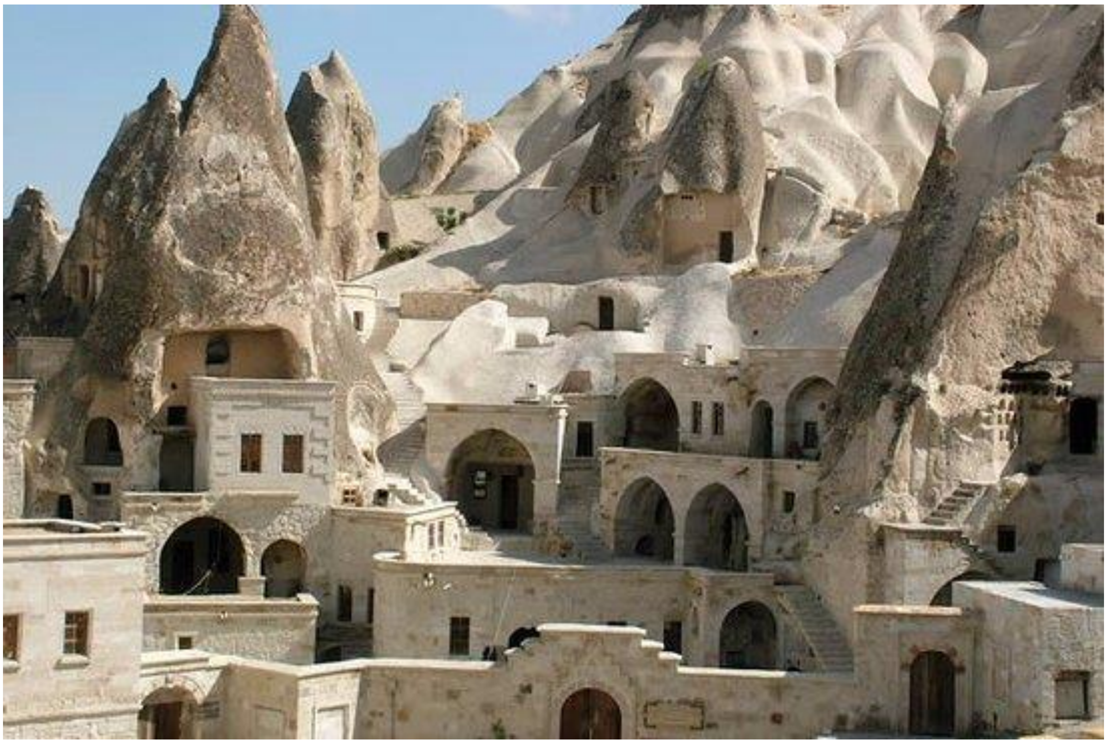

Figure 5.14 Historical masonary buildings in Capaddocia

Figure 5.15 Kaymakli underground city

5.2 Chemicals

Diammonium hydrogen phosphate (DAP) (CAS Number: 7783– 28–0, assay 98.0%, ACS) was purchased from Alfa Aesar. Calcium chloride (CAS Number: 10043–52-4, assay 96% extra pure, anhydrous) was purchased from Acros Organics. All water used was de-ionized.

5.3 Method

Within the scope of this thesis, accelerated aging tests (freeze-thaw and thermal degradation) prepared using experimental design were applied in order to derive the mathematical expressions of time-dependent changes for four different stone types unique to Anatolia (Ankara, Bitlis, Mardin, Nevsehir). As a comparison, weathering cabinet was used to observe the difference between manual and automated tests.

As the second part of the study, DAP consolidant, a new generation preservative, have been applied to all samples. In order to measure the effectiveness of the DAP, comparison tests were made using TEOS and the stability of the application was examined by weathering after the consolidant application.

As the last part of the study we have completed soft capping simulation study to analyse the effectiveness of soft capping on our stones.

Figure 5.16 shows the summary of the methodology.

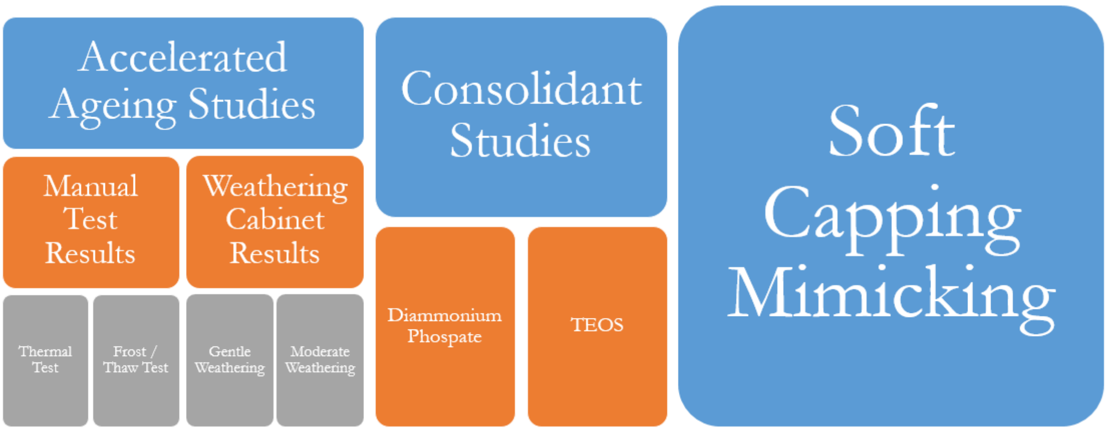

Figure 5.16 Summary of the methodology of the thesis

5.3.1 Preparation of the Samples

After supplying the stone samples from local quarries, all specimens have been cut to 5 cm x 5 cm x 5 cm cubes by using an industrial saw (Figure 5.17).

Figure 5.17 Ankara Stone is being cut by marble saw

5.3.2 Accelerated Ageing Tests

5.3.2.1 Manual Tests

In this thesis, thermal decomposition and freeze / thaw cycles performed as accelerated aging tests. In order to make a methodological comparison between experiment sets, experimental design method was used in thermal decomposition tests, and a set obtained from experimental design method was modified in freeze/thaw tests and the results were manually evaluated.

For thermal degradation tests, 3 different parameters were analyzed in 5 levels. In such a study, $3^5 = 243$ experiments are required to examine all combinations in an experimental system to be planned with traditional methods. This causes problems in terms of both material supply, analysis difficulty and time management. Where such a large number of experiments need to be carried out, the most common methods are experimental design methods.

In this study, the design summarized in Table 5.13 has been used for thermal degradation experiments. Accordingly, it can be seen that the Central Composite Design type is selected under the Response Surface Method (RSM).

Response Surface Method

Designing with the response surface method (RSM) allows one to quantify the relationships between one or more calculated responses and critical input factors. The central composite design (CCD) is the most common response surface method (RSM) design (CCD). There are three types of design points in a CCD:

(a) two-level factorial or fractional factorial design points

(b) axial points (sometimes called "star" points)

(c) center points

CCD's are designed to estimate the coefficients of a quadratic model. All point descriptions will be in terms of coded values of the factors.

The two-level factorial part of the design consists of all possible combinations of the +1 and -1 levels of the factors. For the two factors case there are four design points:

(-1, -1) (+1, -1) (-1, +1) (+1, +1)

Except for one factor, which has the value +/- Alpha, all of the factors in the star points are set to 0, the midpoint. The star points for a two-factor problem are:

(-Alpha, 0) (+Alpha, 0) (0, -Alpha) (0, +Alpha)

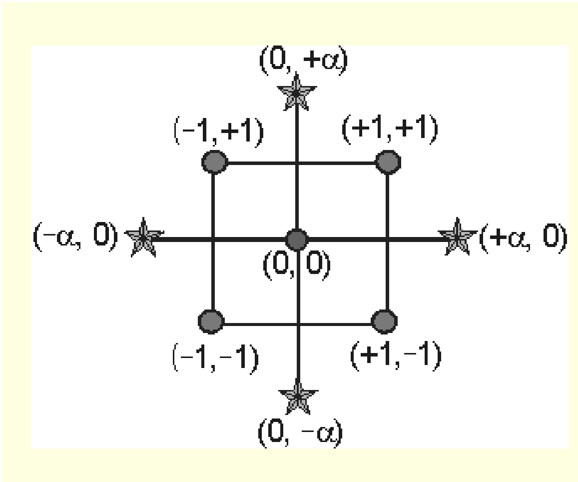

Figure 5.18 Central composite design diagram

For both rotatability and orthogonality of blocks, the value for alpha is determined in each design. The experimenter has the option of selecting one of these values or entering a new one. The rotatable value is the default value.

The star points can also be placed on the face of the cube portion of the design. A face-centered central composite pattern is a known one. By setting the alpha value to one or selecting the Face Centered choice, you can achieve this datum. Each factor only needs three levels in this design.

Center points, as implied by the name, are points with all levels set to coded level 0 - the midpoint of each factor range: (0, 0).

To get a fair estimate of experimental error (pure error), center points are normally replicated 4-6 times. With two variables, for example, the design would have five centered points by necessity.

To summarize, there are five levels of each element in central composite designs: -alpha, -1, 0, 1, and +alpha. The central composite design's construction lends itself to sequential experimentation, which is one of its redeeming qualities. Blocks may be used to create central composite designs.

- **Thermal Degradation**

Thermal decomposition is one of the important mechanical degradation elements based on the expansion of stones in conditions where the continental climate is dominant. Extensive information on the subject has been given in previous chapters.

In the thermal decomposition experiments carried out in this study, samples were exposed to temperatures of 30°C, 50°C , 70°C, 90°C and 110°C for different periods and then taken into baths containing distilled water. According to the experiment plan shown in Table 5.15, the cycle applied for experiment 2 is as follows; 16 hours in a 50°C oven, then 8 hours in a room temperature distilled water bath. In this way, a cycle was obtained and the trial was terminated at the end of 20 cycles.

The tables show the experimental design setup (taken from software) (Table 5.14), levels of parameters (Table 5.15) and final experimental plan for thermal degradation (Table 5.16) at below.

Figure 5.19 and Figure 5.20 shows the laboratory visuals of thermal degradation experiments.

Figure 5.19 T2 series inside the oven at 50°C

Figure 5.20 T2 and T5 series inside the water bath for water treatment phase

Table 5.14 Experimental design setup from software data

Design Summary									
Study Type	Response Surface		**Runs**	15					
Initial Design	Central Composite		**Blocks**	No Blocks					
Design Model	Quadratic								
Factor	**Name**	**Units**	**Type**	**Low Actual**	**High Actual**	**Low Coded**	**High Coded**	**Mean**	**Std. Dev.**
A	Temperature	C	Numeric	50	90	-1	1	70	20.65591118
B	Number of Cycles	day	Numeric	20	40	-1	1	30	10.32795559
C	Duration of exposure	hour	Numeric	16	20	-1	1	18	2.065591118

Table 5.15 Levels of each parameter for ageing procedures

THERMAL		
Durations in the cycles (hour in oven/hour in water)	**Number of cycles (24 hour = 1 cycle)**	**Temperature (°C)**
22/2	10	Room Temperature
20/4	20	50
18/6	30	70
16/8	40	90
14/10	50	110

Table 5.16 Final experimental plan for thermal degradation

Run Number	Temperature (°C)	Number of Cycle (days)	Duration (hour in oven)
T1	30	30	18
T2	50	20	16
T3	50	20	20
T4	50	40	20
T5	50	40	16
T6	70	30	22
T7	70	30	14
T8	70	50	18
T9	70	10	18
T10	70	30	18
T11	90	40	20
T12	90	20	20
T13	90	20	16
T14	90	40	16
T15	110	30	18

- **Frost / Thaw Experiment**

It was stated in the previous chapters that the freeze-thaw event caused serious mechanical damage, especially in conditions dominated by the continental climate.

In this study, experiments were made at -20 ° C, -15 ° C, -5 ° C and 0 ° C in order to investigate the effects of this phenomenon. The samples were kept in refrigerators with manually controlled thermometers and then taken into distilled water baths at room temperature. The cycle of Example 1 in the test set given in Table 5.17 is as follows: 6 hours at -20 ° C followed by 18 hours at room temperature. In this way, one cycle was completed and the trials were terminated, when there was a total of 30 cycles.

Table 5.17 Experimental setup for frost/thaw experiments

Run Number	Temperature (°C)	Duration of Exposure (Frost hour)	Number of Cycle (Days)
F1	-20	6	30
F2	-15	8	40
F3	-15	4	40
F4	-15	4	20
F5	-15	8	20
F6	-5	4	40
F7	-5	4	20
F8	-5	8	40
F9	-5	8	20
F10	0	6	30

Laboratory photo belonging to the cycles is shown in Figure 5.21.

Figure 5.21 F5 series inside the deep freezer at -15^{o}C

5.3.2.2 Weathering Cabinet Tests

In order to make a comparison with manual weathering and deciding right conditions for weathering step of DAP treatment, we took three different blocks for each stone type and used a weathering chamber Sanyo-FE 300H/MP/R20 as can be seen in Figure 5.22.

Deciding weathering conditions can be challenging since the debate continues on the best strategies for simulating the ageing. Simply, there are two edges; applying unrealistic, harsh conditions and applying realistic, mild conditions. Both have certain disadvantages and advantages. In this study, we have applied real mean values (gentle) and maximum/minimum temperatures (moderate) to compare the results.

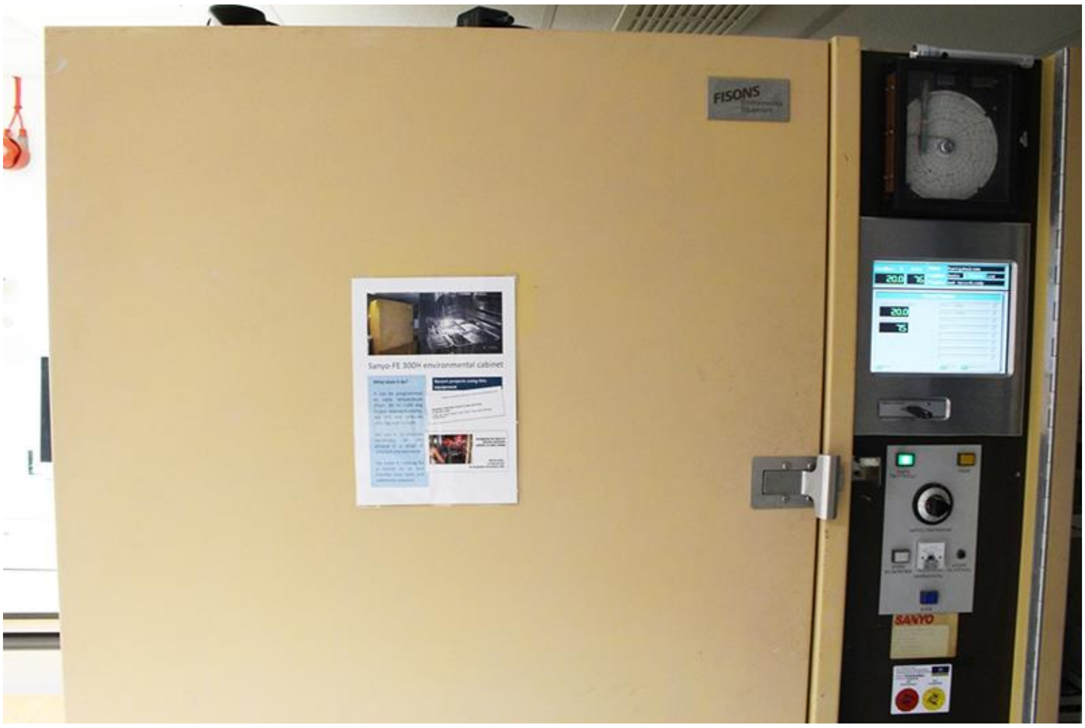

Figure 5.22 Environmental cabinet (Sanyo-FE 300H/MP/R20)

- **Gentle Weathering Conditions**

Table 5.18 shows the real meteorological data from original locations of the samples. In order to investigate the effect of real conditions, first we applied realistic conditions which covers maximum and minimum temperatures of the seasons for overall regions (Figure 5.23). We started as winter conditions and we represented 1 month in 24 hour. Then we analysed the results for physical properties such as surface hardness, color, surface roughness and UPV.

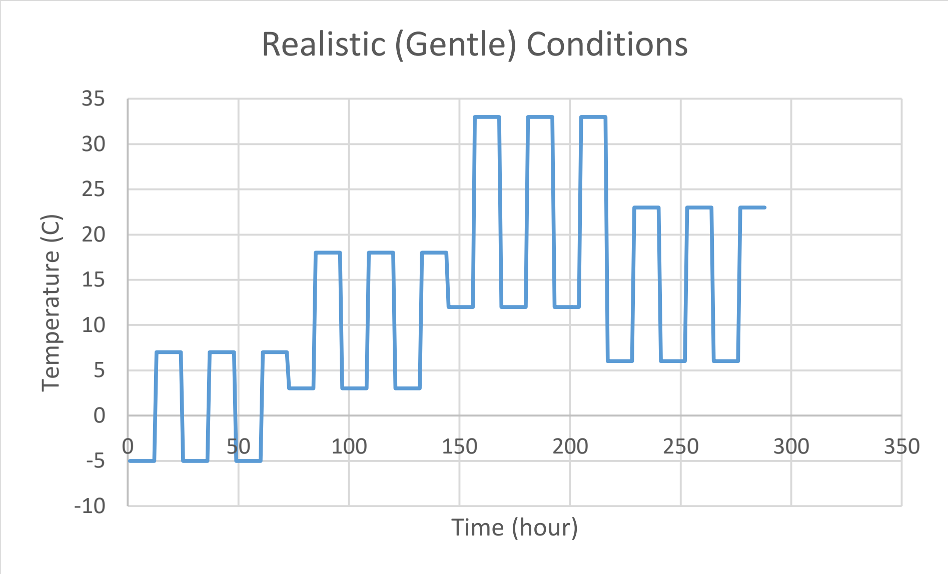

Figure 5.23 Realistic (gentle) conditions for pilot study

Table 5.18 Meteorological data from original locations of the samples

	DEC	JAN	FEB	MAR	APR	MAY	JUN	JUL	AGU	SEP	OCT	NOV
ANKARA												
Average Max Temperature (°C)	6,4	4,1	6,3	11,4	17,3	22,3	26,6	30,2	30,3	25,9	19,8	12,9
Average Min Temperature (°C)	-0,8	-3,3	-2,4	0,5	5,2	9,6	12,8	15,7	15,9	11,7	7	2,4
BITLIS												
Average Max Temperature (°C)	3,2	1,1	2,2	6,1	12,9	19,2	25,3	30,4	30,7	26,2	18,5	10,1
Average Min Temperature (°C)	-4,3	-5,6	-5,8	-2	3,2	7,4	11,5	15,6	15,1	10,7	6,3	0,9
MARDIN												
Average Max Temperature (°C)	8	5,7	7,1	11,4	17,2	23,8	30,5	34,9	34,6	30	22,7	14,4
Average Min Temperature (°C)	2,7	0,5	1,3	4,5	9,6	14,9	20,1	24,4	24,6	20,7	14,5	8
NEVSEHIR												
Average Max Temperature (°C)	5,9	3,7	5,3	10,1	15,7	20,4	24,7	28,3	28,4	24,3	18,1	11,6
Average Min Temperature (°C)	-1,5	-3,8	-2,8	0,5	4,9	8,6	11,4	13,4	13,2	10,1	6,5	2,2

- **Moderate Weathering Conditions**

After observing minimal difference for gentle weathering conditions, maximum (July - Mardin) and minimum (February – Bitlis) temperatures of the year for the cities which samples come from (Table 5.18) have been tested. Each cycle was set according to following program: cooling down to –5°C in 1 h; waiting time at, –5 (±1) C for 11 h; heating up to 35 °C in 1 h, waiting time at 35 (±1) °C for 11 h. The weathering consisted 20 cycles. Figure 5.24 shows the real data collected inside the chamber.

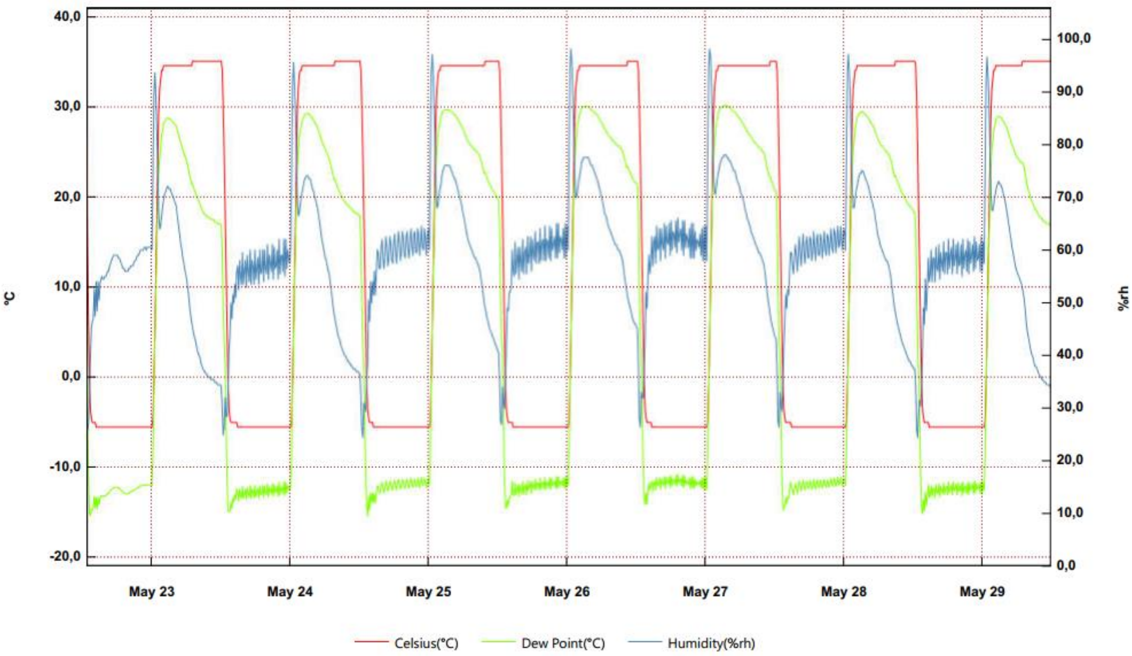

Figure 5.24 Real temperature, relative humidity and dew point data from inside the cabinet. The data collected by using extra USB data logger to check cabinet values

After 20 cycles (20 days) the samples have been collected and analysed for surface hardness, ultrasound pulse velocity and surface roughness.

5.3.3 DAP Treatment

In this study, a research was carried out to measure the effectiveness of DAP, especially on low carbonate stones (Ankara, Nevsehir, Bitlis ones). For this purpose, 1 M DAP solution was prepared in distilled water at room temperature. In previous literature studies, it was observed that Ca^{2+} ion additive increased the effectiveness of DAP especially in low-carbonate stones. For this reason, Ca^{2+} contribution of 1 mM was provided by using $CaCl_2$ in this study. The application was applied to the marked single surfaces of the stone cubes of 5x5x5 cm previously prepared with a brush, as shown in Figure 5.25, with a 2-minute intervals, by applying 20 times. Subsequently, the samples were kept under room conditions for 48 hours and then they were submerged into water to clean from unreacted DAP. Then it was dried in an oven at 40 ° C for 24 hours. Later, the samples were taken into desiccators and then analysed.

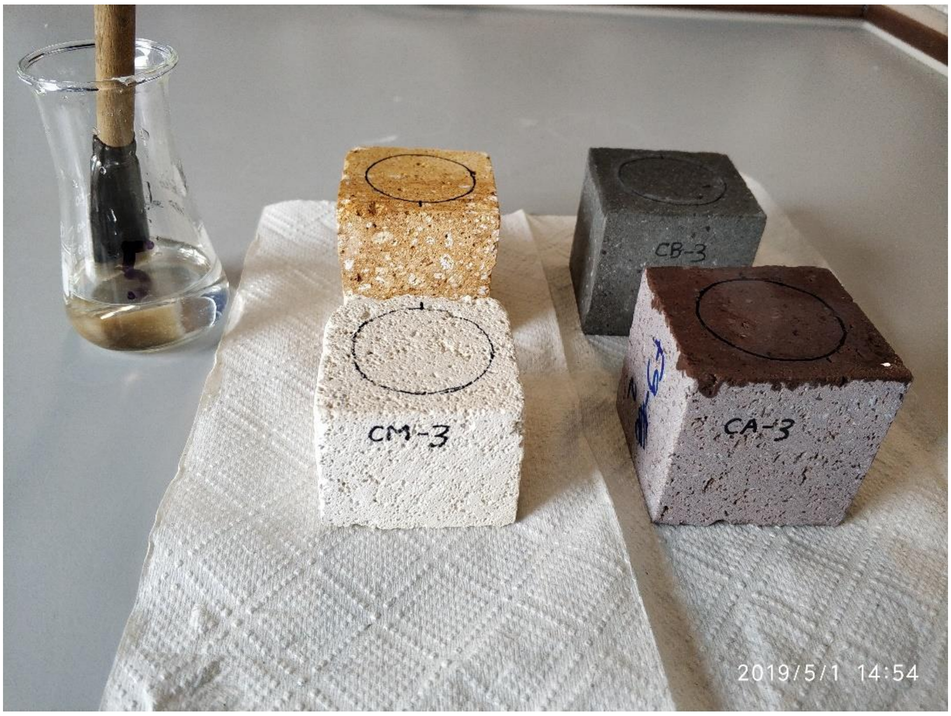

Figure 5.25 Application of DAP treatment

- **TEOS Treatment**

TEOS is the most common consolidant used for silicate stones both in the literature and field. Therefore, we used a commercial product (Wacker Silres BS OH 100) as a TEOS source for comparison.

The TEOS treatment has been applied by following the manufacturer's instructions for the product. First, we rinsed the stones with de-ionized water and dried at 40◦ C. Then we applied the product by brushing for 20 times with two minutes intervals. After that, we left the samples at in room temperature for one week and then carried out the analysis without any operation.

5.3.4 Analytical Techniques

The samples were exposed to different physical and mechanical analysis.

- **Weight**

Weight measurements were taken to determine the amount of consolidant remaining in the stone. Measurements were taken as dry weights before application of the treatment, and after rinsing and drying steps, and the difference in weight (in g and %) calculated.

- **Water Absorption**

Water can affect porous stone by dissolving the original material, causing freeze and thaw impact and creating a medium for water soluble salts. Therefore, it is important to determine water transportation properties for built heritage materials.

In this study two different standards have been used to determine water absorption. Firstly, BS EN 13755:2008 (Natural stone test methods — Determination of water absorption at atmospheric pressure) has been followed for untreated samples. The method consists of gradual immersion of samples in water and calculating the percentage of absorbed water as % of initial dry weight (5.1). Since the procedure involves total immersion of samples, it cannot be used reliably to determine the impacts of treatment on one side of the cubic samples. Therefore, we applied BS EN 16302:2013 (Conservation of cultural heritage — Test methods — Measurement of water absorption by pipe method) which uses Karsten tubes on single surfaces, to investigate the difference between treated and untreated surfaces.

$$\text{Ab (wt\%)} = [(\text{Wetweight} - \text{Dryweight})/\text{Dryweight}] \times 100. \quad (5.1)$$

Figure 5.26 Water absorption analysis with Karsten tube

The theory of the pipe method depends on the measurement of the rate of the absorbed water by using a standardized tube (Karsten tube) with specific volume and height (Figure 5.26). The tube is filled until the zero point and height difference is recorded with respect to time. The measurements for treated surfaces taken 2 days later than rinsing and drying procedure.

- **Surface Hardness**

Surface hardness properties are often used to estimate the mechanical durability of the materials, especially in the field. In this study, hardness measurements were made using a dynamic hardness test based on a rebound technique (Equotip, Proceq, Switzerland) 550 Leeb with D probe (Figure 5.27). Nine single impact measurements were taken for treated and untreated surfaces for each replicate. Three samples were used for each condition. The calculations based on dynamic rebound testing method according to Leeb (Figure 5.28).

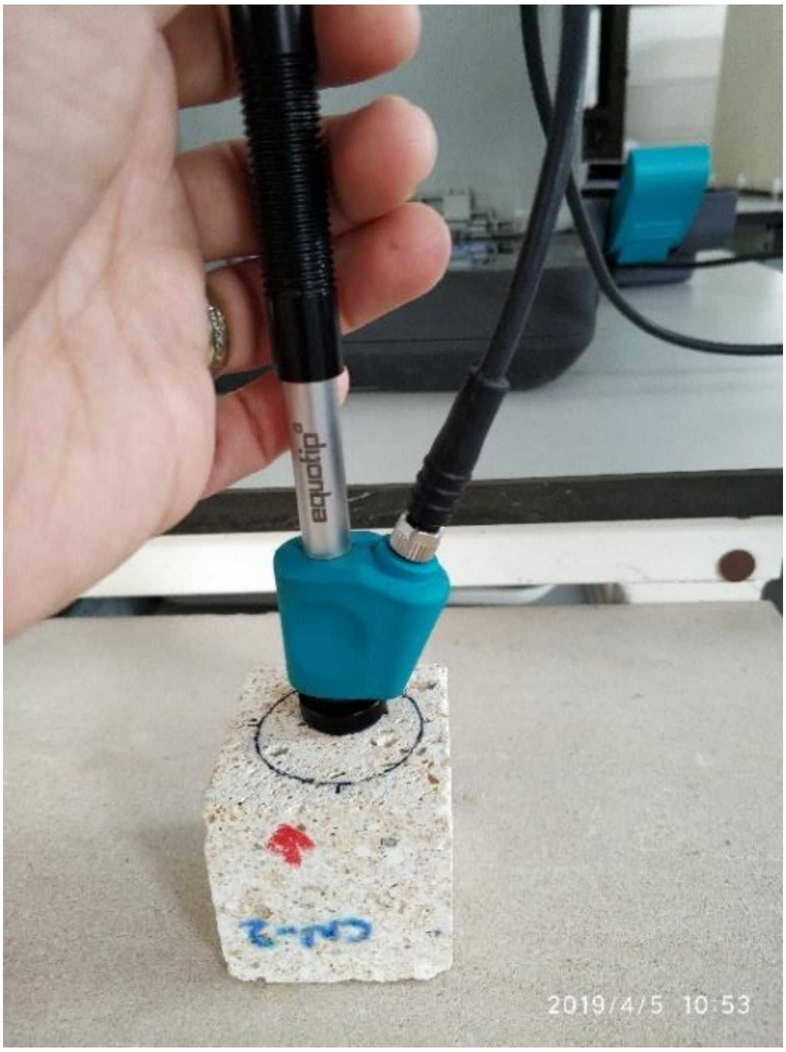

Figure 5.27 Surface hardness analysis with Equotip, Proceq

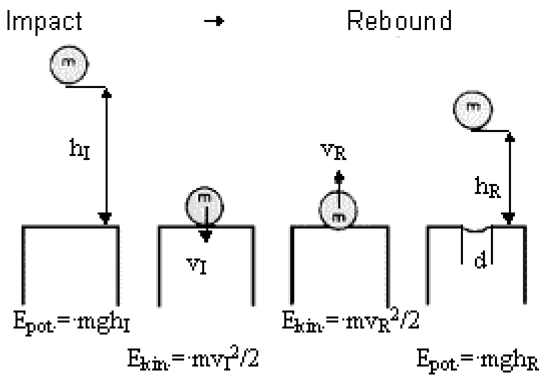

Figure 5.28 Theoretical diagram of rebound testing

- **Ultrasonic Pulse Velocity (UPV) Analysis**

Ultrasonic pulse velocity (UPV) tests are carried out to determine the sealing efficiency of consolidants on micro-cracks. In this study, UPV analysis was carried out using a Pundit Lab (+) (Proceq, Switzerland) (Figure 5.29). The transducers were located directly opposite one another on the consolidated and opposite surfaces. The width of the samples varied between 40 – 45 mm. Calculations were made individually for each sample by using exact distance between the transducers. The measurements were repeated three times for each sample. Analysis was carried out on dry samples.

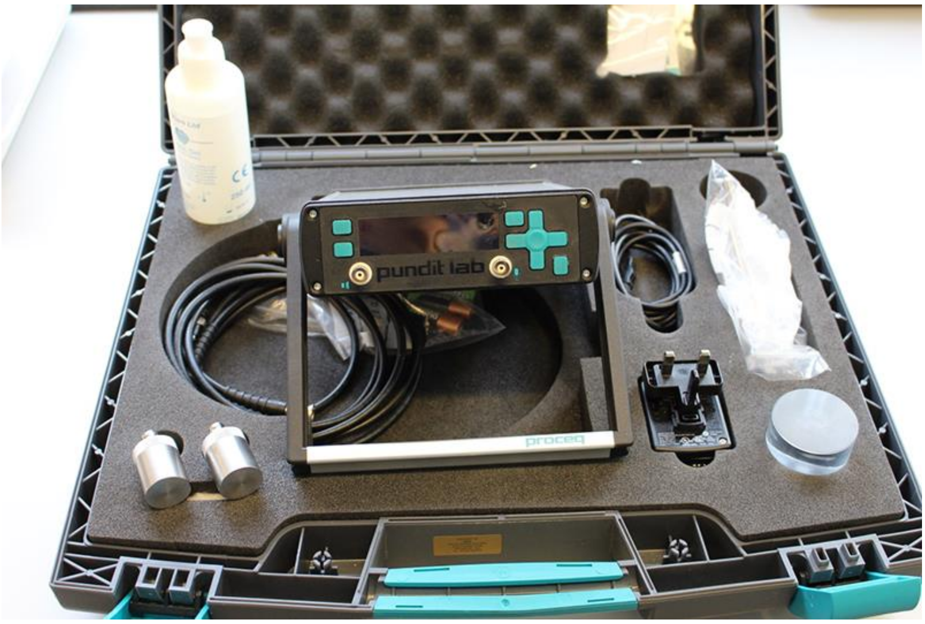

Figure 5.29 Ultrasonic Pulse Velocity (UPV) Analysis Equipment (Pundit Lab+, Proceq)

- **Drilling Resistance Measurement System (DRMS) Analysis**

In this study, we used DRMS (Sint Technology) (Figure 5.30). Measurements were taken from consolidated and untreated surfaces on the same samples. Two holes were drilled for each analysis. Rotational speed was 800 rpm. Drill radius was 5 mm. Drilling rate was 10 mm/min. Reference measurements were carried out on a standard block between each measurement and results standardized for each sample by using reference measurements.

Figure 5.30 DRMS Analysis Equipment (SINT Technology)

- **Color Difference**

Color difference is one of the most common analysis on stone heritage especially for treated façades. According to CIE standards, if ΔE values are smaller than 3.5; it means acceptable change which is not recognizable by untrained human vision.

In this study, a hand held spectrophotometer (Konika Minolta CM-700d) (Figure 5.31) was used to determine color properties. Nine spots were measured on each sample, and three samples were used for each stone type. All measurements were taken on dry samples. Calculations are made according to CIE2004 standard.

Figure 5.31 Hand held spectrophotometer (Konika Minolta CM-700d)

- **Surface Roughness**

Surface roughness measurements are used to determine material loss from the surface due to the environmental factors or the effects of consolidants on the sample surface.

In this study, an optical roughness profiler, the TraceIt (Innowep) (Figure 5.32), was used to determine the surface roughness. The samples were marked to ensure that the same spot could be located before and after treatment and weathering. Each analysis was repeated three times for each sample. Rz (Mean Roughness Depth) values have been calculated. X axis values for Rz were taken for making a clearer comparison, since the samples did not show any orientation.

Figure 5.32 Surface roughness experimental setup (TraceIt, Innowep)

5.3.5 Soft Capping Experiments

Soft capping is basically the technique that uses high plants on structures to protect them from temperature variations. Since it effects the appearance of the site, it is usually applied in ruins and on horizontal line. However, there are different methods that uses microorganism for conservation (Carter & Viles, 2005; de la Rosa et al., 2013; Gadd & Dyer, 2017; Gowell et al., 2015) and they are applicable on vertical walls and whole buildings. Therefore, we have decided to simulate a potential lichen application on our stones rather than applying soft capping as understood in literature. In order to find the suitable mimicking agent, we selected certain criteria such as; being water permeable, moisture permeable, being thin, being adhesive and non-toxic property. After investigating different options, we decided to use fabric band aids for this purpose. Two samples and two controls have been prepared for each stone type. A programmed light source used to mimic sunlight (Figure 5.34). Water sprayed once a day to mimic rainfall. Temperature difference have been measured by using two probes (Tiny Tag) on the surface and inside the sample, as can be seen in Figure 5.33. The samples are prepared and exposed to climatic conditions to determine the effect of temperature and light. The same temperature conditions used as described in Moderate Weathering Conditions section, with adding of rainfall simulation.

The difference on the temperature values can be found in Results section.

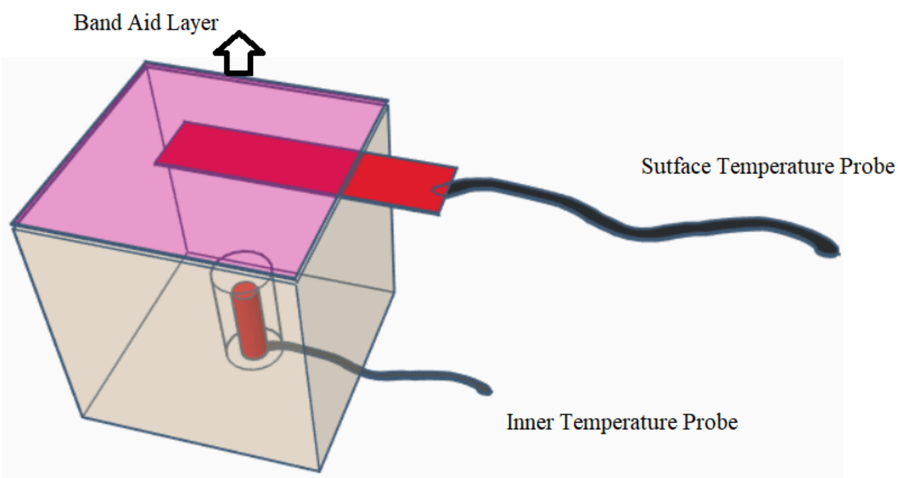

Figure 5.33 Visual description of soft capping mimicking setup for the samples

Figure 5.34 Real setup for soft capping experiment. The image shows covered and uncovered (control) samples for Mardin and Nevsehir stones. Lamp is installed about 20 cm above the stones. All soft capping experiment carried out inside the weathering chamber.

6
RESEARCH FINDINGS

6.1 Accelerated Ageing Studies

For accelerated ageing studies, we have been applied two different procedure, as explained in Materials and Method section. Firstly, in order to decide weathering conditions after DAP treatment, we have put the samples into weathering cabinet and collected certain data. Secondly, we carried out manual weathering, which consist thermal degradation and frost/thaw tests, as explained in previous section. Finally, we have compared the weathering techniques.

6.1.1 Weathering Cabinet Results

As explained in the previous section, the tests carried out in the cabin were carried out under two different plans, gentle and moderate ones. Under conditions called gentle or realistic, real meteorological data were used exactly, and in moderate conditions, the observed maximum and minimum temperatures for all four regions were selected and experiments were carried out by repeating them. Samples were analyzed with different analysis methods and comparisons were made.

6.1.1.1 Gentle (Realistic) Conditions

- Surface Hardness

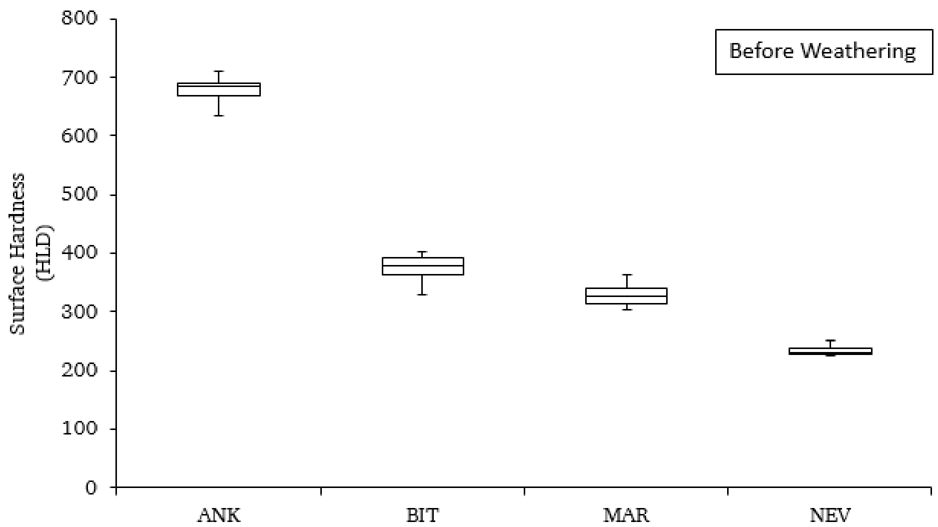

	ANK	BIT	MAR	NEV
Min	601	330	303	225
Median	685.5	379	326	230.5
Max	712	402	364	254

Figure 6.1 Surface hardness results before gentle weathering

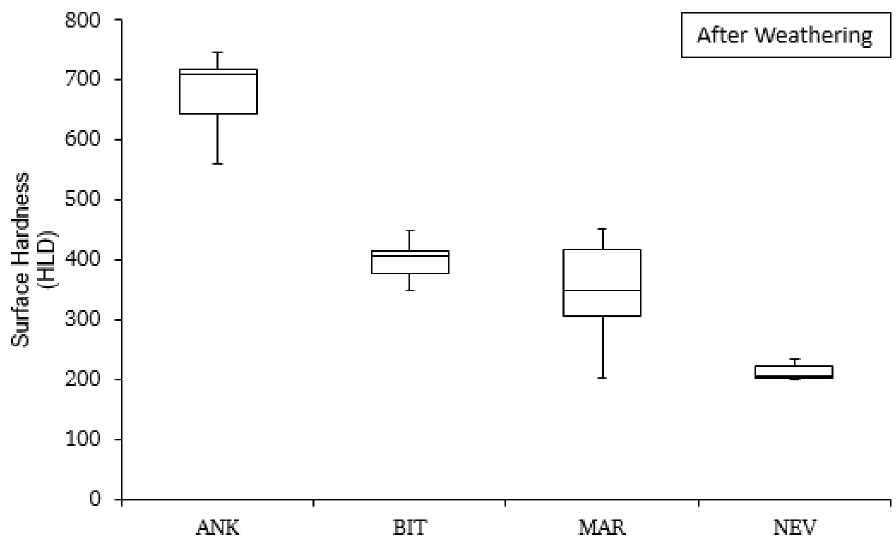

	ANK	BIT	MAR	NEV
Min	562	348	204	201
Median	709	405	350	206
Max	747	449	451	234

Figure 6.2 Surface hardness results after gentle weathering

• While a decrease was expected in the median values of all samples, an increase was observed. This could be because of combined frost and thaw and thermal degradation procedure happened inside the cabinet.

• A decrease in minimum values was observed in all samples except Bitlis stone. An increase in the maximum values was observed in all samples except Nevşehir stone. When these two results are evaluated together, it is seen that there is a general range widening as a result of weathering using cabin.

• However, it is an expected result that the obtained changes are also smaller, since the applied temperature values are at a less aggressive level than thermal degradation or frost/thaw simulation.

- Ultrasonic Pulse Velocity

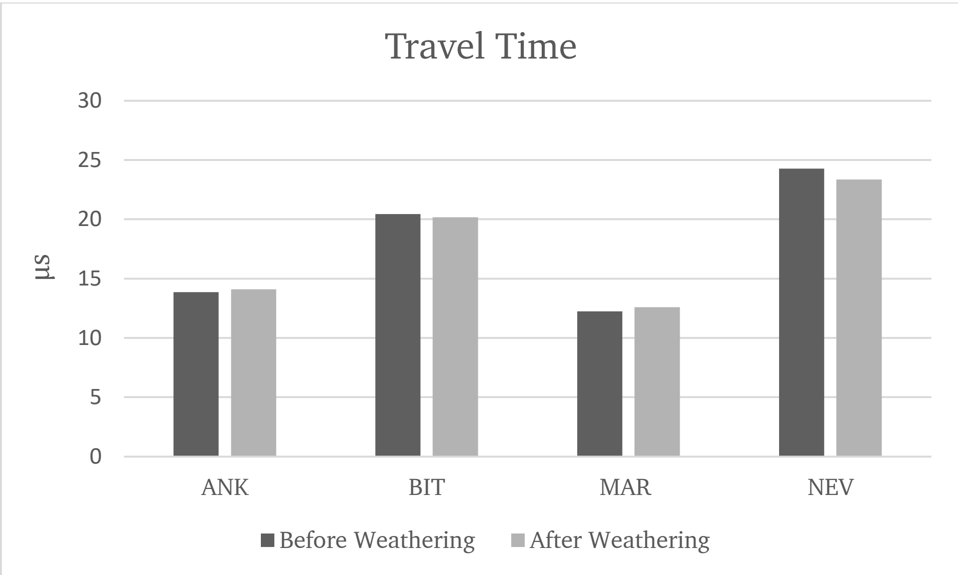

Figure 6.3 Travel time (µs) for Ultrasonic Pulse Velocity (UPV) analysis for gentle weathering

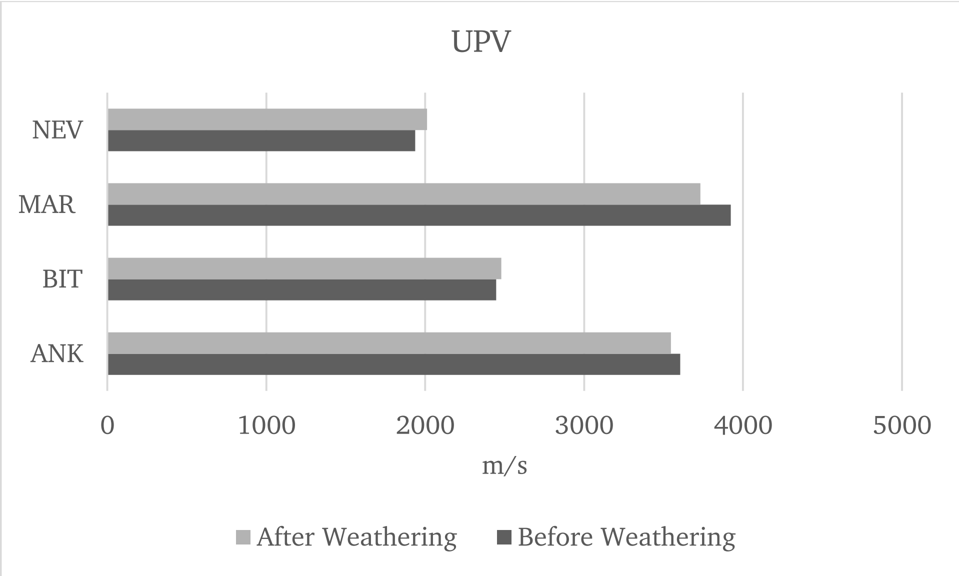

Figure 6.4 Velocity values (m/s) for Ultrasonic Pulse Velocity (UPV) analysis for gentle weathering

Since UPV results give information about the structural integrity of the material, it is expected that UPV values will decrease in m/s and travel time will increase as a result of aging processes. As a result of gentle weathering performed here, a small decrease was observed in UPV values in Mardin and Ankara stones, while a partial increase was observed for Bitlis and Nevsehir ones.

When the results are evaluated proportionally, it can be said that very high changes are not observed in parallel with other analyses. The reason for this is that no aggressive conditions are used in the method applied.

6.1.1.2 Moderate Weathering Conditions

- Surface Hardness

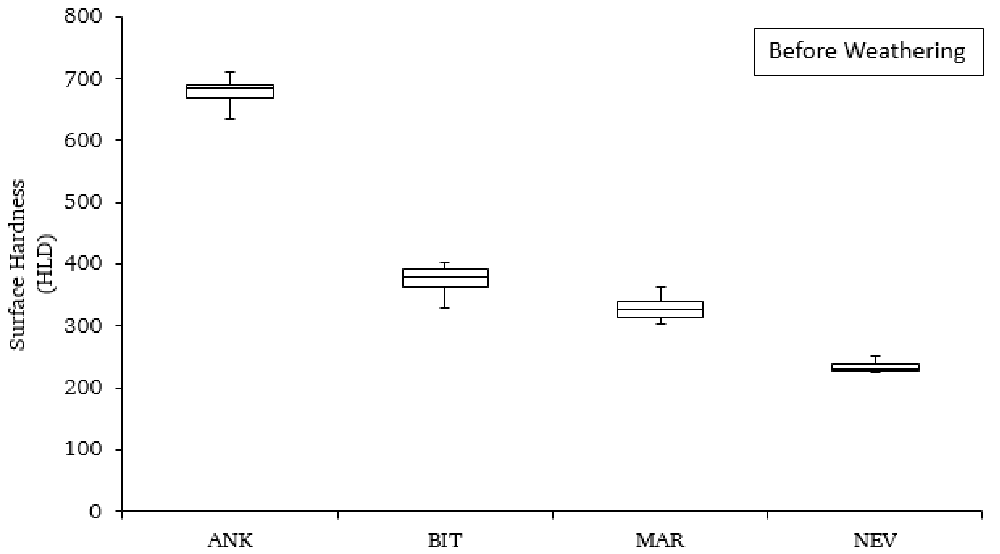

	ANK	BIT	MAR	NEV
Min	601	330	303	225
Median	685.5	379	326	230.5
Max	712	402	364	254

Figure 6.5 Surface hardness results before moderate weathering conditions

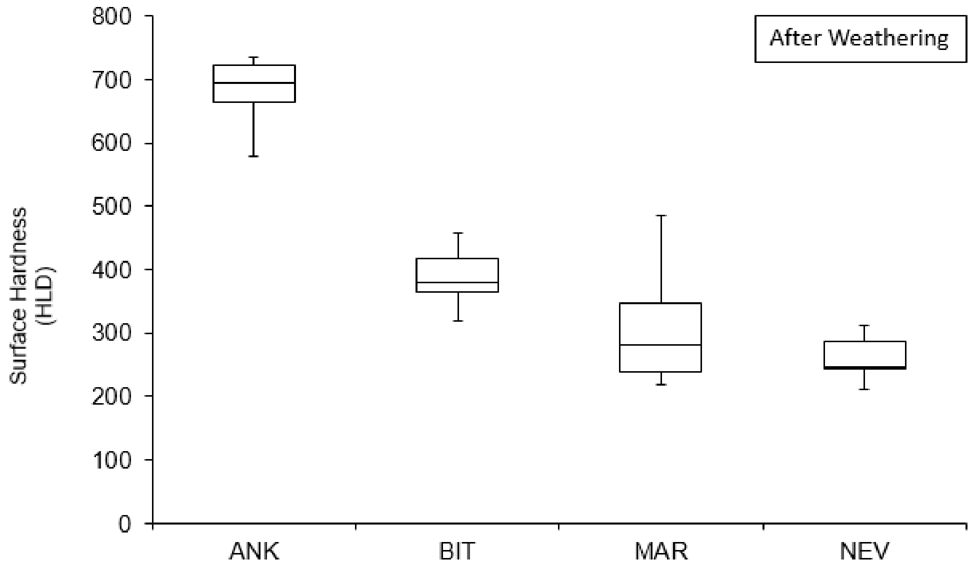

	ANK	BIT	MAR	NEV
Min	360	319	220	212
Median	695	381	282.5	247
Max	735	459	486	313

Figure 6.6 Surface hardness results after moderate weathering conditions

• Similar to the results of gentle weathering, an increase in the median values was observed in all samples except Mardin stone.

• Apart from this, minimum values for all samples decreased, this decrease was very dramatic especially in Ankara and Mardin stones. Similarly, in all of the samples, maximum values also increased, and the highest increase was on Mardin stone. Accordingly, it can be said that the widening of the ranges of values is observed as a result of moderate weathering in all of the samples and especially in Mardin stone.

• However, it can be said that the reason why the changes are somewhat greater than the results of gentle weathering is directly related to the slightly more aggressive conditions applied.

- Surface Roughness Results

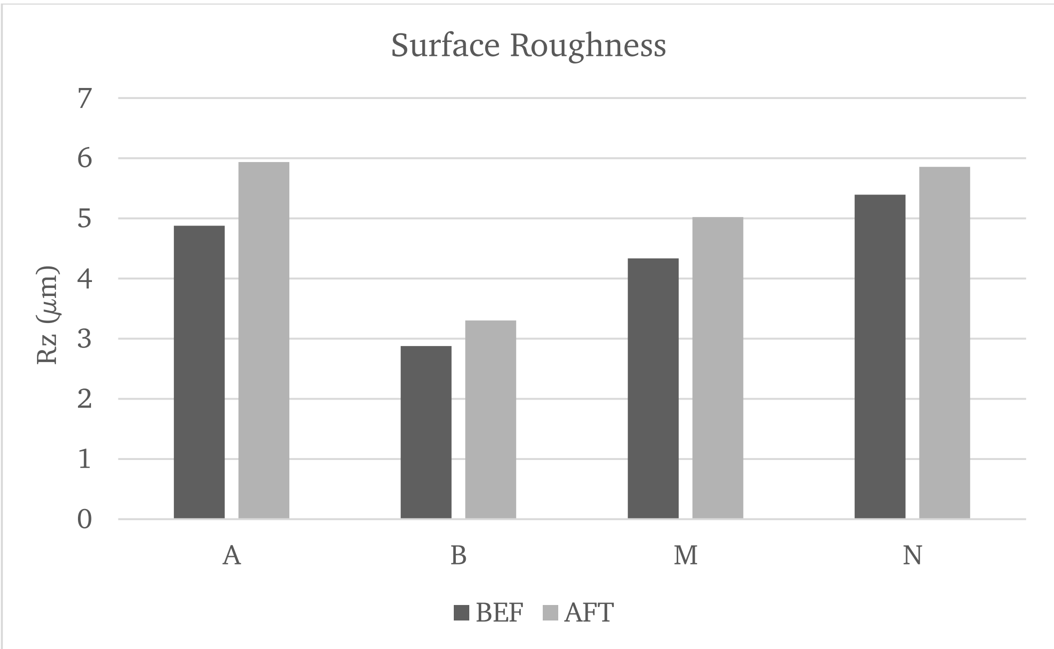

Figure 6.7 Surface roughness results before and after moderate weathering conditions

Surface roughness can give information about the porosity and wear on the surface of the material. As a result of aging, the roughness is expected to increase as a result of micro particles that will break off the surface or change with temperature difference. As can be seen in the Figure 6.7, it was observed that the surface roughness increased in all samples. The increase in all samples compared to other analyses indicates that the surface roughness can be suggested as a good technique for natural aging conditions. These results are also consistent with the results of other performance tests conducted throughout the thesis.

6.1.2 Manual Test Results

6.1.2.1 Thermal Degradation

In this section, the effects of thermal degradation on four different stone types have been investigated by using a 3-factor and 3-level response surface model on the Design Expert software, as explained in the Materials & Methods section. The samples obtained were evaluated by examining their surface hardness, ultrasonic pulse velocity and surface roughness properties. The results were shown by presenting the real data firstly, then ANOVA analysis, which provides information about the significance of the results, and then, information on the consistency of statistical equivalents was presented with tables where mean values, standard deviation values, PRESS value and R-Squared value are given. Finally, model equations for all significant results in ANOVA analysis are shown over both coded values and actual values.

During the analysis of the results, while deriving the model equation, first the most comprehensive model, the cubic model, was selected, then the final model was obtained by evaluating the elimination of each term one by one. The reason to follow such a path and not to use a standard linear or parabolic equations is that it is aimed to obtain a model equation with higher accuracy. In this case, it can be analyzed how each parameter affects the equivalence with other parameters in the obtained equations, but it is difficult to interpret how a single parameter affects the result individually.

- **Surface Hardness**

  <u>Ankara</u>

Table 6.1 Surface hardness results for Ankara stone after thermal degradation

Experimental Parameters				Surface Hardness		
	Temperature (°C)	Number of Cycle (days)	Duration of Exposure (hour)	Mean	Min	Max
AT-1	30	30	18	664.00	462.00	767.33
AT-2	50	20	16	717.00	594.33	767.00
AT-3	50	20	20	714.67	613.67	768.33
AT-4	50	40	20	691.67	506.67	771.33
AT-5	50	40	16	655.67	496.00	766.33
AT-6	70	30	22	643.33	390.00	775.00
AT-7	70	30	14	716.00	586.00	779.00
AT-8	70	50	18	681.00	463.67	783.33
AT-9	70	10	18	716.00	591.67	776.00
AT-10	70	30	18	704.33	569.00	763.33
AT-11	90	40	20	706.67	585.00	771.33
AT-12	90	20	20	687.33	523.00	783.67
AT-13	90	20	16	682.67	532.67	760.67
AT-14	90	40	16	700.67	568.67	772.33
AT-15	110	30	18	706.67	566.33	792.00

Table 6.2 ANOVA Analysis of surface hardness results for Ankara stone

ANOVA for Response Surface Reduced Cubic Model						
Analysis of variance table [Partial sum of squares - Type III]						
	Sum of		Mean	F	p-value	
Source	Squares	df	Square	Value	Prob > F	
Model	6169.381	7	881.3401	4.175615	0.0394	significant
A-Temperature	437.5069	1	437.5069	2.072821	0.1931	
B-Number of Cycles	855.5625	1	855.5625	4.053486	0.0840	
C-Duration of exposure	2640.222	1	2640.222	12.50885	0.0095	
AB	1850.347	1	1850.347	8.766579	0.0211	
AC	66.125	1	66.125	0.313287	0.5931	
A^2	73.93646	1	73.93646	0.350296	0.5726	
A^2C	2248.34	1	2248.34	10.65219	0.0138	
Residual	1477.478	7	211.0683			
Cor Total	7646.859	14				

Table 6.3 Statistical analysis of model of surface hardness for Ankara stone

Std. Dev.	14.52819	R-Squared	0.806786
Mean	692.5111	Adj R-Squared	0.613572
C.V. %	2.0979	Pred R-Squared	-0.20855
PRESS	9241.622	Adeq Precision	7.00248

Table 6.4 Final equation in terms of coded factors for surface hardness of Ankara stone

Final Equation in Terms of Coded Factors:					
	R1	=			
	694.4264				
	5.229167	* A			
	-7.3125	* B			
	-18.1667	* C			
	15.20833	* A * B			
	-2.875	* A * C			
	-1.79554	* A^2			
	23.70833	* A^2 * C			

Table 6.5 Final equation in terms of actual factors for surface hardness of Ankara stone

Final Equation in Terms of Actual Factors:		
	R1	=
	-1705.15	
	74.58365	* Temperature
	-6.05417	* Number of Cycles
	141.1615	* Duration of exposure
	0.076042	* Temperature * Number of Cycles
	-4.22083	* Temperature * Duration of exposure
	-0.53793	* Temperature^2
	0.029635	* Temperature^2 * Duration of exposure

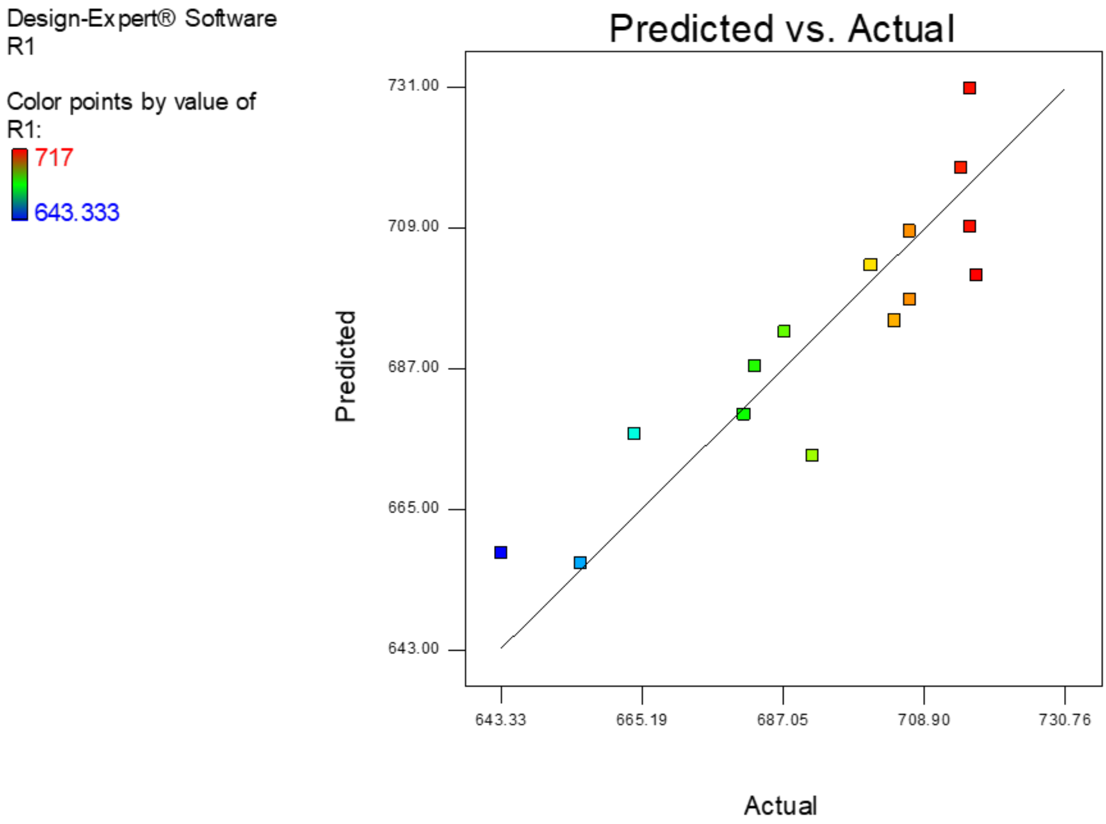

Figure 6.8 Predicted vs. actual values of surface hardness for Ankara stone

Bitlis

Table 6.6 Surface hardness results for Bitlis stone after thermal degradation

Experimental Parameters				Surface Hardness		
	Temperature (°C)	Number of Cycle (days)	Duration of Exposure (hour)	Mean	Min	Max
BT-1	30	30	18	391.00	325.33	457.00
BT-2	50	20	16	405.33	367.33	456.67
BT-3	50	20	20	394.67	309.33	503.00
BT-4	50	40	20	369.00	305.33	424.67
BT-5	50	40	16	371.75	293.00	434.75
BT-6	70	30	22	390.00	346.00	446.00
BT-7	70	30	14	411.67	370.00	474.00
BT-8	70	50	18	391.67	353.00	431.67
BT-9	70	10	18	377.33	330.00	414.67
BT-10	70	30	18	394.67	343.67	487.00
BT-11	90	40	20	379.00	269.67	440.67
BT-12	90	20	20	387.00	330.67	428.00
BT-13	90	20	16	400.67	328.00	452.67
BT-14	90	40	16	385.33	287.33	448.33
BT-15	110	30	18	393.00	334.00	465.50

Table 6.7 ANOVA analysis of surface hardness results for Bitlis stone

ANOVA for Response Surface Reduced Cubic Model						
Analysis of variance table [Partial sum of squares - Type III]						
	Sum of		Mean	F	p-value	
Source	Squares	df	Square	Value	Prob > F	
Model	1729.801	7	247.1145	7.621216	0.0078	significant
A-Temperature	14.53516	1	14.53516	0.448276	0.5246	
B-Number of Cycles	102.7222	1	102.7222	3.168039	0.1183	
C-Duration of exposure	368.1602	1	368.1602	11.35437	0.0119	
AB	161.2509	1	161.2509	4.973111	0.0610	
A^2	29.82695	1	29.82695	0.919888	0.3695	
C^2	230.2888	1	230.2888	7.1023	0.0322	
A^2B	773.5352	1	773.5352	23.85647	0.0018	
Residual	226.9718	7	32.42455			
Cor Total	1956.773	14				

Table 6.8 Statistical analysis of model of surface hardness for Bitlis stone

Std. Dev.	5.694256		R-Squared	0.884007
Mean	389.4722		Adj R-Squared	0.768014
C.V. %	1.462044		Pred R-Squared	0.591545
PRESS	799.2537		Adeq Precision	9.441976

Table 6.9 Final equation in terms of coded factors for surface hardness of Bitlis stone

Final Equation in Terms of Coded Factors:			
	R1	=	
	384.4679		
	0.953125	* A	
	3.583333	* B	
	-4.79688	* C	
	4.489583	* A * B	
	1.241587	* A^2	
	3.44992	* C^2	
	-13.9063	* A^2 * B	

Table 6.10 Final equation in terms of actual factors for surface hardness of Bitlis stone

Final Equation in Terms of Actual Factors:		
	R1	=
	1266.402	
	-15.6619	* Temperature
	-18.2482	* Number of Cycles
	-33.4477	* Duration of exposure
	0.509167	* Temperature * Number of Cycles
	0.107401	* Temperature ^ 2
	0.86248	* Duration of exposure ^ 2
	-0.00348	* Temperature ^ 2 * Number of Cycles

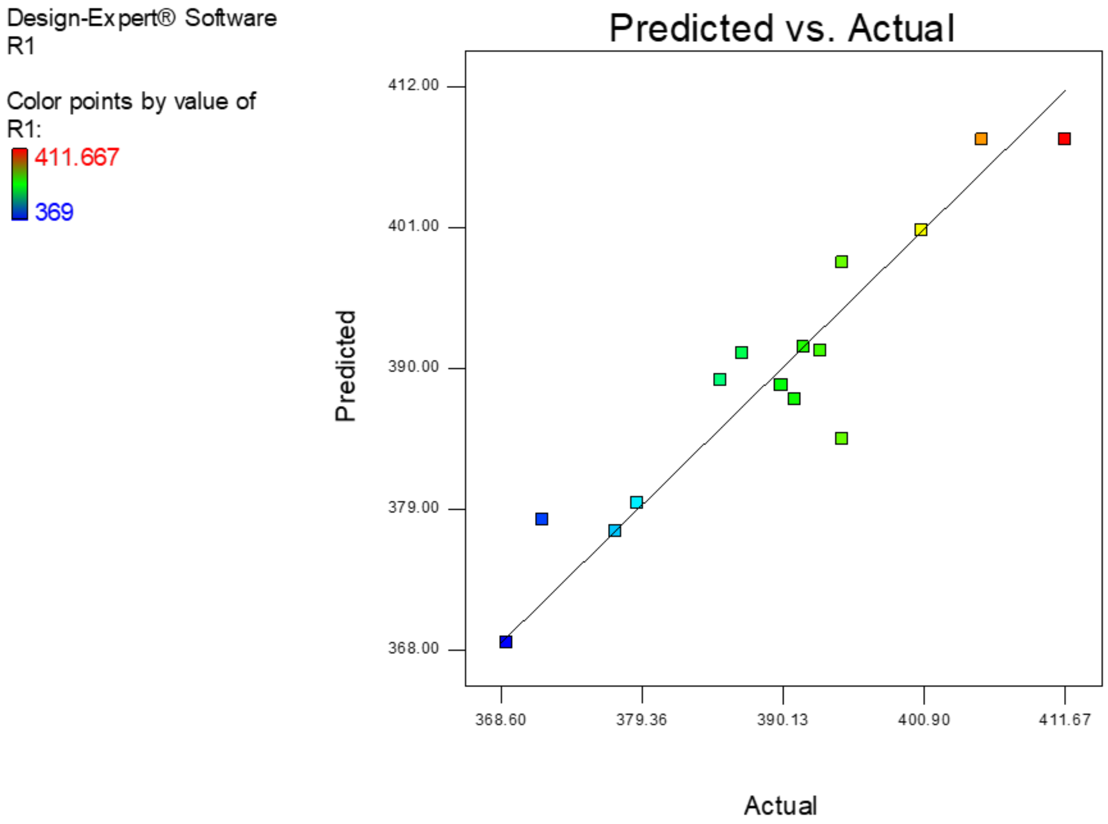

Figure 6.9 Predicted vs. actual values of surface hardness for Bitlis stone

Mardin

Table 6.11 Surface hardness results for Mardin stone after thermal degradation

Experimental Parameters				Surface Hardness		
	Temperature (°C)	Number of Cycle (days)	Duration of Exposure (hour)	Mean	Min	Max
MT-1	30	30	18	320.67	238.33	434.33
MT-2	50	20	16	306.33	205.67	418.00
MT-3	50	20	20	289.33	227.00	375.67
MT-4	50	40	20	257.67	208.67	327.67
MT-5	50	40	16	266.33	207.33	371.33
MT-6	70	30	22	286.00	207.33	469.33
MT-7	70	30	14	280.67	219.33	365.67
MT-8	70	50	18	301.33	235.00	420.33
MT-9	70	10	18	302.00	213.67	442.33
MT-10	70	30	18	263.33	205.00	371.67
MT-11	90	40	20	263.67	213.67	371.33
MT-12	90	20	20	282.67	221.00	399.33
MT-13	90	20	16	365.00	235.00	500.00
MT-14	90	40	16	282.67	208.00	406.67
MT-15	110	30	18	322.00	213.33	525.00

Table 6.12 ANOVA analysis of surface hardness results for Mardin stone

ANOVA for Response Surface Reduced Cubic Model						
Analysis of variance table [Partial sum of squares - Type III]						
	Sum of		Mean	F	p-value	
Source	Squares	df	Square	Value	Prob > F	
Model	11208.39	13	862.1841	23.55774	0.1600	not significant
A-Temperature	0.888889	1	0.888889	0.024287	0.9016	
B-Number of Cycles	0.222222	1	0.222222	0.006072	0.9505	
C-Duration of exposure	14.22222	1	14.22222	0.388598	0.6451	
AB	110.0139	1	110.0139	3.005945	0.3331	
AC	715.6806	1	715.6806	19.55477	0.1416	
BC	642.0139	1	642.0139	17.54195	0.1492	
A^2	2444.844	1	2444.844	66.80126	0.0775	
B^2	1094.399	1	1094.399	29.90262	0.1151	
C^2	317.8179	1	317.8179	8.683842	0.2083	
ABC	378.125	1	378.125	10.33163	0.1920	
A^2B	1841.84	1	1841.84	50.3252	0.0892	
A^2C	1184.507	1	1184.507	32.36467	0.1108	
AB^2	321.0069	1	321.0069	8.770977	0.2073	
Residual	36.59877	1	36.59877			
Cor Total	11244.99	14				

Nevsehir

Table 6.13 Surface hardness results for Nevsehir stone after thermal degradation

Experimental Parameters				Surface Hardness		
	Temperature (°C)	Number of Cycle (days)	Duration of Exposure (hour)	Mean	Min	Max
NT-1	30	30	18	266.00	218.33	355.67
NT-2	50	20	16	249.33	215.00	310.00
NT-3	50	20	20	248.67	216.00	288.00
NT-4	50	40	20	253.67	211.00	351.33
NT-5	50	40	16	270.33	216.67	357.00
NT-6	70	30	22	251.67	211.33	334.67
NT-7	70	30	14	255.00	207.33	336.67
NT-8	70	50	18	231.00	201.33	281.00
NT-9	70	10	18	252.33	214.67	292.33
NT-10	70	30	18	242.00	200.67	285.33
NT-11	90	40	20	264.33	220.67	323.33
NT-12	90	20	20	251.00	206.33	326.00
NT-13	90	20	16	256.33	202.33	333.67
NT-14	90	40	16	250.67	204.33	349.33
NT-15	110	30	18	266.67	205.67	376.00

Table 6.14 ANOVA analysis of surface hardness results for Nevsehir stone

ANOVA for Response Surface Reduced Cubic Model						
Analysis of variance table [Partial sum of squares - Type III]						
	Sum of		Mean	F	p-value	
Source	Squares	df	Square	Value	Prob > F	
Model	1352.746	10	135.2746	6.495931	0.0432	significant
A-Temperature	0.173611	1	0.173611	0.008337	0.9316	
B-Number of Cycles	227.5556	1	227.5556	10.92729	0.0298	
C-Duration of exposure	15.34028	1	15.34028	0.736645	0.4391	
AB	42.01389	1	42.01389	2.01752	0.2285	
AC	82.34722	1	82.34722	3.95434	0.1176	
BC	1.125	1	1.125	0.054023	0.8276	
A^2	686.5479	1	686.5479	32.96825	0.0046	
C^2	141.7572	1	141.7572	6.807223	0.0595	
ABC	153.125	1	153.125	7.353111	0.0534	
A^2B	364.1736	1	364.1736	17.48773	0.0139	
Residual	83.29808	4	20.82452			
Cor Total	1436.044	14				

Table 6.15 Statistical analysis of model of surface hardness for Nevsehir stone

Std. Dev.	4.563389	R-Squared	0.941995
Mean	253.9333	Adj R-Squared	0.796982
C.V. %	1.797082	Pred R-Squared	-0.1282
PRESS	1620.15	Adeq Precision	8.880049

Table 6.16 Final equation in terms of coded factors for surface hardness of Nevsehir stone

Final Equation in Terms of Coded Factors:		
	R1	=
	244.6923	
	0.104167	* A
	-5.33333	* B
	-0.97917	* C
	-2.29167	* A * B
	3.208333	* A * C
	0.375	* B * C
	5.956731	* A^2
	2.706731	* C^2
	4.375	* A * B * C
	9.541667	* A^2 * B

Table 6.17 Final equation in terms of actual factors for surface hardness of Nevsehir stone

Final Equation in Terms of Actual Factors:		
	R1	=
	-115.613	
	12.74535	* Temperature
	25.40104	* Number of Cycles
	-8.05849	* Duration of exposure
	-0.54229	* Temperature * Number of Cycles
	-0.24792	* Temperature * Duration of exposure
	-0.74687	* Number of Cycles * Duration of exposure
	-0.05667	* Temperature^2
	0.676683	* Duration of exposure^2
	0.010938	* Temperature * Number of Cycles * Duration of exposure
	0.002385	* Temperature^2 * Number of Cycles

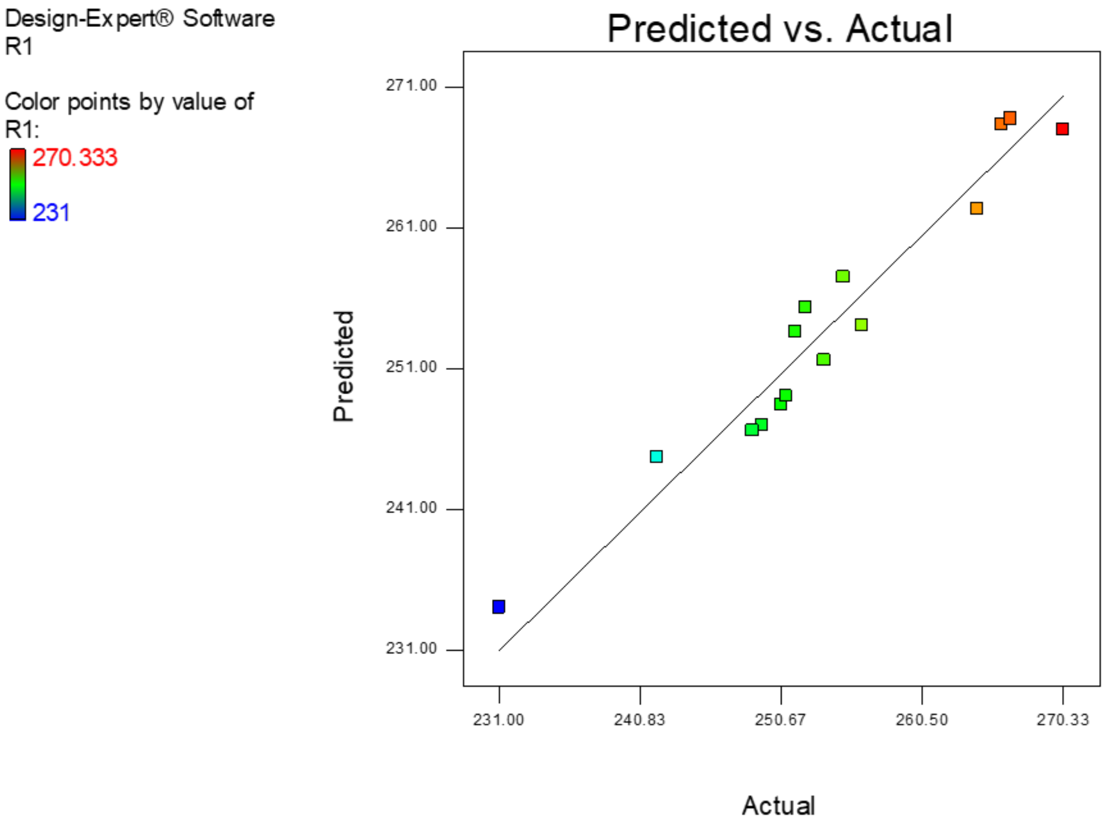

Figure 6.10 Predicted vs. actual values of surface hardness for Nevsehir stone

Conclusion:

• p-values less than 0.05 were observed in ANOVA analyses of Ankara, Bitlis and Nevsehir stones. This shows that the statistical evaluation made is significant. The high dispersion observed in other surface hardness analyses made on Mardin stones may be the reason for this situation. The most important reason for this is the dense pitting on the surface.

• R^2 values for Ankara, Bitlis and Nevsehir ones, respectively; 0.81, 0.88 and 0.94. This gives information about the accuracy of the models.

• It has been observed that common parameters for all models are A, B, C, AB and A^2. However, two of the models also have AC and C^2 parameters. Accordingly, it can be said that the most effective parameter in all models is temperature (A).

• Coefficients of parameters vary in models. The most important reason for this is the use of a modified cubic model.

• Summarizing the results, it can be said that the surface hardness results based on temperature, exposure time and cycle amount could be mathematically modelled for Ankara, Bitlis and Nevsehir stones in thermal degradation experiments.

- **Ultrasonic Pulse Velocity (UPV)**

Ankara

Table 6.18 UPV results for Ankara stone after thermal degradation

Experimental Parameters				
	Temperature (°C)	Number of Cycle (days)	Duration of Exposure (hour)	Ultrasonic Pulse Velocity (m/s)
AT-1	30	30	18	4225.33
AT-2	50	20	16	4373.67
AT-3	50	20	20	3969.33
AT-4	50	40	20	4213.67
AT-5	50	40	16	3768.67
AT-6	70	30	22	4348.67
AT-7	70	30	14	4027.33
AT-8	70	50	18	4168.67
AT-9	70	10	18	4047.67
AT-10	70	30	18	4286.67
AT-11	90	40	20	3902.00
AT-12	90	20	20	4065.33
AT-13	90	20	16	3690.00
AT-14	90	40	16	4287.33
AT-15	110	30	18	3698.67

Table 6.19 ANOVA analysis of UPV results for Ankara stone

ANOVA for Response Surface Reduced Cubic Model						
Analysis of variance table [Partial sum of squares - Type III]						
	Sum of		Mean	F	p-value	
Source	Squares	df	Square	Value	Prob > F	
Model	627890.335	8	78486.29193	4.5101	0.0414	significant
A-Temperature	128522.25	1	128522.25	7.385	0.0348	
B-Number of Cycles	6214.694	1	6214.694444	0.357	0.5720	
C-Duration of exposure	28336.111	1	28336.11111	1.628	0.2491	
AB	78936.888	1	78936.88889	4.536	0.0772	
AC	320.888	1	320.8888889	0.018	0.8964	
BC	982.722	1	982.7222222	0.056	0.8201	
A^2	60564.279	1	60564.27984	3.480	0.1114	
ABC	324012.5	1	324012.5	18.61	0.0050	
Residual	104413.842	6	17402.30706			
Cor Total	732304.177	14				

Table 6.20 Statistical analysis of model of UPV results for Ankara stone

Std. Dev.	131.9178042	R-Squared	0.857417388
Mean	4071.533333	Adj R-Squared	0.667307239
C.V. %	3.24000305	Pred R-Squared	-0.280544475
PRESS	937748.069	Adeq Precision	7.51347397

Table 6.21 Final equation in terms of coded factors for UPV of Ankara stone

Final Equation in Terms of Coded Factors:		
	Untitled	=
	4126.348837	
	-89.625	* A
	19.70833333	* B
	42.08333333	* C
	99.33333333	* A * B
	-6.333333333	* A * C
	11.08333333	* B * C
	-51.38953488	* A^2
	-201.25	* A * B * C

Table 6.22 Final equation in terms of actual factors for UPV of Ankara stone

Final Equation in Terms of Actual Factors:		
	Untitled	=
	23533.51453	
	-270.2324128	* Temperature
	-676.7083333	* Number of Cycles
	-1041.0625	* Duration of exposure
	9.552916667	* Temperature * Number of Cycles
	14.93541667	* Temperature * Duration of exposure
	35.77291667	* Number of Cycles * Duration of exposure
	-0.128473837	* Temperature^2
	-0.503125	* Temperature * Number of Cycles * Duration of exposure

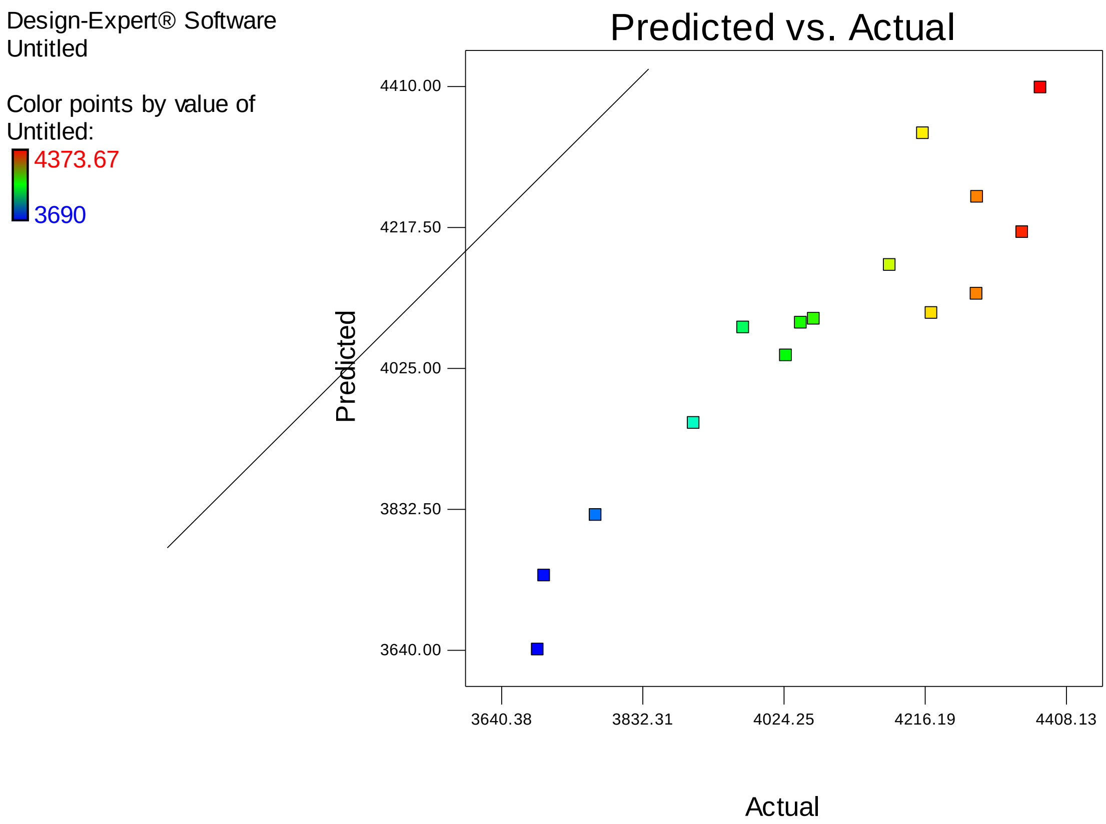

Figure 6.11 Predicted vs. actual Values of UPV for Ankara Stone

Bitlis

Table 6.23 UPV results for Bitlis stone after thermal degradation

Experimental Parameters				
	Temperature (°C)	Number of Cycle (days)	Duration of Exposure (hour)	Ultrasonic Pulse Velocity (m/s)
BT-1	30	30	18	2815.33
BT-2	50	20	16	2798.00
BT-3	50	20	20	2900.67
BT-4	50	40	20	2733.33
BT-5	50	40	16	2856.67
BT-6	70	30	22	2852.33
BT-7	70	30	14	2843.67
BT-8	70	50	18	2911.00
BT-9	70	10	18	2814.00
BT-10	70	30	18	2817.67
BT-11	90	40	20	2691.33
BT-12	90	20	20	2763.67
BT-13	90	20	16	2862.33
BT-14	90	40	16	2727.00
BT-15	110	30	18	2737.67

Table 6.24 ANOVA analysis of UPV results for Bitlis stone

ANOVA for Response Surface Reduced Cubic Model						
Analysis of variance table [Partial sum of squares - Type III]						
Source	Sum of Squares	df	Mean Square	F Value	p-value Prob > F	
Model	51545.75002	9	5727.305558	3.129782225	0.1109	Not significant
A-Temperature	9983.340278	1	9983.340278	5.455563814	0.0667	
B-Number of Cycles	4704.5	1	4704.5	2.570852966	0.1698	
C-Duration of exposure	1184.506944	1	1184.506944	0.647293696	0.4576	
AB	1225.125	1	1225.125	0.669490114	0.4504	
AC	1615.013889	1	1615.013889	0.882551439	0.3906	
BC	3321.125	1	3321.125	1.814884484	0.2358	
A^2	6563.666688	1	6563.666688	3.586825799	0.1168	
ABC	10440.125	1	10440.125	5.70518149	0.0625	
A^2B	16277.50694	1	16277.50694	8.895116804	0.0307	
Residual	9149.687016	5	1829.937403			
Cor Total	60695.43704	14				

Mardin

Table 6.25 UPV results for Mardin stone after thermal degradation

Experimental Parameters				
	Temperature (°C)	Number of Cycle (days)	Duration of Exposure (hour)	Ultrasonic Pulse Velocity (m/s)
MT-1	30	30	18	2936.67
MT-2	50	20	16	3244.00
MT-3	50	20	20	2830.00
MT-4	50	40	20	1477.00
MT-5	50	40	16	2577.00
MT-6	70	30	22	2983.00
MT-7	70	30	14	2207.00
MT-8	70	50	18	2687.67
MT-9	70	10	18	4154.67
MT-10	70	30	18	2407.67
MT-11	90	40	20	1462.50
MT-12	90	20	20	2127.67
MT-13	90	20	16	3344.00
MT-14	90	40	16	2347.00
MT-15	110	30	18	2584.50

Table 6.26 ANOVA analysis of UPV results for Mardin stone

ANOVA for Response Surface Reduced Cubic Model						
Analysis of variance table [Partial sum of squares - Type III]						
Source	Sum of Squares	df	Mean Square	F Value	p-value Prob > F	
Model	5961344.62	7	851620.66	7.744	0.0075	Signifi.
A-Temperature	150382.3767	1	150382.3767	1.367	0.2805	
B-Number of Cycles	2735853.835	1	2735853.835	24.879	0.0016	
C-Duration of exposure	301088	1	301088	2.738	0.1420	
AC	43046.67014	1	43046.67014	0.391	0.5514	
A^2	99849.44723	1	99849.44723	0.908	0.3724	
B^2	1086643.169	1	1086643.169	9.881	0.0163	
A^2C	1668510.418	1	1668510.418	15.173	0.0059	
Residual	769744.984	7	109963.5691			
Cor Total	6731089.604	14				

Table 6.27 Statistical analysis of model of UPV results for Mardin stone

Std. Dev.	331.6075529	R-Squared	0.885643331
Mean	2624.688889	Adj R-Squared	0.771286663
C.V. %	12.63416606	Pred R-Squared	0.1947128
PRESS	5420460.3	Adeq Precision	10.33066971

Table 6.28 Final equation in terms of coded factors for UPV of Mardin stone

Final Equation in Terms of Coded Factors:		
	Untitled 2	=
	2295.282051	
	-96.94791667	* A
	-413.5104167	* B
	194	* C
	-73.35416667	* A * C
	71.83653846	* A^2
	236.9823718	* B^2
	-645.8541667	* A^2 * C

Table 6.29 Final equation in terms of actual factors for UPV of Mardin stone

Final Equation in Terms of Actual Factors:		
	Untitled 2	=
	74036.73558	
	-2031.421434	* Temperature
	-183.5404647	* Number of Cycles
	-3730.486979	* Duration of exposure
	111.190625	* Temperature * Duration of exposure
	14.7113101	* Temperature^2
	2.369823718	* Number of Cycles^2
	-0.807317708	* Temperature^2 * Duration of exposure

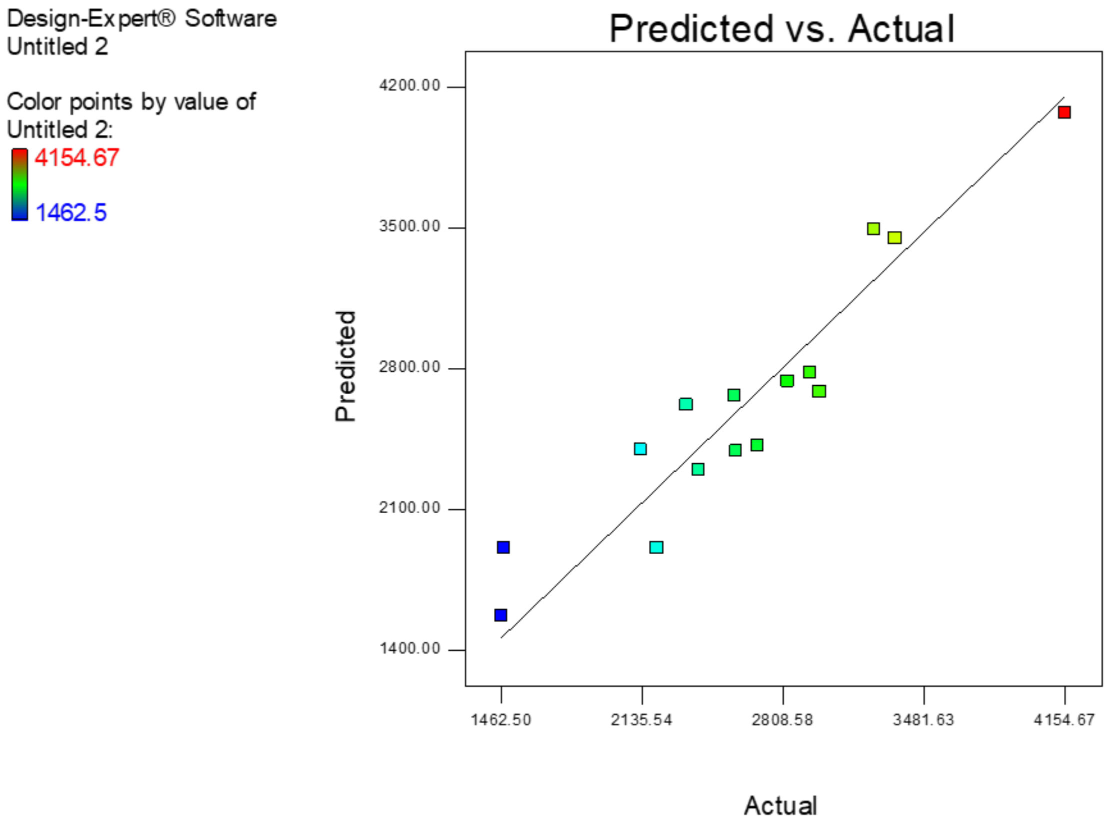

Figure 6.12 Predicted vs. actual values of UPV for Mardin stone

Nevsehir

Table 6.30 UPV results for Nevsehir stone after thermal degradation

Experimental Parameters				
	Temperature (°C)	Number of Cycle (days)	Duration of Exposure (hour)	Ultrasonic Pulse Velocity (m/s)
NT-1	30	30	18	1889.00
NT-2	50	20	16	2002.33
NT-3	50	20	20	1952.33
NT-4	50	40	20	1769.33
NT-5	50	40	16	1737.67
NT-6	70	30	22	1930.33
NT-7	70	30	14	2140.33
NT-8	70	50	18	1664.67
NT-9	70	10	18	1756.00
NT-10	70	30	18	2158.00
NT-11	90	40	20	1988.33
NT-12	90	20	20	2000.00
NT-13	90	20	16	1981.67
NT-14	90	40	16	1925.00
NT-15	110	30	18	1888.33

Table 6.31 ANOVA analysis of UPV results for Nevsehir stone

ANOVA for Response Surface Reduced Cubic Model						
Analysis of variance table [Partial sum of squares - Type III]						
	Sum of		Mean	F	p-value	
Source	Squares	df	Square	Value	Prob > F	
Model	271689.6481	10	27168.96481	17.2184023	0.0073	significant
A-Temperature	0.222222222	1	0.222222222	0.000140834	0.9911	
B-Number of Cycles	4170.888889	1	4170.888889	2.643311709	0.1793	
C-Duration of exposure	3333.660131	1	3333.660131	2.112715801	0.2197	
AB	17986.72222	1	17986.72222	11.39913211	0.0279	
A^2	45607.69231	1	45607.69231	28.90399393	0.0058	
B^2	131001.9231	1	131001.9231	83.02281035	0.0008	
C^2	8376.923077	1	8376.923077	5.308896844	0.0826	
A^2B	6944.444444	1	6944.444444	4.401059775	0.1039	
AB^2	11808.44444	1	11808.44444	7.483632459	0.0521	
C^3	14600.69444	1	14600.69444	9.253228177	0.0383	
Residual	6311.611111	4	1577.902778			
Cor Total	278001.2593	14				

Table 6.32 Statistical analysis of model of UPV results for Nevsehir stone

Std. Dev.	39.72282439	R-Squared	0.977296466
Mean	1918.888889	Adj R-Squared	0.92053763
C.V. %	2.070095076	Pred R-Squared	-0.260038356
PRESS	350292.2497	Adeq Precision	14.13035823

Table 6.33 Final equation in terms of coded factors for UPV of Nevsehir stone

Final Equation in Terms of Coded Factors:			
	Untitled	=	
	2132.666667		
	-0.166666667	* A	
	-22.83333333	* B	
	28.05555556	* C	
	47.41666667	* A * B	
	-64.16666667	* A^2	
	-108.75	* B^2	
	-27.5	* C^2	
	-41.66666667	* A^2 * B	
	54.33333333	* A * B^2	
	-20.13888889	* C^3	

Table 6.34 Final equation in terms of actual factors for UPV of Nevsehir stone

Final Equation in Terms of Actual Factors:		
	Untitled	=
	12955.83333	
	-3.9625	* Temperature
	109.4291667	* Number of Cycles
	-2185.347222	* Duration of exposure
	0.065416667	* Temperature * Number of Cycles
	0.152083333	* Temperature^2
	-2.989166667	* Number of Cycles^2
	129.0625	* Duration of exposure^2
	-0.010416667	* Temperature^2 * Number of Cycles
	0.027166667	* Temperature * Number of Cycles^2
	-2.517361111	* Duration of exposure^3

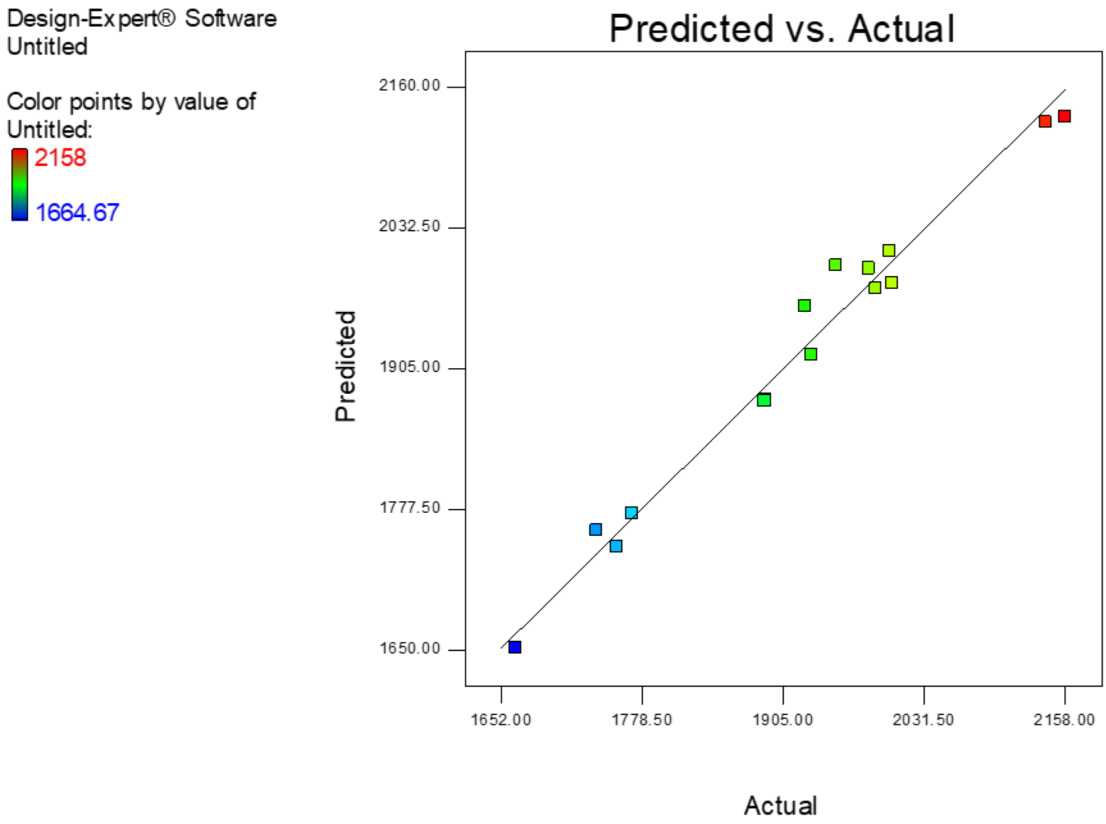

Figure 6.13 Predicted vs. actual values of UPV for Nevsehir stone

Conclusion:

• The p-values obtained from ANOVA analysis for Ankara, Mardin and Nevsehir stones are 0.04, 0.0075 and 0.0075, respectively. This shows that the analyses are meaningful for these stones.

• The obtained R^2 values are at a high level.

• The most repetitive parameters are A, B, C, A^2 and B^2. Accordingly, it can be said that the most effective parameter is temperature (A), followed by the cycle quantity (B).

• In summary, we can say that UPV is a method that gives meaningful mathematical models in Ankara, Mardin and Nevsehir stones for thermal aging experiments based on temperature, exposure time and cycle amount.

- **Surface Roughness**

Ankara

Table 6.35 Surface roughness results for Ankara stone after thermal degradation

Experimental Parameters				
	Temperature (°C)	Number of Cycle (days)	Duration of Exposure (hour)	Surface Roughness (Rz) (μm)
AT-1	30	30	18	18.84
AT-2	50	20	16	21.09
AT-3	50	20	20	19.54
AT-4	50	40	20	21.08
AT-5	50	40	16	20.33
AT-6	70	30	22	18.69
AT-7	70	30	14	20.75
AT-8	70	50	18	25.43
AT-9	70	10	18	19.33
AT-10	70	30	18	20.23
AT-11	90	40	20	21.74
AT-12	90	20	20	19.07
AT-13	90	20	16	25.23
AT-14	90	40	16	20.05
AT-15	110	30	18	20.18

Table 6.36 ANOVA analysis of surface roughness results for Ankara stone

ANOVA for Response Surface Reduced Cubic Model						
Analysis of variance table [Partial sum of squares - Type III]						
	Sum of		Mean	F	p-value	
Source	Squares	df	Square	Value	Prob > F	
Model	56.53178	10	5.653178	13.47773	0.0115	significant
A-Temperature	2.650384	1	2.650384	6.318776	0.0658	
B-Number of Cycles	18.56639	1	18.56639	44.26409	0.0027	
C-Duration of exposure	5.514669	1	5.514669	13.14751	0.0222	
AB	1.36125	1	1.36125	3.245354	0.1460	
AC	1.686672	1	1.686672	4.021192	0.1154	
BC	12.85245	1	12.85245	30.6415	0.0052	
A^2	0.217167	1	0.217167	0.517747	0.5116	
B^2	6.970792	1	6.970792	16.61905	0.0151	
ABC	3.850313	1	3.850313	9.179524	0.0388	
A^2B	12.11736	1	12.11736	28.88898	0.0058	
Residual	1.677783	4	0.419446			
Cor Total	58.20957	14				

Table 6.37 Statistical analysis of model of surface roughness results for Ankara stone

Std. Dev.	0.647646	R-Squared	0.971177
Mean	20.78098	Adj R-Squared	0.899119
C.V. %	3.116535	Pred R-Squared	-0.19013
PRESS	69.27715	Adeq Precision	12.48508

Table 6.38 Final equation in terms of coded factors for surface roughness of Ankara stone

Final Equation in Terms of Coded Factors:		
	R1	=
	20.25374	
	0.407	* A
	1.523417	* B
	-0.58708	* C
	-0.4125	* A * B
	-0.45917	* A * C
	1.2675	* B * C
	-0.10594	* A^2
	0.600224	* B^2
	0.69375	* A * B * C
	-1.7405	* A^2 * B

Table 6.39 Final equation in terms of actual factors for surface roughness of Ankara stone

Final Equation in Terms of Actual Factors:		
	R1	=
	37.47847	
	-0.56503	* Temperature
	-1.15097	* Number of Cycles
	2.250937	* Duration of exposure
	0.027636	* Temperature * Number of Cycles
	-0.06351	* Temperature * Duration of exposure
	-0.05803	* Number of Cycles * Duration of exposure
	0.012789	* Temperature^2
	0.006002	* Number of Cycles^2
	0.001734	* Temperature * Number of Cycles * Duration of exposure
	-0.00044	* Temperature^2 * Number of Cycles

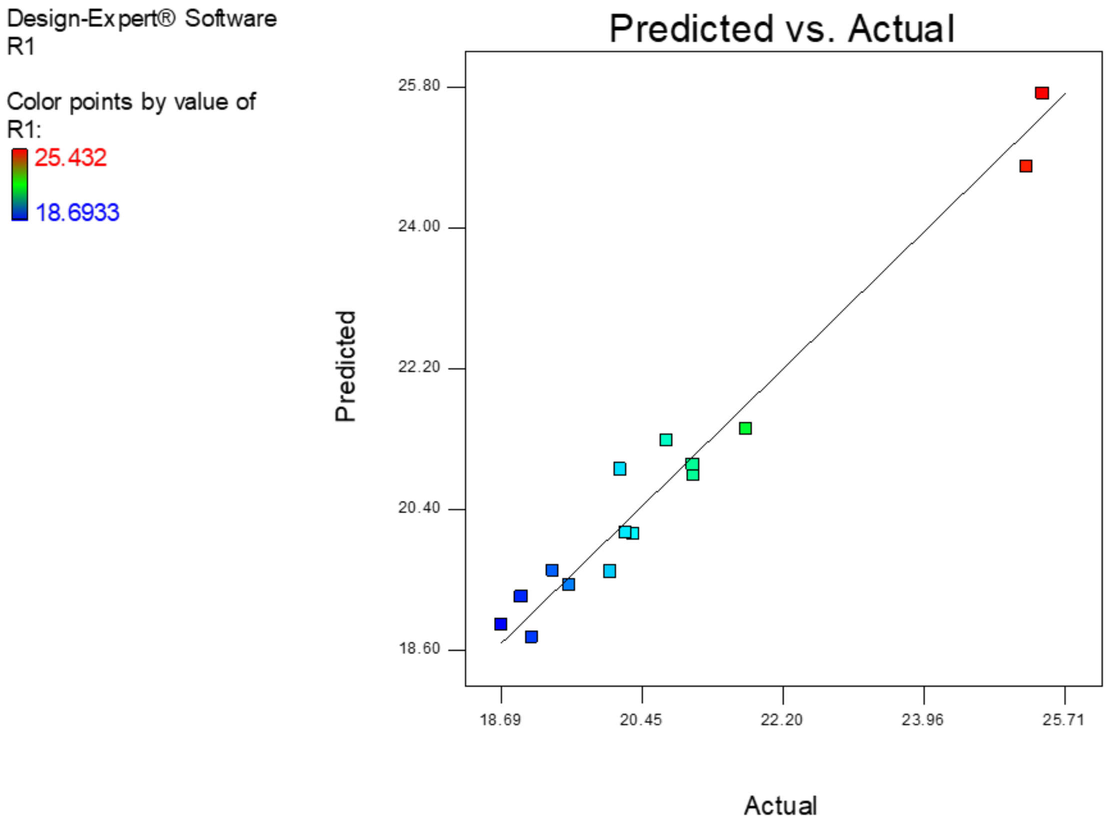

Figure 6.14 Predicted vs. actual values of surface roughness for Ankara stone

Bitlis

Table 6.40 Surface roughness results for Bitlis stone after thermal degradation

	Experimental Parameters			
	Temperature (°C)	Number of Cycle (days)	Duration of Exposure (hour)	Surface Roughness (Rz) (μm)
BT-1	30	30	18	23.62
BT-2	50	20	16	25.63
BT-3	50	20	20	24.01
BT-4	50	40	20	23.19
BT-5	50	40	16	20.49
BT-6	70	30	22	23.04
BT-7	70	30	14	22.44
BT-8	70	50	18	23.11
BT-9	70	10	18	23.64
BT-10	70	30	18	23.82
BT-11	90	40	20	21.85
BT-12	90	20	20	23.60
BT-13	90	20	16	28.37
BT-14	90	40	16	26.01
BT-15	110	30	18	29.60

Table 6.41 ANOVA analysis of surface roughness results for Bitlis stone

ANOVA for Response Surface Reduced Cubic Model						
Analysis of variance table [Partial sum of squares - Type III]						
	Sum of		Mean	F	p-value	
Source	Squares	df	Square	Value	Prob > F	
Model	78.88228	13	6.067867	12673.62	0.0070	significant
A-Temperature	17.9151	1	17.9151	37418.28	0.0033	
B-Number of Cycles	0.141158	1	0.141158	294.828	0.0370	
C-Duration of exposure	0.183013	1	0.183013	382.2481	0.0325	
AB	0.437892	1	0.437892	914.6009	0.0210	
AC	12.43093	1	12.43093	25963.8	0.0040	
BC	3.064875	1	3.064875	6401.436	0.0080	
A^2	5.367481	1	5.367481	11210.76	0.0060	
B^2	0.141957	1	0.141957	296.4987	0.0369	
C^2	0.818999	1	0.818999	1710.598	0.0154	
ABC	1.707244	1	1.707244	3565.827	0.0107	
A^2B	5.045639	1	5.045639	10538.55	0.0062	
A^2C	5.09593	1	5.09593	10643.59	0.0062	
AB^2	1.849147	1	1.849147	3862.211	0.0102	
Residual	0.000479	1	0.000479			
Cor Total	78.88275	14				

Table 6.42 Statistical analysis of model of surface roughness results for Bitlis stone

Std. Dev.	0.021881	R-Squared	0.999994
Mean	24.16203	Adj R-Squared	0.999915
C.V. %	0.09056	Pred R-Squared	0.998443
PRESS	0.122807	Adeq Precision	431.5616

Table 6.43 Final equation in terms of coded factors for surface roughness of Bitlis stone

Final Equation in Terms of Coded Factors:		
	R1	=
	23.83031	
	1.496458	* A
	-0.13283	* B
	0.15125	* C
	0.233958	* A * B
	-1.24654	* A * C
	0.618958	* B * C
	0.696106	* A^2
	-0.11321	* B^2
	-0.27191	* C^2
	-0.46196	* A * B * C
	-1.12313	* A^2 * B
	-1.12871	* A^2 * C
	-0.67992	* A * B^2

Table 6.44 Final equation in terms of actual factors for surface roughness of Bitlis stone

Final Equation in Terms of Actual Factors:		
	R1	=
	213.8031	
	-5.30728	* Temperature
	-4.84313	* Number of Cycles
	-5.56276	* Duration of exposure
	0.081665	* Temperature * Number of Cycles
	0.201007	* Temperature * Duration of exposure
	0.111791	* Number of Cycles * Duration of exposure
	0.03556	* Temperature ^ 2
	0.022665	* Number of Cycles ^ 2
	-0.06798	* Duration of exposure ^ 2
	-0.00115	* Temperature * Number of Cycles * Duration of exposure
	-0.00028	* Temperature ^ 2 * Number of Cycles
	-0.00141	* Temperature ^ 2 * Duration of exposure
	-0.00034	* Temperature * Number of Cycles ^ 2

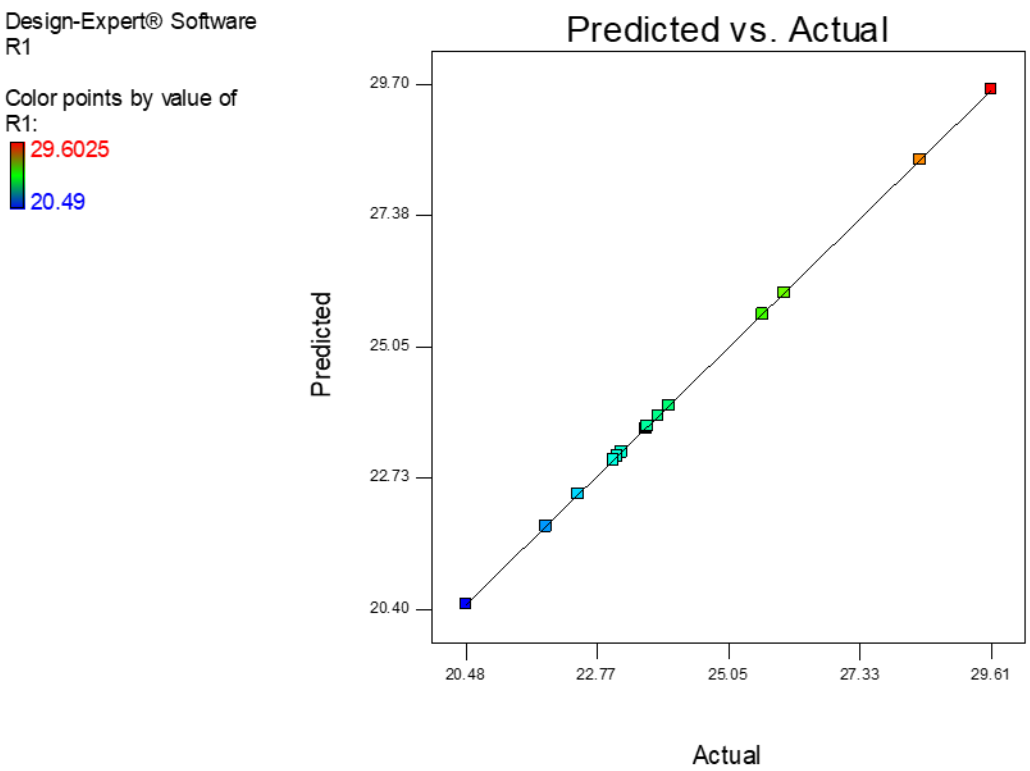

Figure 6.15 Predicted vs. actual values of surface roughness for Bitlis stone

Mardin

Table 6.45 Surface roughness results for Mardin stone after thermal degradation

Experimental Parameters				
	Temperature (°C)	Number of Cycle (days)	Duration of Exposure (hour)	Surface Roughness (Rz) (μm)
MT-1	30	30	18	13.49
MT-2	50	20	16	15.33
MT-3	50	20	20	14.51
MT-4	50	40	20	17.69
MT-5	50	40	16	18.08
MT-6	70	30	22	15.66
MT-7	70	30	14	18.84
MT-8	70	50	18	17.05
MT-9	70	10	18	11.82
MT-10	70	30	18	19.69
MT-11	90	40	20	17.76
MT-12	90	20	20	16.28
MT-13	90	20	16	14.23
MT-14	90	40	16	17.20
MT-15	110	30	18	13.96

Table 6.46 ANOVA analysis of surface roughness results for Mardin stone

ANOVA for Response Surface Reduced Cubic Model						
Analysis of variance table [Partial sum of squares - Type III]						
	Sum of		Mean	F	p-value	
Source	Squares	df	Square	Value	Prob > F	
Model	68.19494	11	6.19954	162.5118	0.0007	significant
A-Temperature	0.038875	1	0.038875	1.019043	0.3871	
B-Number of Cycles	27.18667	1	27.18667	712.6583	0.0001	
C-Duration of exposure	5.066806	1	5.066806	132.8188	0.0014	
AB	0.276396	1	0.276396	7.245316	0.0743	
AC	1.82055	1	1.82055	47.72303	0.0062	
BC	0.1379	1	0.1379	3.614845	0.1534	
A^2	25.05757	1	25.05757	656.8471	0.0001	
B^2	19.46956	1	19.46956	510.3657	0.0002	
C^2	4.29209	1	4.29209	112.5108	0.0018	
ABC	0.451092	1	0.451092	11.8247	0.0413	
A^2C	3.763923	1	3.763923	98.66569	0.0022	
Residual	0.114445	3	0.038148			
Cor Total	68.30938	14				

Table 6.47 Statistical analysis of model of surface roughness results for Mardin stone

Std. Dev.	0.195316	R-Squared	0.998325
Mean	16.10739	Adj R-Squared	0.992182
C.V. %	1.212585	Pred R-Squared	0.943357
PRESS	3.869234	Adeq Precision	45.27944

Table 6.48 Final equation in terms of coded factors for surface roughness of Mardin stone

	R1	=
	19.78983	
	0.049292	* A
	1.303521	* B
	-0.79583	* C
	-0.18588	* A * B
	0.477042	* A * C
	-0.13129	* B * C
	-1.50404	* A^2
	-1.32577	* B^2
	-0.62248	* C^2
	-0.23746	* A * B * C
	0.970042	* A^2 * C

Table 6.49 Final equation in terms of actual factors for surface roughness of Mardin stone

Final Equation in Terms of Actual Factors:		
	R1	=
	-132.885	
	3.077154	* Temperature
	0.36104	* Number of Cycles
	9.261359	* Duration of exposure
	0.009756	* Temperature * Number of Cycles
	-0.14002	* Temperature * Duration of exposure
	0.034991	* Number of Cycles * Duration of exposure
	-0.02559	* Temperature^2
	-0.01326	* Number of Cycles^2
	-0.15562	* Duration of exposure^2
	-0.00059	* Temperature * Number of Cycles * Duration of exposure
	0.001213	* Temperature^2 * Duration of exposure

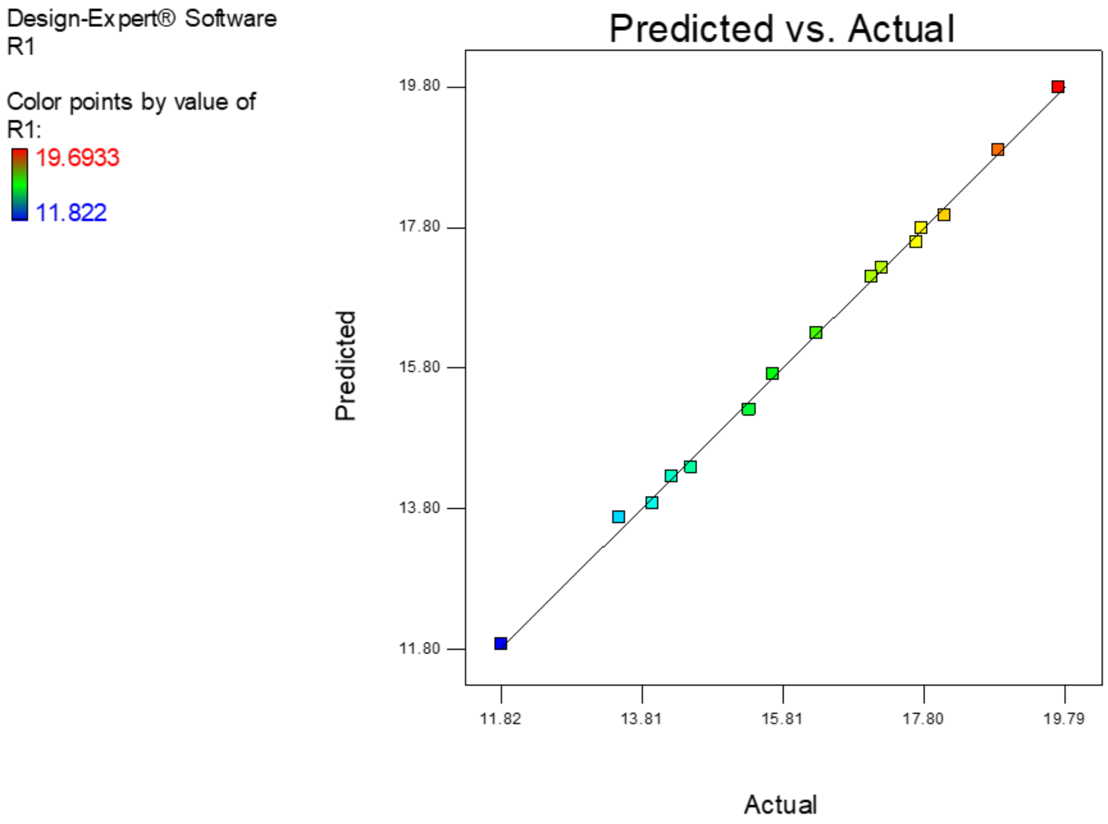

Figure 6.16 Predicted vs. actual values of surface roughness for Mardin stone

Nevsehir

Table 6.50 Surface roughness results for Nevsehir stone after thermal degradation

Experimental Parameters				
	Temperature (°C)	Number of Cycle (days)	Duration of Exposure (hour)	Surface Roughness (Rz) (μm)
NT-1	30	30	18	20.91
NT-2	50	20	16	21.74
NT-3	50	20	20	20.87
NT-4	50	40	20	26.82
NT-5	50	40	16	27.52
NT-6	70	30	22	24.14
NT-7	70	30	14	24.14
NT-8	70	50	18	28.48
NT-9	70	10	18	17.70
NT-10	70	30	18	27.13
NT-11	90	40	20	19.45
NT-12	90	20	20	26.01
NT-13	90	20	16	19.38
NT-14	90	40	16	16.08
NT-15	110	30	18	20.69

Table 6.51 ANOVA Analysis of Surface Roughness Results for Nevsehir Stone

ANOVA for Response Surface Reduced Cubic Model						
Analysis of variance table [Partial sum of squares - Type III]						
	Sum of		Mean	F	p-value	
Source	Squares	df	Square	Value	Prob > F	
Model	190.7872	9	21.19858	5.479618	0.0378	significant
A-Temperature	0.023835	1	0.023835	0.006161	0.9405	
B-Number of Cycles	58.08623	1	58.08623	15.0147	0.0117	
C-Duration of exposure	4.423135	1	4.423135	1.143335	0.3338	
AB	58.24532	1	58.24532	15.05583	0.0116	
AC	16.71914	1	16.71914	4.321727	0.0922	
A^2	20.6626	1	20.6626	5.341072	0.0688	
B^2	4.124981	1	4.124981	1.066266	0.3491	
A^2B	24.22157	1	24.22157	6.261031	0.0543	
AB^2	15.19928	1	15.19928	3.928859	0.1043	
Residual	19.34312	5	3.868624			
Cor Total	210.1304	14				

Table 6.52 Statistical analysis of model of surface roughness results for Nevsehir stone

Std. Dev.	1.966882	R-Squared	0.907947
Mean	22.73614	Adj R-Squared	0.742252
C.V. %	8.650903	Pred R-Squared	-1.44455
PRESS	513.6734	Adeq Precision	7.656283

Table 6.53 Final equation in terms of coded factors for surface roughness of Nevsehir stone

Final Equation in Terms of Coded Factors:		
	R1	=
	24.33094	
	-0.05458	* A
	2.694583	* B
	0.525781	* C
	-2.69827	* A * B
	1.445646	* A * C
	-1.03339	* A^2
	-0.46173	* B^2
	-2.46077	* A^2 * B
	-1.94931	* A * B^2

Table 6.54 Final equation in terms of actual factors for surface roughness of Nevsehir stone

Final Equation in Terms of Actual Factors:		
	R1	=
	163.9343	
	-3.34784	* Temperature
	-5.61711	* Number of Cycles
	-2.26699	* Duration of exposure
	0.131115	* Temperature * Number of Cycles
	0.036141	* Temperature * Duration of exposure
	0.015872	* Temperature^2
	0.063609	* Number of Cycles^2
	-0.00062	* Temperature^2 * Number of Cycles
	-0.00097	* Temperature * Number of Cycles^2

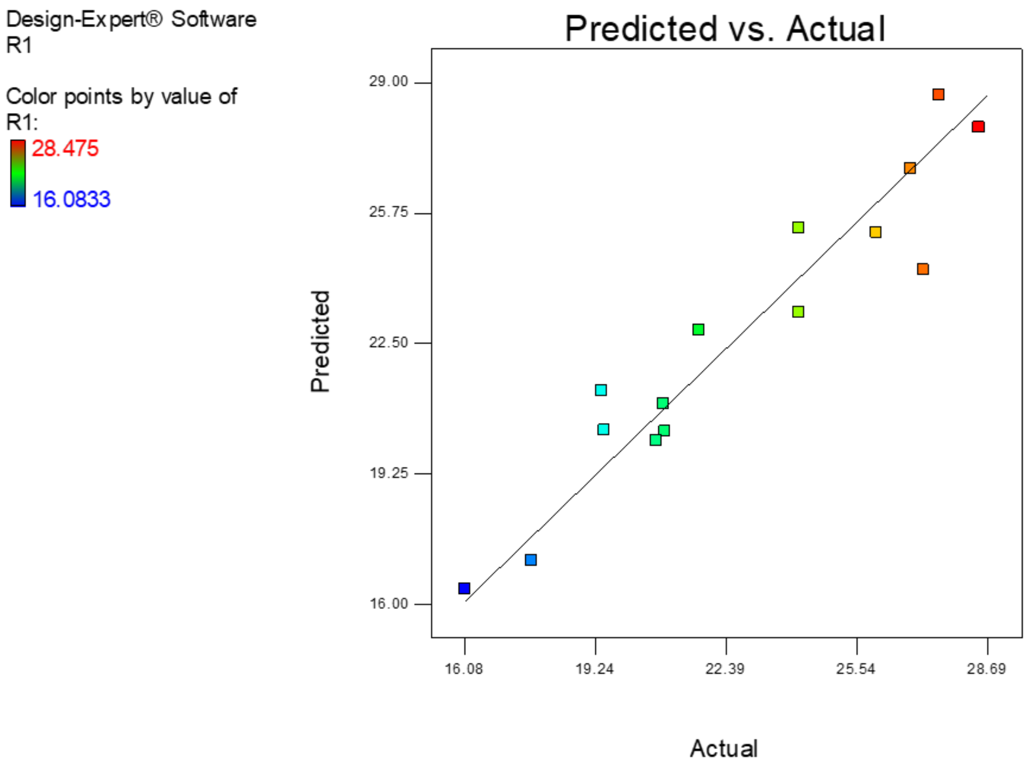

Figure 6.17 Predicted vs. actual values of surface roughness for Nevsehir stone

Conclusion:

• Low p-values were observed for all samples. This shows that surface roughness analysis is meaningful for all stones.

• All of the R^2 values are above 0.9, ie 0.99 for Bitlis and Mardin ones. This shows that the accuracy of the models is very high.

• When the selected parameters are examined, it is seen that the parameters A, B, C, AB, AC, A^2 are common in all of the examples. Accordingly, it is seen that the most effective parameter is again temperature (A).

6.1.2.2 Frost – Thaw Results

- **Surface Hardness**

- It has been observed that the general values are compatible with the other surface hardness results (ANK>BIT>MAR>NEV).
- The values again fluctuate in a large range. For this reason, it is important that the results are not perceived as net values and evaluated together with other analyses.
- It was considered to be a common starting value for all samples and the results were evaluated accordingly. The reason for this is that it will not be possible to get the initial state of the stones in the examinations to be made on naturally aged samples in the field studies and it is aimed to establish an analogy with field studies on this subject. However, if the initial values are known, it should be considered that more accurate mathematical evaluations can be made for samples aged under laboratory conditions by analyzing the differences between them.

Ankara

Table 6.55 Surface hardness results of Ankara stone after frost/thaw procedure

	Temperature (°C)	Duration of Exposure (Frost hour)	Number of Cycle (Days)	Mean Surface Hardness (HLD)
FA1	-20	6	30	676.33
FA2	-15	8	40	688.00
FA3	-15	4	40	670.67
FA4	-15	4	20	738.33
FA5	-15	8	20	702.33
FA6	-5	4	40	666.33
FA7	-5	4	20	682.33
FA8	-5	8	40	713.00
FA9	-5	8	20	665.67
FA10	0	6	30	687.33

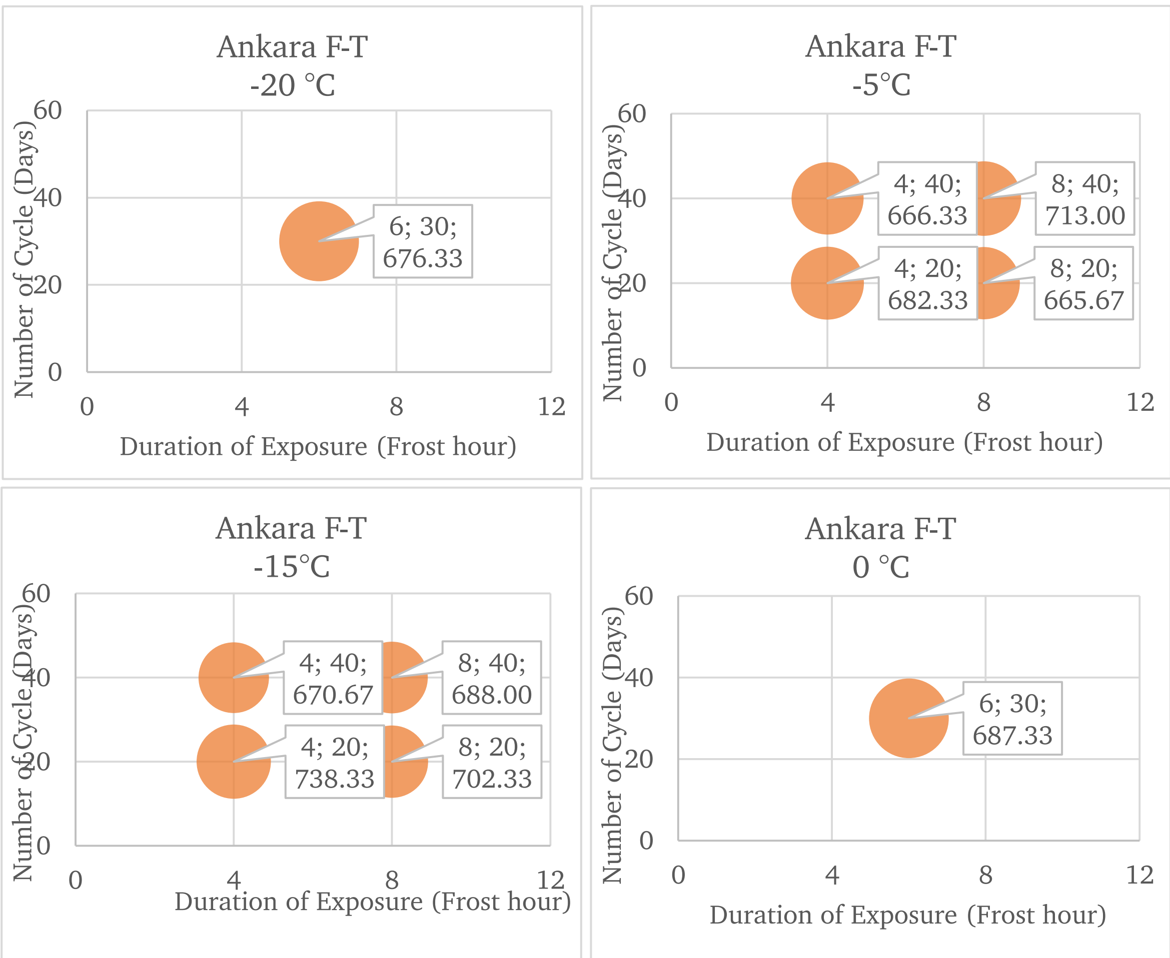

Figure 6.18 Surface hardness results of Ankara stone after frost/thaw procedure

• On the basis of temperature averages, it was observed that the lowest average value was at -20°C and the hardness values increased towards 0, as expected, except -15°C. However, attention should be paid to the fact that the differences are at the level of 1% and that the analysis is distributed in a wide range.

• In terms of cycle number, it is seen that the samples with 40 cycles at -5°C degrees, 4 hours exposure, show 16 HLD lower hardness compared to the samples with 20 cycles, and this difference reaches 68 HLD at -15°C and 4 hours exposure. Similarly, samples with 40 cycles at -15°C and 8 hours exposure showed 14 HLD lower values than samples with 20 cycles. However, in tests conducted at -5°C, it was observed that increasing cycle values for 8 hours exposure did not cause a decrease in hardness.

• When looking at different exposure times for the same cycle periods, a decrease of 17 HLD is observed when increasing from 4 hours to 8 hours in a 20 cycle series for -5°C degrees, but there is no decrease depending on the period for 40-day cycles, similar situation is observed for -15°C.

• If a general comment is to be made for Ankara stone that surface hardness is quite high at the beginning, the most important variable in freezing damage is the temperature during freezing and the other effects (duration of exposure to freezing or the number of repetitions of the cycle) are at similar levels.

Bitlis

Table 6.56 Surface hardness results of Bitlis stone after frost/thaw procedure

	Temperature (°C)	Duration of Exposure (Frost hour)	Number of Cycle (Days)	Mean Surface Hardness (HLD)
FB1	-20	6	30	370.33
FB2	-15	8	40	378.00
FB3	-15	4	40	378.00
FB4	-15	4	20	389.67
FB5	-15	8	20	373.67
FB6	-5	4	40	393.67
FB7	-5	4	20	374.00
FB8	-5	8	40	382.00
FB9	-5	8	20	377.00
FB10	0	6	30	387.00

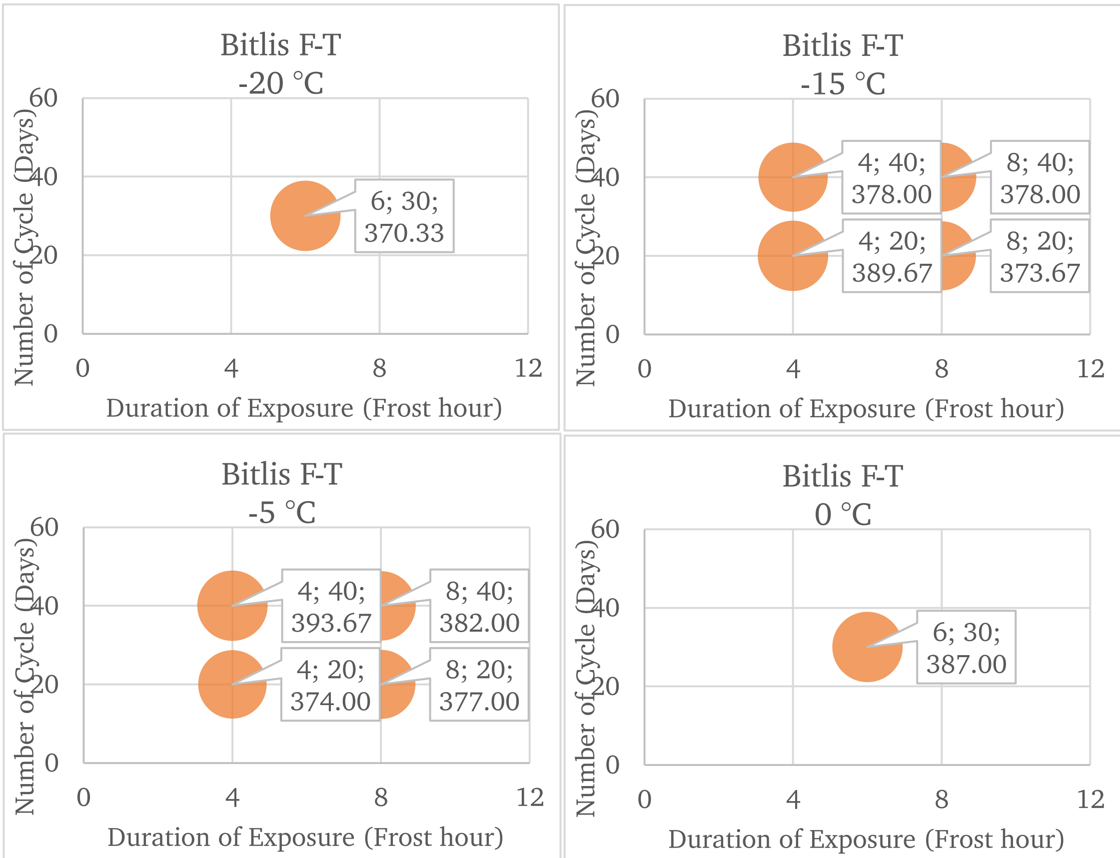

Figure 6.19 Surface hardness results of Bitlis stone after frost/thaw procedure

• Among the samples examined, it is the stone type with the highest HLD values after Ankara stone.

• It is the type of stone that can be exposed to the highest frost damage due to the continental climate of its geography (can be seen in Table 5.18). However, the surface hardness of all stones was the least altered.

• In terms of temperature values, it has been observed that the average values from -20°C to 0°C are 370, 379, 381 and 387 HLD, respectively. This revealed the direct proportion between the decrease in freezing temperatures and the decrease in surface hardness.

• When the samples are examined in fixed cycle amounts, while the hardness decreased with the exposure time for 20 cycles for -15°C, it remained constant for 40 cycles. However, an increase of 3 HLD was observed when going from 4-hour exposure to 8-hour exposure for 20 cycles at -5°C, while a decrease of 11 HLD was observed when going from 4 hours to 8 hours for 40 cycles.

• When examined for constant exposure periods, a decrease of 11 HLD is observed when going from 20 cycles to 40 cycles in trials of 4 hours freezing at -15°C, while an increase of 5 HLD in the same cycle increase in 8 hour trials has been observed. When the same analysis was made for -5°C, it was observed that the cycle amounts and surface hardness varied in direct proportion for both fixed times.

• When all the data are analyzed together, it can be said that for Bitlis stone, cycle amount and exposure time do not have a significant effect on the hardness, but the exposure temperature does.

Mardin

Table 6.57 Surface hardness results of Mardin stone after frost/thaw procedure

	Temperature (°C)	Duration of Exposure (Frost hour)	Number of Cycle (Days)	Mean Surface Hardness (HLD)
FM1	-20	6	30	343.67
FM2	-15	8	40	318.67
FM3	-15	4	40	333.67
FM4	-15	4	20	251.00
FM5	-15	8	20	319.00
FM6	-5	4	40	304.00
FM7	-5	4	20	331.00
FM8	-5	8	40	249.00
FM9	-5	8	20	284.00
FM10	0	6	30	237.00

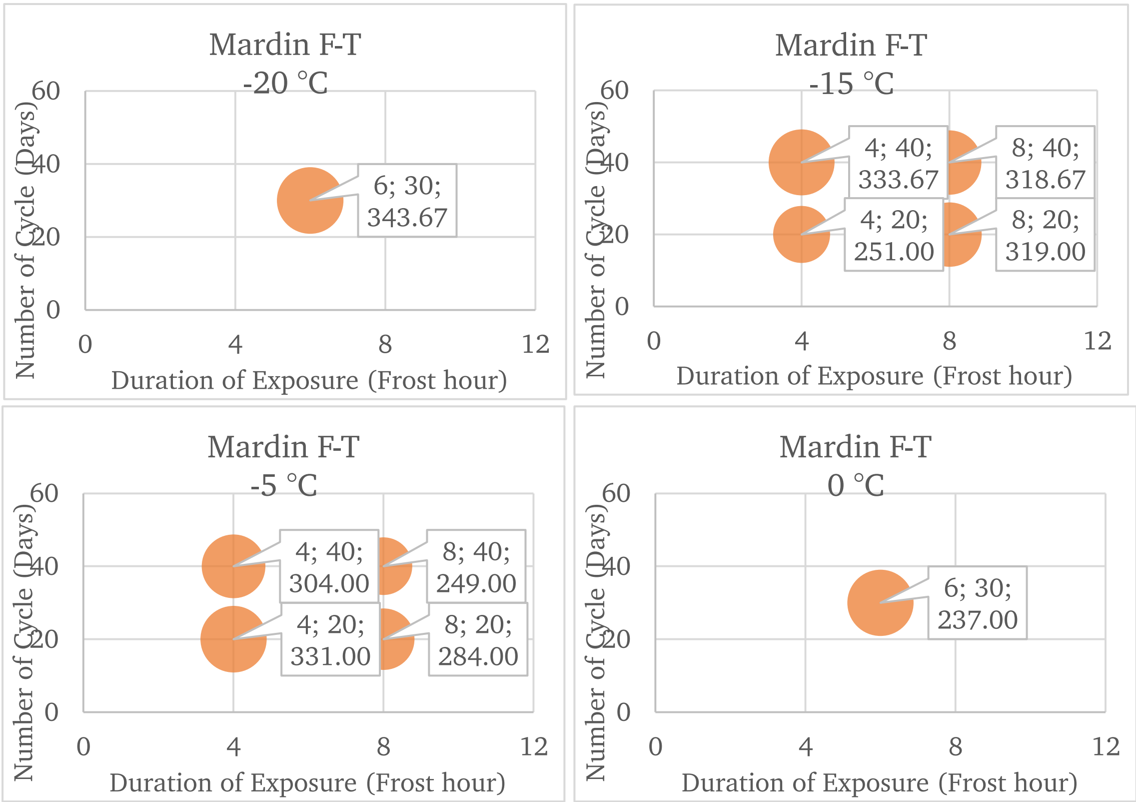

Figure 6.20 Surface hardness results of Mardin stone after frost/thaw procedure

• As in other examples, Mardin stones have preserved the same order as in the raw form of the samples. Accordingly, surface values after freezing cycles are less than Ankara and Bitlis stones and higher than Nevşehir one.

• Due to the nature of the analysis, the porous structure on the surface of Mardin stone, we could not collect as many values as in the other examples. For this reason, it should not be forgotten that different methods should be evaluated in surface hardness examinations, especially for stones with high surface heterogeneity.

• When the change depending on the temperature is examined, contrary to expectations, higher surface hardness was observed at lower temperature values. When the values were examined, it was seen that the hardness values were 343, 305, 292 and 237 HLD, respectively, from -20°C to 0°C.

• From the perspective of fixed cycle times, for -15°C, the hardness increased by 68 HLD with increasing exposure time at 20 cycles, while at 40 cycles, the hardness decreased by 15 HLD with increasing exposure time. When examined for -5°C, it was seen that the hardness decreased with increasing exposure times for both 40 cycles and 20 cycles. Accordingly, it can be said that exposure times and hardness decrease are observed with a rate of 75%.

• When examined for constant exposure periods, it was observed that the hardness increase was observed with the increase in the number of cycles in the 4-hour cycles for -15°C, while the value remained constant in the 8-hour cycle. For -5°C, it can be said that there is a decrease in surface hardness with an increase in cycle amount for both exposure durations. Here, similar to the exposure time, it can be said that the increase in cycle amount by 75% adversely affects the surface hardness.

• When a general evaluation is made for the surface hardness due to freezing in Mardin stone, it can be said that the cycle time and the cycle amount inversely affect the hardness as expected, but the temperature directly affects the hardness.

<u>Nevsehir</u>

Table 6.58 Surface hardness results of Nevsehir stone after frost/thaw procedure

	Temperature (°C)	Duration of Exposure (Frost hour)	Number of Cycle (Days)	Mean Surface Hardness (HLD)
FN1	-20	6	30	253.00
FN2	-15	8	40	249.00
FN3	-15	4	40	247.00
FN4	-15	4	20	247.00
FN5	-15	8	20	244.67
FN6	-5	4	40	243.33
FN7	-5	4	20	242.50
FN8	-5	8	40	244.50
FN9	-5	8	20	248.50
FN10	0	6	30	236.00

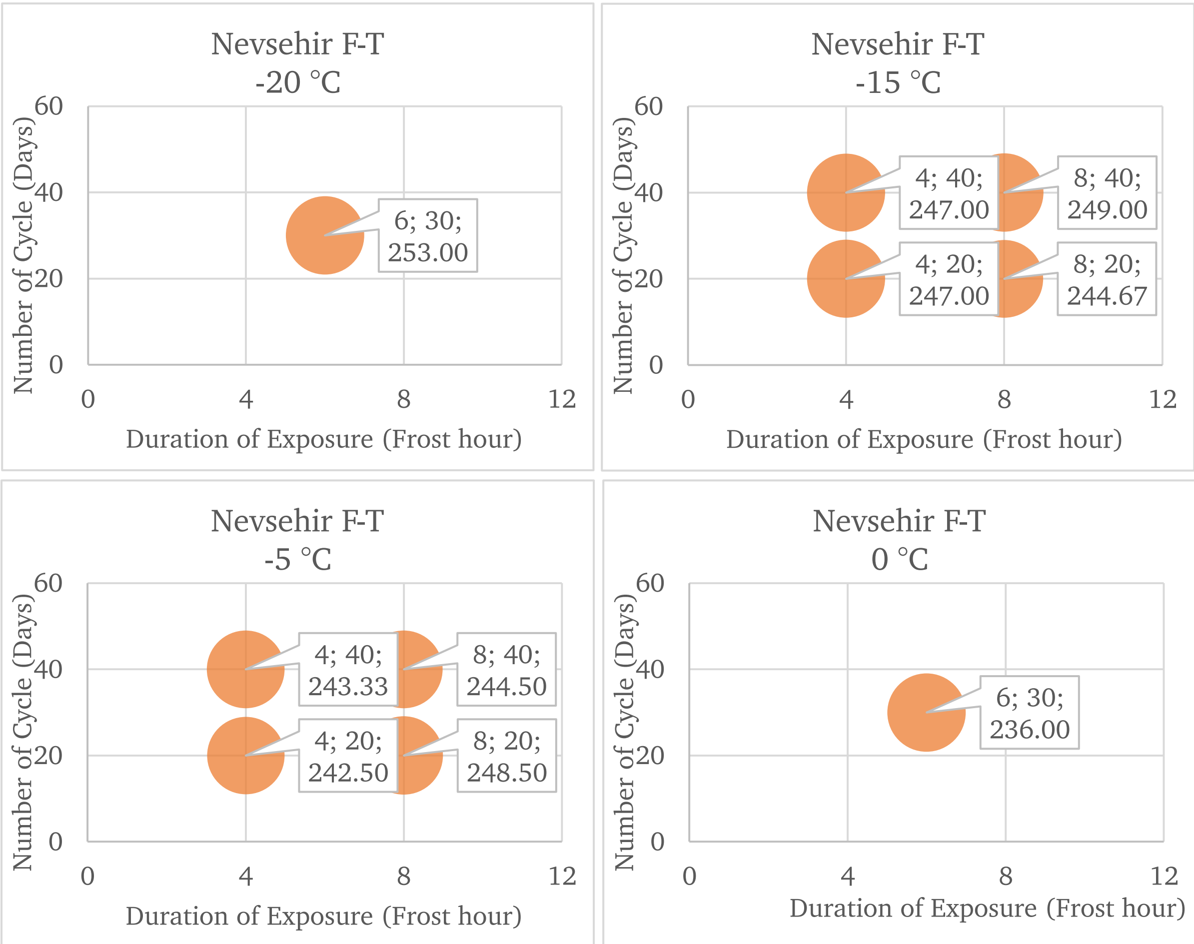

Figure 6.21 Surface hardness results of Nevsehir stone after frost/thaw procedure

• Nevsehir stone has the lowest surface hardness compared to other stones.

• When examined in terms of temperature, it is seen that there is an increase in hardness values with the temperature decrease, similar to Mardin stone. Average values are as follows from -20°C to 0; 253, 247, 244, 236 HLD.

• When looking at Nevsehir stone in general, it is seen that the biggest change as a result of different parameters is 6 HLD. In general, this may lead us to conclude that the cycle amount and exposure time are not effective in terms of the surface hardness values of these stones.

- **Ultrasonic Pulse Velocity (UPV)**

<u>Ankara</u>

Table 6.59 UPV results of Ankara stone after frost/thaw procedure

	Temperature (°C)	Duration of Exposure (Frost hour)	Number of Cycle (Days)	Ultraonic Pulse Velocity (m/s)
FA1	-20	6	30	4331.00
FA2	-15	8	40	4345.00
FA3	-15	4	40	4331.00
FA4	-15	4	20	4242.70
FA5	-15	8	20	3642.30
FA6	-5	4	40	3774.70
FA7	-5	4	20	3691.30
FA8	-5	8	40	3866.70
FA9	-5	8	20	3206.00
FA10	0	6	30	4194.00

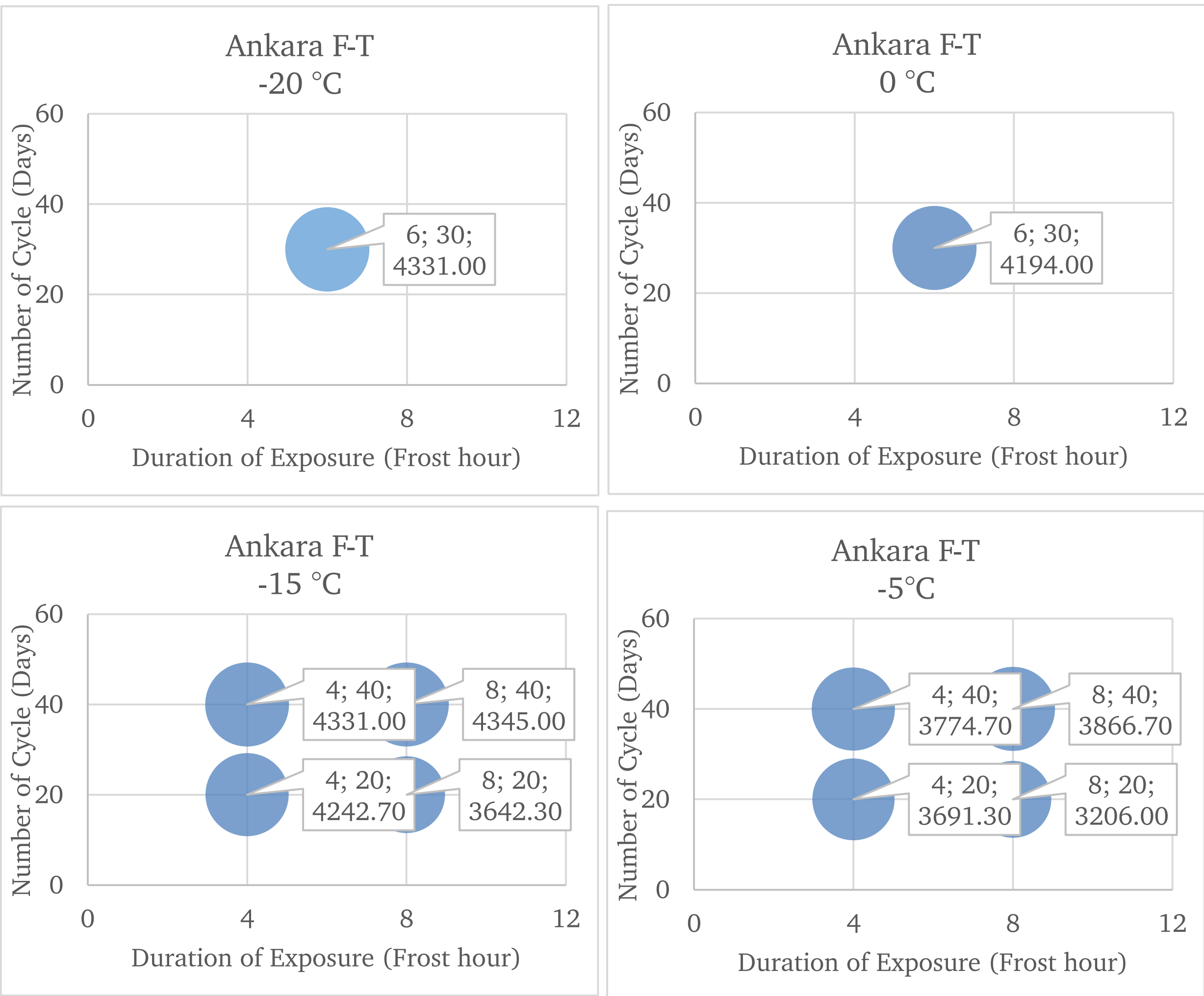

Figure 6.22 UPV results of Ankara stone after frost/thaw procedure

• When examined in terms of temperature values, it was observed that the expected ultrasonic velocity decrease was not observed with the decrease in temperature. Considering together with its surface hardness, it can be said that Ankara stone is generally resistant to freezing degradation.

• When examined according to exposure time in constant cycle amount, an increase of 15 m/s was observed when going from 4 hours to 8 hours for -15°C, 40 cycles, while a decrease of 600 m/s was observed in 20 cycles. For -5°C, an increase of approximately 90 m/s was observed when increasing from 4 hours to 8 hours in 40 cycles, while a decrease of 485 m/s was observed as a result of the same change in 20 cycles.

• Looking at the constant exposure times, it was seen that the ultrasonic speed increased with increasing cycle amounts in all cycles, despite the fixed exposure times.

Bitlis

Table 6.60 UPV results of Bitlis stone after frost/thaw procedure

	Temperature (°C)	Duration of Exposure (Frost hour)	Number of Cycle (Days)	Ultrasonic Pulse Velocity (m/s)
FB1	-20	6	30	2694.00
FB2	-15	8	40	2714.67
FB3	-15	4	40	2711.00
FB4	-15	4	20	2776.67
FB5	-15	8	20	2498.33
FB6	-5	4	40	2791.00
FB7	-5	4	20	2541.67
FB8	-5	8	40	2371.00
FB9	-5	8	20	2694.67
FB10	0	6	30	2700.33

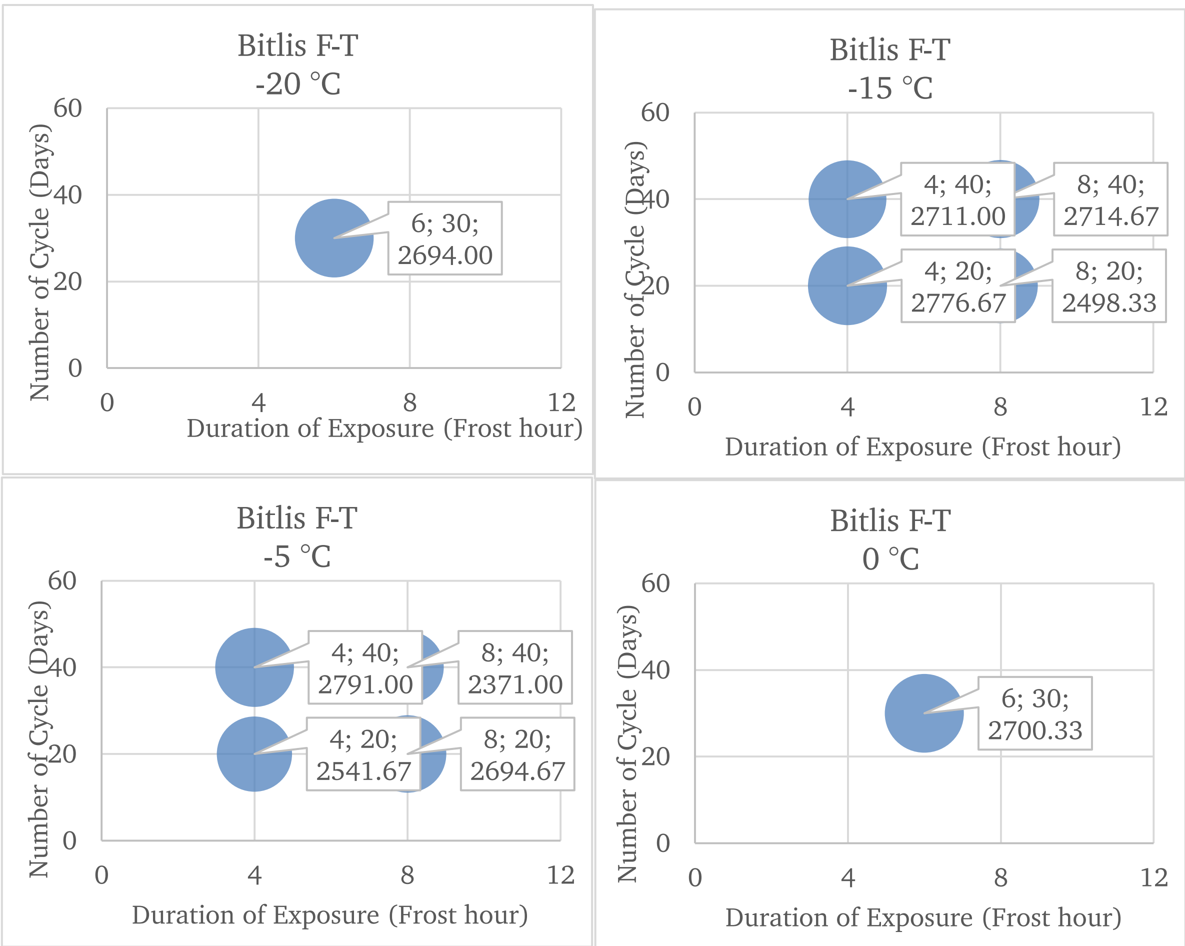

Figure 6.23 UPV results of Bitlis stone after frost/thaw procedure

• When the temperature-based ultrasonic velocities of Bitlis stones are examined, it is seen that, while a decrease is expected with a decrease in temperature, an increase is observed (similar to Ankara stone).

• Looking at the exposure times at constant cycle amounts, it can be said that for -15°C, a decrease of 278 m/s is observed in the exposure times that increase from 4 hours to 8 hours in 20 cycles, while there is almost no change for 40 cycles. For -5°C, when increasing from 4 hours to 8 hours in 20 cycles, a decrease of 420 m/s was observed, while an increase of 153 m/s was observed in 20 cycles.

• Looking at the constant exposure times, a decrease was observed in the cycle amount of 4 hours exposure for -15°C, while an increase in 8 hours exposure was observed. A similar situation can be said for -5°C.

• When evaluated in general, as a result of the examination of the freeze-thaw strength of Bitlis stone, it can be said that the temperature affects inversely, but the other parameters examined do not show a statistically significant change.

Mardin

Table 6.61 UPV results of Mardin stone after frost/thaw procedure

	Temperature (°C)	Duration of Exposure (Frost hour)	Number of Cycle (Days)	Ultrasonic Pulse Velocity (m/s)
FM1	-20	6	30	2512.00
FM2	-15	8	40	3450.00
FM3	-15	4	40	2961.33
FM4	-15	4	20	2373.67
FM5	-15	8	20	3433.67
FM11	-5	4	40	2713.00
FM12	-5	4	20	2586.00
FM13	-5	8	40	1244.00
FM14	-5	8	20	3984.00
FM15	0	6	30	2268.33

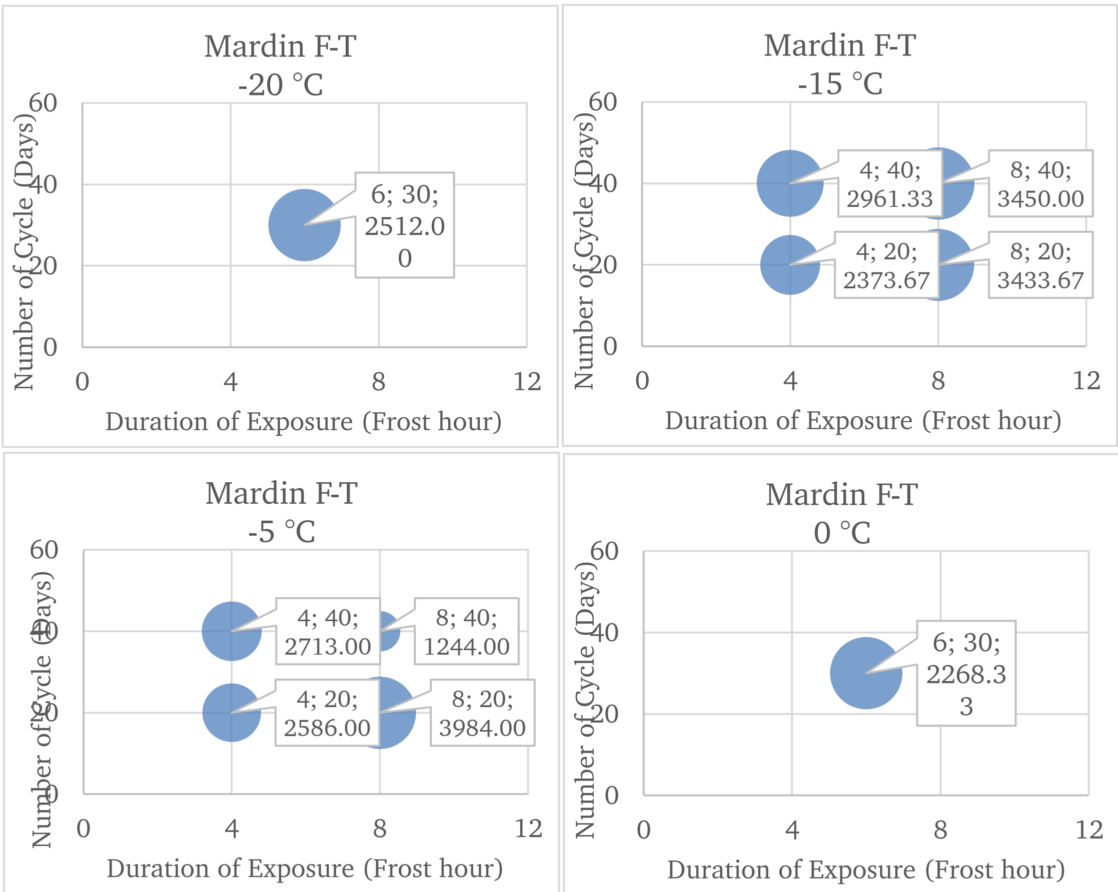

Figure 6.24 UPV results of Mardin stone after frost/thaw procedure

• When the graphics are analyzed for the temperature, it can be said that there is no correlation depending on the temperature.

• When examined in terms of constant exposure values, it was observed that a decrease of 2740 m/s was observed when going from 20 cycles to 40 cycles as a result of 8 hours of exposure only for -5°C, and in the samples other than this, an increase was observed with the cycle time.

• In constant cycle times, when the variable exposure durations are examined, it is observed that a decrease is observed in the experiment of 40 cycles at -5°C, and an increase is observed in the samples other than this, depending on the exposure time.

• Finding similar results in both UPV values and surface hardness values in Mardin stone may lead us to conclude that the stone becomes more durable after freeze-thaw cycles. However, due to reasons such as the heterogeneous nature of the stones and the small number of samples, it can be said that different analysis techniques and more samples should be studied in order to verify this hypothesis.

Nevsehir

Table 6.62 UPV results of Nevsehir stone after frost/thaw procedure

	Temperature (°C)	Duration of Exposure (Frost hour)	Number of Cycle (Days)	Ultrasonic Pulse Velocity (m/s)
FN1	-20	6	30	1907.33
FN2	-15	8	40	2008.33
FN3	-15	4	40	1834.33
FN4	-15	4	20	2019.00
FN5	-15	8	20	2047.00
FN11	-5	4	40	1861.33
FN12	-5	4	20	2037.33
FN13	-5	8	40	1909.00
FN14	-5	8	20	2018.00
FN15	0	6	30	2019.00

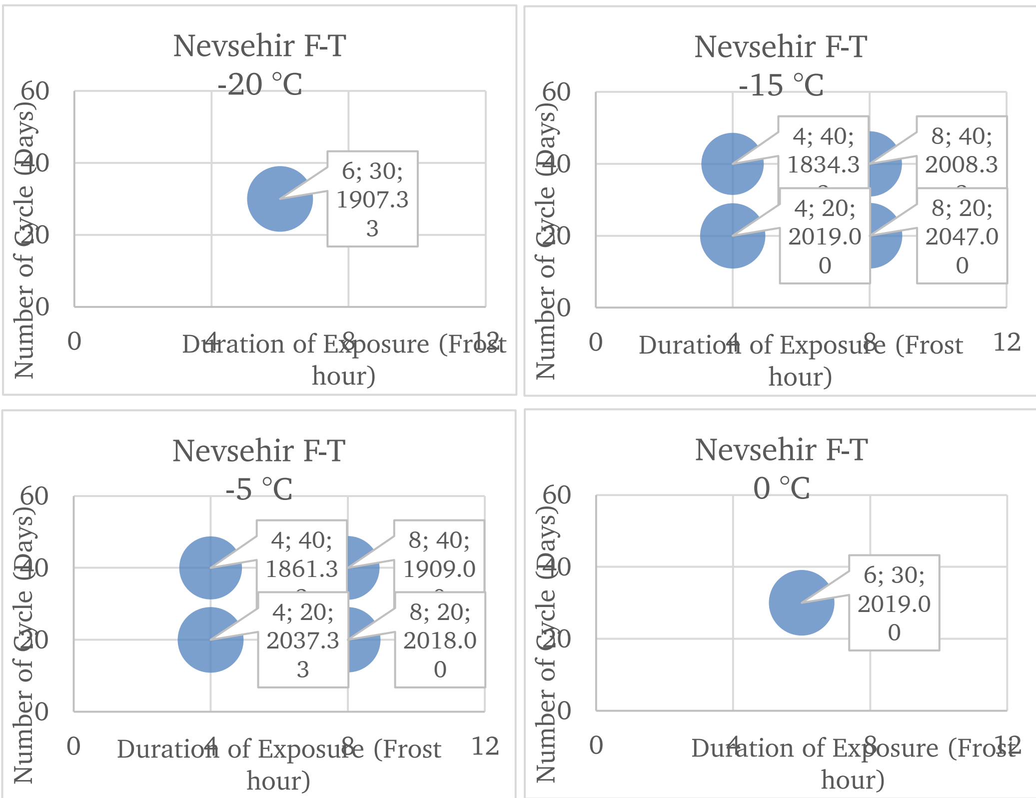

Figure 6.25 UPV results of Nevsehir stone after frost/thaw procedure

• When the evaluation is made in terms of temperature values, it is seen that there is a decrease of about 100 m/s in speed when going from 0°C to -20°C, but the intermediate values are very close to each other.

• Looking at the number of cycles at constant exposure time, it was observed in all trials that the speed decreased as the number of cycles increased.

• Looking at the exposure times versus the constant cycle times, it was observed that an inversely proportional change was observed in all of the trials except the 20-cycle trial at -5°C.

- **Surface Roughness**

In surface roughness analysis, both numerical values and topographic images are taken.

<u>Ankara</u>

Table 6.63 Surface roughness results of Ankara stone after frost/thaw procedure

	Temperature (°C)	Duration of Exposure (Frost hour)	Number of Cycle (Days)	Surface Roughness Rz (μm)
FA1	-20	6	30	34.68
FA2	-15	8	40	36.69
FA3	-15	4	40	37.78
FA4	-15	4	20	33.11
FA5	-15	8	20	35.57
FA11	-5	4	40	37.06
FA12	-5	4	20	35.54
FA13	-5	8	40	36.48
FA14	-5	8	20	35.71
FA15	0	6	30	31.24

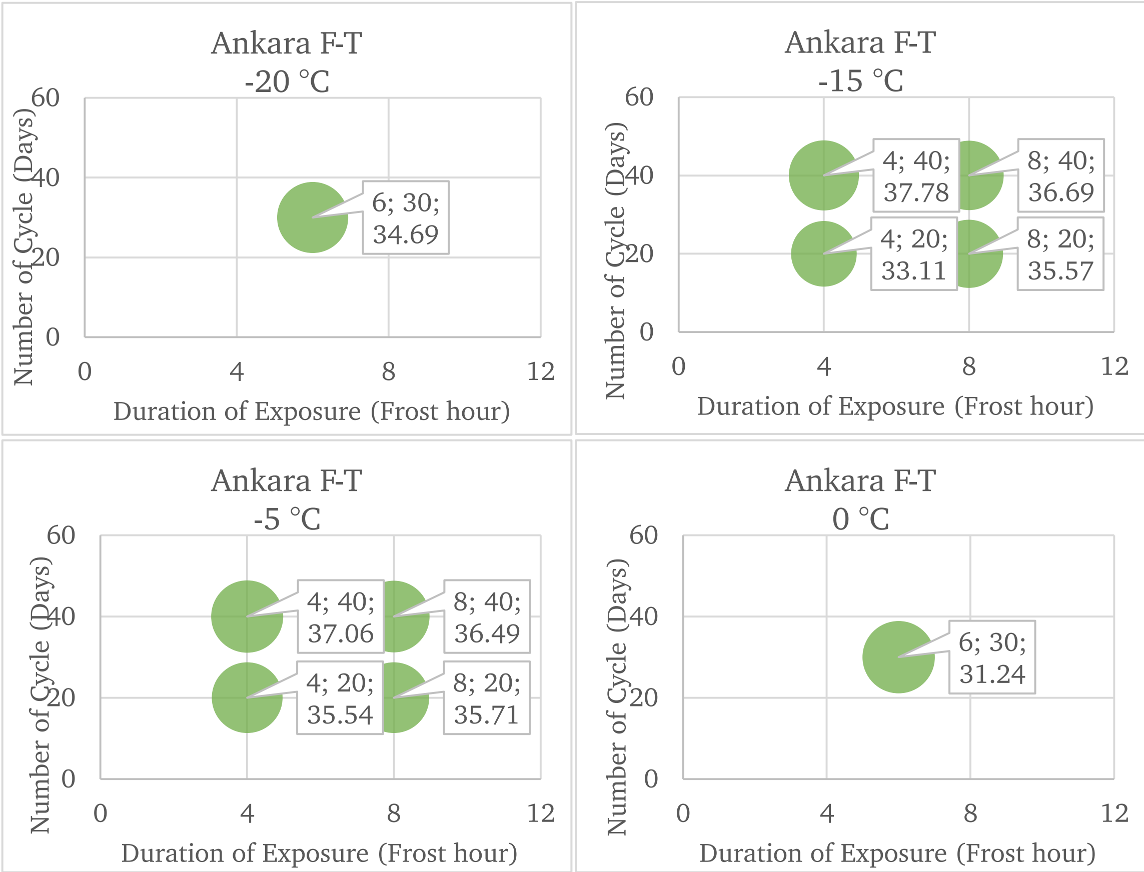

Figure 6.26 Surface roughness results of Ankara stone after frost/thaw procedure

• When the surface roughness is examined in terms of freezing temperatures, it is seen that the roughness slightly increases from -20°C to -5°C for Ankara stone, but decreases again at 0°C degrees.

• Looking at the cycle amount at constant exposure times, it was observed that the roughness of the samples increased between 1-4 μm with the increasing cycle time.

• No correlation could be established between exposure time and roughness in constant cycle amounts.

Bitlis

Table 6.64 Surface roughness results of Bitlis stone after frost/thaw procedure

	Temperature (°C)	Duration of Exposure (Frost hour)	Number of Cycle (Days)	Surface Roughness Rz (μm)
FB1	-20	6	30	32.30
FB2	-15	8	40	31.64
FB3	-15	4	40	31.28
FB4	-15	4	20	31.88
FB5	-15	8	20	29.75
FB6	-5	4	40	31.42
FB7	-5	4	20	30.01
FB8	-5	8	40	30.91
FB9	-5	8	20	32.34
FB10	0	6	30	28.99

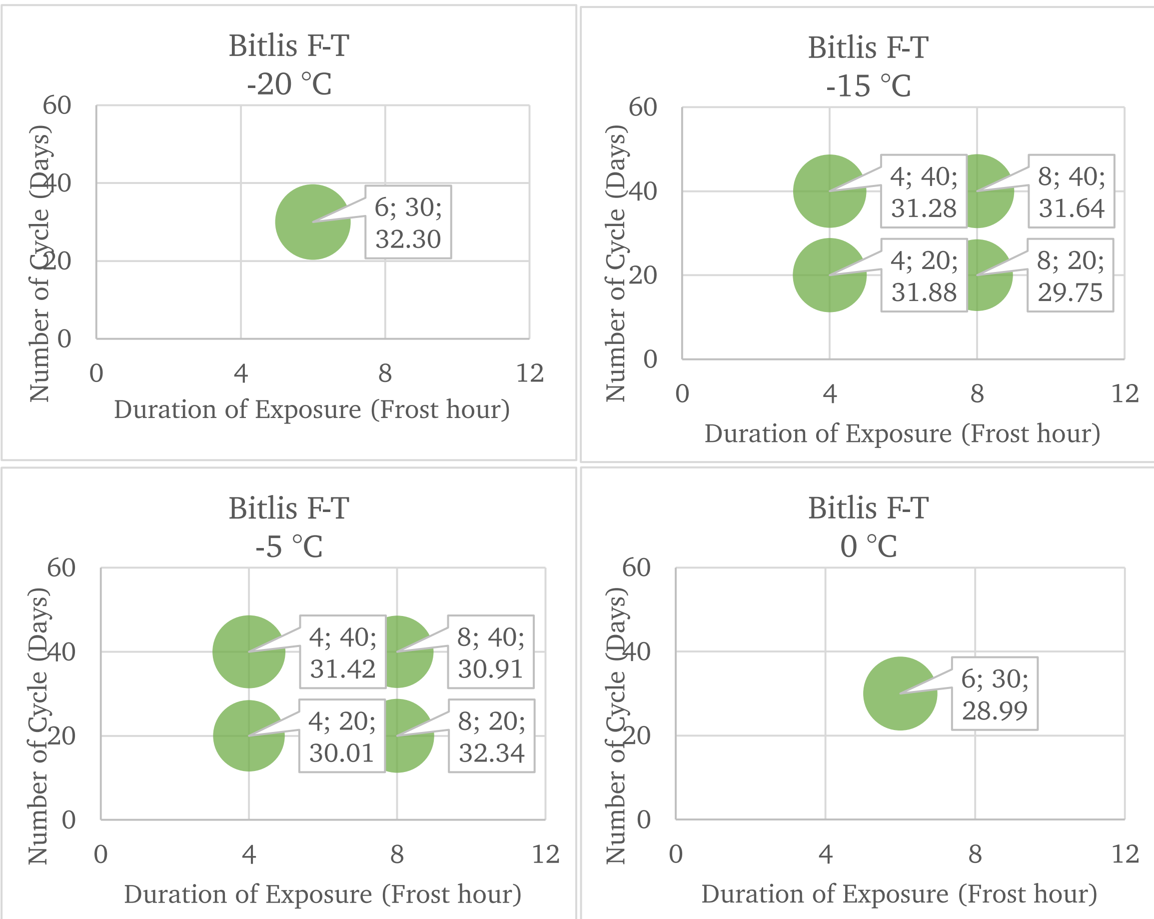

Figure 6.27 Surface roughness results of Bitlis stone after frost/thaw procedure

• When the effect of the freezing effect on the roughness on Bitlis stones is examined, it is observed that the values at -15°C and -5°C degrees are very close to each other, but there is an increase in roughness around 3μm from 0°C to -20°C.

• When looking at the change in fixed exposure times according to the amount of cycles, in some of the experiments, an increase of 1μm is observed, while some decrease at the same level is observed. Accordingly, it can be said that the number of cycles for Bitlis stone generally does not affect the roughness in freezing damage.

• A similar situation is also valid for exposure times in fixed cycle amounts.

• In this case, it can be said that the most effective parameter for these examples is temperature change.

Mardin

Table 6.65 Surface roughness results of Mardin stone after frost/thaw procedure

	Temperature (°C)	Duration of Exposure (Frost hour)	Number of Cycle (Days)	Surface Roughness Rz (μm)
FM1	-20	6	30	14.46
FM2	-15	8	40	14.35
FM3	-15	4	40	15.86
FM4	-15	4	20	12.67
FM5	-15	8	20	15.07
FM6	-5	4	40	13.67
FM7	-5	4	20	14.25
FM8	-5	8	40	15.45
FM9	-5	8	20	14.18
FM10	0	6	30	14.79

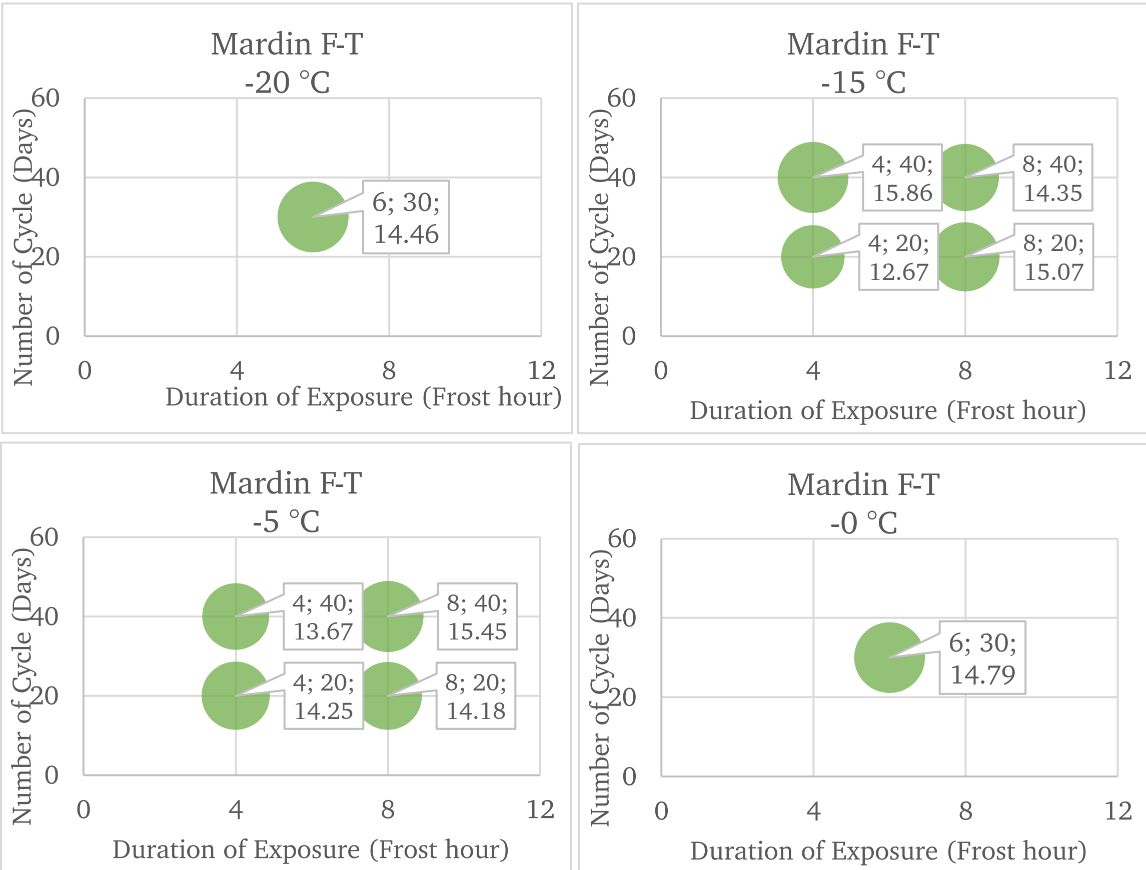

Figure 6.28 Surface roughness results of Mardin stone after frost/thaw procedure

• When looking at the effect of freezing temperature in Mardin stone, it is seen that the change in roughness values is less than 1% when the average values are considered.

• When the constant exposure values are examined, the roughness increased with the increase in the cycle amount at -15°C at 4 hours exposures, while a decrease of 0.6 μm was observed in 8 hour exposures. A similar situation was observed in the trials at -5°C.

• When the exposure times are evaluated in constant cycle amounts, it can be said that both increase and decrease are observed for both temperature values and there is no correlation.

• Generally, we can say that the freezing effect does not cause a significant change on the roughness for Mardin stone.

Nevsehir

Table 6.66 Surface roughness results of Nevsehir stone after frost/thaw procedure

	Temperature (°C)	Duration of Exposure (Frost hour)	Number of Cycle (Days)	Surface Roughness Rz (μm)
FN1	-20	6	30	23.68
FN2	-15	8	40	22.35
FN3	-15	4	40	16.93
FN4	-15	4	20	23.63
FN5	-15	8	20	30.84
FN6	-5	4	40	22.65
FN7	-5	4	20	29.63
FN8	-5	8	40	25.07
FN9	-5	8	20	44.78
FN10	0	6	30	52.62

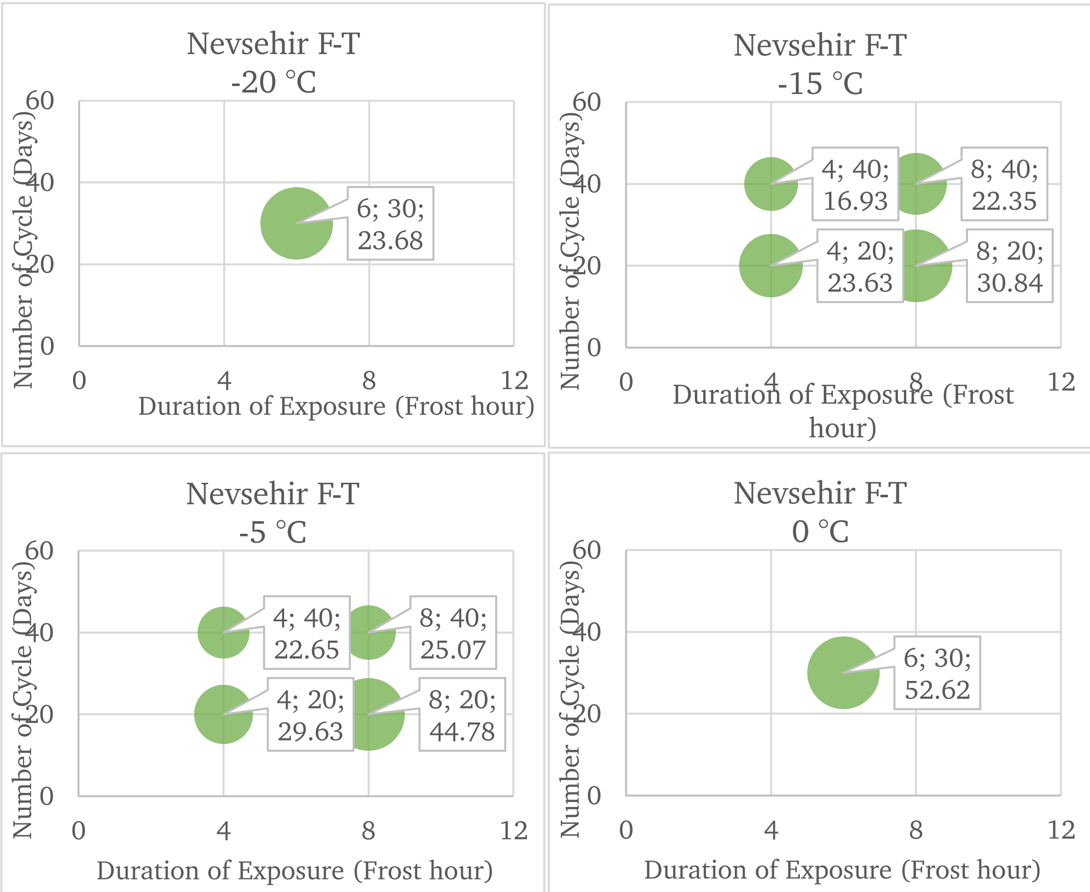

Figure 6.29 Surface roughness results of Nevsehir stone after frost/thaw procedure

• Compared to other stones, it is the type of stone that has the widest distribution of roughness as a result of frost damage.

• When the temperature values are examined, it is seen that the roughness decreases by 20 μm levels as the temperatures are decreased. The reason for this situation may be that the particles on the surface of this heterogeneous stone type are separated from the structure by the effect of freeze-thaw.

• When looking at cycle amounts at constant exposure values, a reduction in roughness of 8-20 μm was observed in all of the samples. The reason for this may be that the particles were removed from the structure more easily by means of water as a result of the samples being immersed in water after the freezing stage during the trials.

• In constant cycle values, as the exposure time increased, the roughness of all samples increased. This may be because more pits occur in the structure.

• Images can also be examined for more detailed analysis of the examples.

• In summary, the frost damage in Nevsehir stone showed different correlations for all three parameters; it has been observed that it decreases as the freezing temperature decreases and the number of cycles increases, but increases as the exposure time increases.

6.2 Consolidant Studies

6.2.1 Diammonium Hydrogen Phosphat (DAP) Treatment Results

Table 6.67 displays the abbreviations used in following graphs and tables to avoid any misunderstanding between the samples.

Table 6.67 Samples and abbreviations presented in further sections

Sample	**Abbreviation**
DAP Treated Samples Before Treatment	B-DAP
DAP Treated Samples After Treatment (Before Weathering)	A-DAP
Untreated Control Sample (Before Weathering)	UT-BW
DAP Treated Samples after 20 days of Weathering	A-DAP-AW
Control Samples after 20 days of Weathering	UT-AW
TEOS Treated Samples Before Treatment	B-TEOS
TEOS Treated Samples After Treatment	A-TEOS

- **Weight**

The amount of consolidant absorbed by the stone is calculated using weight measurements (Sassoni et al., 2013)

Table 6.68 shows the results for each stone form. The dry weight results for DAP/Ca procedure are compatible with literature values (0.1-0.3 percent (Sassoni et al., 2013)). Although the Mardin stone had the most $CaCO_3$ material, it had the smallest weight difference after treatment. This can be explained by the relatively low rate of water absorption shown in Table 5, because the amount increase in weight caused by DAP/Ca treatment is found to be very similar to maximum water saturation in other experiments (Sassoni et al., 2013, 2016).

For all stone kinds, the weight disparity for TEOS treatment is greater than for DAP treatment. The main reason for this is that the two merged applications use separate mechanisms. Following that, DAP treatment is based on the reaction (5.1) between stone and DAP to form HAP. As shown in the equation, the by-products of this reaction (ammonium carbonate, carbon dioxide, and water) are both innocuous and volatile, implying that no unwanted residues are needed to linger in the stone (Sassoni, 2018).

However, because the reaction uses stone as the $CaCO_3$ source, the reaction should not greatly increase weight because 10 moles of $CaCO_3$ (1000 g) are required to form 1 mole of HAP (988 g). In our case, the weight increased slightly because we used an additional Ca^{2+} source.

TEOS, on the other hand, enters the capillary pores and reacts with moisture to form a silica gel binder $(SiO_2)_{aq}$. Because there is no reaction between stone and TEOS, the weight of more than DAP increases when SiO_2 is produced.

Table 6.68 Weight differences mean and standard deviations between before and after the treatments (n=3)

	ANK	BIT	MAR	NEV
Weight Difference After DAP Treatment (g)	0.46 ± 0.06	0.41 ± 0.06	0.23 ± 0.14	0.44 ± 0.12
Weight Difference After DAP Treatment (%)	0.17± 0.02	0.23±0.03	0.15 ± 0.09	0.28 ± 0.07
Weight difference after TEOS treatment (g)	1.26±0.17	1.56±0.15	1.56±0.07	1.65±0.03
Weight difference after TEOS treatment (%)	0.44±0.06	0.88±0.09	1.04±0.03	1.02±0.06

- **Water Absorption**

Table 6.69 shows the water absorption results of untreated samples according to BS EN 13755: 2008 standard.

Table 6.69 Water absorption mean and standard deviations percentage of untreated samples (n= 3)

	ANK	BIT	MAR	NEV
Water Absorption (%)	4.53 ± 0.10	20.18 ± 0.09	12.72 ± 4.29	24.48 ± 1.49

Figure 6.30 depicts the effects of the treated samples prior to and following the application. The study was carried out on all stone forms, but Ankara stone absorbed less than 5 mL in 60 minutes, which was insignificant for plotting.

The findings revealed that the water transport properties of the Bitlis and Nevsehir stones decreased significantly but did not change significantly, whereas the absorption potential of the Mardin stone remained nearly unchanged. This is a significant finding for the Consolidant because most other Consolidants (such as TEOS) make the surface hydrophobic. This exposes the sample to further decay because the water can remain behind the treatment and makes aqueous application after consolidation more difficult (Borsoi et al., 2016). The results were also found to be consistent with previous DAP treatments (Borsoi et al., 2016; Sassoni et al., 2013).

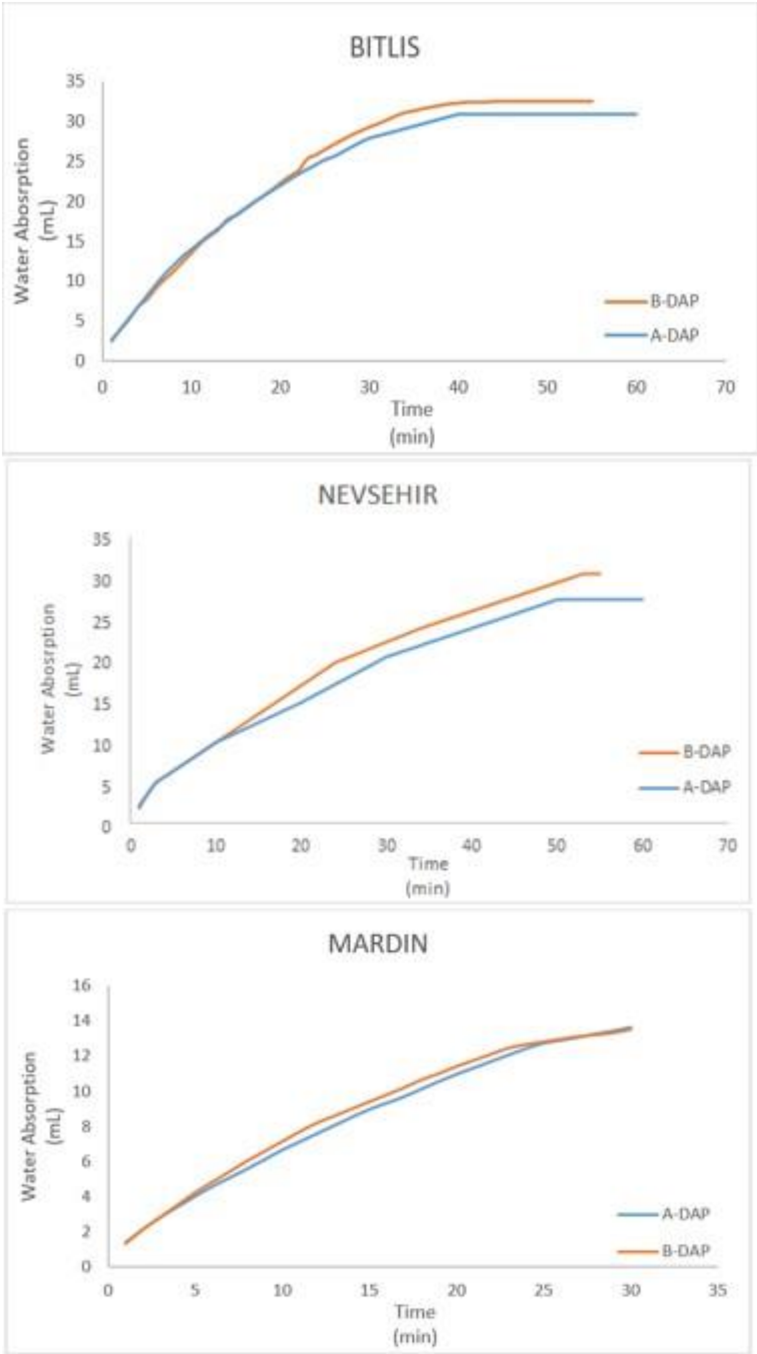

Figure 6.30 Water absorption capacities of Bitlis, Nevsehir and Mardin stones, before DAP/Ca treatment (B-DAP) and after DAP/Ca treatment (A-DAP)

- **Surface Hardness**

When all of the stones in Figure 6.31 are compared, it is clear that Ankara stone has the highest hardness values (near stainless steel and above the rest of the metals) even before treatment. On the other hand, Nevsehir stone is discovered to be the softest of all. This explains the carved churches and underground towns in Cappadocia, as soft stones are better for carving. Mardin stone, like Nevsehir stone, has soft surfaces. This is the reason for the popularity of carvings on buildings in Midyat and Mardin. The Mardin stone, on the other hand, displayed scattered Equotype data, and data on this stone was difficult to obtain due to pits and surface heterogeneity.

Ankara, Mardin, and Nevsehir stones have improved mechanically on their surfaces after DAP/Ca treatment. TEOS treatment, on the other hand, had no effect on surface hardness in Ankara, Bitlis, or Mardin stones, but Nevsehir stone showed higher surface hardness efficiency after TEOS treatment. However, the variations are insignificant, and the results are highly uncertain. These results are consistent with literature values, which show that surface hardness increases by less than 5% (Chen et al., 2016) and 2% (Mol et al., 2017) after TEOS application. This can be viewed as a positive result because the consolidant does not cause a significant change in the surface and internal structure of the sample. These results are compounded by DRMS data where higher resistance was observed over the 15 mm profiles sampled under the combined surfaces.

The weathering process reduced surface hardness in all specimens, but DAP/Ca treatment reduced weathering degradation in Ankara, Bitlis, and Nevsehir stones by a small amount (compare to UT-AW and A-DP-AW samples in Figure 6.31).

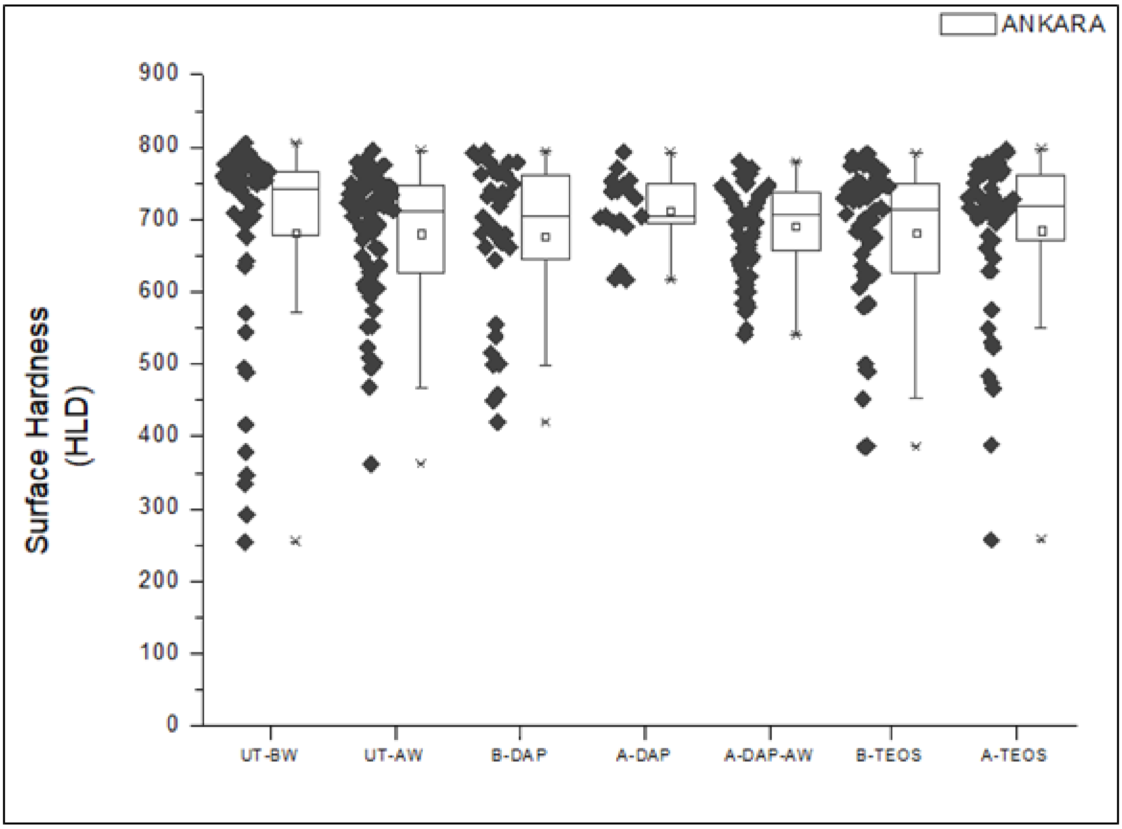
ANKARA
Surface Hardness (HLD)
900
800
700
600
500
400
300
200
100
0
UT-BW
UT-AW
B-DAP
A-DAP
A-DAP-AW
B-TEOS
A-TEOS

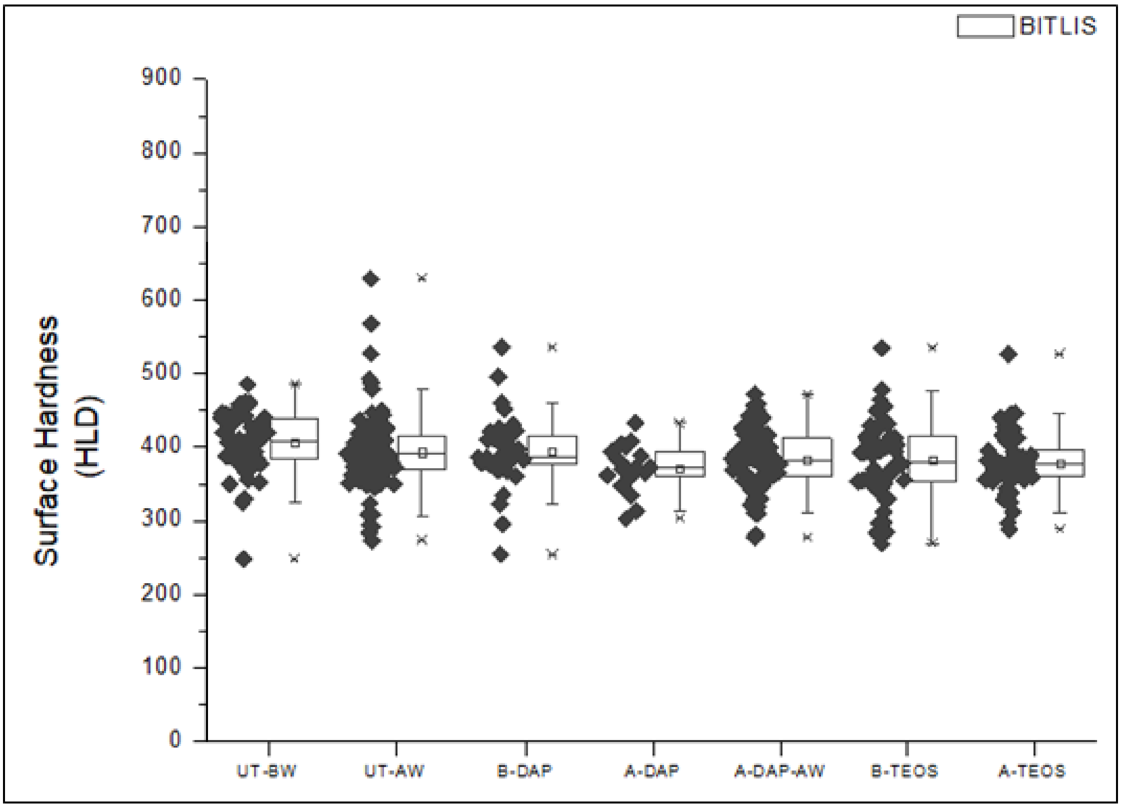
BITLIS
Surface Hardness (HLD)
900
800
700
600
500
400
300
200
100
0
UT-BW
UT-AW
B-DAP
A-DAP
A-DAP-AW
B-TEOS
A-TEOS

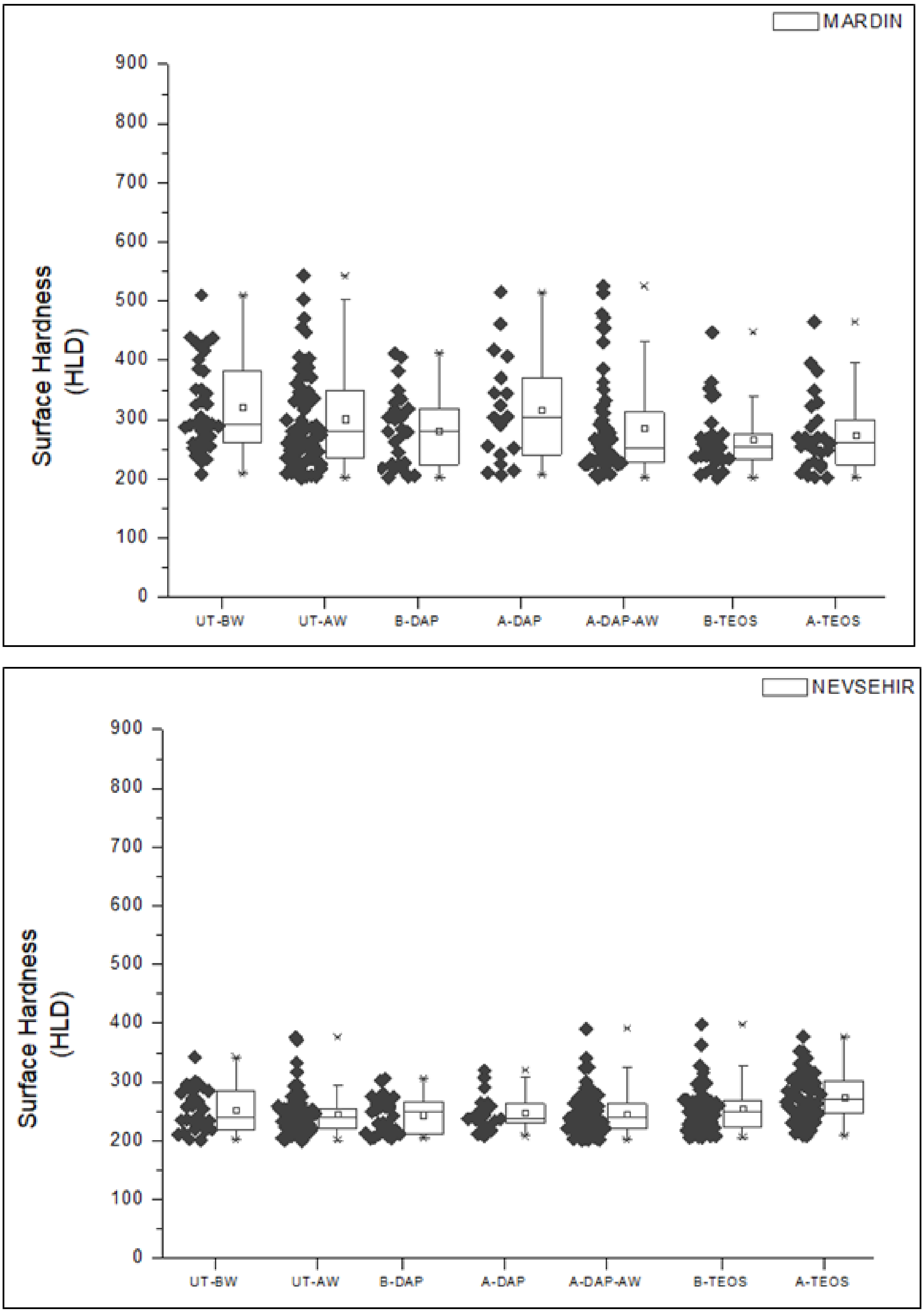

Figure 6.31 Surface hardness results with real data and boxplot charts of all stones

- **Ultrasonic Pulse Velocity (UPV) Analysis**

Data from UPV have been found in the literature to provide a valid link with compressive strength (Vasanelli et al., 2015). It is also recognized as a significant parameter for consolidation efficiency or level of weathering (Pamplona et al., 2010).

UPV findings (Figure 6) reveal that Ankara stone has the greatest UPV values before and after treatment, while Nevsehir stone has the lowest values. DAP/Ca treatment improved the UPV values (4-15%) for all rock types (Figure 6.32). This can be due to the development of HAP within pores, as seen in earlier studies (Sassoni & Franzoni, 2014).

TEOS treatment didn't seem to affect Ankara and Bitlis stones, but it affected Mardin slightly higher than DAP/Ca (15% for DAP/Ca and 18% for TEOS) and Nevsehir stone (6%). Weathering cycles did not have a drastic effect on UPV values on any of the samples. While it has previously been stated in the literature that UPV values are decreased by up to 65 percent and 32.33 with weathering steps. However, these experiments consisted of severe weather conditions (such as 1 hour at 400°C), whereas mild weather conditions were implemented in this thesis.

Mardin stone has the highest standard deviation values (as can be seen in Figure 6.32) which are presumably the product of bedding. This is therefore consistent with the effects of water absorption.

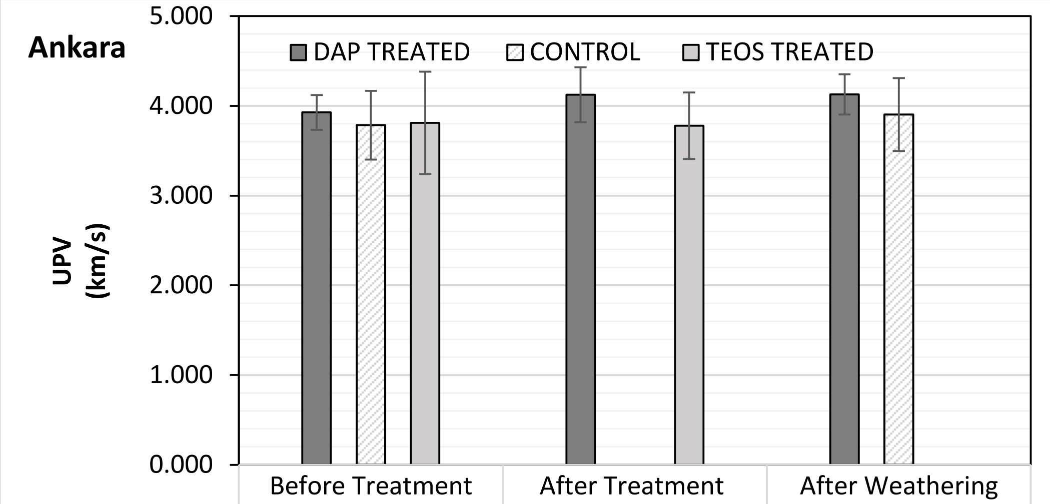

	Before Treatment	After Treatment	After Weathering
DAP TREATED	3.927	4.126	4.129
CONTROL	3.785		3.903
TEOS TREATED	3.810	3.780	

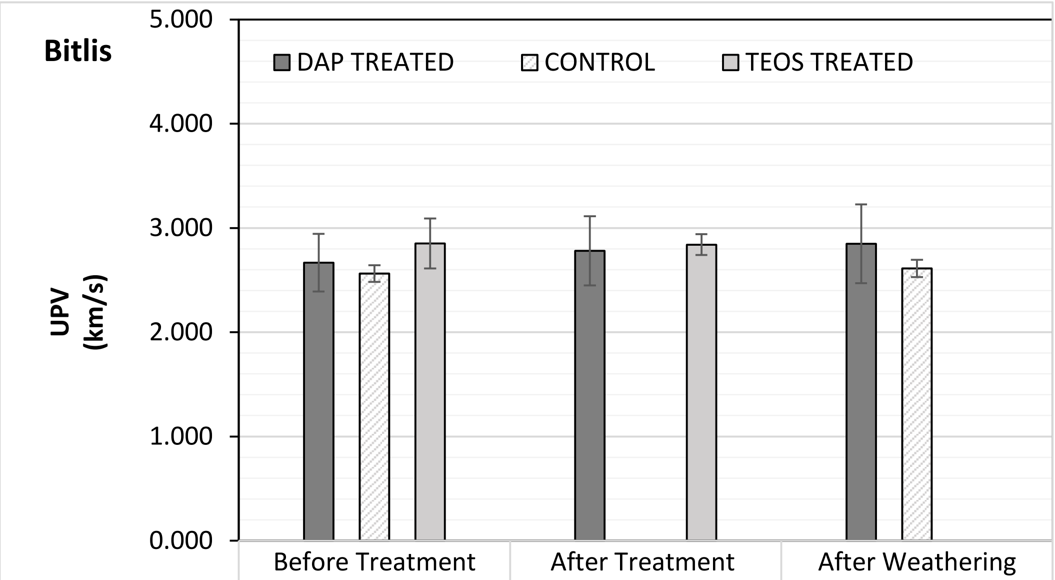

	Before Treatment	After Treatment	After Weathering
DAP TREATED	2.667	2.780	2.847
CONTROL	2.562		2.612
TEOS TREATED	2.850	2.840	

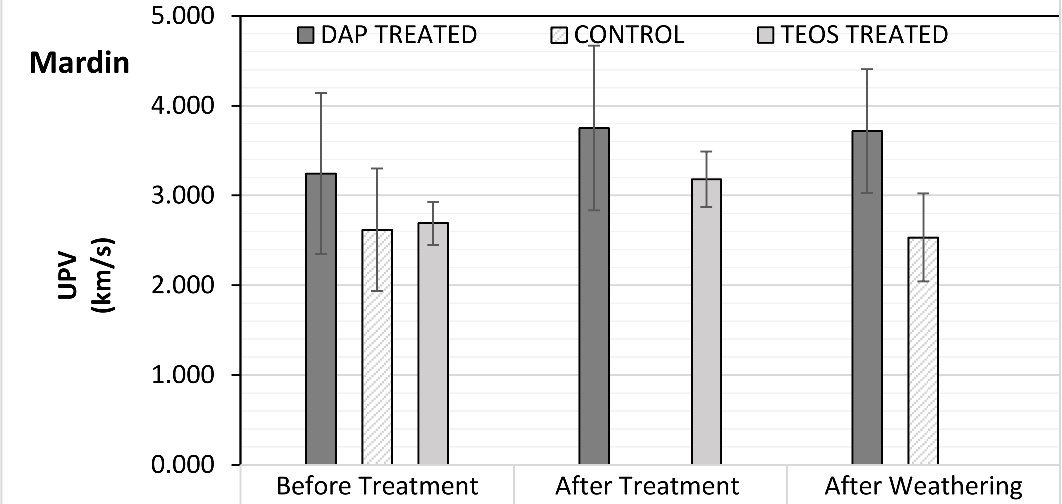

	Before Treatment	After Treatment	After Weathering
DAP TREATED	3.245	3.752	3.717
CONTROL	2.618		2.532
TEOS TREATED	2.690	3.180	

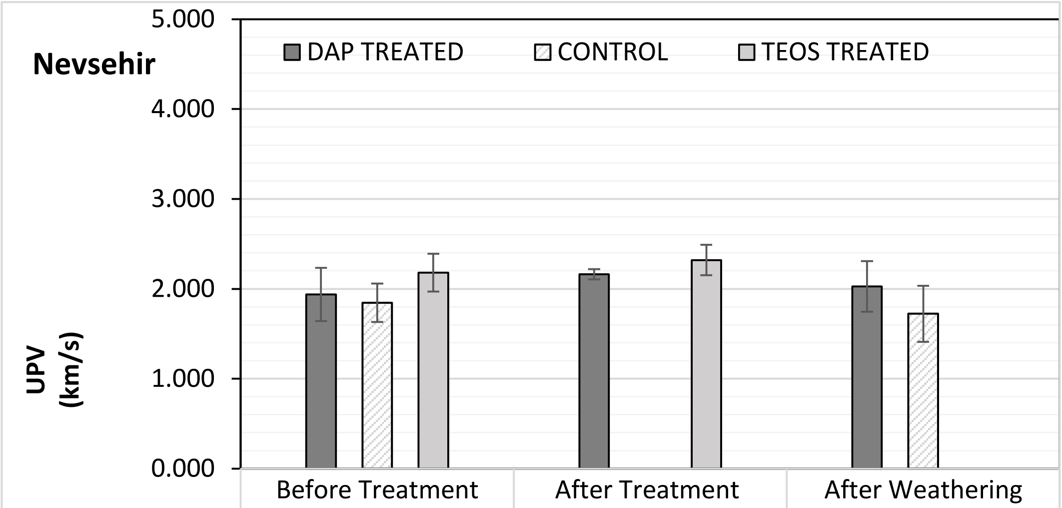

	Before Treatment	After Treatment	After Weathering
DAP TREATED	1.938	2.161	2.027
CONTROL	1.845		1.722
TEOS TREATED	2.180	2.320	

Figure 6.32 Average UPV results for all samples. Darker bars represent the treated DAP/Ca samples, grey bars represent TEOS treated samples and stripe bars represent the control samples. For control samples, “After Treatment” column represents the UPV value before weathering.

- **DRMS (Drilling Resistance Measurement System)**

Figure 6.33 shows the results for DAP/Ca treated and untreated surfaces. (Ankara stone couldn't be measured because it exceeded the limits of the equipment which is 100 N.)

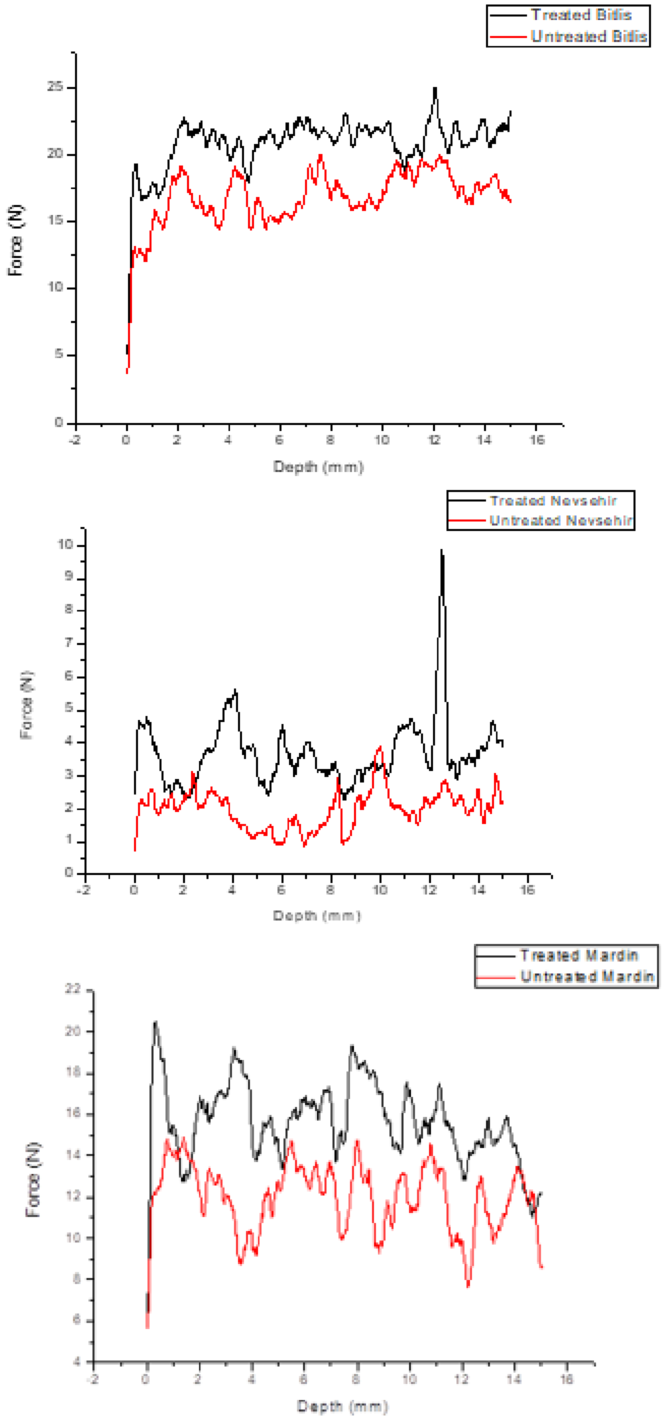

Figure 6.33 Average values (n=2) for DRMS data for Bitlis, Mardin and Nevsehir stones

The findings indicated that DAP/Ca treatment improved the drilling resistance value (~5 N for Bitlis and Mardin and ~2 N for Nevsehir) for each litotype. The results are also consistent with the literature data, showing an improvement in DRMS results between 2N (Sassoni et al., 2017) and 8N (Matteini et al., 2011) for DAP-treated limestones and 6N for DAP-treated silicate stones (Molina et al., 2018). In Nevsehir stone, it is very clear that the DAP/Ca treatment increased very significantly in certain points (e.g. at 13 mm depth). It may be linked to the creation of HAP crystal within the pores. The high porosity of Mardin stone induced variance in DRMS results, while the homogeneous structure of Bitlis one resulted in the lowest deviation. In a recent report, Molina et al. pointed out that caution is required in interpreting DRMS data for heterogeneous samples. In addition, penetration depth and drilling resistance are considered to be closely related to the direction of application of bedded stones. The probability of bedding should also be put into question in the first place when applying the consolidations.

- **Color Difference**

ΔE results are shown in Table 6.70.

Table 6.70 Average color difference (ΔE) data (n=3) for treated and control samples. All calculations referred to raw (untreated + unweathered) surfaces. Color difference for control samples calculated before and after weathering

	Control Weathering	DAP Treatment	DAP Treatment + Weathering	TEOS Treatment
ANKARA	0.75 (±0.18)	1.04(± 0.82)	0.74 (±0.58)	3.27 (±2.02)
BITLIS	1.33 (±1.14)	4.32 (±2.14)	1.63 (±0.82)	9.18 (±2.25)
MARDIN	1.43 (±0.77)	0.94 (±0.52)	1.12 (±0.42)	3.81 (±0.91)
NEVSEHIR	4.37 (±2.87)	0.43 (±0.20)	1.80 (±1.62)	5.36 (±1.15)

Due to its multicolored nature, Nevsehir stone has a high standard deviation in color measurements. After DAP/Ca treatment, which is a very significant property for a consolidant, none of the stones except Bitlis resulted in ΔE>3.5 (mostly affected by lower L values). This is the greatest downside of polymeric solids, as they can induce a change of color. This also can be seen from TEOS results. All of the samples resulted in ΔE>3.5, except Ankara, and this is very close to a limit value. In terms of L*, a*, b*, all TEOS treated samples leads to lower L* and higher b* after treatment i.e. darkening and yellowing.

Weathering cycles have not changed the visual properties of control samples for Ankara, Bitlis and Mardin stones. Only Nevsehir one was affected by accelerated weathering, but the shift was not consistent with each sample, as one of the stones was yellower (displayed higher b* value), the other was bluer (displayed lower b* value), and one was darker (displayed lower L* value), while the other was lighter (shown higher L* value). This may be caused by the high and visibly heterogeneous mineralogical content of the material, since all the samples clearly showed different appearances.

- **Surface Roughness**

Figure 6.34 shows mean Rz values in units of micrometers for treated surfaces (before treatment, after treatment and after weathering) and control samples (before and after weathering). Figure 6.35 shows visual impression, 2D and 3D topography of corresponding samples (Corresponding abbreviations can be found in Table 6.67).

In the literature, HAP structure has been seen to be improved by rougher samples (Naidu et al., 2017; Sassoni, 2018; Sassoni et al., 2015) while the impact of the consolidation on roughness parameters has hardly been studied. In this analysis, therefore, we decided to make a distinction between treated, untreated and weathered surfaces.

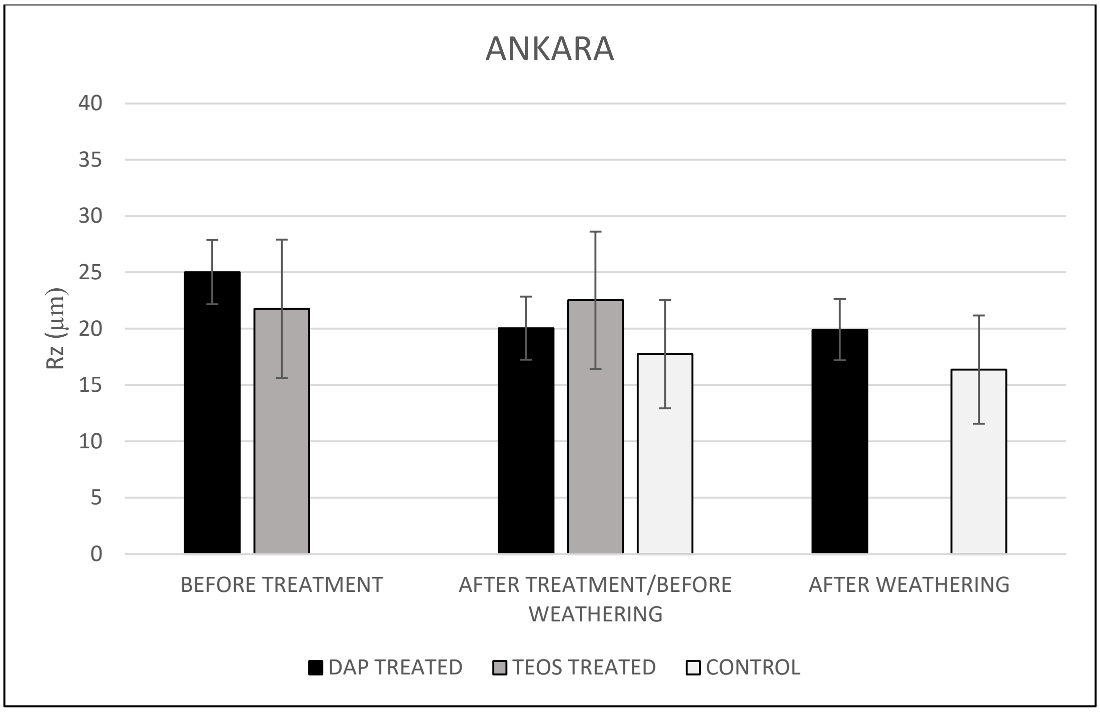
ANKARA
Rz (µm)
40
35
30
25
20
15
10
5
0
BEFORE TREATMENT
AFTER TREATMENT/BEFORE WEATHERING
AFTER WEATHERING
DAP TREATED
TEOS TREATED
CONTROL

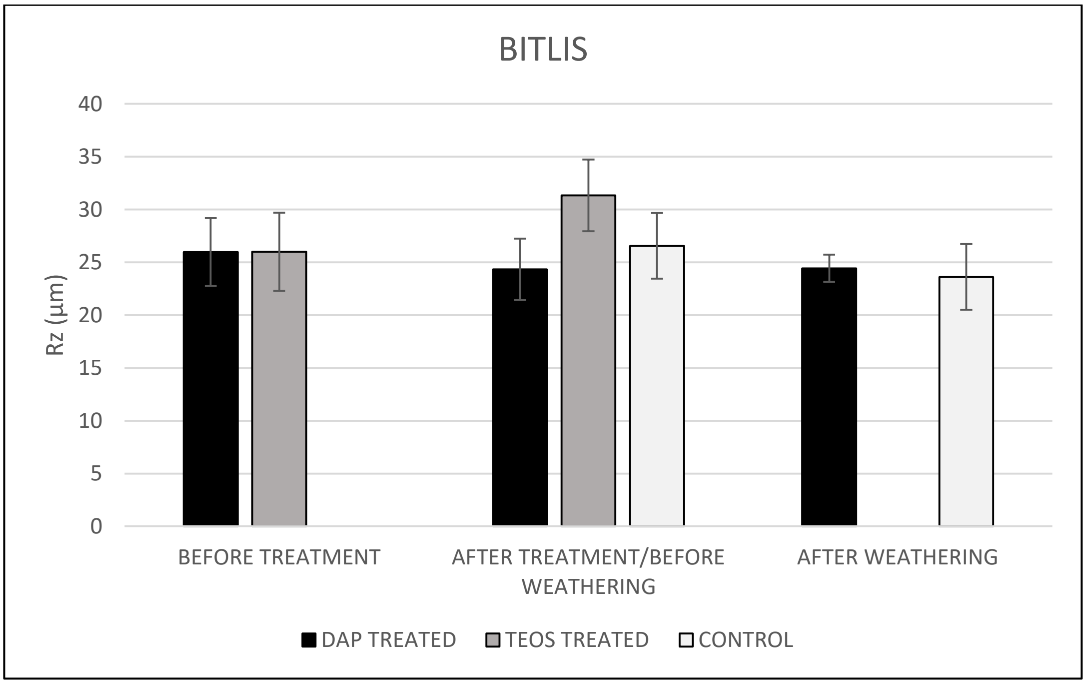
BITLIS
Rz (µm)
40
35
30
25
20
15
10
5
0
BEFORE TREATMENT
AFTER TREATMENT/BEFORE WEATHERING
AFTER WEATHERING
DAP TREATED
TEOS TREATED
CONTROL

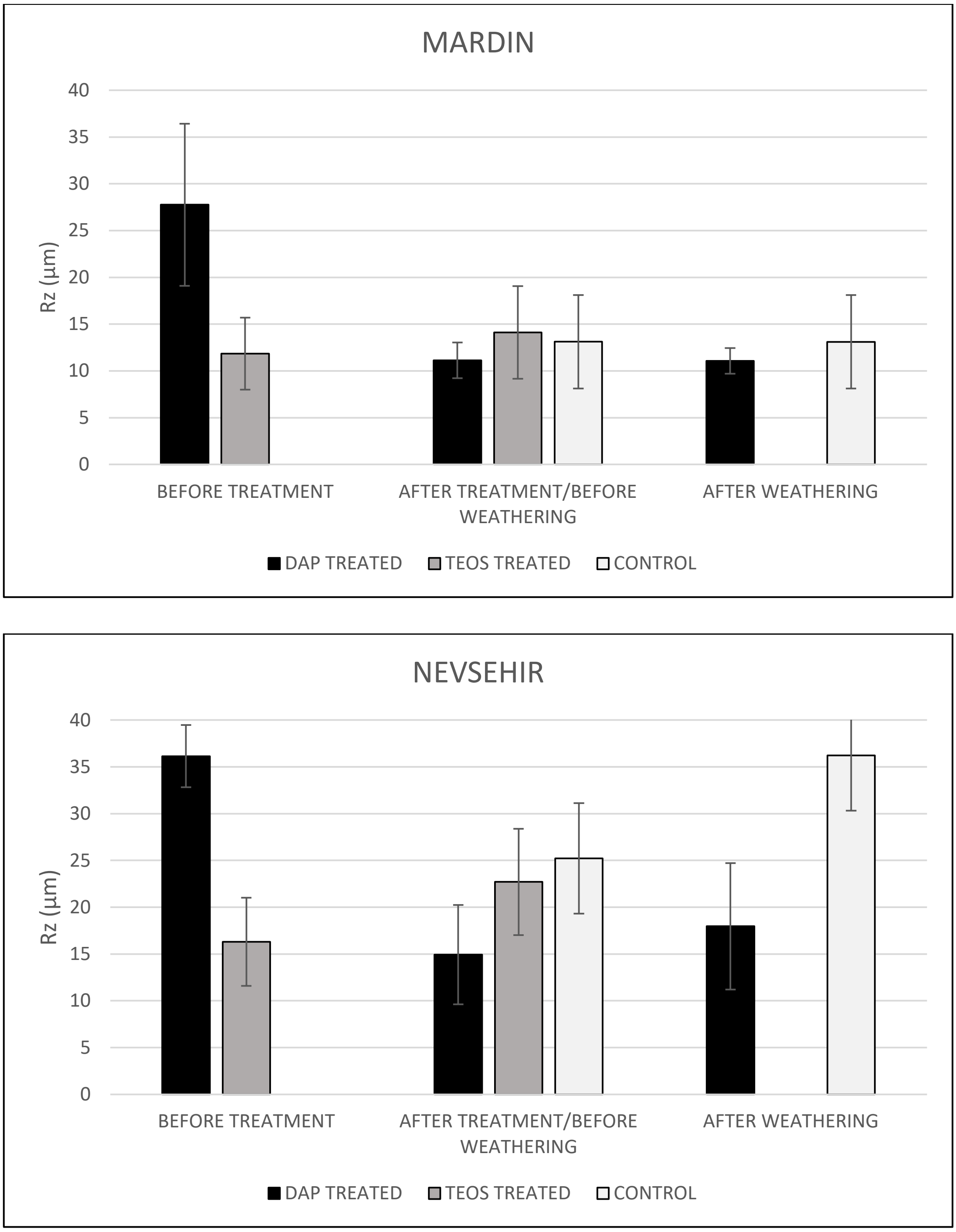

Figure 6.34 Surface roughness (Rz) values for all samples (n=3). Black bars represent DAP/Ca treated samples, grey bars represent TEOS treated samples and white bars represent control samples. Second column shows after treatment values for DAP/Ca and TEOS treated samples and before weathering values for control samples.

ANKARA	Visual Impression	2D Topography	3D Topography
B-DAP	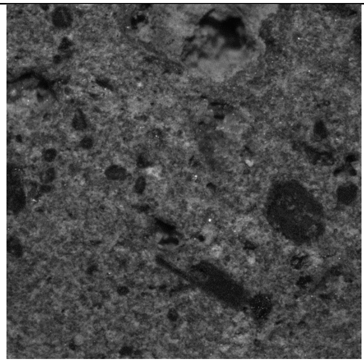	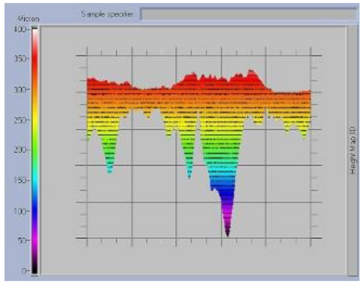	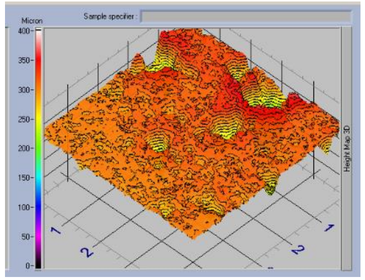
A-DAP	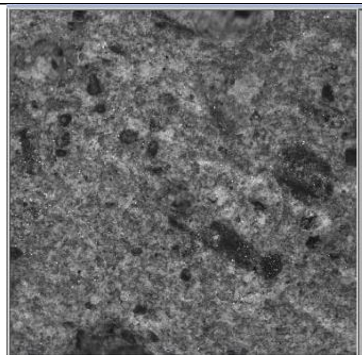	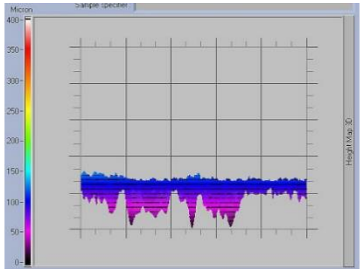	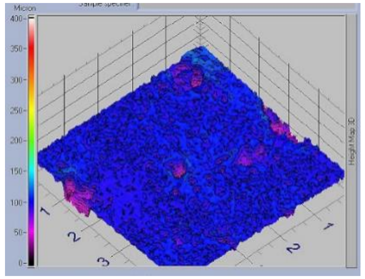
A-DAP-AW	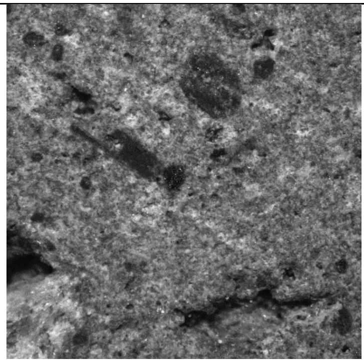	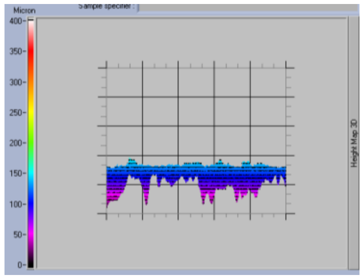	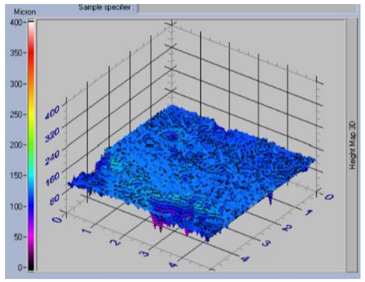

Figure 6.35 (a) Visual impression and topography images for DAP treated Ankara stone

ANKARA	Visual Impression	2D Topography	3D Topography
UT-BW	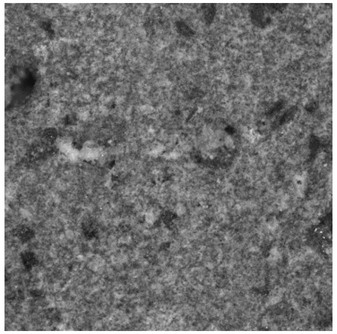	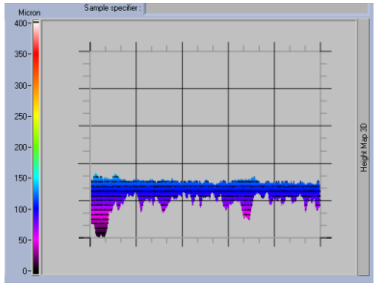	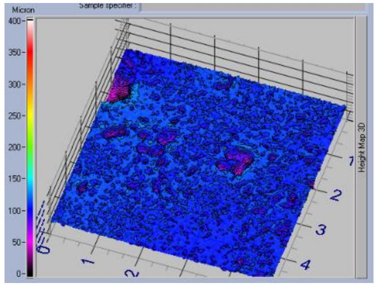
UT-AW	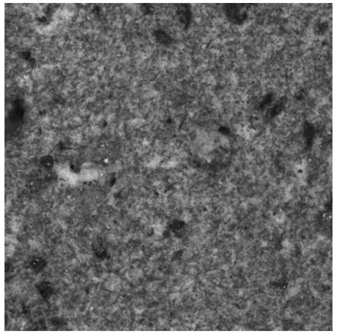	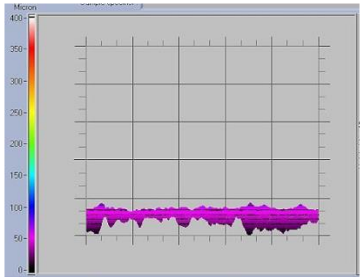	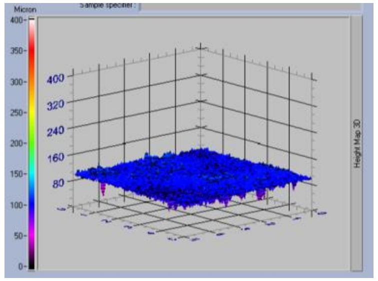

Figure 6.35 (b) Visual impression and topography images for control samples of Ankara stone

ANKARA	Visual Impression	2D Topography	3D Topography
B-TEOS	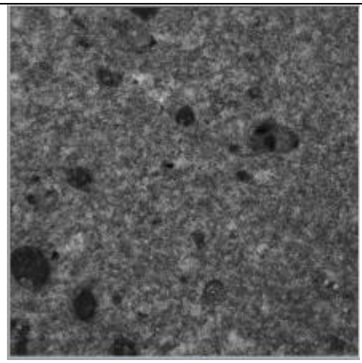	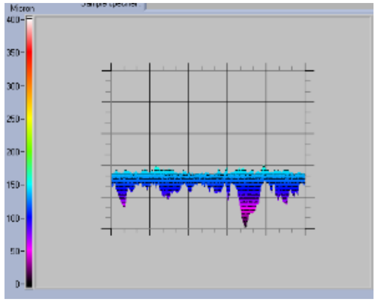	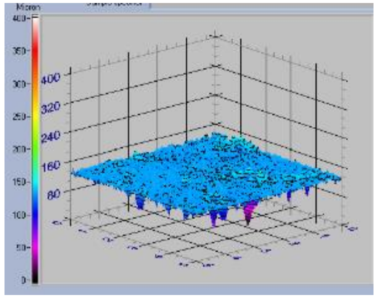
A-TEOS	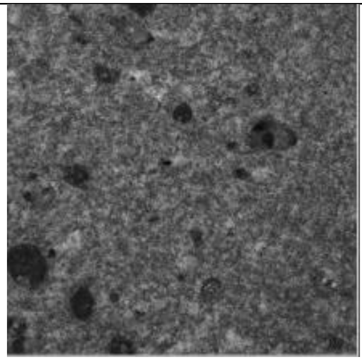	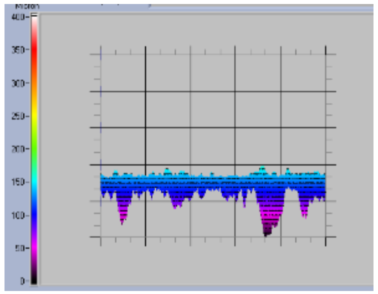	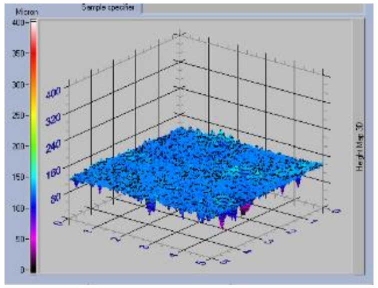

Figure 6.35 (c) Visual impression and topography images for TEOS treated Ankara stone

BİTLİS	Visual Impression	2D Topography	3D Topography
B-DAP	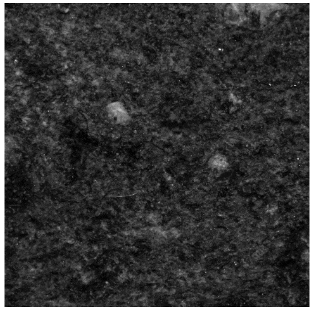	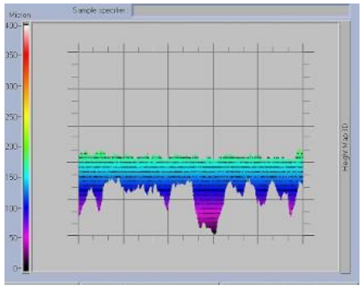	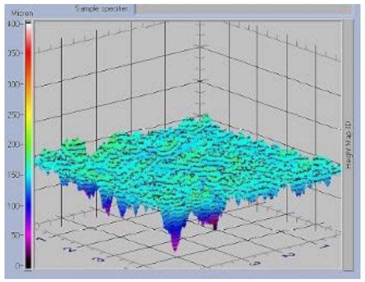
A-DAP	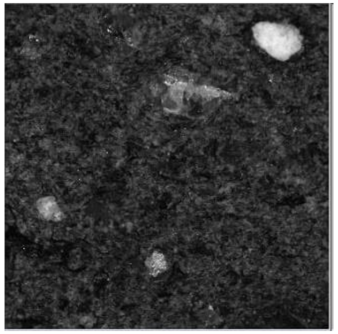	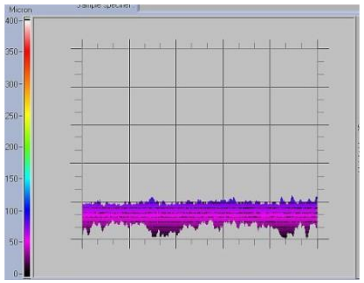	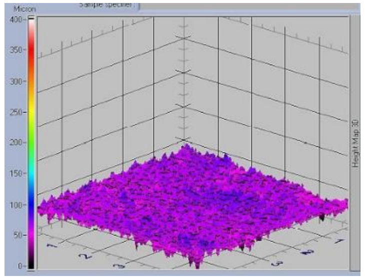
A-DAP-AW	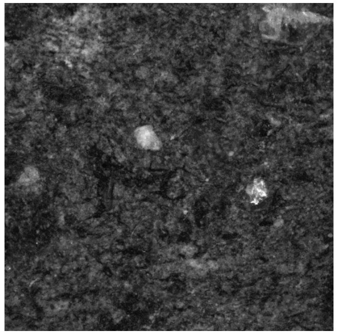	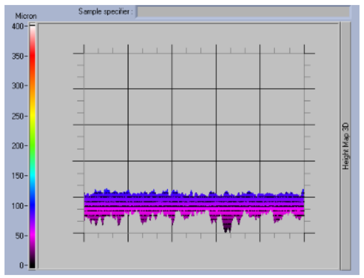	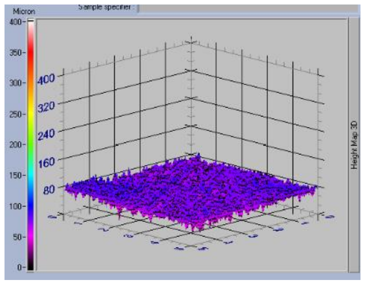

Figure 6.35 (d) Visual impression and topography images for DAP treated Bitlis stone

BİTLİS	Visual Impression	2D Topography	3D Topography
UT-BW	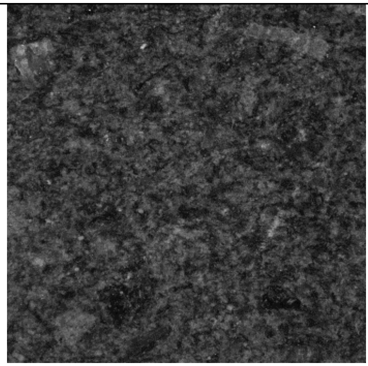	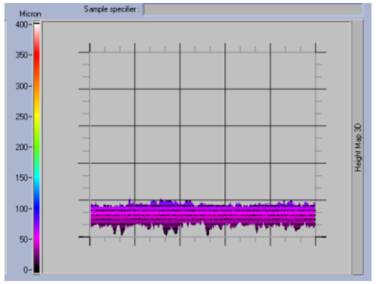	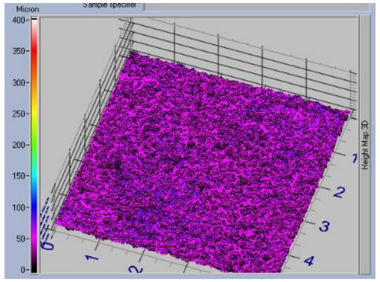
UT-AW	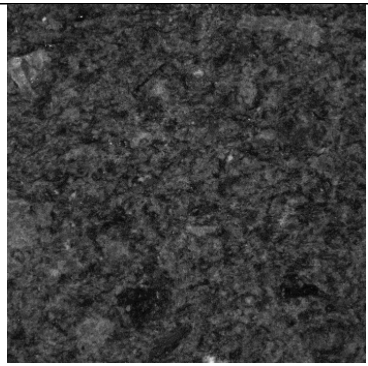	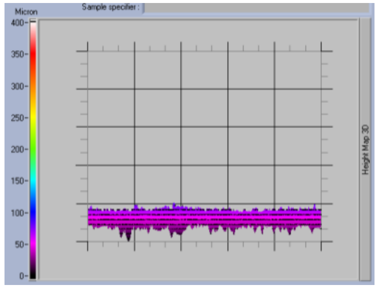	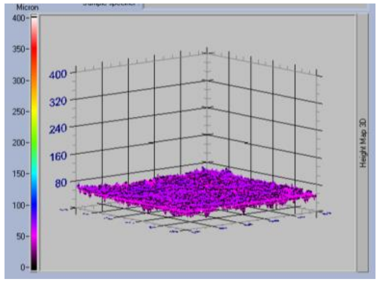

Figure 6.35 (e) Visual impression and topography images for control samples of Bitlis stone

BİTLİS	Visual Impression	2D Topography	3D Topography
B-TEOS	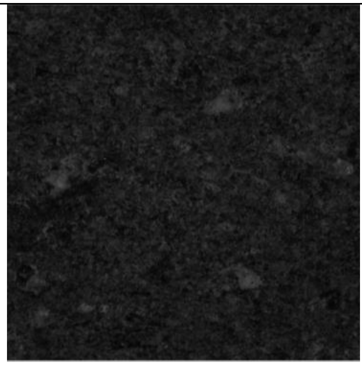	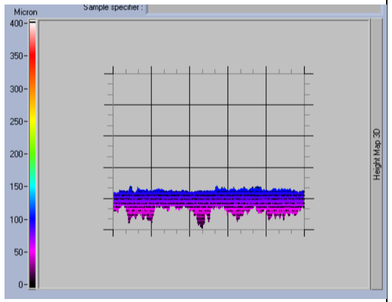	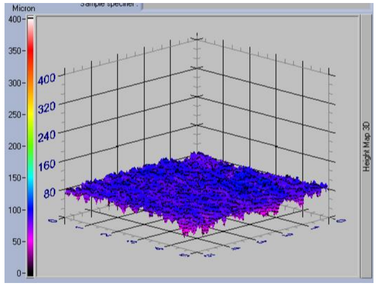
A-TEOS	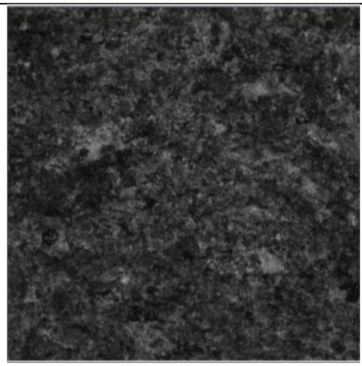	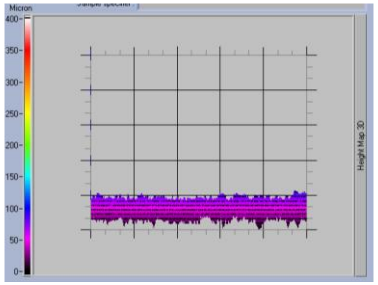	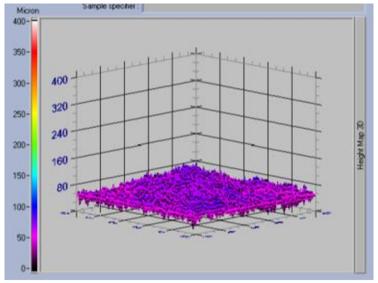

Figure 6.35 (f) Visual impression and topography images for TEOS treated Bitlis stone

MARDIN	Visual Impression	2D Topography	3D Topography
B-DAP	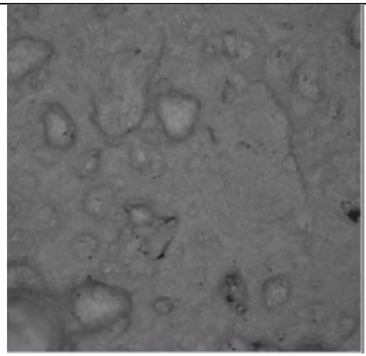	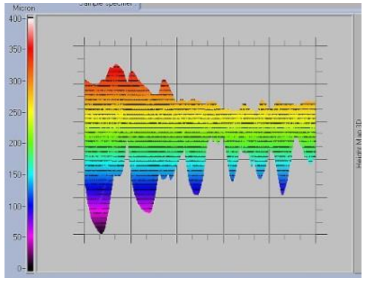	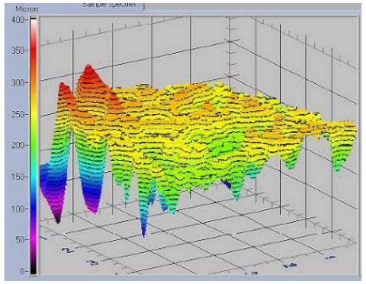
A-DAP	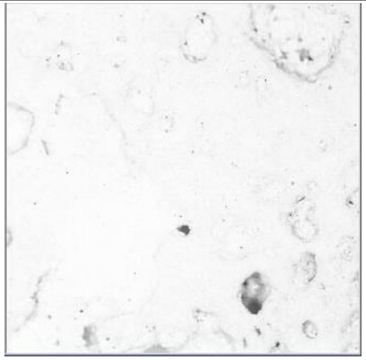	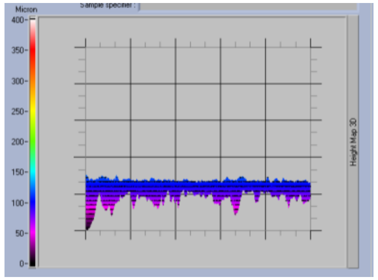	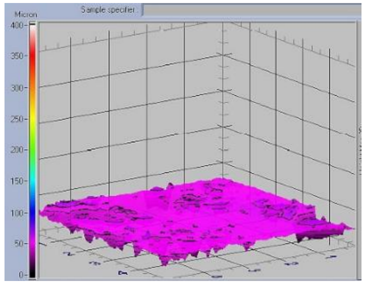
A-DAP-AW	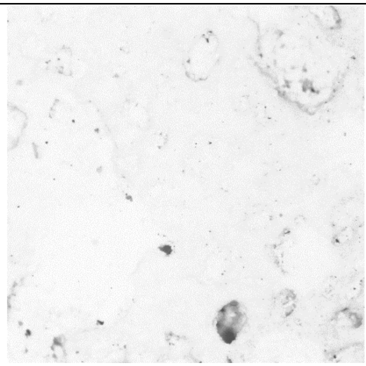	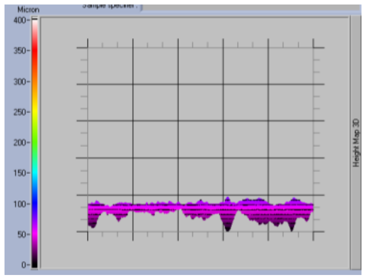	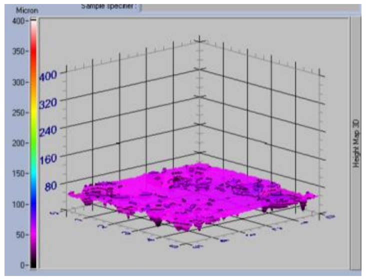

Figure 6.35 (g) Visual impression and topography images for DAP treated Mardin stone

MARDIN	Visual Impression	2D Topography	3D Topography
UT-BW	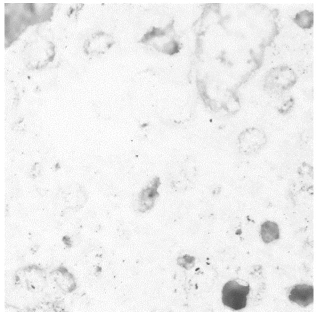	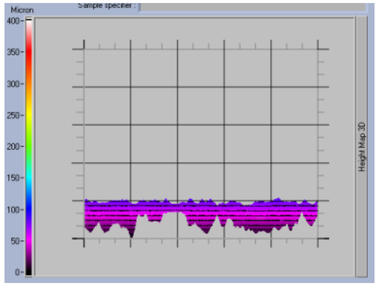	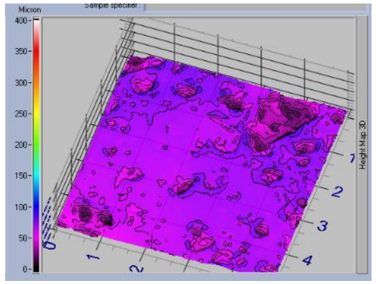
UT-AW	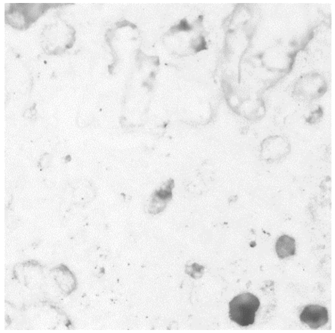	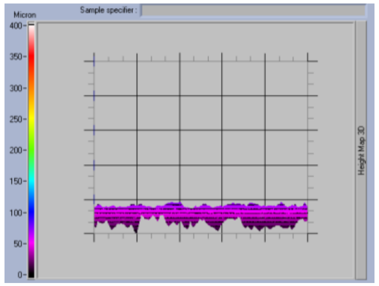	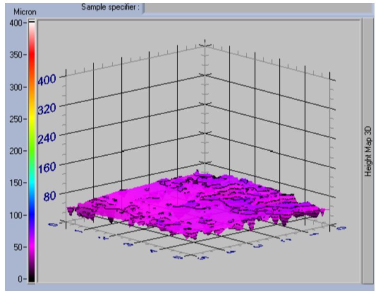

Figure 6.35 (h) Visual impression and topography images for control samples of Mardin stone

MARDIN	Visual Impression	2D Topography	3D Topography
B-TEOS	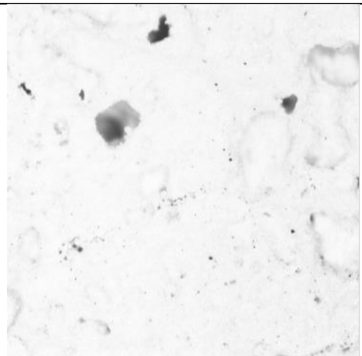	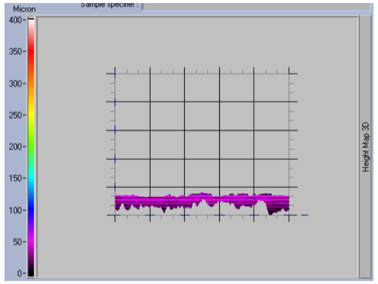	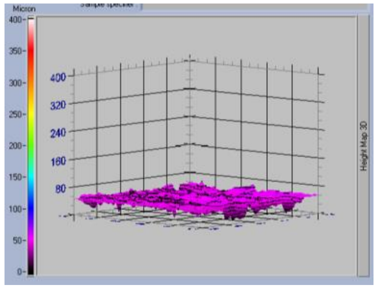
A-TEOS	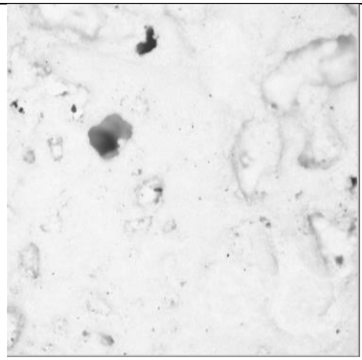	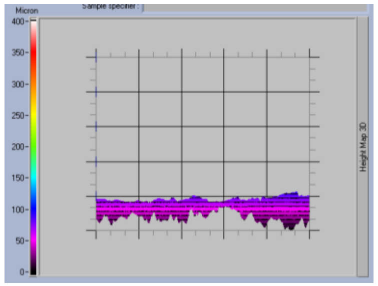	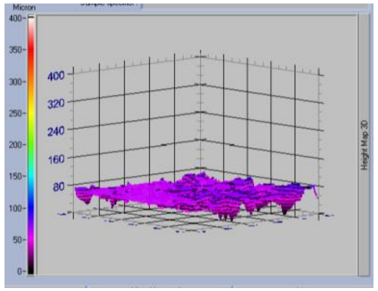

Figure 6.35 (i) Visual impression and topography images for TEOS treated Mardin stone

NEVSEHIR	Visual Impression	2D Topography	3D Topography
B-DAP	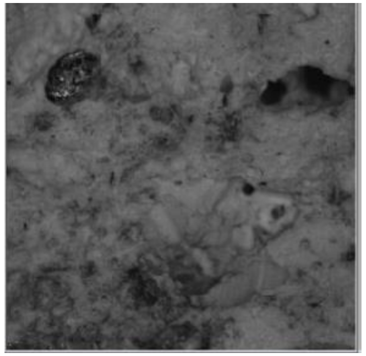	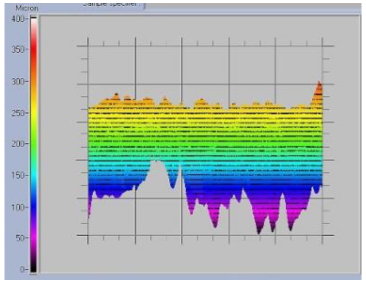	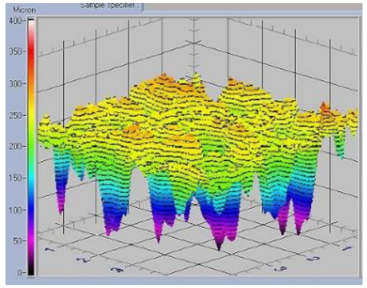
A-DAP	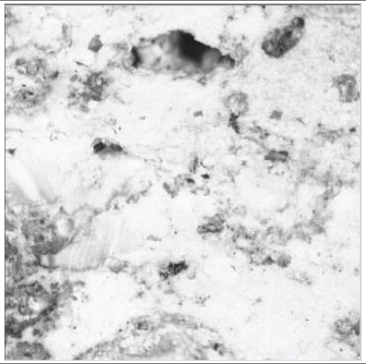	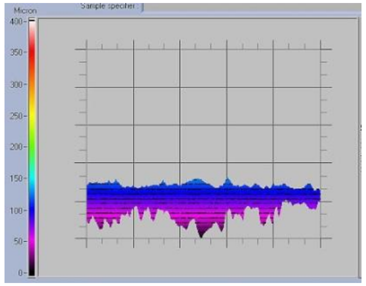	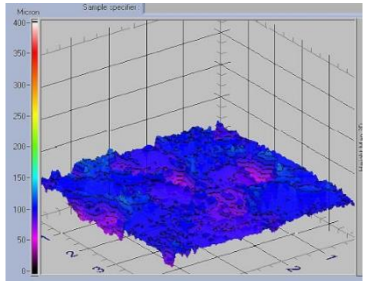
A-DAP-AW	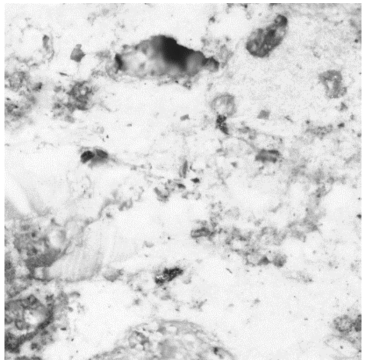	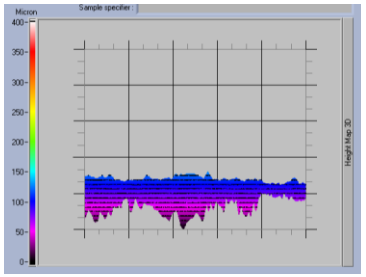	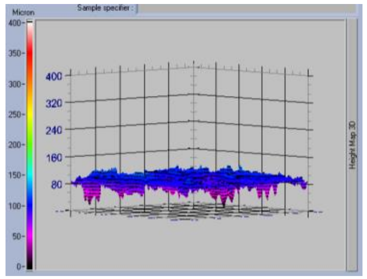

Figure 6.35 (j) Visual impression and topography images for DAP treated Nevsehir stone

NEVSEHIR	Visual Impression	2D Topography	3D Topography
UT-BW	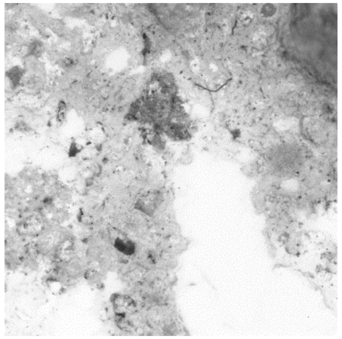	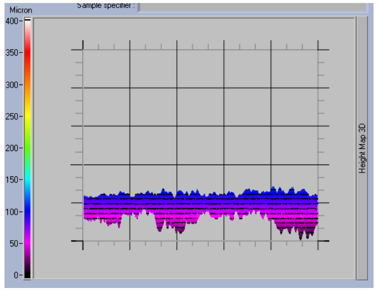	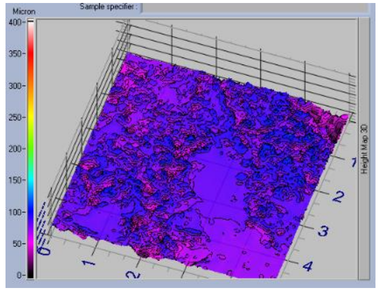
UT-AW	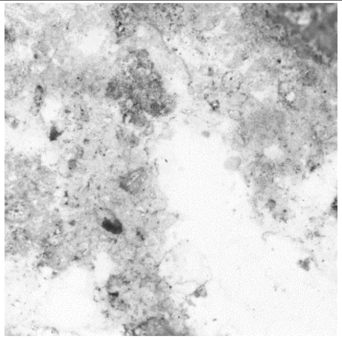	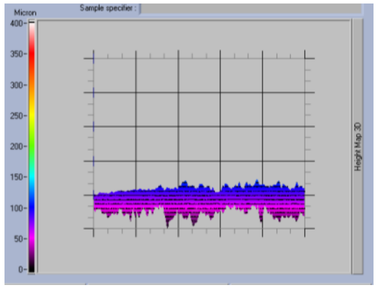	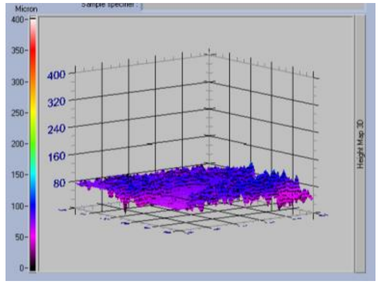

Figure 6.35 (k) Visual impression and topography images for control samples of Nevsehir stone

NEVSEHIR	Visual Impression	2D Topography	3D Topography
B-TEOS	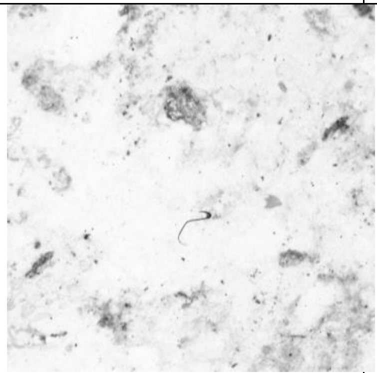	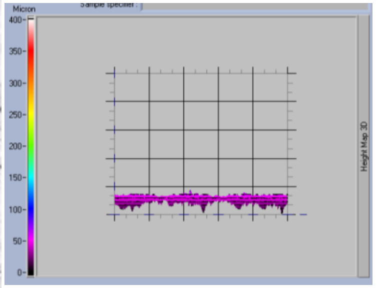	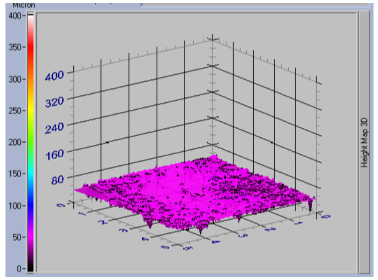
A-TEOS	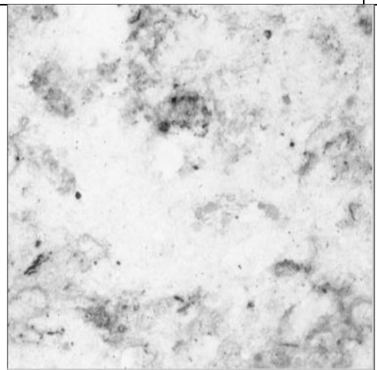	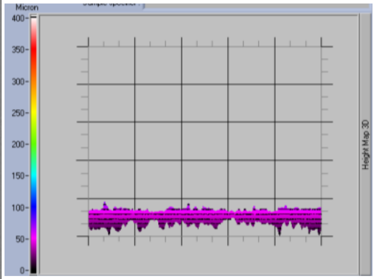	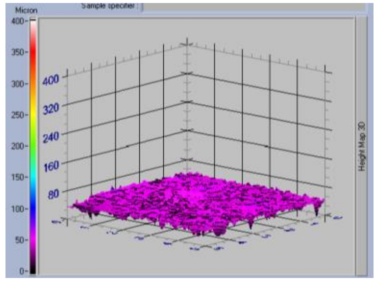

Figure 6.35 (l) Visual impression and topography images for TEOS treated Nevsehir stone

The followings can be drawn after considering Figure 6.35 and Table 6.71 together: DAP/Ca treatment filled the pits and reduced roughness for all samples, while TEOS induced heterogeneous aggregation and increased roughness, as can be seen in the topography photos.

For both DAP/Ca treated and control samples, weathering did not impact surface roughness (<%1) of the Ankara, Bitlis and Mardin stones. However, DAP/Ca treatment resulted in less mineral loss due to Nevsehir stone weathering (25.22 μm with 36.22 μm for control sample, 14.92 μm for 17.96 μm with DAP/Ca treatment).

Table 6.71 Mean surface roughness values (μm) (n=3)

	Ankara	Bitlis	Mardin	Nevsehir
B-DAP	25.02 (±2.86)	25.96 (±3.22)	27.76 (±8.66)	36.14 (±3.32)
A-DAP	20.04 (±2.81)	24.32 (±2.90)	11.14 (±1.90)	14.92 (±5.32)
A-DAP-AW	19.91 (±2.71)	24.43 (±1.29)	11.08 (±1.36)	17.96 (±6.74)
B-TEOS	21.76 (±6.14)	25.99 (±3.70)	11.85 (±3.84)	16.29 (±4.71)
A-TEOS	22.53 (±6.09)	31.32 (±3.40)	14.13 (±4.95)	22.70 (±5.69)
UT-BW	17.74 (±5.08)	26.56 (±3.13)	13.12 (±4.77)	25.22 (±4.97)
UT-AW	16.38 (±4.60)	23.62 (±3.12)	13.11 (±5.35)	36.22 (±6.98)

6.3 Soft Capping Mimicking Results

As explained in Materials & Method section, a simulation study has been carried out to see the effect of lichen on surface and core temperatures, by using fabric layers. Following program set for 24 hours on the cabinet. The experiment carried out for two days. A light source used to simulate daylight during hot temperature intervals as it can be seen in previous section.

- -5°C for 6 hour
- +35°C for 6 hour
- Rainfall simulation
- -5°C for 6 hour
- +35°C for 6 hour

Figure 6.36 shows the temperature results from inside, surface and difference between surface and inside of Mardin and Nevsehir stones. Figure 6.37 shows the internal temperature data from the cabinet.

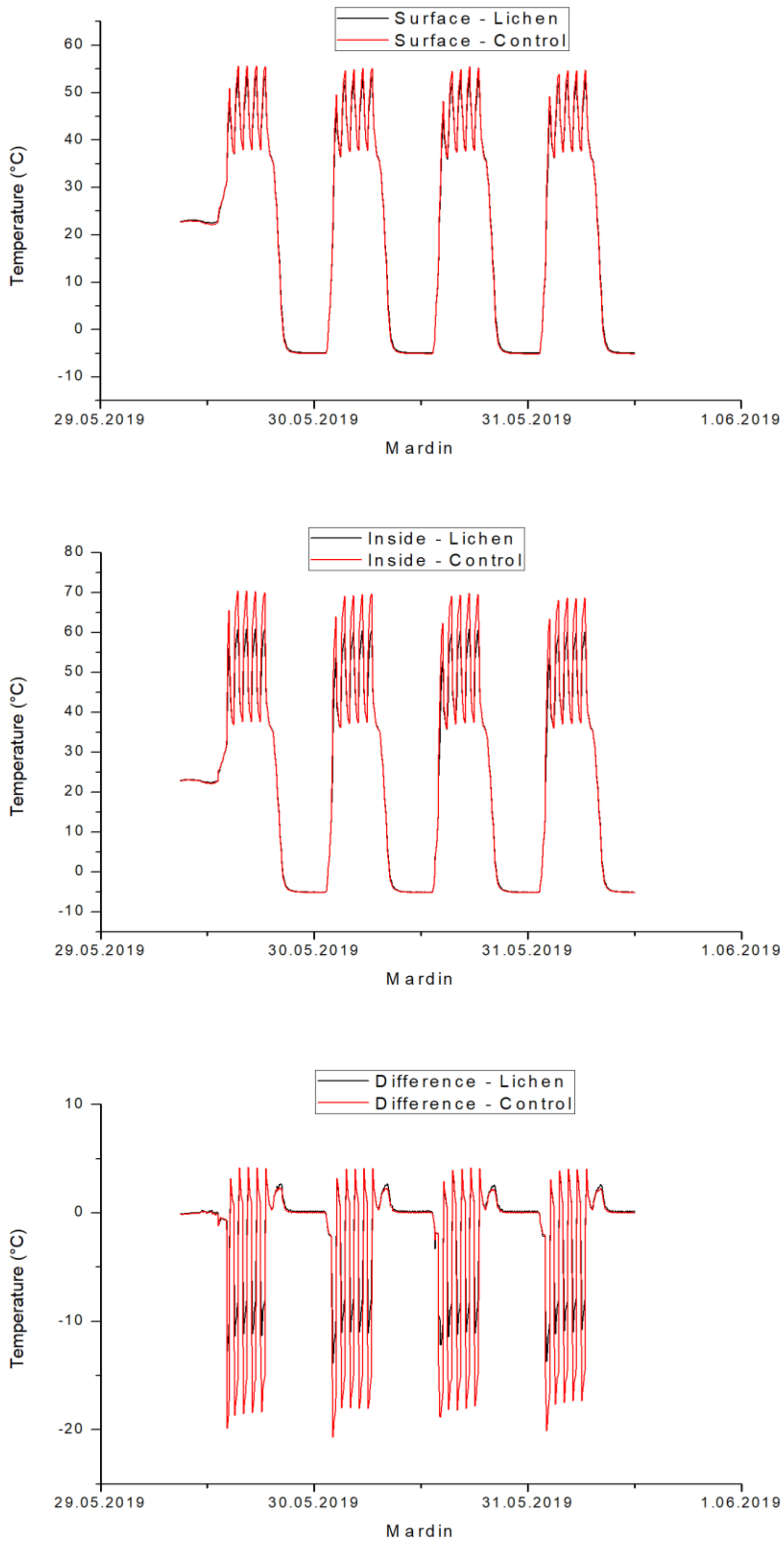

Figure 6.36 (a) Temperature data from the probes inside and surface of Mardin stone

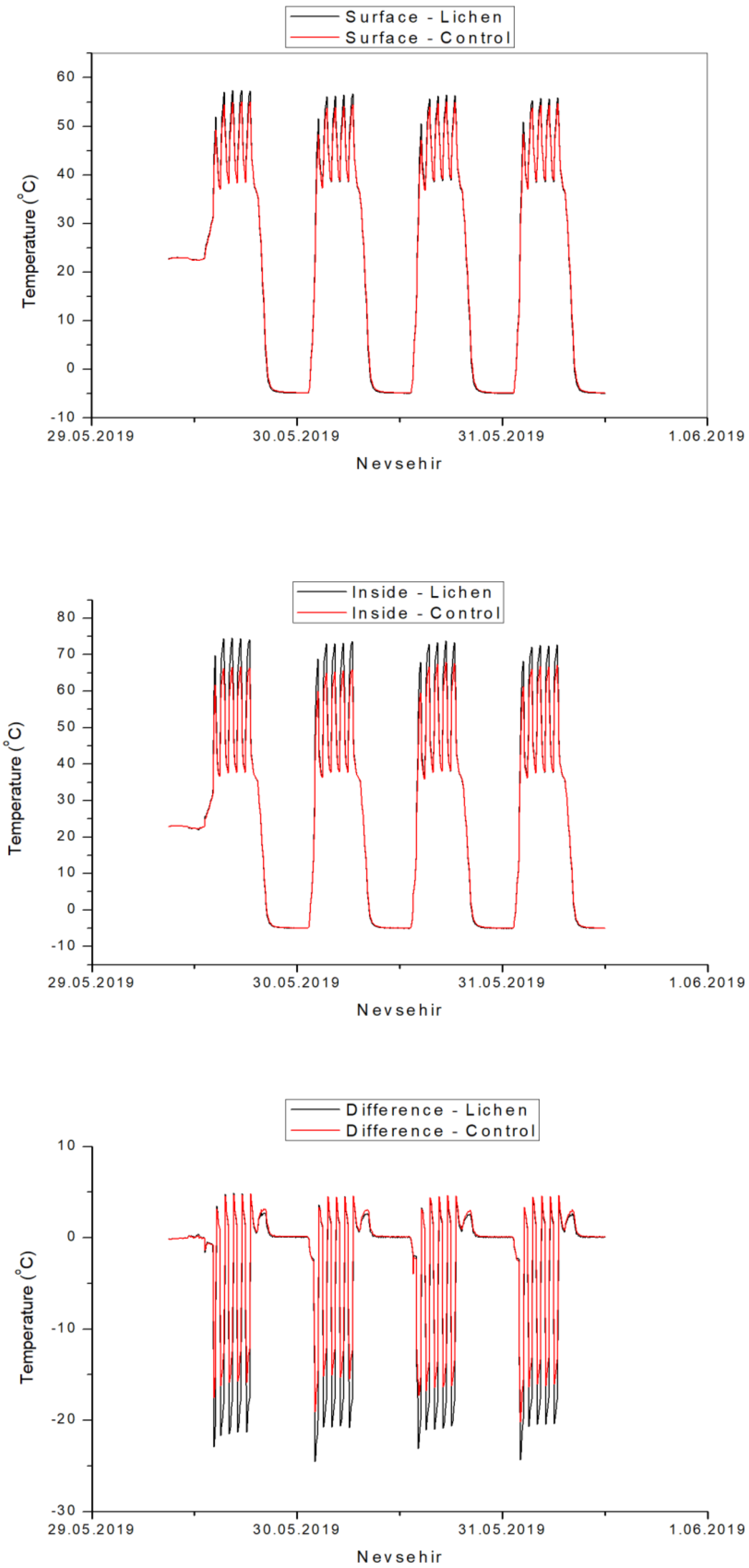

Figure 6.36 (b) Temperature data from the probes inside and surface of Nevsehir stone

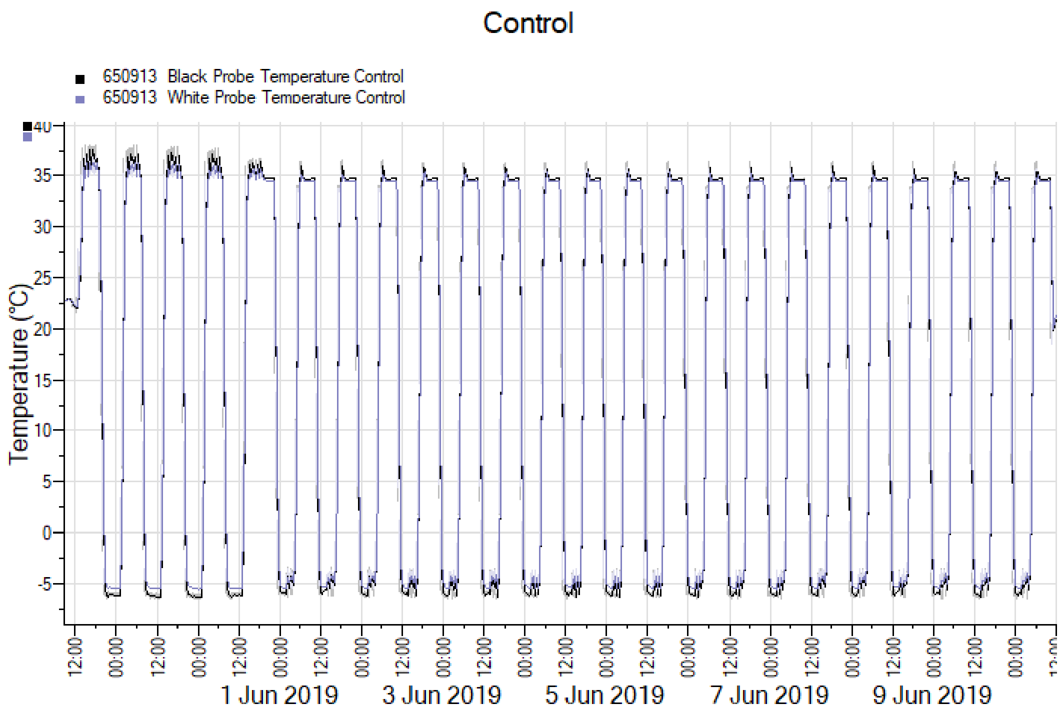

Figure 6.37 Temperature data from cabinet during the simulation experiments

The results show that:

- For both stone types, inner and surface temperatures are greater than set temperature (35°C). This is caused by light source placed on the samples. The dramatic increase in surface temperature (up to 60°C) reminded us to be careful about consideration of consolidant formulation and decision on the field.
- For both stone types, temperature difference change with fabric layer. For Mardin, the difference decreased around 10°C for summer conditions. That means, the use of a microorganism can be investigated to prevent thermal shock damage on this kind of stones. For Nevsehir stone, the difference increased with the use of band layer. That may be because of the temperature conductivity of the stone is lower than the layer. It can also be observed by inside temperatures, where band layers caused an increase for Nevsehir stone.
- There is no difference for winter conditions for both stones.

7

RESULTS AND DISCUSSION

In this study, the degradation properties of the samples were investigated by using four different stone types (Ankara, Bitlis, Mardin, Nevsehir) taken from different regions of Anatolia and the improvements in various properties after consolidant application were evaluated.

In the first part of the study, frost-thaw and thermal degradation experiments were carried out in laboratory conditions within the scope of manual weathering. The final states of the samples were analyzed by surface hardness, ultrasonic pulse velocity and surface roughness techniques. As a result of frost-thaw experiments, it was observed that there were differences in various physical properties, although it was different for each stone. In thermal degradation experiments, experimental design method was used by using Design Expert 7.0 software. In this way, more comprehensive results were obtained with fewer trials. As a result of thermal degradation experiments, decay equations based on mathematical expressions were obtained. According to this, it can be said that, especially by using experimental design methods, models connecting the degradation to the relevant parameters have been obtained and successful observations have been made.

In the second part of the study, DAP consolidant, a new generation treatment that has become increasingly popular in recent years, was applied for the first time in the literature on stones from Ankara, Bitlis, Mardin and Nevsehir. Samples were analyzed before and after application. Overall findings show that DAP/Ca treatment caused an improvement on surface roughness, internal cohesion observed by UPV, mechanical strength observed by DRMS, without causing a negative change in surface hardness, color or water absorption. Weathering did not cause significant differences between DAP/Ca treated and control samples for most of the characteristics analysed. However, there is some evidence that the

DAP/Ca treatment maintained surface hardness after weathering. That may be caused by the mild conditions which were used in the accelerated weathering test in this study and further investigation should be done with more extreme conditions to observe the effects of weathering on both consolidant treatments. In these experiments, DAP/Ca proved to be effective for limestone, ignimbrites and andesite, whilst TEOS, which is a favourable option for silicate stones in the field, only performed better for Nevsehir stone (ignimbrite) at least in terms of improving surface hardness. However, it caused alteration in both color and surface roughness. On the other hand, it should be noted that relatively short curing time may have limited TEOS performance and further investigation should be done on TEOS based consolidants to make a better comparison. Despite the general opinion about the compatibility of DAP treatment and limestone, DAP/Ca did not show better performance on Mardin stone (limestone) than on the other stones (andesite and ignimbrite) in this study. The results illustrate that DAP can be an effective option for a variety of lithotypes with lower $CaCO_3$ contents and requires more investigation.

In the last part of the thesis, a simulation study, was carried out to investigate the long-term usability of the soft capping technique, which is rarely used in the literature, on Mardin and Nevsehir stones. During this study, the specimens were covered with a cover simulating the vegetation layer and subjected to the weathering process. The results were evaluated in terms of temperature difference and the changes in thermal conductivity properties were shown. Accordingly, it was observed that the thermal conductivity changed during the high temperature cycle in which the summer simulation was performed for both stone types. While this change is in the form of a decrease in conductivity in Mardin stone, it has increased in Nevsehir stone. As a result, it can be said that the soft capping technique is a technique that can be used to prevent higher degree of damage due to temperature in places where it is not possible to restore, especially in Mardin stone.

Future Perspectives

• At the end of the study, it was observed that time-dependent changes could be obtained as a result of accelerated aging. However, in order for these evaluations to be based on healthier foundations, it would be very useful to conduct similar analyzes on old samples taken from the field and re-evaluate the aging equations with these data.

• The effect of experimental design, which is not used very often in laboratory aging in the field of cultural heritage, on reducing the number of experiments has been observed. It will be beneficial to use such methods, which are made using software, more in this field.

• Only two of the accelerated aging techniques (thermal and freeze-thaw) were used during the study. However, in the real environment, it is known that there are many different degradation parameters such as salt, UV, pollution, mechanical load. More comprehensive data can be obtained with experimental sets in which these effects are present. For even more realistic data, effects in the field need to be simulated simultaneously.

• In the consolidant application part of the study, important data were obtained regarding the effectiveness of DAP application, the effectiveness of which has not been studied much in the literature in stones with low calcium carbonate content. In recent publications for the development of this application, different approaches have been made, such as adding Mg^{2+} ion, adding organic components to support crystallization, or using nanoparticles to gain different properties.

• In this study, weathering studies were carried out under laboratory conditions after the DAP application. However, for these substrate and DAP combinations, it is not known what changes occur under actual atmospheric conditions. Research can be done on this subject.

REFERENCES

Agan, C., & Cicek, F. (2020). Some rock mass, chemical, physical, thermal, and mechanical properties of Mardin limestone, Turkey. *Arabian Journal of Geosciences*, *13*(4), 188. https://doi.org/10.1007/s12517-020-5146-x

Akın, M., Dinçer, İ., Özvan, A., Oyan, V., & Tapan, M. (2016). İgnimbiritlerdeki Kılcal Su Emme Özelliğinin Ahlat Selçuklu Mezar Taşlarının Bozunmasındaki Rolü. *Jeoloji Mühendisliği Dergisi*, 149–149. https://doi.org/10.24232/jeoloji-muhendisligi-dergisi.295428

Akın, M., Özvan, A., Dinçer, İ., & Topal, T. (2017). Evaluation of the physico-mechanical parameters affecting the deterioration rate of Ahlat ignimbrites (Bitlis, Turkey). *Environmental Earth Sciences*, *76*(24). https://doi.org/10.1007/s12665-017-7175-7

Akkurt, I., Altindag, R., Basyigit, C., & Kilincarslan, S. (2008). The effect of barite rate on the physical and mechanical properties of concretes under F–T cycle. *Materials & Design*, *29*(9), 1793–1795. https://doi.org/10.1016/j.matdes.2008.03.013

Al-Omari, A., Brunetaud, X., Beck, K., & Al-Mukhtar, M. (2014). Effect of thermal stress, condensation and freezing–thawing action on the degradation of stones on the Castle of Chambord, France. Environmental Earth Sciences, 71(9), 3977–3989. https://doi.org/10.1007/s12665-013-2782-4

Alves, C., Figueiredo, C., & Sanjurjo-Sánchez, J. (2020). Rock Features and Alteration of Stone Materials Used for the Built Environment: A Review of Recent Publications on Ageing Tests. Geosciences, 10(3), 91. https://doi.org/10.3390/geosciences10030091

Altindag, R., Alyildiz, I. S., & Onargan, T. (2004). Mechanical property degradation of ignimbrite subjected to recurrent freeze–thaw cycles. *International Journal of Rock Mechanics and Mining Sciences*, *41*(6), 1023–1028. https://doi.org/10.1016/j.ijrmms.2004.03.005

Altindag, R., Sengun, N., guney, avni, Mutlutürk, M., karaguzel, remzi, & Onargan, T. (2006). The integrity loss of physicomechanical properties of building stones when subjected to recurrent cycles of freeze–thaw (f-t) process. In *Fracture and Failure of Natural Building Stones* (pp. 363–372). Springer.

Aly, N., Gomez–Heras, M., Hamed, A., Álvarez de Buergo, M., & Soliman, F. (2015). The influence of temperature in a capillary imbibition salt weathering simulation test on Mokattam limestone. *Materiales de Construcción*, *65*(317), e044. https://doi.org/10.3989/mc.2015.00514

Amirkiyaei, V., Ghasemi, E., & Faramarzi, L. (2020). Determination of P-wave Velocity of Carbonate Building Stones During Freeze–Thaw Cycles. *Geotechnical and Geological Engineering*. https://doi.org/10.1007/s10706-020-01409-z

Andrew, C., Young, M., Tonge, K. H., Robert Gordon University, Masonry Conservation Research Group, Historic Scotland, & Technical Conservation Research and Education Division. (1994). *Stone cleaning: A guide for practitioners*. Historic Scotland ; Robert Gordon University.

Andriani, G. F., & Germinario, L. (2014). Thermal decay of carbonate dimension stones: Fabric, physical and mechanical changes. *Environmental Earth Sciences*, *72*(7), 2523–2539. https://doi.org/10.1007/s12665-014-3160-6

Angeli, M. (2007). *Multiscale study of stone decay by salt crystallization in porous networks*. (PhD Thesis, Université de Cergy Pontoise, France)

Arıkan, F., Ulusay, R., & Aydın, N. (2007). Characterization of weathered acidic volcanic rocks and a weathering classification based on a rating system. *Bulletin of Engineering Geology and the Environment*, *66*(4), 415–430. https://doi.org/10.1007/s10064-007-0087-0

Asmus, J. F., Guattari, G., Lazzarini, L., Musumeci, G., & Wuerker, R. F. (1973). Holography in the Conservation of Statuary. *Studies in Conservation*, *18*(2), 49–63. https://doi.org/10.2307/1505458

Avsar, A. O., & Güleç, A. (2019). Ahlat Selçuklu Meydan Mezarlığı Mezar Taşları Analiz Çalışmaları ve Konservasyon Önerileri. *Restorasyon ve Konservasyon Çalışmaları Dergisi*, *22*, 3-16 https://dergipark.org.tr/en/download/article-file/856083

Bakis, A. (2019). Increasing the Durability and Freeze-Thaw Strength of Concrete Paving Stones Produced from Ahlat Stone Powder and Marble Powder by Special Curing Method. *Advances in Materials Science and Engineering*, *2019*, 1–14. https://doi.org/10.1155/2019/3593710

Barriuso, B. C., Botticelli, G., Cuzman, O. A., Osticioli, I., Tiano, P., & Matteini, M. (2017). Conservation of calcareous stone monuments: Screening different diammonium phosphate based formulations for countering phototrophic colonization. *Journal of Cultural Heritage*, *27*, 97–106. https://doi.org/10.1016/j.culher.2017.03.002

Bartoli, F., Municchia, A. C., Futagami, Y., Kashiwadani, H., Moon, K. H., & Caneva, G. (2014). Biological colonization patterns on the ruins of Angkor temples (Cambodia) in the biodeterioration vs bioprotection debate. *International Biodeterioration & Biodegradation*, *96*, 157–165. https://doi.org/10.1016/j.ibiod.2014.09.015

Baykara, T., & Işık, M. C. (2016). Physical Characterization, Microstructural Evaluation, and Condition Assessment of Ancient Ahlat Tombstones in the Seljukian Cemetery of Ahlat (Turkey). *International Journal of Architectural Heritage*, *10*(8), 1025–1040. https://doi.org/10.1080/15583058.2016.1181227

Benavente, D. Garcia del Cura, M.A. & Ordonez, S. (2001). Quantification of salt weathering in porous stones using an experimental continuous partial immersion method. *Engineering Geology*, *59*, 313-325. https://doi.org/10.1016/S0013-7952(01)00020-5

Benavente, D., Martínez-Martínez, J., Cueto, N., & García-del-Cura, M. A. (2007). Salt weathering in dual-porosity building dolostones. *Engineering Geology*, *94*(3–4), 215–226. https://doi.org/10.1016/j.enggeo.2007.08.003

Bernal, J. L. P., & Bello, M. A. (2003). Modeling sulfur dioxide deposition on calcium carbonate. *Industrial & Engineering Chemistry Research*, *42*(5), 1028–1034. https://doi.org/10.1021/ie020426h

Binal, A. (2009). A new laboratory rock test based on freeze–thaw using a steel chamber. *Quarterly Journal of Engineering Geology and Hydrogeology*, *42*(2), 179–198. https://doi.org/10.1144/1470-9236/08-040

Borsoi, G., Lubelli, B., van Hees, R., Veiga, R., & Silva, A. S. (2016). Understanding the transport of nanolime consolidants within Maastricht limestone. *Journal of Cultural Heritage*, *18*, 242–249. https://doi.org/10.1016/j.culher.2015.07.014

Bracci, S., & Melo, M. J. (2003). Correlating natural ageing and Xenon irradiation of Paraloid® B72 applied on stone. *Polymer Degradation and Stability*, *80*(3), 533–541. https://doi.org/10.1016/S0141-3910(03)00037-5

Briones, C. C., & Viles, H. (2018). An Assessment of the Role of an Open Shelter in Reducing Soiling and Microbial Growth on the Archaeological Site of the Bishop's Palace, Witney, England. *Conservation and Management of Archaeological Sites*, *20*(1), 2–17. https://doi.org/10.1080/13505033.2018.1430437

Camuffo, D., Del Monte, M., & Sabbioni, C. (1983). Origin and growth mechanisms of the sulfated crusts on urban limestone. *Water, Air, and Soil Pollution*, *19*(4), 351–359. https://doi.org/10.1007/BF00159596

Caneva, G., Gasperini, R., & Salvadori, O. (2008). Endolithic colonization of stone in six Jewish cemeteries in urban environment. *Proceedings of the 11th Int. Congress on Deterioration and Conservation of Stone,* September 15-20*,* Torun, Poland, (49–56).

Careddu, N., & Marras, G. (2013). The effects of solar UV radiation on the gloss values of polished stone surfaces. *Construction and Building Materials*, *49*, 828–834. https://doi.org/10.1016/j.conbuildmat.2013.09.010

Carter, N. E. A., & Viles, H. A. (2005). Bioprotection explored: The story of a little known earth surface process. *Geomorphology*, *67*(3), 273–281. https://doi.org/10.1016/j.geomorph.2004.10.004

Chen, W., Dai, P., Yuan, P., & Zhang, J. (2016). Effect of inorganic silicate consolidation on the mechanical and durability performance of sandstone used in historical sites. *Construction and Building Materials*, *121*, 445–452. https://doi.org/10.1016/j.conbuildmat.2016.06.008

Ciferri, O., Tiano, P., & Mastromei, G. (Eds.). (2000). *Of Microbes and Art: The Role of Microbial Communities in the Degradation and Protection of Cultural Heritage*. Springer US. https://doi.org/10.1007/978-1-4615-4239-1

Concha-Lozano, N., Gaudon, P., Pages, J., de Billerbeck, G., Lafon, D., & Eterradossi, O. (2012). Protective effect of endolithic fungal hyphae on oolitic limestone buildings. *Journal of Cultural Heritage*, *13*(2), 120–127. https://doi.org/10.1016/j.culher.2011.07.006

Coombes, M. A., Viles, H. A., & Zhang, H. (2018). Thermal blanketing by ivy (Hedera helix L.) can protect building stone from damaging frosts. *Scientific Reports*, *8*(1), 9834. https://doi.org/10.1038/s41598-018-28276-2

Crispim, C. A., & Gaylarde, C. C. (2005). Cyanobacteria and Biodeterioration of Cultural Heritage: A Review. *Microbial Ecology*, *49*(1), 1–9. https://doi.org/10.1007/s00248-003-1052-5

de Buergo, M. A., & González, R. F. (2003). Protective patinas applied on stony façades of historical buildings in the past. *Construction and Building Materials*, *17*(2), 83–89. https://doi.org/10.1016/S0950-0618(02)00107-1

de la Rosa, J. P. M., Warke, P. A., & Smith, B. J. (2013). Lichen-induced biomodification of calcareous surfaces: Bioprotection versus biodeterioration. *Progress in Physical Geography: Earth and Environment*, *37*(3), 325–351. https://doi.org/10.1177/0309133312467660

Del Monte, M., Sabbioni, C., & Zappia, G. (1987). The origin of calcium oxalates on historical buildings, monuments and natural outcrops. *Science of The Total Environment*, *67*(1), 17–39. https://doi.org/10.1016/0048-9697(87)90063-5

Demirdag, S. (2013). Effects of freezing–thawing and thermal shock cycles on physical and mechanical properties of filled and unfilled travertines. *Construction and Building Materials*, *47*, 1395–1401. https://doi.org/10.1016/j.conbuildmat.2013.06.045

Di Bonaventura, M. P., Del Gallo, M., Cacchio, P., Ercole, C., & Lepidi, A. (1999). Microbial formation of oxalate films on monument surfaces: Bioprotection or biodeterioration? *Geomicrobiology Journal*, *16*(1), 55–64.

Diaz Gonçalves, T., & Brito, V. (2014). Alteration kinetics of natural stones due to sodium sulfate crystallization: Can reality match experimental simulations? *Environmental Earth Sciences*, *72*(6), 1789–1799. https://doi.org/10.1007/s12665-014-3085-0

Dinçer, İ., & Bostancı, M. (2019). Capillary water absorption characteristics of some Cappadocian ignimbrites and the role of capillarity on their deterioration. *Environmental Earth Sciences*, *78*(1). https://doi.org/10.1007/s12665-018-7993-2

Doehne, E. F., & Price, C. A. (2010). *Stone conservation: An overview of current research* (2nd ed). Getty Conservation Institute, California, USA.

Doehne, E., Selwitz, C., & Carson, D. (2002). The Damage Mechanism Of Sodium Sulfate In Porous Stone, *Proceedings of the SALTeXPERT Meeting, Prague, ARCCHIP and GCI (*23*)*

Dorn, R. (2013). Rock Coatings in *Treatise on Geomorphology (4)*, 70–97, Elsevier Inc https://doi.org/10.1016/B978-0-12-374739-6.00066-X

ElBaghdady, K. Z., Tolba, S. T., & Houssien, S. S. (2019). Biogenic deterioration of Egyptian limestone monuments: Treatment and conservation. *Journal of Cultural Heritage*, *38*, 118–125. https://doi.org/10.1016/j.culher.2019.02.005

El-Gohary, M. (2011). Chemical deterioration of egyptian limestone affected by saline water. *International Journal of Conservation Science 2(1),* 17-28.

Erdal, M., Simsek, O. (2004). Investigation of some mechanical and physical properties of the ahlat stone (ignimbrite). *Gazi University Journal of Science 17(4),* 71-78

Eren Sarıcı, D. (2016). Thermal deterioration of marbles: Gloss, color changes. *Construction and Building Materials*, *102*, 416–421. https://doi.org/10.1016/j.conbuildmat.2015.10.200

Erguler, Z. A. (2009). Field-based experimental determination of the weathering rates of the Cappadocian tuffs. *Engineering Geology*, *105*(3–4), 186–199. https://doi.org/10.1016/j.enggeo.2009.02.003

European Commission. Raphael Programme & Domstiftung Regensburg. (2001). *Turm—Fassade—Portal:* Schnell + Steiner. https://books.google.com.tr/books?id=oyfqAAAAMAAJ

Fassina, V., Ott, Heinrich. & Zezza, Fulvio. (1994) *The conservation of monuments in the Mediterranean basin: Stone and monuments, methodologies for the analyses of weathering and conservation: Proceedings of the 3rd international symposium, Venice, 22-25 June 1994*

Favero-Longo, S. E., & Viles, H. A. (2020). A review of the nature, role and control of lithobionts on stone cultural heritage: Weighing-up and managing biodeterioration and bioprotection. *World Journal of Microbiology & Biotechnology*, *36*(7), 100. https://doi.org/10.1007/s11274-020-02878-3

Ferrero, A. M., & Marini, P. (2001). Experimental Studies on the Mechanical Behaviour of two Thermal Cracked Marbles. *Rock Mechanics and Rock Engineering*, *34*(1), 57–66. https://doi.org/10.1007/s006030170026

Flatt, R. J. (2002). Salt damage in porous materials: How high supersaturations are generated. *Journal of Crystal Growth*, *242*(3–4), 435–454. https://doi.org/10.1016/S0022-0248(02)01429-X

Franzoni, E., Sassoni, E., & Graziani, G. (2015). Brushing, poultice or immersion? The role of the application technique on the performance of a novel hydroxyapatite-based consolidating treatment for limestone. *Journal of Cultural Heritage*, *16*(2), 173–184. https://doi.org/10.1016/j.culher.2014.05.009

Gadd, G. M., & Dyer, T. D. (2017). Bioprotection of the built environment and cultural heritage. *Microbial Biotechnology*, *10*(5), 1152–1156. https://doi.org/10.1111/1751-7915.12750

Garcia-Talegon, J., Vicente, M. A., Vicente-Tavera, S., & Molina-Ballesteros, E. (1998). Assessment of chromatic changes due to artificial ageing and/or conservation treatments of sandstones. *Color Research & Application*, *23*(1), 46–51. https://doi.org/10.1002/(SICI)1520-6378(199802)23:1<46::AID-COL7>3.0.CO;2-3

Garcia-Vallès, M., Vendrell-Saz, M., Molera, J., & Blazquez, F. (1998). Interaction of rock and atmosphere: Patinas on Mediterranean monuments. *Environmental Geology*, *36*(1–2), 137–149. https://doi.org/10.1007/s002540050329

Germinario, L., Andriani, G. F., & Laviano, R. (2015). Decay of calcareous building stone under the combined action of thermoclastism and cryoclastism: A laboratory simulation. *Construction and Building Materials*, *75*, 385–394. https://doi.org/10.1016/j.conbuildmat.2014.11.035

Gherardi, F., & Toniolo, L. (2015). *Report and database on commercial consolidants and protective coatings* (2015)5214449; NANO-CATHEDRAL. EU. www.nanocathedral.eu

Ghobadi, M. H., Taleb Beydokhti, A. R., Nikudel, M. R., Asiabanha, A., & Karakus, M. (2016). The effect of freeze–thaw process on the physical and mechanical properties of tuff. *Environmental Earth Sciences*, *75*(9). https://doi.org/10.1007/s12665-016-5664-8

Ghobadi, M. H., & Torabi-Kaveh, M. (2014). Assessing the potential for deterioration of limestones forming Taq-e Bostan monuments under freeze–thaw weathering and karst development. *Environmental Earth Sciences*, *72*(12), 5035–5047. https://doi.org/10.1007/s12665-014-3373-8

Gorbushina, A. (2003). Microcolonial fungi: Survival potential of terrestrial vegetative structures. *Astrobiology*, *3*(3), 543–554. https://doi.org/10.1089/153110703322610636

Goudie, A. S. (1999). A comparison of the relative resistance of limestones to frost and salt weathering. *Permafrost and Periglacial Processes*, *10*(4), 309–316. https://doi.org/10.1002/(SICI)1099-1530(199910/12)10:4<309::AID-PPP330>3.0.CO;2-C

Goudie, Andrew S, & Viles, H. A. (2000). The Thermal Degradation of Marble. *GEOGRAPHICA*, *XXXV*, 7–10.

Gowell, M. R., Coombes, M. A., & Viles, H. A. (2015). Rock-protecting seaweed? Experimental evidence of bioprotection in the intertidal zone: Rock-Protecting Seaweed. *Earth Surface Processes and Landforms*, *40*(10), 1364–1370. https://doi.org/10.1002/esp.3736

Graziani, G., Sassoni, E., & Franzoni, E. (2015). Consolidation of porous carbonate stones by an innovative phosphate treatment: Mechanical strengthening and physical-microstructural compatibility in comparison with TEOS-based treatments. *Heritage Science*, *3*(1), 1. https://doi.org/10.1186/s40494-014-0031-0

Graziani, G., Sassoni, E., Franzoni, E., & Scherer, G. W. (2016). Hydroxyapatite coatings for marble protection: Optimization of calcite covering and acid resistance. *Applied Surface Science*, *368*, 241–257. https://doi.org/10.1016/j.apsusc.2016.01.202

Gulotta, D., Villa, F., Cappitelli, F., & Toniolo, L. (2018). Biofilm colonization of metamorphic lithotypes of a renaissance cathedral exposed to urban atmosphere. *Science of the Total Environment*, *639*, 1480–1490. https://doi.org/10.1016/j.scitotenv.2018.05.277

Günal, V. (2011). The Possitive Effects of Tourism and The Case of The Traditional Stone Art in Midyat District. *Marmara Geographical Review*, *24*, 433–471.

Hajpal, M., & Török, A. (2004). Mineralogical and colour changes of quartz sandstones by heat. *Environmental Geology*, *46*(3–4). https://doi.org/10.1007/s00254-004-1034-z

Hu, Y., Duan, T., Xian, P., & Chen, L. (2019). Freeze-Thaw Cycle Effect on Sputtering Rate of Water-Saturated Yellow Sandstone under Impact Loading. *Advances in Civil Engineering*, *2019*, 1–12. https://doi.org/10.1155/2019/2549603

Huang Kezhong. (2003). A Study on Ancient Structural Materials and Their Preservation. *Southeast Culture*, *09*, 93–96.

Inigo, A. C., Vicente-Tavera, S., & Rives, V. (2004). MANOVA-Biplot statistical analysis of the effect of artificial ageing (freezing/thawing) on the colour of treated granite stones. *Color Research and Application*, *29*(2), 115–120. https://doi.org/10.1002/col.10236

Inkpen, R. J., Viles, H. A., Moses, C., Baily, B., Collier, P., Trudgill, S. T., & Cooke, R. U. (2012). Thirty years of erosion and declining atmospheric pollution at St Paul's Cathedral, London. Atmospheric Environment, 62, 521–529. https://doi.org/10.1016/j.atmosenv.2012.08.055Iucolano, F., Colella, A., Liguori, B., & Calcaterra, D. (2019). Suitability of silica nanoparticles for tuff consolidation. *Construction and Building Materials*, *202*, 73–81. https://doi.org/10.1016/j.conbuildmat.2019.01.002

Jaynes, S. M., & Cooke, R. U. (1987). Stone weathering in Southeast England. *Atmospheric Environment (1967)*, *21*(7), 1601–1622. https://doi.org/10.1016/0004-6981(87)90321-0

Karaca, Z., Hamdi Deliormanli, A., Elci, H., & Pamukcu, C. (2010). Effect of freeze–thaw process on the abrasion loss value of stones. *International Journal of Rock Mechanics and Mining Sciences*, *47*(7), 1207–1211. https://doi.org/10.1016/j.ijrmms.2010.07.003

Kaya, A. C. (2008). *The usage of Midyat stone as a covering and building material researching.* (MSc Thesis) University of Cukurova, Adana

Kazancı, N., & Gürbüz, A. (2014). Jeolojik Miras Nitelikli Türkiye Doğal Taşları. *Türkiye Jeoloji Bülteni / Geological Bulletin of Turkey*, *57*(1), 19–44. https://doi.org/10.25288/tjb.298752

Kwiatkowski, D., Löfvendahl, R., & ICOMOS Sweden. (2004). *Proceedings of the 10th International Congress on Deterioration and Conservation of Stone: Stockholm June 27—July 2, 2004* (Issue v. 2). ICOMOS Sweden. https://books.google.com.tr/books?id=Ag-jygAACAAJ

La Iglesia, A., González, V., López-Acevedo, V., & Viedma, C. (1997). Salt crystallization in porous construction materials I Estimation of crystallization pressure. *Journal of Crystal Growth*, *177*(1–2), 111–118. https://doi.org/10.1016/S0022-0248(96)01072-X

Lam dos Santos, J. P., Rosa, L. G., & Amaral, P. M. (2011). Temperature effects on mechanical behaviour of engineered stones. *Construction and Building Materials*, *25*(1), 171–174. https://doi.org/10.1016/j.conbuildmat.2010.06.042

Le Pennec, J.-L., Bourdier, J.-L., Froger, J.-L., Temel, A., Camus, G., & Gourgaud, A. (1994). Neogene ignimbrites of the Nevsehir plateau (Central Turkey): Stratigraphy, distribution and source constraints. *Journal of Volcanology and Geothermal Research*, *63*(1–2), 59–87. https://doi.org/10.1016/0377-0273(94)90018-3

Lee, C., Jo, Y., & Kim, J. (2011). Damage evaluation and conservation treatment of the tenth century Korean rock-carved Buddha statues. *Environmental Earth Sciences*, *64*, 1–14. https://doi.org/10.1007/s12665-010-0809-7

Liu, Q., Zhang, B., Shen, Z., & Lu, H. (2006). A crude protective film on historic stones and its artificial preparation through biomimetic synthesis. *Applied Surface Science*, *253*(5), 2625–2632. https://doi.org/10.1016/j.apsusc.2006.05.032

Liu, Q., Zhang, B., & Yang, G. (2010). Investigation on Application of Biomimetic Technology to the Conservation of Longmen Grottoes. *Applied Mechanics and Materials*, *26–28*. https://doi.org/10.4028/www.scientific.net/AMM.26-28.43

Liu, Q., & Zhang, B.J. (2007). Syntheses of a novel nanomaterial for conservation of historic stones inspired by nature. *Materials Letters*, *61*, 4976–4979. https://doi.org/10.1016/j.matlet.2007.03.104

Lopez-Arce, P., & Doehne, E. (2006). *Kinetics of sodium sulfate efflorescence as observed by humidity cycling with ESEM*. Proceedings of the Heritage, Weathering & Conservation Conference, Madrid, Spain

López-Arce, P., Varas-Muriel, M. J., Fernández-Revuelta, B., Álvarez de Buergo, M., Fort, R., & Pérez-Soba, C. (2010). Artificial weathering of Spanish granites subjected to salt crystallization tests: Surface roughness quantification. *CATENA*, *83*(2–3), 170–185. https://doi.org/10.1016/j.catena.2010.08.009

Łukaszewicz, J. W., & Niemcewicz, P. (2008). *11th International Congress on Deterioration and Conservation of Stone, 15-20 September 2008, Torun, Poland: Proceedings* (Issue v. 2). Uniwersytetu Mikołaja Kopernika. https://books.google.com.tr/books?id=RKljQwAACAAJ

Mahmutoglu, Y. (1998). Mechanical Behaviour of Cyclically Heated Fine Grained Rock. *Rock Mechanics and Rock Engineering*, *31*(3), 169–179. https://doi.org/10.1007/s006030050017

Martínez-Martínez, J., Benavente, D., Gomez-Heras, M., Marco-Castaño, L., & García-del-Cura, M. Á. (2013). Non-linear decay of building stones during freeze–thaw weathering processes. *Construction and Building Materials*, *38*, 443–454. https://doi.org/10.1016/j.conbuildmat.2012.07.059

Matteini, M., Rescic, S., Fratini, F., & Botticelli, G. (2011). Ammonium Phosphates as Consolidating Agents for Carbonatic Stone Materials Used in Architecture and

Cultural Heritage: Preliminary Research. *International Journal of Architectural Heritage*, *5*(6), 717–736. https://doi.org/10.1080/15583058.2010.495445

Mauro Francesco, La Russa, Silvestro Antonio, Ruffolo, Natalia, Rovella, Cristina Maria, Belfiore, Paola, Pogliani, Claudia, Pelosi, Maria, Andaloro, & Gino Mirocle, Crisci. (2014). Cappadocian ignimbrite cave churches: Stone degradation and conservation strategies. *Periodico Di Mineralogia*, *83*(2), 187–206. https://doi.org/10.2451/2014PM0011

May, E., & Jones, M. (Eds.). (2006). *Conservation science: Heritage materials*. RSC Pub.

McCabe, S., Smith, B. J., & Warke, P. A. (2007). Preliminary observations on the impact of complex stress histories on sandstone response to salt weathering: Laboratory simulations of process combinations. *Environmental Geology*, *52*(2), 251–258. https://doi.org/10.1007/s00254-006-0531-7

McIlroy de la Rosa, J. P., Warke, P. A., & Smith, B. J. (2014). The effects of lichen cover upon the rate of solutional weathering of limestone. *Geomorphology*, *220*, 81–92. https://doi.org/10.1016/j.geomorph.2014.05.030

Ministry of Culture and Tourism. (2021) Türkiye Geneli Korunması Gerekli Taşınmaz Kültür Varlığı İstatistiği. Retrieved from https://kvmgm.ktb.gov.tr/TR-44798/turkiye-geneli-korunmasi-gerekli-tasinmaz-kultur-varlig-.html

Ministry of Culture and Tourism. (2021) UNESCO. Retrieved from https://kvmgm.ktb.gov.tr/TR-44393/unesco.html

Mol, L., Gomez-Heras, M., Brassey, C., Green, O., & Blenkinsop, T. (2017). The benefit of a tough skin: Bullet holes, weathering and the preservation of heritage. *Royal Society Open Science*, *4*(2), 160335. https://doi.org/10.1098/rsos.160335

Molina, E., Fiol, C., & Cultrone, G. (2018). Assessment of the efficacy of ethyl silicate and dibasic ammonium phosphate consolidants in improving the durability of two building sandstones from Andalusia (Spain). *Environmental Earth Sciences*, *77*(8). https://doi.org/10.1007/s12665-018-7491-6

Monte, M. (2017). *Experimental evidence of oxalate formation by fungal strains on marble samples* in Molecular Biology and Cultural Heritage (pp. 263–266). https://doi.org/10.1201/9780203746578-36

Mottershead, D., & Lucas, G. (2000). The role of lichens in inhibiting erosion of a soluble rock. *The Lichenologist*, *32*(6), 601–609. https://doi.org/10.1006/lich.2000.0300

Mutlutürk, M., Altindag, R., & Türk, G. (2004). A decay function model for the integrity loss of rock when subjected to recurrent cycles of freezing–thawing and heating–

cooling. *International Journal of Rock Mechanics and Mining Sciences*, *41*(2), 237–244. https://doi.org/10.1016/S1365-1609(03)00095-9

Naidu, S., Blair, J. M., & Scherer, G. W. (2017). Nucleation, Growth and Evolution of Hydroxyapatite Films on Calcite. *MRS Proceedings*, *1656*, 3–8. https://doi.org/10.1557/opl.2014.814

Naidu, S., Liu, C., & Scherer, G. W. (2015). Hydroxyapatite-based consolidant and the acceleration of hydrolysis of silicate-based consolidants. *Journal of Cultural Heritage*, *16*(1), 94–101. https://doi.org/10.1016/j.culher.2014.01.001

Olaru, M., Aflori, M., Simionescu, B., Doroftei, F., & Stratulat, L. (2010). Effect of SO2 Dry Deposition on Porous Dolomitic Limestones. *Materials*, *3*(1), 216–231. https://doi.org/10.3390/ma3010216

Önenç, İ., Kıral, N., Erkanol, D., & Tullukcu, A. (2006). *"Mardin stone" the stone of civilizations.* Geological Congress of Turkey.

Ordóñez, S., Fort, R., & Garcia del Cura, M. A. (1997). Pore size distribution and the durability of a porous limestone. *Quarterly Journal of Engineering Geology and Hydrogeology*, *30*(3), 221–230. https://doi.org/10.1144/GSL.QJEG.1997.030.P3.04

Orhan, M., Işık, N. S., Topal, T., & Özer, M. (2006). Effect of weathering on the geomechanical properties of andesite, Ankara – Turkey. *Environmental Geology*, *50*(1), 85–100. https://doi.org/10.1007/s00254-006-0189-1

Ozcelik, Y., Careddu, N., & Yilmazkaya, E. (2012). The effects of freeze–thaw cycles on the gloss values of polished stone surfaces. *Cold Regions Science and Technology*, *82*, 49–55. https://doi.org/10.1016/j.coldregions.2012.05.007

Ozguven, A., & Ozcelik, Y. (2013). Investigation of some property changes of natural building stones exposed to fire and high heat. *Construction and Building Materials*, *38*, 813–821. https://doi.org/10.1016/j.conbuildmat.2012.09.072

Ozguven, A., & Ozcelik, Y. (2014). Effects of high temperature on physico-mechanical properties of Turkish natural building stones. *Engineering Geology*, *183*, 127–136. https://doi.org/10.1016/j.enggeo.2014.10.006

Özışık, M. N. (1985). *Heat transfer: A basic approach*. McGraw-Hill.

Ozkaya, I. (1974). Stratigraphy of sason and baykan areass SE Turkey. *Geological Bulletin of Turkey*, *17*, 51–72.

Özşen, H., Bozdağ, A., & İnce, İ. (2017). Effect of salt crystallization on weathering of pyroclastic rocks from Cappadocia, Turkey. *Arabian Journal of Geosciences*, *10*(12). https://doi.org/10.1007/s12517-017-3027-8

Özvan, A., Dinçer, İ., Akın, M., Oyan, V., & Tapan, M. (2015). Experimental studies on ignimbrite and the effect of lichens and capillarity on the deterioration of Seljuk Gravestones. *Engineering Geology*, *185*, 81–95. https://doi.org/10.1016/j.enggeo.2014.12.001

Pamplona, M., Ahmad, A., Simon, S., Aßel, E., & Theissen, A. (2010). *Ultrasonic pulse velocity – a tool for the condition assessment of outdoor marble sculptures. The 8th International Symposium on the Conservation of Monuments in the Mediterranean Basin: Monument Damage Hazards & Rehabilitation Technologies.* Patras, Greece

Parchert, K. J., Spilde, M. N., Porras-Alfaro, A., Nyberg, A. M., & Northup, D. E. (2012). Fungal Communities Associated with Rock Varnish in Black Canyon, New Mexico: Casual Inhabitants or Essential Partners? *Geomicrobiology Journal*, *29*(8), 752–766. https://doi.org/10.1080/01490451.2011.619636

Pinna, D. (2014). Biofilms and lichens on stone monuments: Do they damage or protect? *Frontiers in Microbiology*, *5*, 133. https://doi.org/10.3389/fmicb.2014.00133

Poli, T., Toniolo, L., & Sansonetti, A. (2006). Durability of Protective Polymers: The Effect of UV and Thermal Ageing. *Macromolecular Symposia*, *238*(1), 78–83. https://doi.org/10.1002/masy.200650611

Pouli, P., Fotakis, C., Hermosin, B., Saiz-Jimenez, C., Domingo, C., Oujja, M., & Castillejo, M. (2008). The laser-induced discoloration of stonework; a comparative study on its origins and remedies. *Spectrochimica Acta Part A: Molecular and Biomolecular Spectroscopy*, *71*(3), 932–945. https://doi.org/10.1016/j.saa.2008.02.031

Price, C. A. (1982). The Evaluation of Stone Preservatives. In *Conservation of Historic Stone Buildings and Monuments* (pp. 329–340). The National Academies Press. https://doi.org/10.17226/514

Price, C., & Brimblecombe, P. (1994). Preventing salt damage in porous materials. *Studies in Conservation 39(2),* 90-93. https://doi.org/10.1179/sic.1994.39.Supplement-2.90

Přikryl, R. (2013). Durability assessment of natural stone. *Quarterly Journal of Engineering Geology and Hydrogeology*, *46*(4), 377–390. https://doi.org/10.1144/qjegh2012-052

Rampazzi, L., Andreotti, A., Bonaduce, I., Colombini, M. P., Colombo, C., & Toniolo, L. (2004). Analytical investigation of calcium oxalate films on marble monuments. *Talanta*, *63*(4), 967–977. https://doi.org/10.1016/j.talanta.2004.01.005

Rob, P. J. van H. (2004). 3. DAMAGE ANALYSIS AS A STEP TOWARDS COMPATIBLE REPAIR MORTARS. In *Characterisation of Old Mortars with Respect to their Repair* (pp. 107–152). RILEM Publications SARL. 10.1617/2912143675.007

Rodríguez-Gordillo, J., & Sáez-Pérez, M. P. (2006). Effects of thermal changes on Macael marble: Experimental study. *Construction and Building Materials*, *20*(6), 355–365. https://doi.org/10.1016/j.conbuildmat.2005.01.061

Rodriguez-Navarro, C., & Doehne, E. (1999). Salt weathering: Influence of evaporation rate, supersaturation and crystallization pattern. *Earth Surface Processes and Landforms*, *24*(3), 191–209. https://doi.org/10.1002/(SICI)1096-9837(199903)24:3<191::AID-ESP942>3.0.CO;2-G

Rodriguez-Navarro, C., & Ruiz-Agudo, E. (2018). Nanolimes: From synthesis to application. *Pure and Applied Chemistry*, *90*(3), 523–550. https://doi.org/10.1515/pac-2017-0506

Rothert, E., Eggers, T., Cassar, J., Ruedrich, J., Fitzner, B., & Siegesmund, S. (2007). Stone properties and weathering induced by salt crystallization of Maltese Globigerina Limestone. *Geological Society, London, Special Publications*, *271*, 189–198. https://doi.org/10.1144/GSL.SP.2007.271.01.19

Sáez-Pérez, M. P., & Rodríguez-Gordillo, J. (2008). The Influence of Solar Radiation on the Deterioration of the Marble Columns in the Courtyard of the Lions in the Alhambra. *Studies in Conservation*, *53*(3), 145–157. https://doi.org/10.1179/sic.2008.53.3.145

Şahin, K., Yılmaz, A., & Günel, A. (2013). Midyat taşı ve taş işçiliği: doğal ve kültürel çevre ilişkileri. *The Journal of International Social Research*, *6*(24), 12.

Sari, M., Karpuz, C., & Ayday, C. (2010). Estimating rock mass properties using Monte Carlo simulation: Ankara andesites. *Computers & Geosciences*, *36*(7), 959–969. https://doi.org/10.1016/j.cageo.2010.02.001

Sassoni, E. (2018). Hydroxyapatite and Other Calcium Phosphates for the Conservation of Cultural Heritage: A Review. *Materials*, *11*(4), 557. https://doi.org/10.3390/ma11040557

Sassoni, E., & Franzoni, E. (2014). Sugaring marble in the Monumental Cemetery in Bologna (Italy): Characterization of naturally and artificially weathered samples and first results of consolidation by hydroxyapatite. *Applied Physics A*, *117*(4), 1893–1906. https://doi.org/10.1007/s00339-014-8629-3

Sassoni, E., Franzoni, E., Pigino, B., Scherer, G. W., & Naidu, S. (2013). Consolidation of calcareous and siliceous sandstones by hydroxyapatite: Comparison with a TEOS-based consolidant. *Journal of Cultural Heritage*, *14*(3), e103–e108. https://doi.org/10.1016/j.culher.2012.11.029

Sassoni, E., Graziani, G., & Franzoni, E. (2015). Repair of sugaring marble by ammonium phosphate: Comparison with ethyl silicate and ammonium oxalate and pilot application to historic artifact. *Materials & Design*, *88*, 1145–1157. https://doi.org/10.1016/j.matdes.2015.09.101

Sassoni, E., Graziani, G., & Franzoni, E. (2016). An innovative phosphate-based consolidant for limestone. Part 1: Effectiveness and compatibility in comparison with ethyl silicate. *Construction and Building Materials*, *102*, 918–930. https://doi.org/10.1016/j.conbuildmat.2015.04.026

Sassoni, E., Graziani, G., Ridolfi, G., Bignozzi, M. C., & Franzoni, E. (2017). Thermal behavior of Carrara marble after consolidation by ammonium phosphate, ammonium oxalate and ethyl silicate. *Materials & Design*, *120*, 345–353. https://doi.org/10.1016/j.matdes.2017.02.040

Sassoni, E., Naidu, S., & Scherer, G. W. (2011). The use of hydroxyapatite as a new inorganic consolidant for damaged carbonate stones. *Journal of Cultural Heritage*, *12*(4), 346–355. https://doi.org/10.1016/j.culher.2011.02.005

Scheerer, S., Ortega-Morales, O., & Gaylarde, C. (2009). Microbial deterioration of stone monuments—An updated overview. *Advances in Applied Microbiology*, *66*, 97–139. https://doi.org/10.1016/S0065-2164(08)00805-8

Schnabel, L. (2014). Lectures on Materials Science for Architectural Conservation. *Studies in Conservation*, *59*(2), 123–124. https://doi.org/10.1179/0039363014Z.000000000151

Semerci, F. (2008). *A study on Mardin limestone as a construction component*. (MSc Theis) İstanbul Teknik Üniversitesi, Fen Bilimleri Enstitüsü

Sena da Fonseca, B., Ferreira Pinto, A. P., Piçarra, S., & Montemor, M. F. (2017). Artificial aging route for assessing the potential efficacy of consolidation treatments applied to porous carbonate stones. *Materials and Design*, *120*, 10–21. Scopus. https://doi.org/10.1016/j.matdes.2017.02.001

Sena da Fonseca, Bruno, Ferreira Pinto, A. P., Piçarra, S., & Montemor, M. de F. (2018). Challenges of Alkoxysilane-Based Consolidants for Carbonate Stones: From Neat TEOS to Multipurpose Hybrid Nanomaterials. In M. Hosseini & I. Karapanagiotis (Eds.), *Advanced Materials for the Conservation of Stone* (pp. 185–207). Springer International Publishing. https://doi.org/10.1007/978-3-319-72260-3_9

Sengun, N. (2014). Influence of thermal damage on the physical and mechanical properties of carbonate rocks. *Arabian Journal of Geosciences*, *7*(12), 5543–5551. https://doi.org/10.1007/s12517-013-1177-x

Siedel, H., & Hubrich, K. (2000). *Results of Laser Cleaning on Encrusted Oolithic Limestone of Angel Sculptures from the Cologne Cathedral*. 9th International Congress on Deterioration and Conservation of Stone, Italy.

Siegesmund, S., & Snethlage, R. (Eds.). (2011). *Stone in Architecture*. Springer Berlin Heidelberg. https://doi.org/10.1007/978-3-642-14475-2

Smith, B. J., Srinivasan, S., Gomez-Heras, M., Basheer, P. A. M., & Viles, H. A. (2011). Near-surface temperature cycling of stone and its implications for scales of surface deterioration. Geomorphology, 130(1–2), 76–82. https://doi.org/10.1016/j.geomorph.2010.10.005

Sonmez, H., Gokceoglu, C., Medley, E. W., Tuncay, E., & Nefeslioglu, H. A. (2006). Estimating the uniaxial compressive strength of a volcanic bimrock. *International Journal of Rock Mechanics and Mining Sciences*, *43*(4), 554–561. https://doi.org/10.1016/j.ijrmms.2005.09.014

Souza-Egipsy, V., Wierzchos, J., Sancho, C., Belmonte Ribas, Á., & Ascaso, C. (2004). Role of biological soil crust cover in bioweathering and protection of sandstones in a semi-arid landscape (Torrollones de Gabarda, Huesca, Spain). *Earth Surface Processes and Landforms*, *29*, 1651–1661. https://doi.org/10.1002/esp.1118

Steiger, M., Charola, A. E., & Sterflinger, K. (2011). Weathering and Deterioration. In S. Siegesmund & R. Snethlage (Eds.), *Stone in Architecture* (pp. 227–316). Springer Berlin Heidelberg. https://doi.org/10.1007/978-3-642-14475-2_4

Sternberg, T., Viles, H., Cathersides, A., & Edwards, M. (2010). Dust particulate absorption by ivy (Hedera helix L) on historic walls in urban environments. *The Science of the Total Environment*, *409*(1), 162–168. https://doi.org/10.1016/j.scitotenv.2010.09.022

Tan, X., Chen, W., Yang, J., & Cao, J. (2011). Laboratory investigations on the mechanical properties degradation of granite under freeze–thaw cycles. *Cold Regions Science and Technology*, *68*(3), 130–138. https://doi.org/10.1016/j.coldregions.2011.05.007

Taylor-George, S., Palmer, F., Staley, J. T., Borns, D. J., Curtiss, B., & Adams, J. B. (1983). Fungi and bacteria involved in desert varnish formation. *Microbial Ecology*, *9*(3), 227–245. https://doi.org/10.1007/BF02097739

Tesser, E., Lazzarini, L., & Bracci, S. (2018). Investigation on the chemical structure and ageing transformations of the cycloaliphatic epoxy resin EP2101 used as stone consolidant. *Journal of Cultural Heritage*, *31*, 72–82. https://doi.org/10.1016/j.culher.2017.11.002

Topal, T., & Doyuran, V. (1997). Engineering geological properties and durability assessment of the Cappadocian tuff. *Engineering Geology*, *47*(1–2), 175–187. https://doi.org/10.1016/S0013-7952(97)00017-3

Topal, T., & Doyuran, V. (1998). Analyses of deterioration of the Cappadocian tuff, Turkey. *Environmental Geology*, *34*(1), 5–20. https://doi.org/10.1007/s002540050252

Topal, Tamer, & Sözmen, B. (2003). Deterioration mechanisms of tuffs in Midas monument. *Engineering Geology*, *68*(3–4), 201–223. https://doi.org/10.1016/S0013-7952(02)00228-4

Uğur, İ., & Toklu, H. Ö. (2020). Effect of multi-cycle freeze-thaw tests on the physico-mechanical and thermal properties of some highly porous natural stones. *Bulletin of Engineering Geology and the Environment*, *79*(1), 255–267. https://doi.org/10.1007/s10064-019-01540-z

Van, T. T., Beck, K., & Al-Mukhtar, M. (2007). Accelerated weathering tests on two highly porous limestones. *Environmental Geology*, *52*(2), 283–292. https://doi.org/10.1007/s00254-006-0532-6

Vasanelli, E., Colangiuli, D., Calia, A., Sileo, M., & Aiello, M. A. (2015). Ultrasonic pulse velocity for the evaluation of physical and mechanical properties of a highly porous building limestone. *Ultrasonics*, *60*, 33–40. https://doi.org/10.1016/j.ultras.2015.02.010

Viles, H. A. (2013). Durability and conservation of stone: Coping with complexity. *Quarterly Journal of Engineering Geology and Hydrogeology*, *46*(4), 367–375. https://doi.org/10.1144/qjegh2012-053

Viles, Heather A. (2005). Can stone decay be chaotic? In A. V. Turkington (Ed.), *Stone Decay in the Architectural Environment* (Vol. 390, pp. 11–16). Geological Soc Amer Inc. https://doi.org/10.1130/2005.2390(02)

Wakefield, R. D., & Jones, M. S. (1998). An introduction to stone colonizing micro-organisms and biodeterioration of building stone. *Quarterly Journal of Engineering Geology and Hydrogeology*, *31*(4), 301–313. https://doi.org/10.1144/GSL.QJEG.1998.031.P4.03

Wang, P., Xu, J., Liu, S., & Wang, H. (2016). Dynamic mechanical properties and deterioration of red-sandstone subjected to repeated thermal shocks. *Engineering Geology*, *212*, 44–52. https://doi.org/10.1016/j.enggeo.2016.07.015

Warscheid, Th., & Braams, J. (2000). Biodeterioration of stone: A review. *International Biodeterioration & Biodegradation*, *46*(4), 343–368. https://doi.org/10.1016/S0964-8305(00)00109-8

Wasserman, I. (2004). The efficiency of surface treatments on enhancement of the durability of limestone cladding stones. *Materials and Structures*, *38*(275), 99–105. https://doi.org/10.1617/14068

Wedekind, W., Gross, C. J., Hoffmann, A., & Siegesmund, S. (2018). Damage phenomenon and petrophysical properties of sandstones at the Phnom Bakheng Temple (Angkor, Cambodia): First investigations and possible conservation measures. Environmental Earth Sciences, 77(21), 735. https://doi.org/10.1007/s12665-018-7915-3

Werner, M. (1991). Research on cleaning methods applied to historical stone monuments. *Science, Technology and European Cultural Heritage* https://doi.org/10.1016/B978-0-7506-0237-2.50120-9

Williams, R. B. G., & Robinson, D. A. (1981). Weathering of sandstone by the combined action of frost and salt. *Earth Surface Processes and Landforms*, *6*(1), 1–9. https://doi.org/10.1002/esp.3290060102

Winkler, E. M. (1997). *Stone in Architecture*. Springer Berlin Heidelberg. https://doi.org/10.1007/978-3-662-10070-7

X Wang. (2004). Investigation on the restoration techniques of ancient wall. *Traditional Chinese Architecture and Gardens*, *1*, 20–22.

Yang, F., Liu, Y., Zuo, G., Zhu, Y., Zhang, B., & Hua, P. (2012). Biomimetic fluorapatite films for conservation of historic calcareous stones. *Chinese Science Bulletin*, *57*. https://doi.org/10.1007/s11434-012-5026-1

Yavuz, A.B., & Topal, T. (2007). Thermal and salt crystallization effects on marble deterioration: Examples from Western Anatolia, Turkey. *Engineering Geology*, *90*(1–2), 30–40. https://doi.org/10.1016/j.enggeo.2006.11.005

Yavuz, Ali Bahadır, & Topal, T. (2016). Effects of different drying temperatures on the physical and mechanical properties of some marbles (Muğla, Turkey) during salt crystallization tests. *Environmental Earth Sciences*, *75*(11). https://doi.org/10.1007/s12665-016-5806-z

Yavuz, H., Altindag, R., Sarac, S., Ugur, I., & Sengun, N. (2006). Estimating the index properties of deteriorated carbonate rocks due to freeze–thaw and thermal shock weathering. *International Journal of Rock Mechanics and Mining Sciences*, *43*(5), 767–775. https://doi.org/10.1016/j.ijrmms.2005.12.004

Yavuz, H., Demirdag, S., & Caran, S. (2010). Thermal effect on the physical properties of carbonate rocks. *International Journal of Rock Mechanics and Mining Sciences*, *47*(1), 94–103. https://doi.org/10.1016/j.ijrmms.2009.09.014

Yavuz, Huseyin. (2011). Effect of freeze–thaw and thermal shock weathering on the physical and mechanical properties of an andesite stone. *Bulletin of Engineering Geology and the Environment*, *70*(2), 187–192. https://doi.org/10.1007/s10064-010-0302-2

Young, M. E. (1993). Stone cleaning of granite buildings and monuments: The use of colour measurement in stone cleaning trials. *Conservation Science in the U.K.: Preprints of the Meeting Held in Glasgow, May 1993*, 20.

Zarzuela, R., Moreno-Garrido, I., Blasco, J., Gil, M. L. A., & Mosquera, M. J. (2018). Evaluation of the effectiveness of CuONPs/SiO2-based treatments for building stones against the growth of phototrophic microorganisms. *Construction and Building Materials*, *187*, 501–509. https://doi.org/10.1016/j.conbuildmat.2018.07.116

Zhang, W. (2015). Experimental study of the effect of thermal damage on resistivity and mechanical properties of sandstone. *Acta Geodynamica et Geomaterialia*, 185–192. https://doi.org/10.13168/AGG.2015.0056

Zornoza-Indart, A., López-Arce, P., & López-Polín, L. (2017). Durability of traditional and new nanoparticle based consolidating products for the treatment of archaeological stone tools: Chert artifacts from Atapuerca sites (Burgos, Spain). *Journal of Cultural Heritage*, *24*, 9–21. https://doi.org/10.1016/j.culher.2016.10.019

PUBLICATIONS FROM THESIS

Papers

1. Celik, S. E., Gulen, J., & Viles, H. A. (2020). Evaluating the effectiveness of DAP as a consolidant on Turkish building stones. *Construction and Building Materials*, *262*, 120765. https://doi.org/10.1016/j.conbuildmat.2020.120765

Projects

1. TUBITAK 2214 International Doctoral Research Fellowship Programme. Development of green conservation techniques on unique Anatolian stones. Grant No: 1059B141700359. 02.2019 – 06.2019